EFMC6 KTH

Electronic version

Abstracts

Volume 1

KTH
VETENSKAP
OCH KONST

EFMC6 KTH - EUROMECH Fluid Mechanics Conference 6
Royal Institute of Technology STOCKHOLM, JUNE 26-30 2006

Preface

The EUROMECH Fluid Mechanics Conference 6 (EFMC 6) is held at KTH in Stockholm during June 26-30, 2006. These two volumes of abstracts comprise all presentations of the conference, including nine plenary lectures, and more than 400 contributed papers, which are presented either in oral sessions or during five different mini-symposia. The page numbers given here corresponds to the presentation number found in the conference programme booklet. At the end of each volume you will find a list of all authors and the page number(s) where their abstract appear. The **bold** page numbers correspond to presenting authors.

We like to thank the EFMC committee for their work with the evaluation and selection process. We also like to thank Veronica Eliasson and Bengt Fallenius for help with preparing the printed version of these volumes.

Henrik Alfredsson, chairman EFMC6
Jens Fransson, scientific secretary EFMC6

Euromech Fluid Mechanics Lecturer

Invited Lecturers

LIQUID SLOSHING IN CYLINDRICAL CONTAINERS

E.J. HOPFINGER
LEGI/CNRS, UJF, B.P. 53, 38041 Grenoble, France

Liquid sloshing is frequently encountered in liquid storage tanks subjected to external forces. It is also an every-day problem as we often experience sloshing and spilling by dropping inadvertently a cap of coffee or by shaking a glass of water. In the latter case spilling may be prevented by a bifurcation of the wave motion to a stable swirling mode. However, the frequency and excitation amplitude tuning for getting one or the other modes is very narrow and what seems to be at first sight a simple problem turns out to be complex in detail. An overview of the theory of sloshing is given in the book by Ibrahim (2005)

The main part of my presentation will be on sloshing in partially filled circular and square-base cylindrical containers subjected to sway (horizontal periodic excitation). The low viscosity fluid motion is controlled by three parameters which are the liquid depth, the excitation frequency and excitation amplitude. Experimental results, obtained for a range of excitation frequencies excitation amplitudes in the limit of large fluid depth will be discussed with emphasis on the bounds of existence of the different wave amplitude responses, namely plane waves, swirling waves and resonant breaking waves. It is shown that plane wave motions bifurcate to a swirling motion at finite wave amplitude (cubic non-linearity). The swirl has a hard-spring behaviour, is very robust and can generate a rotation of the liquid. In the chaotic regime wave breaking occurs quasi periodically: growth of plane wave amplitude, collapse, irregular swirl and again growth of plane wave amplitude. The scenario of three-dimensional breaking is best illustrated by experiments conducted in the square-base container of base dimension L. The spanwise destabilisation of the wave crest of wavelengths L and $L/2$ is interpreted as parametric instability.

The second part of my talk will illustrate sloshing phenomena due to axial excitations, specifically by subjecting a liquid layer of uneven free surface to a step change in axial acceleration and by higher frequency vibrations, leading to capillary wave breaking. The step change can be produced by dam-break or liquid reorientation (Baumbach et al 2005) leading to geysering. This problem is relevant for space applications where liquid fuel tanks are exposed to large changes in axial accelerations. On collapse of the geyser violent liquid sloshing occurs. The striking phenomenon is the considerable height of the geyser, similar to what is observed at the surface of the impacting coffee cup (Milgram 1969). Periodic vertical acceleration leads to Faraday instability and, at sufficiently large excitation frequency and amplitude to capillary wave breaking. The breaking characteristics and emerging drop sizes are discussed on hand of recent experiments similar to those of Goodridge et al (1999).

Boumbach, V, Hopfinger, E.J. & Cartellier A. 2005 The transient behaviour of a large bubble in a vertical tube. J. Fluid mech. 524, pp 131-142
Ibrahim, R.A. 2005 Liquid sloshing dynamics. Cambridge University Press
Milgram, J. H. 1969. The motion of a fluid in a cylindrical container with a free surface following vertical impact. J. Fluid Mech. 37, pp. 435- 448
Goodridge, C.L. Hentschel, H.G.E. and Lathrop, D.P. 1999 Breaking Faraday waves: critical slowing of droplet ejection rates. Phys. Ref. Lett. 82, pp. 3062-3065

Continuum Models in Industrial Applications.

Hilary Ockendon[d]

A continuum model is often a model at the macrolevel of a process which has a very complicated discrete structure at the microlevel. This talk describes some situations in which a relatively simple continuum model can be used to give useful results in an industrial setting. Two cases will be considered.

1. The Fanno model is traditionally used to model turbulent gas flow in long pipes. The unsteady version of this model turns out to be appropriate for problems as diverse as explosions in coalmines, pressure transducers in extreme situations and the high speed spinning of manmade fibres. These applications show that a well-known model can still contain unexpected results.

2. A more unconventional modelling task is posed by the deformation of a mass of entangled fibres. Here the dynamics of the microstructure are governed by frictional interactions between fibres and the bending and stretching of individual fibres. In spite of the complicated microstructure, it is possible to construct a useful macroscopic model of the material as an anisotropic viscous fluid when it is in tension and as a linear anisotropic elastic material when in compression. The model builds on ideas from liquid crystals and fibre reinforced materials and introduces the concept of “entanglement” to quantify the state of the material. Practical examples include the movement of fibres in the carding machine and the packing of glass fibre insulation.

[d] Mathematical Institute, University of Oxford, 24-29 St Giles, Oxford

Progress in Reynolds' problem: transition to turbulence in a pipe

R.R. Kerswell*

The problem of understanding the nature of pressure-driven fluid flow through a circular straight pipe remains one of the oldest problems in fluid mechanics. At low flow rates, the realised solution named after Hagen[1] and Poiseuille[2] is steady, unidirectional and parabolic in profile. For increased level of driving, however, the flow can easily be triggered into a spatially and temporally disordered 3-dimensional state[3]. This transition is abrupt, dependent on the level of ambient disturbances in the system and, at least close to the threshold flow rate, transient. The recent discovery of travelling wave solutions in this system[4,5] has at last provided a theoretical stepping stone towards rationalising the transition process. I will discuss these waves, evidence for their relevance to the transitional dynamics and the current level of our understanding.

*Dept. of Mathematics, University of Bristol, U.K.

[1]Hagen, *Poggendorfs Annalen def Physik und Chemie* **16**, 423 (1839)
[2]Poiseuille, *C.R. Acad. Sci. Paris* **11**, 961 (1840)
[3]Reynolds, *Proc. R. Soc. Lond.* **35**, 84 (1883)
[4]Faisst & Eckhardt *Phys. Rev. Lett.* **91**, 22 (2003)
[5]Wedin & Kerswell *J. Fluid Mech.* **508**, 333 (2004)

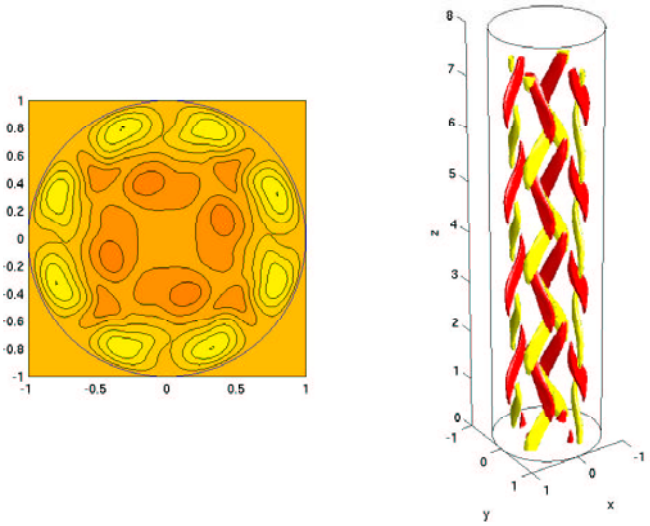

Figure 1: A travelling wave with 4-fold rotational symmetry. On the left, a slice across the pipe showing fast and slow streaks in the stream velocity (light/dark respectively). On the right, isocontours of the streamwise vorticity (+/-60% of maximum shown).

Slip Behavior at Liquid/Solid Interfaces: Comparison Between Hydrodynamic and Molecular Scale Simulations

S. M. Troian[a], N. V. Priezjev[b] and A. A. Darhuber[a]

The development of micro- and nanofluidic devices for the transport and mixing of liquid films, droplets and bubbles requires accurate characterization of the boundary conditions at liquid/solid interfaces. The smaller the dimensions of the device, the more dominant is the influence of surface conditions on flow behavior. Of practical concern in systems with large surface to volume ratio are the significant frictional losses induced by the celebrated no-slip condition. While it is true that this empirical boundary condition has proven remarkably successful in reproducing most commonplace flows, there exist notable examples of non-inertial flows for which the no-slip condition leads to a divergent shear stress including corner flows, coating flows and capillary spreading of a droplet. Various slip models have been used to regularize the shear stress singularity but these are mostly phenomenological in origin and provide no general understanding of the nature of momentum transport at liquid-solid interfaces. During the past decade, high resolution experimental measurements have determined that slip can occur along solid boundaries treated with non-wetting silanized coatings and along substrates with little surface roughness. The flow of high molecular polymer melts also generates much larger slip lengths than do simple liquids especially at high shear rates.

Using molecular dynamics (MD) simulations of liquid films in steady planar shear at very low Reynolds number, we have examined what transport coefficients govern the degree of slip and whether the slip length for simple liquids[1] and polymer melts is shear-rate dependent[2]. The simulations elucidate the role of the liquid in-plane structure factor and diffusion coefficient near the solid substrate, the role of wall roughness[3], and variations in wall surface energy[4] in establishing the slip length. Comparisons between molecular scale simulations, simplified molecular models based on the fluctuation–dissipation theorem, and continuum Stokes flow solutions indicate excellent agreement between the hydrodynamic and molecular level models provided the characteristic size of the substrate inhomogeneity is about an order of magnitude larger than the diameter of the liquid particles. We will conclude this talk with a general discussion of what liquid/solid characteristics lead to deviations between these various approaches and a generalization of slip based on the Navier slip condition.

---

[a] School of Engineering and Applied Science, Princeton University, Princeton, NJ, 08544, USA.

[b] Dept. of Mechanical Engineering, Michigan State Univ., East Lansing, MI 48824, USA.

[1] Thompson and Troian, *Nature* **389**, 360 (1997).

[2] Priezjev and Troian, *Phys. Rev. Lett,* **92**, 018302 (2004).

[3] Priezjev and Troian, *J. Fluid Mech.* **554**, 25 (2006).

[4] Priezjev, Darhuber and Troian, *Phys. Rev. E* **71**, 041608 (2005).

Wind Turbine Wake Structures

J. N. Sørensen[a]

Modern wind turbines are often clustered in wind parks in order to reduce the overall installation and maintenance expenses. An unwanted effect, however, is that the turbulence intensity in the wake is increased because of the interaction from the wakes of the surrounding wind turbines. As a consequence, dynamic loadings are increased that may excite the structural parts of the individual wind turbine and enhance fatigue loadings. The turbulence created from wind turbine wakes are mainly due to the dynamics of the vortices originating from the rotor blades. The vortices are formed as a result of the rotor loading. To analyse the genesis of the wake, it is thus necessary to include descriptions of the aerodynamics of both the rotor and the wake. Although many wake studies have been performed over the last two decades, a lot of basic questions still need to be clarified in order to elucidate the dynamic behavior of individual as well as multiple interactive wakes behind wind turbines[1].

In the past years the author and his group has developed a numerical technique for studying wind turbine wakes[2]. In this model the gross flow field around the rotor is simulated by the Navier-Stokes equations, using either direct or large eddy simulation, with the rotor loading represented by body forces. This technique enables to study wake dynamics without having to resolve in detail the viscous boundary layer of the rotor blades. The computational results are compared to experiments and analysed for their content of organized anisotropic and coherent structures. The computations form the background for the development of a low-dimensional wake turbulence model based on proper orthogonal decomposition.

In the presentation we show and discuss recent results from simulations of single and multiple wakes (see the figure below[3]) and demonstrate how they can be used to create low-dimensional turbulence models. Furthermore, we present a new analytical wake model based on helical vortices[4].

---

[a] DTU Fluid Mechanics, Bldg. 403, DK-2800 Lyngby, Denmark.

[1] Vermeer et al., *Progress in Aerospace Sciences*, **39**, 467 (2003).

[2] Sørensen and Shen, *J. Fluids Engineering*, **124**, 393 (2002).

[3] Troldborg et al., *European Wind Turbine Conference, EWEC 2006*, Athens (2006).

[4] Okulov and Sørensen, submitted *J. Fluid Mech.*, (2006).

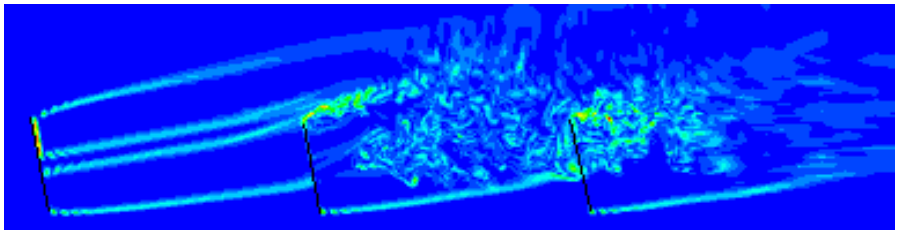

Figure 1: Development of wake formed by three rotors in a row inclined 9.6^{o}.

The power of bubbles: Unconventional microfluidics

Sascha Hilgenfeldt*

Microfluidics has been both a fertile field of fundamental fluid mechanics research and an exciting area for innovative applications in various fields, including lab-on-a-chip functions, biochemistry, biomedicine, and bioengineering. We give an overview on the physics behind a novel method of driving flows on the microscale and its many uses: *bubble-driven streaming flow*.

Streaming flow is steady fluid motion induced by fast, oscillatory displacements of a boundary, which by themselves would not lead to significant fluid transport. In the micron-scale set-ups we utilize, the steady streaming is a creeping flow governed by the Stokes equation. Using microbubbles attached to a wall of a microfludic device as the fast-moving boundaries allows for significant oscillation amplitudes and convenient driving by ultrasound. The resulting streaming is very fast compared to other microfluidic flows and exerts strong shear forces on transported objects. Changes in driving frequency, ultrasound amplitude, or the topography of the substrate surface allow for translational or rotational flows, reversal of flow direction, or mixing.

The theoretical description of the streaming flow is intricate because of the need for boundary layer matching at both the bubble boundary and the wall. The final result for the far-field flow, however, can be expressed as a sum of analytically known Stokes singularities, providing us with a simple mathematical toolbox to describe and predict the various behaviors encountered in experiment.

Like the streaming flow, the steady hydrodynamic stress on transported objects is a known function of experimental parameters and results in forces ranging from pN to many nN. We discuss several applications to trap, deform, separate, and porate lipid membranes or whole cells. In a lab-on-a-chip setting, bubble streaming microfluidics provides very large throughput for these and other applications without the need for sophisticated micromanufacturing.

*ESAM and Mechanical Engineering, Northwestern University, 2145 Sheridan Rd, Evanston, IL 60208

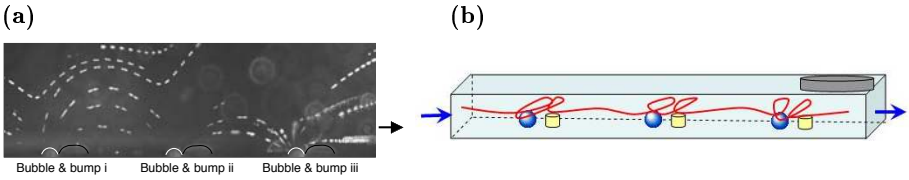

Figure 1: An example of flows caused by oscillating bubbles adhering to a wall. (a) Combinations of bubbles and "bumps" (protrusions on a substrate, seen in side view) effect fast unidirectional transport (streaks are fluorescent tracer particles). (b) The same set-up with different bubble/bump geometry induces convoluted fluid trajectories and can serve as a micromixer. Both set-ups transport fluid and suspended particles from left to right, but (a) is optimized for throughput, while (b) combines thorough mixing and fast flow.

Fluid mechanics of phase change

Gustav Amberg[a]

One crucial step in almost all materials processes is solidification in one form or other. The conditions under which the melt resolidifies will be crucial for the final microstructure of the material. The size and morphology of the individual grains that make up a polycrystalline material, the homogeneity of a monocrystal, the actual phase that is formed, as well as its local composition, is determined by the interplay between local heat and mass transfer and the thermodynamics of the phase change. Even though the microstructure of the material may change considerably during subsequent cooling and following process steps, the foundation has been laid at the point of solidification. Since local heat and mass transfer governs the phase change, it is obvious that any convection in the melt will be paramount in determining the structure of the material, thus making this an area of important applications that should interest fluid dynamicists. Aside from the technological processes referred to above, there are also numerous phenomena in nature where the interplay of convection and phase change is crucial, from the formation of ice on sea and lakes, to solidification of magma into rock.

In this lecture I will outline some basic solidification phenomena, following a path of increasing geometrical complexity, and discuss different effects of convection and fluid flow as I go along. In the simplest situation, a solid growing very slowly may form a planar interface, but as the driving force for phase change increases, this becomes unstable to shape perturbations, which may develop into highly complex patterns. One common morphology is a dendritic crystal, which grows in a tree-like shape. Eventually a complex solid-liquid two-phase system is formed. In all of these processes the presence of convection and melt motion will have a crucial effect on the structures that are formed. As an example, in forced convection past a growing array of dendrites, the dendritic forest will tend to tilt upstream into the wind. Around a single, large, slowly growing crystal, natural convection may be important, causing an enhanced growth downwards, in the direction of gravity. Many relevant materials processes involve free liquid melt surfaces, and in such cases additional important driving forces for fluid motion are capillarity and wetting, and surface tension gradients due to temperature or concentration gradients.

In discussing these problems I will also have to briefly introduce the phase field method, a diffuse interface method where model equations for phase change are derived using the principles of phenomenological non-equilibrium thermodynamics.

[a] KTH Mechanics, SE-100 44 Stockholm, Sweden.

Premixed Turbulent combustion based on the Level Set Approach

N. Peters[a] and J. Ewald[b]

In premixed turbulent combustion a thin flame front interacts with a turbulent flow field at many scales, ranging from the integral length scale down to the Kolmogorov scale. Depending on whether the flame thickness l_F is larger or smaller than the Kolmogorov scale l_k, two different regimes of interaction can be defined: 1. the corrugated flamelet regime where $l_F \leq l_k$ and 2. the thin reaction zones regime where $l_F \geq l_k$. In the first case the entire flame structure including the preheat zone can be assumed as quasi-steady with the consequence that its interaction with the flow its characterized by the laminar burning velocity alone. In the second case Kolmogorov eddies may enter into the preheat zone but not into the thin reaction zone, which now may be assumed as quasi-steady. Since the smallest eddies will wrinkle the reaction zone, its curvature will become large. The product of the molecular diffusivity and the curvature represents a velocity. This velocity is of the same order of magnitude or larger than the laminar burning velocity and therefore determines the interaction with the flow in the second regime.

Modelling premixed turbulent combustion is traditionally based on the progress variable as the dependent scalar. It will be argued that this approach is physically not sound. Therefore a level set formulation is proposed to derive suitable model equations. In these equations a better distinction can be made between the physical phenomena occurring in the two regimes mentioned above. Finally a joint formulation for the turbulent burning velocity is derived which contains the two regimes as distinet limits.

The resulting combustion model is applied to two premixed configurations with spark ignition, a cylindrical vessel and a SI engine with complex geometry. For the latter case simulations are shown for engines for homogeneous and as well as for stratified charge. At the end of the talk a LES simulation of a turbulent flame on a slot burner will be presented.

---

[a] Institut für Technische Verbrennung, RWTH, D-52056 Aachen, Germany
[b] FEV, D-52078 Aachen, Germany

[1] Peters, J. Fluid Mech. **384**, 107 (1999)
[2] Wenzel and Peters, Combust. Sci. and Techn. **158**, 273 (2000)
[3] Peters et al., Proceedings of the Combustion Institute **28**, 235 (2000)
[4] Peters et al., Combust. Theory Modelling **5**, 363 (2001)
[5] Wenzel and Peters, Combust. Sci. Tech. **177**, 1095 (2005)

Generation of magnetic fields by turbulent flows

S. Fauve*, F. Pétrélis†

The generation of a magnetic field by the flow of an electrically conducting fluid, i.e. the dynamo effect, has been first considered to explain the origin of the magnetic fields of planets, stars and galaxies. It has been also studied in relation with several applied problems such as liquid metal cooling of nuclear reactors, liquid metal electromagnets and instabilities in toroidal plasmas. Magnetic field generation by laminar flows is fairly well understood and dynamos generated by simple but clever flow geometries have been successfully observed in experiments performed a few years ago in Karlsruhe and Riga.

However, the effect of turbulence on dynamo threshold and saturation still involves many open problems. We have shown that small scale turbulent fluctuations only slightly modify the dynamo threshold predicted as if the mean flow were acting alone, in agreement with the Karlsrhue and Riga experimental observations [1]. On the contrary, large scale fluctuations of eddies generating the field can strongly inhibit the dynamo effect, as shown in an analytically tractable example. Thus, the behaviour of the dynamo threshold of strongly turbulent flows as a function of the kinetic Reynolds number, is still an open problem involving many conflicting statements in the literature.

The nonlinearly saturated dynamo regime also depends on the Reynolds number of the flow generating the magnetic field. We show that different scaling laws can be obtained for the magnetic energy generated in the vicinity of the threshold [2] and compare them to the values measured in Karlsruhe and Riga. The importance of the Coriolis force, crucial for astrophysical or geophysical dynamos, is also shortly discussed.

Dynamos generated by strongly turbulent flows of liquid metal as well as astrophysical or geophysical dynamos, cannot be studied with direct numerical simulations of the equations of magnetohydrodynamics in a realistic parameter range. Progress in this direction thus strongly relies on experimental observations and several groups in the world are trying to generate a turbulent dynamo [3]. We will shortly review these efforts and show how the study of fluctuations and transport of a magnetic field by the flow of a liquid metal can give insights in the relevant mechanisms of turbulent dynamos [4] [5].

*Laboratoire de Physique Statistique, Ecole Normale Supérieure, 24 rue Lhomond 75005 Paris, France.

†Laboratoire de Physique Statistique, Ecole Normale Supérieure, 24 rue Lhomond 75005 Paris, France.

[1] Fauve and Pétrélis, *Peyresq Lectures on Nonlinear Phenomena, Ed. J-A Sepulchre, World Scientific* **2**, 1 (2003).

[2] Pétrélis and Fauve, *Eur. Phys. J. B* **22**, 273 (2001).

[3] Fauve and Lathrop, *Fluid Dynamics and Dynamos in Astrophysics and Geophysics, A. Soward et al., Eds.* 393 (2005).

[4] Bourgoin et al., *Phys. Fluids* **14**, 3046 (2002).

[5] Pétrélis et al., *Phys. Rev. Lett.* **90**, 174501 (2003).

Session 1

Linear dynamics of a separated flow over a rounded backward facing step : global modes and optimal perturbations

O. Marquet[a], D. Sipp[a], J.-M. Chomaz[a], L. Jacquin[a]

The global linear stability of a two-dimensional flow over a rounded backward facing step to three-dimensional transverse perturbations is numerically investigated. The steady two- dimensional base flow is obtained through time-dependent simulations and Newton-Raphson convergence methods. The streamlines of a typical base flow is given in Fig. 1. The generalized eigenvalue problem is solved using the Implicitly Restarted Arnoldi Method implemented in the ARPACK library. The most unstable linear mode is three-dimensional, non-oscillating and appears at a critical Reynolds number of Re=675. The associated eigenmode is localized within the separation bubble (see Fig. 2), and the reconstruction of the total flow shows a three-dimensional deformation of this recirculation region. The adjoint stability problem is solved in order to locate the core of the instability and to determine the influence of numerical boundary conditions on the direct stability problem. Our results suggest that the characteristics of the global mode are mainly dictated by the recirculation zone of the base flow. Finally, thanks to a gradient-based optimization algorithm, we study the optimal perturbations of the system, i.e. the initial perturbation which maximizes the energy at time t=T. We show that strong gains may be obtained which are associated to the growth of three-dimensional convective instabilities in the shear layer.

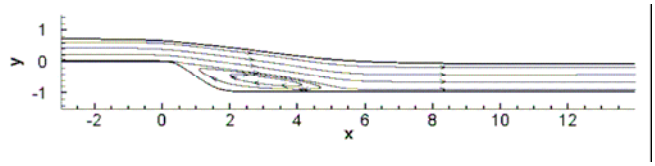

Fig. 1 : Streamlines of the basic flow at Re=800

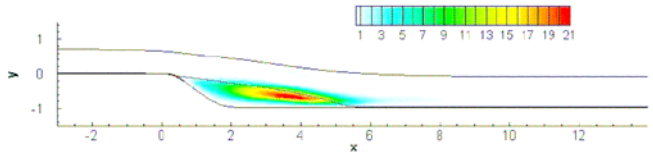

Fig. 2 : Typical energy repartition of most unstable eigenmode at Re=800 and k=2.

[a] ONERA / DAFE, 8 rue des Vertugadins 92190 Meudon, France

Global stability of jets and sensitivity of the mode to inflow perturbations.

F. Giannetti* and P. Luchini*

Recent experiments on coaxial jets [1] have revealed, for particular values of the parameters, the existence of a self-exciting mechanism between the vortical structures created inside the nozzle and the jet evolution in the external region. The spectral analysis of the experimental data indicates that when this occurs, the flow field in the proximity of the nozzle exit is modulated by the instability of the external shear layer and consequently is characterized by a single dominant frequency. Numerical simulations on geometries resembling the experimental set up [2] confirm this behavior and show an unexpected sensitivity of the flow field to the imposed inflow conditions. Computations performed on simplified geometries, in fact, exhibit a remarkably different evolution of the system according as the full geometry (nozzle + jet) is simulated or only the region downstream of the exit is considered. This behavior brings evidence of a strong feedback between different locations of the flow and suggests the presence of an unstable global mode [3].

In this paper we perform a linear stability analysis on a jet emerging from a converging nozzle. The aim is to investigate the possible existence of an unstable global mode and to study its main characteristics. The steady axially-symmetric base flow is obtained trough the numerical solution of the incompressible Navier-Stokes equations and an immersed-boundary technique is used to represents the nozzle geometry. The first instability of the steady flow is studied by linearizing the governing equations and using a normal mode expansion. The resulting numerical eigenvalue problem is solved numerically and a parametric study is performed to evaluate the critical Reynolds number. The properties of the adjoint eigenfunctions are analyzed in order to study the receptivity of the system to initial conditions and to external forcing. The sensitivity of the jet to the imposed inflow and outflow conditions and the existence of localized feedbacks are determined through a stability analysis to perturbations of the differential operator, a technique originally developed to study the stability of the wake behind a circular cylinder [4] [5] . The spatial characteristics of the product of the direct and adjoint modes are analyzed to identify the regions where the instability mechanism acts and to determine the locations where the feedback is stronger. In order to verify the results, the stability analysis is repeated on several restricted domains, allowing in this way a direct comparison of the influence of the inflow and outflow conditions on the eigenvalues.

*DIMEC, University of Salerno, Via Ponte Don Melillo, 84084 Fisciano (SA), Italy.

[1] Buresti G., *Documenti del Dip. di Ing. Aerospaziale di Pisa*, **DDIA 2002-1** (2002).

[2] Tessicini et al. , *Proc. XV AIMeTA Congress of Theoret. and Appl. Mech.*, **SP FL 20** (2001).

[3] Huerre and Monkewitz, *Annual Review of Fluid Mechanics*,**22**,pp 473-537 (1990).

[4] Giannetti and Luchini, *V Euromech Fluid Mechanics Conference*, Toulouse, August 24-28, 2003.

[5] Giannetti and Luchini, *Journal of Fluid Mechanics*, (submitted) .

Oscillating growth in convection dominated systems

G. Coppola*, L. de Luca*

In the context of the linear stability analysis of non parallel open flows, such as wakes, jets, boundary layers and separation bubbles, the concept of global modes has been employed in order to describe the dynamics of the flow disturbances. By considering the model problem of the linearized Ginzburg Landau equation with spatially varying coefficients, Cossu and Chomaz[1] firstly demonstrated that the simultaneous excitation of different global modes in a non normal system can be advocated in order to describe wave packets convectively propagating in open flow systems. In recent papers these concepts have been applied to real flows problems such as the stability of a falling liquid curtain[2], and the two dimensional temporal analysis of boundary layer flows along a flat plate[3].

The case illustrated by the model of the falling curtain presents a situation in which the non normal character of the operator involved in the global analysis produces a transient evolution that is characterized by a periodic oscillating pattern, which appears to be as important for the physical description of the system as the occurrence of the growth itself. However, while the relations between non normality of a linear operator and the transient growth of its solution operator norm has been a wide theme of research in hydrodynamic stability in the past years, the theme of oscillating transient growth and of its relations with non normality of the operator has received less attention.

In this work, the study of oscillating norm behavior in linear evolutionary systems is addressed. A link between the occurrence of oscillating patterns in the energy evolution of the solutions and the nonorthogonality of linear global modes is illustrated; moreover, a distinction between transient and asymptotic oscillations is made. The analysis carried out shows that special frequency signatures associated to transient oscillations can be explained by means of suitable "synchronizations" between global modes, and some frequency selection rules are also proposed. The physical importance of such oscillating behaviors is stressed by reconsidering the model for the linear stability of the falling liquid curtain studied by Schmid and Henningson and by considering different physical models arising in the context of the linearized formulation of some convection dominated systems over finite length domains.

*DETEC, Univ. di Napoli 'Federico II', Italy.

[1]Cossu and Chomaz *Phys. Rev. Lett.* **78**, 4387 (1997).
[2]Schmid and Henningson *J. Fluid Mech.* **463**, 163 (2002).
[3]Ehrenstein and Gallaire *J. Fluid Mech.* **536**, 209 (2005).

Control of instabilities in a cavity-driven separated boundary-layer flow

E. Åkervik*, J. Hœpffner *, U. Ehrenstein† and D. S. Henningson *

A two-dimensional incompressible boundary-layer flow along a smooth-edged cavity is considered. Unstable global modes appear above a critical inflow Reynolds number ($Re_{\delta_0^*}$) of approximatively 300 for the considered aspect ratio of the cavity.

We aim at stabilizing the flow using feedback control. Sensors measure shear stress at the downstream lip of the cavity, where the unstable modes are most energetic, and actuators apply blowing and suction upstream, where sensitivity is highest. The optimal control loop, in the form of control and estimation feedback gains, is computed through the solution of two Riccati equations. The high dimentionality of this strongly nonparallel flow, once discretized, challenges the design of an optimal feedback controller. A reduced dynamic model is thus constructed for small perturbations to the basic flow by selecting the least stable eigenmodes of the linearized Navier-Stokes equations for this geometry.

The flow system is discretized using Chebyshev collocation in both the streamwise and wall-normal direction and the global eigenmodes are computed by means of the Krylov-Arnoldi method as described in Ehrenstein&Gallaire (2005)[1]. Flow stabilization is demonstrated using a model reduced to 50 states, provided the actuators are smooth, with slow time scales.

Figure 1 shows the streamwise velocity component of the most unstable eigenmode at the inflow Reynolds number of $Re_{\delta_0^*} = 325$.

*KTH Mechanics , SE-100 44 Stockholm, Sweden.
†Laboratoire J.A. Dieudonne , Parc Valrose, F-06108 Nice Cedex 02, France
[1]Ehrenstein and Gallaire, *J. Fluid Mech.* **536**, 209 (2005).

Figure 1: Streamwise velocity component of the most unstable eigenmode.

The stability of multiple wing-tip vortices

E. J. Whitehead*, J. P. Denier* and S. M. Cox*

The stability of wing-tip vortices is a problem that has received much attention in the past 20 years due to their importance in the aerodynamics industry, where they are the limiting factor that sets minimum spacing between following aircraft, both in flight and during take-off and landing. Work to date can be divided into two, not necessarily distinct, camps. The first approach follows the early work of Crow[1] in which the stability of a vortex pair is considered, the resulting instability now commonly referred to as the Crow instability. The second approach focus on the stability of a single vortex, which is typically taken to be given by the asymptotic solution for a single tip-vortex far downstream of the trailing edge, as was first derived by Batchelor[2].

Unlike much of the previous work on the stability of tip vortices we have considered the stability of a multi-vortex system. The combined vortex flow is taken as a combination of Batchelor vortices, who strengths, extents and positions can be adjusted. Our results indicate that the optimal position, in terms of the maximal streamwise growth rate of an infinitesimally small disturbance, for a four-vortex configuration has all vortices aligned along the axis representing the aerofoil trailing edge; see the accompanying figure. The horizontal locations of the vortices along this axis that yield the maximal streamwise growth rate as a function of the relative vortex strengths will also be described. If time permits, recent work on the question of the absolute instability of multi-vortex flows will also be presented.

*School of Mathematical Sciences, The University of Adelaide, South Australia 5005, Australia.

[1] Crow, *AIAA J.*, **8**, 2172 (1970).

[2] Batchelor, *J. Fluid Mech.*, **20**, 645 (1964).

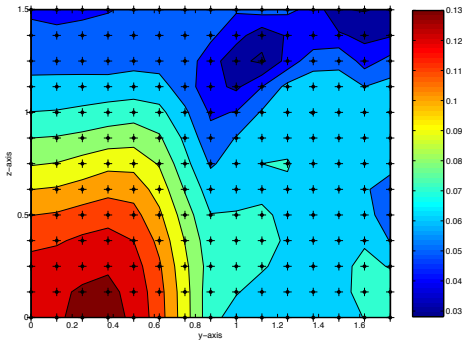

Figure 1: Contour plot of the maximum growth rate as a function of secondary-vortex position. The vortices are aligned symmetrically with respect to the z-axis. The primary vortex is situated at $(y, z) = (2, 0)$.

The dispersal, decay and instability of multiple trailing-line vortices

Peter W. Duck*

The importance of the dispersal, decay and breakdown of trailing-line vortices is now a key aerodynamic issue. The classical flow that has spawned much research activity over many years has been the (viscous) solution of Batchelor[1], describing the downstream evolution of a solitary vortex generated behind one side of a wing. Various aspects of the stability of this flow have been presented over the years (see for example[2] [3] [4]). The dominant mode of instability is generally of short wavelength (and is therefore inviscid), and as a consequence growth rates are quite large (which can lead to breakdown, which is advantageous from a practical point of view).

In this paper the approach adopted involves (i) the determination of the downstream evolution of a multiple vortex system and (ii) an investigation of the short-wavelength (inviscid) stability of this developing flow. The theory is mathematically rational, being based on the assumption of large Reynolds numbers.

Consider first the downstream developing baseflow; assuming a uniform flow far outside the trailing vortex system, it is then possible to reduce the Navier-Stokes equations to the following nondimensional form:

$$U_X + v_y + w_z = 0, \quad UU_X + vU_y + wU_z = U_{yy} + U_{zz},$$

$$Uv_X + vv_y + wv_z = v_{yy} + v_{zz} - p_y, \quad Uw_X + vw_y + ww_z = w_{yy} + w_{zz} - p_z.$$

Here (U, v, w) are the velocity components in the (X, y, z) directions respectively, and p is pressure; the scaling in the downstream direction X is long, and includes a Reynolds number factor (implying a slow downstream flow evolution, compared to the vertical y and crossflow z directions). Correspondingly the velocity components in the y and z directions are an order smaller in Reynolds number than the X component. The system is parabolic in nature (the streamwise diffusion terms have been eliminated), and can therefore be solved in a 'marching' fashion, downstream from some prescribed initial conditions. A variety of such conditions have been implemented, including two counter-rotating vortices and various systems involving four vortices.

When considering the stability of the base states (as described above), it is possible to perform a 2D (inviscid) stability analysis, which reduces the (in)stability problem to the following partial eigenvalue problem (in which either the streamwise wavenumber α is specified and the wavespeed c is treated as an eigenvalue, or vice versa):

$$\frac{\partial^2 \tilde{p}}{\partial y^2} + \frac{\partial^2 \tilde{p}}{\partial z^2} - \frac{2}{U-c}\frac{\partial U}{\partial y}\frac{\partial \tilde{p}}{\partial y} - \frac{2}{U-c}\frac{\partial U}{\partial z}\frac{\partial \tilde{p}}{\partial z} - \alpha^2 \tilde{p} = 0,$$

where $\tilde{p}$ is the pressure eigenfunction. Using this type of approach, it is feasible to rapidly and efficiently investigate different vortex configurations, in order to optimise trailing-vortex characteristics with regard to dispersal, decay and breakdown.

*School of Mathematics, University of Manchester, England

[1] Batchelor, *J. Fluid Mech.* **20**, 645 (1964).
[2] Lessen et al. *J. Fluid Mech.* **63**, 743 (1974)
[3] Lessen & Paillet *J. Fluid Mech.* **65**, 769 (1974)
[4] Duck & Foster, *ZAMP* **31**, 524 (1980)

Stability of pulsatile flow through a pipe

Linganagari Abhijeeth Reddy*, Kirti Chandra Sahu†, Rama Govindarajan†

Pulsatile flow through a pipe has been a topic of interest[1] because of its relevance to the blood flow through arteries. (Arterial flow is of course very complicated but we confine ourselves here to the effect of the pulsatile nature of the flow.) Stability of pulsatile flow in a plane channel has been studed by Straatman et al. using a Floquet analysis. They find that pulsatile flow is always destabilising[2]. In a recent paper[3] Fedele et al. have studied the stability of pulsatile pipe flow for axisymmetric disturbances. Although all eigen modes are decaying, a small transient growth of the disturbances was found for a short time. In this work, we depart in two ways from the study of Fedele et al. (1) the flow is taken to be periodic but not sinusoidal, which is closer to arterial flow, (2) we consider non-axisymmetric disturbances which are often more unstable. Prescribing periodic velocity profiles at the inlet, we solve the Navier-Stokes equation directly using a full-multigrid algorithm on a parallel machine[4] to get the basic flow. A Floquet stability analysis is then conducted. A sample basic flow is plotted in figure 1(a) in terms of the deviation from the mean. For two different frequencies the neutral stability curves are plotted in figure 1(b). It can be seen that the flow is linearly unstable unlike either Poiseuille flow, or the findings of Fedele et al. Details of the approach[5] and a study of the effect of asymmetry of the periodic flow will be presented at the conference.

*IIT Guwahati, India
†Jawaharlal Nehru Centre for Advanced Scientific Research, Bangalore, India

[1]Pedley, *Perspectives in Fluid Dynamics* **chapter 3**, (2000).
[2]Straatman et al., *Phys. Fluids* **14**, 6 (2002).
[3]Fedele et al., *European J. of Mech.* **237**, 24 (2005).
[4]Venkatesh et al., *Current Science* **589**, 88(4) (2005).
[5]Sahu and Govindarajan, *J. Fluid Mech.* **325**, 531 (2005).

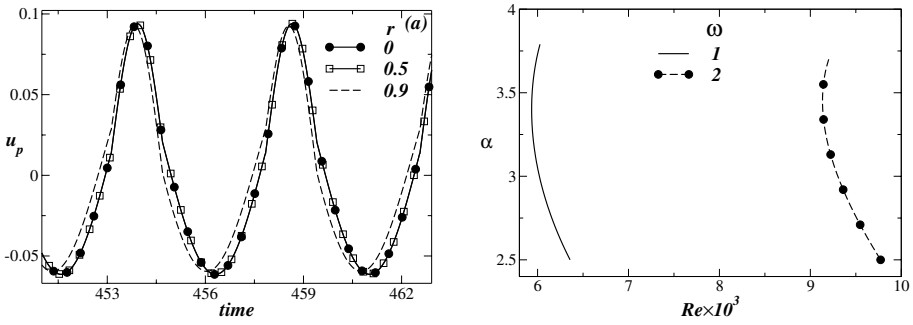

Figure 1: (a) Deviation from the mean profile at different radial locations. The amplitude of the deviation falls off to zero at the wall. (b) Neutral Reynolds number Vs wave number (α) of the disturbances for different frequencies of the inlet unsteady profile.

Steady and pulsatile flow through a locally constricted tube

M. D. Griffith[*†], T. Leweke[*], K. Hourigan[†] and M. C. Thompson[†]

Flows, both steady and pulsatile, through a circular tube with an axisymmetric blockage of varying size are studied experimentally and numerically. The geometry consists of a long straight tube and a blockage which is semi-circular in cross-section. This geometry is selected as an idealized model of a stenosed artery. The stenosis has been simplified to a single-parameter blockage, the aim being to highlight fundamental behaviours of constricted flows. The chosen Reynolds numbers (Re), defined using the average inlet velocity and unblocked tube diameter, are in a range relevant to blood flows in the larger arteries. Recent work[1] has shown the outlet length to be an important parameter, particularly for the onset of instabilities in pulsatile flow. The experiments and simulations have been designed to remove, as far as possible, the effect of outlet length on the flow downstream of the blockage. Experimentally, a water flow is considered inside a tube of 19 mm diameter, which has an unblocked length of 2 m both upstream and downstream of the blockage. The flow is characterised using dye visualisations and Particle Image Velocimetry. These results are complemented by spectral-element numerical simulations.

At low Reynolds numbers, the flow is steady and characterised by a jet emanating from the constriction, surrounded by an axisymmetric recirculation zone, the length of which increases linearly with Reynolds number. Figure 1 shows the streamlines and vorticity field from an axisymmetric simulation, at Re = 100 and blockage by area of 75%. The work of Sherwin and Blackburn[1] on the flow through a similar geometry with the same reduction in area showed that the jet loses axisymmetry at a critical Reynolds number of 722. Results from our numerical simulations indicate a similar stability threshold for the present geometry, a transition we aim to qualify experimentally. The effect of a variation in blockage size on the onset and mode of instability is investigated, revealing a change in the azimuthal mode number as the blockage size is decreased. The transition to a time-dependent state at higher Reynolds numbers, downstream of the blockage, is also studied.

The second part of the study looks at flows subject to a pulsatile inlet condition, which more closely describe the type of flow found in the cardio-vascular system. We characterise the stability of such flows, focusing particularly on the effect of the blockage size on any loss of flow-axisymmetry or transition to turbulence.

[*]IRPHE, CNRS/Universités Aix-Marseille, BP 146, F-13384 Marseille Cedex 13, France
[†]FLAIR, Dept. of Mechanical Engineering, Monash University (Melbourne), 3800, Australia
[1]Sherwin and Blackburn, *J. Fluid Mech.* **533**, 297 (2005).

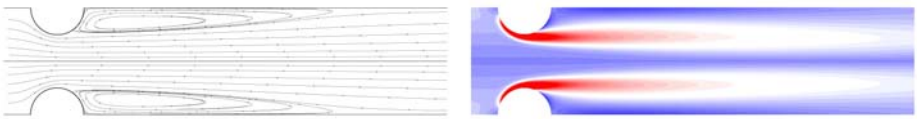

Figure 1: Streamlines and vorticity of the steady flow, at Re = 100 and 75% blockage.

Instability and Transition of Pulsatile Flow in Stenotic/Constricted Pipes.

Spencer J. Sherwin*, Hugh Blackburn†

An idealisation of an arterial blockage or stenosis, potentially generated by atherosclerosis disease is a smooth sinusoidally varying stenotic (constricted) tube. Although most physiological flow conditions are typically laminar, turbulent flow states are possible when a stenosis is present.

The instability modes arising within simple non-reversing pulsatile flows in a circular tube with a smooth axisymmetric constriction are examined using global Floquet stability analysis and direct numerical simulation. The sectionally averaged pulsatile flow is represented with one harmonic component superimposed on a time-mean flow. In prior work[1] we identified a period-doubling absolute instability mechanism associated with alternating tilting of the vortex rings that are ejected out of the stenosis throat with each pulse, as shown in figure 1(a). In this paper[2] we show that while this is the primary instability mode for comparatively larger reduced velocities associated with long pulse periods (or low Womersley numbers), for lower reduced velocities that are associated with shorter pulse periods the primary instability typically manifests as azimuthal waves (Widnall instability modes) of low wavenumber that grow on each vortex ring as shown in figure 1(b). It is also shown that the shear layer of the steady axisymmetric flow is convectively unstable at still shorter temporal periods, and at Reynolds numbers well below the onset of the first three-dimensional absolute instability mode.

*Department of Aeronautics, Imperial College London, UK
†CSIRO, Manufacturing and Infrastructure Technology, Australia

[1] Three-dimensional instabilities and transition of steady and pulsatile axisymmetric stenotic flows by S.J. Sherwin and H.M. Blackburn, *J. Fluid Mech.* ,**533**, 297-327, (2005).

[2] Instability modes and transition of pulsatile stenotic flow: pulse-period dependence by H.M. Blackburn and S.J. Sherwin, submitted to *J. Fluid Mech.* , (2005).

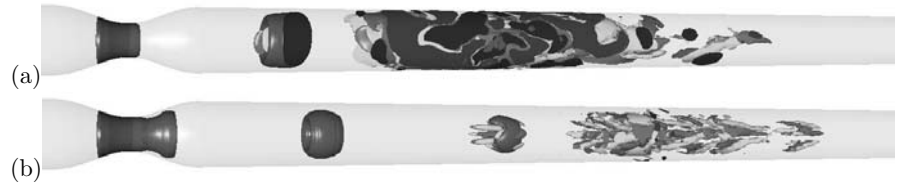

Figure 1: Transitional flow under (a) Period doubling instability and (b) Wavy mode instability.

Pulsatile flows in pipes with finite curvature

S.L.Waters and J.H.Siggers
School of Mathematical Sciences, University of Nottingham,
University Park, Nottingham, NG7 2RD, UK

Motivated by the study of blood flow in a curved artery, we consider fluid flow through a curved pipe of uniform curvature, δ, driven by a prescribed pulsatile axial pressure gradient. The curved pipe has finite (as opposed to asymptotically small) curvature, and we determine the effects of both the centrifugal and Coriolis forces on the flow. The flow is parameterised by δ, the Dean number, D, the Womersley number, α, and a secondary streaming Reynolds number, R_s. Asymptotic solutions are developed for the case when $D \ll 1$, $R_s \ll 1$ and $\delta \ll 1$, using regular perturbation techniques. For intermediate values of the governing parameters a pseudospectral code is used to obtain numerical solutions. For flows driven by a purely oscillatory pressure gradient ($D = 0$) we identify three distinct classes of stable solutions: 2π-periodic symmetric, 2π-periodic asymmetric, and asymmetric solutions that are either quasi-periodic, or periodic with period $2\pi k$ for $k \in \mathbb{N}$. The transition between solutions is dependent on the value of δ; thus pipes with finite curvature may exhibit qualitatively different transitions between the solution classes as the governing parameters are varied from those of curved pipes with asymptotically small curvature. When $\alpha \gg 1$, matched asymptotic expansions are used to simplify the system, and the resulting equations are solved analytically for $R_s \ll 1$, $\delta \ll 1$ and numerically for larger parameter values. We then determine the effect of a non-zero steady component of the pressure gradient ($D \neq 0$), and show that, for certain parameter values, when D is above a critical value the periodic asymmetric solutions regain spatial symmetry. Finally, we show that the effects of finite curvature can lead to substantial quantitative differences in the wall shear stress distribution and discuss the physiological implications of the results for blood flow in arteries.

Convective diffusion process in a pulsating flow trough stenosis.

R. Tuzi*and P. Orlandi*

Cardiovascular flows in a complex geometry, such as a stenosis in blood vessel or artificial valves and stents, are commonly accompanied by separation, stagnation, recirculation and secondary vortex motion. The geometry of a stenotic artery could be complex; it has been frequently simplified as symmetrical and asymmetrical constriction in a cylindrical tube, but it has been also studied on its complex shape by Yakhot *et* al.[1] to investigate the effect of the surface roughness on the flow resistance.

Numerical simulations of the pulsating flow and convection-dominated diffusion process in a tube with local axisymmetric constriction simulating stenosed artery are performed. The flow is characterized by high frequency jets at the narrowest section and flow separation behind the stenosis. It has been observed that the transition to turbulence occurred trough the breakdown of waves and streamwise vortices in the high-shear layers. The postenotic flow became unstable during this vortex generation phase of the cycle, resulting in intense fluctuations in wall shear stress. Vortical and helical structures were formed during the decelerating phase and near the reattachment point downstream of the constriction, accordingly with the experimental findings by Ojha *et* al. [2]

Detecting the occurrence of turbulence is important, in fact turbulence affects the flow resistance, the shear stress acting on the blood vessel wall, tensile stress in the endothelian cell membrane, mass transport from the blood to the vessel wall. Our attention is focused on the effect of wall shear stress and recirculating flow on the concentration distribution in the vessel lumen and on the wall transfer. At this purpose the Navier Stokes and the convection-diffusion equations are solved, to gain a deep insight into the physiological condition for the transport of oxygen or macromolecules such as low density lipoproteins, across the artery wall and their accumulation in the wall. 3D and axisymmetric simulations are performed, as an example in Fig.1a vorticity contours are shown in the accelerating phase and in Fig.1b the contours of a passive scalar inserted at $x_1 = 0$ and with the possibility to exit from the domain at $x_1 = L_1$. These figures are evaluated in the axisymmetric case, the differences with the 3D simulations will be presented at the meeting.

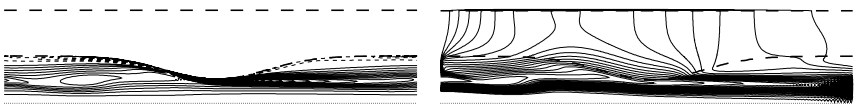

Figure 1: a) Vorticity b) Passive scalar

*Dipartimento di Meccanica e Aeronautica, Università di Roma 'La Sapienza', Via Eudossiana 18, 00184, Italy

[1]Yakhot *et* al.*Journal of Biomechanics* **38**, 1115 (2005).

[2]Ojha *et* al., *J. Fluid Mech.* **203**, 173 (1989).

Haemodynamics of the embryonic chicken heart.

P. Vennemann*, R. Lindken* and J. Westerweel*

To answer the question whether cardiogenesis is regulated through fluid forces, detailed knowledge about the velocity distribution in the embryonic heart is required. The derived wall shear stress distribution can be compared to gene expression patterns to draw conclusions. Micro Particle Image Velocimetry (μPIV) quantitatively resolves the instantaneous velocity distribution *in vivo*. A special polymer coating makes the fluorescent tracer particles bio-inert. The measurement allows the determination of the velocity gradient close to the wall. Figure 1 shows the blood velocity distribution in the central plane of the developing ventricle of a chicken embryo after three days of incubation. The location of the measurement plane is indicated in the scanning electron micrograph from Männer[1]. The eccentricity of the flow profile can be explained by the curvature of the primitive heart tube. Closely following Deans calculation for a curved tube[2] the velocity peak position is found to be shifted into the direction of the inner curvature wall for low Reynolds numbers (Figure 1, insets *a* and *b*). Secondary flow is negligibly small (Figure 1, inset *c*).

*Lab. for Aero- and Hydrodynamics, Delft Technical University, The Netherlands.

[1] J. Männer, *Anat. Rec.* **259**:248-262 (2000).
[2] W. R. Dean, *Phil. Mag. Ser. 7* **4(20)**:673-695 (1928).

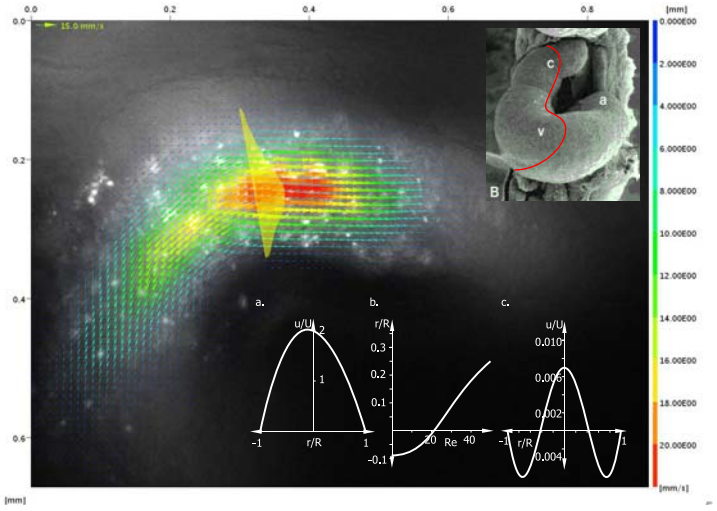

Figure 1: Particle Image Velocimetry in the embryonic chicken heart. Inset *a*: theoretical, axial velocity profile for a curved tube in the plane of coil curvature (r is negative in the direction of the coil center). Inset *b*: theoretical, radial velocity peak position in the plane of coil curvature at varying Reynolds numbers ($R_{tube}/R_{coil} = 1/2$). Inset *c*: theoretical, secondary velocity profile in radial direction.

Global stability of the rotating disk boundary layer and the effects of suction and injection

Christopher Davies*and Christian Thomas*

The rotating disk boundary-layer can be shown to be absolutely unstable, using an analysis that deploys the usual 'parallel-flow' approximation, where the base flow is simplified by taking it to be homogeneous along the radial direction[1]. But for the genuine radially inhomogeneous base flow, numerical simulations indicate that the absolute instability does not give rise to any unstable linear global mode.[2]. This is despite the fact that the temporal growth rates for the absolute instability display a marked increase with radius.

The apparent disparity between the radially increasing strength of the absolute instability and the absence of any global instability can be understood by considering analogous behaviour in solutions of the linearized complex Ginzburg-Landau equation[3]. These solutions show that detuning, arising from the radial variation of the temporal frequency of the absolute instability, may be enough to globally stabilize disturbances. Depending on the precise balance between the radial increase in the growth rates and the corresponding shifts in the frequencies, it is possible for an absolutely unstable flow to remain globally stable.

Similar behaviour has been identified in more recent numerical simulations, where mass injection was introduced at the disk surface but the modified flow still appeared to be globally stable. More interestingly, it was found that globally unstable behaviour was promoted when suction was applied. This is illustrated in the figure, which displays numerical simulation results for the impulse response of a range of inhomogeneous base flows with varying degrees of mass injection and suction. The plots show the evolution of locally computed temporal growth rates at the critical point for the onset of absolute instability. The temporal variation of the negative-valued growth rates for the cases with injection is associated with convective propagation behaviour. But when suction is applied the disturbance eventually displays an increasingly rapid growth at the radial position of the impulse, albeit without any selection of a dominant frequency, as would be more usual for an unstable global mode.

*School of Mathematics, Cardiff University, Cardiff, CF24 4YH, UK

[1]Lingwood, *J. Fluid Mech.* **299**, 17 (1995).

[2]Davies and Carpenter, *J. Fluid Mech.* **486**, 287 (2003).

[3]Hunt and Crighton, *Proc. R. Soc. Lond. A* **435**, 109 (1991).

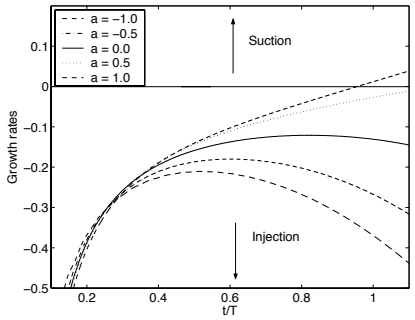

Crossflow instability in rotor-stator flows with throughflow

S. Poncet [*], M.-P. Chauve [*]

We study the formation of new spiral patterns, denoted SRJ2 (figure 1(a)), at the periphery of an enclosed rotor-stator cavity when an axial inward or outward throughflow is superimposed.

Figure 1(b) shows the transition diagrams, obtained from flow visualizations, for three different aspect ratios $G = h/R_2$ in the (Re, V_z^*) plane, where h is the interdisk space, R_2 the rotating disk radius, Re the rotational Reynolds number and V_z^* the dimensionless axial velocity in the radial gap between the rotor and the shroud. Thus, the results of Poncet and Chauve [1] and Rémy *et al.* [2] have been extended for both Batchelor ($G = 0.0857$) and torsional Couette ($G = 0.0171$) type of flows. The SRJ2 spiral rolls appear essentially when an inward throughflow ($V_z^* > 0$) is superimposed but also in the case of an outward throughflow ($V_z^* < 0$) for $G = 0.0857$. Numerical calculations have shown that these structures appear as soon as a strong axial upward flow is created along the shroud, which may be the case when the outward throughflow impinges on it. As the axial velocity profiles exhibit inflexion points, this instability is of crossflow type. From visualizations and velocity measurements, we have determined that these are positive spirals located at the periphery of the cavity along the stator side and characterized by small frequency and phase velocity and large inclination angle and azimuthal wavenumber. The influence of the flow control parameters Re, V_z^* and G on these characteristics have been analysed. There is a strong competition between rotation and throughflow. Nevertheless, the effects of the geometry G and of the throughflow V_z^* seem to be preponderant to be compared to the one of the rotation Re.

*IRPHE, Technopôle Château-Gombert, 13384 Marseille, France.

[1] Poncet and Chauve, *J. Fluid Mech.* **545**, 281 (2005).

[2] Rémy *et al.*, *Phys. Fluids* **17 (1)** (2005).

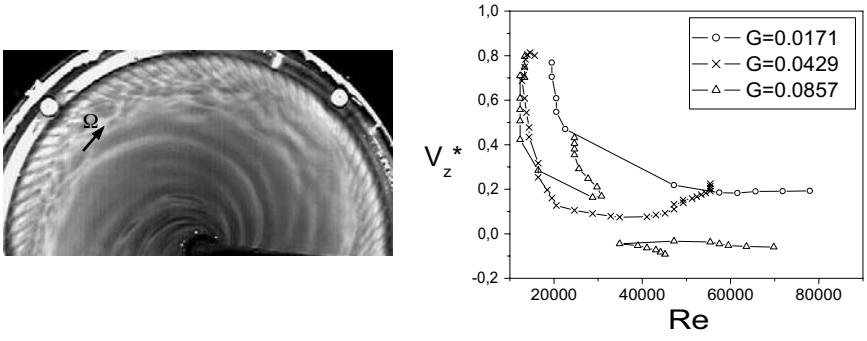

(a) (b)

Figure 1: (a) Visualization of the SRJ2 patterns for $Re = 2.05 \times 10^4$, $V_z^* = 0.515$ and $G = 0.0429$. (b) Existence domains of the SRJ2 spirals in the (Re,V_z^*) plane.

Continuous Spectrum Growth and Modal Instability in Swirling Duct Flow

C. J. Heaton*, N. Peake*

We discuss the acoustics and stability of inviscid ducted swirling flow. Swirling flow arises in many problems, from aeroacoustics to vortex and jet stability. The vorticity in the mean flow complicates the usual acoustic spectrum: there is no simple scalar velocity potential and the unsteady pressure and vorticity are coupled. The spectrum typically contains two distinct families of modes, respectively analogous to the acoustic and vorticity waves found in irrotational flow[1]. In particular a family of so-called nearly-convected modes can be present in the spectrum, often having an infinite accumulation of eigenvalues in the complex plane and we analytically classify this, and describe in which cases the family contains instability modes. We also treat the continuous spectrum of the acoustic-vorticity waves and find that it can be responsible for a new convective instability. The growth rate for this instability is algebraic (rather than exponential), with an exponent that depends on the mean flow and which is given in the analysis.

The stability of swirling inviscid flow has been considered by many previous authors, from Rayleigh's famous stability criterion for axisymmetric perturbations to incompressible rotating fluid to many modern numerical and asymptotic studies. The family of unstable nearly-convected modes we identify (see figure 1 for an example, which shows the complex wavenumber plane for a fixed temporal frequency calculation) is shown to correspond to existing large wavenumber WKB theory[2] and among our results is an extension of their results to finite azimuthal orders. The non-modal instability we identify and investigate is due to the continuous spectrum of the linearised Euler equations, and is in addition to any modal growth that may or may not be present. The continuous spectrum of parallel shear flow can lead to linear growth of the flow energy[3], but here we find that taking a fully three dimensional mean flow leads to a growth rate which can take any value.

*DAMTP, Wilberforce Road, Cambridge CB3 0WA, UK

[1]Golubev and Atassi, *J. Sound Vib.* **209**, 203 (1998).

[2]Leibovich and Stewartson, *J. Fluid Mech.* **126**, 335 (1983).

[3]Landahl, *J. Fluid Mech.* **98**, 243 (1980).

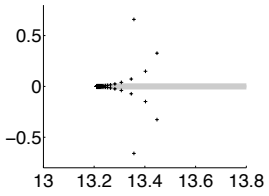

Figure 1: Unstable nearly convected modes (+ signs) and the continuous spectrum (thick grey line) for a swirling flow. These numerics agree very well the the asymptotic analysis to be presented.

Oscillatory jets and triadic instability in a closed rotating flow

Y. Duguet*, J. F. Scott†, L. Le Penven†

Oscillatory shear layers commonly occur in unsteady forced rotating flows and their instabilities are believed to be important for the dynamics of planetary cores. We study the flow inside a closed rotating gas cylinder which is subject to oscillating axial strain. Strain is imposed by a piston and the cylinder height varies like $h(t) = h_0\,(1 + \epsilon \cos\omega_0 t)$. When $\omega_0 < 1$ (with ω_0 non-dimensionalised by twice the rotation rate) and the Ekman number is small –here E=$O(10^{-4})$–, the basic flow is characterised by thin conical oscillatory shear layers (or 'jets'), emanating from the piston corner and reflecting on the walls. The jets are angled out at $\arcsin\omega_0$ with the rotation axis. The viscous structure of this flow is computed using an axisymmetric spectral algorithm. For small ϵ the jetwidth scales like $O(E^{\frac{1}{3}})$ or exceptionnally $O(E^{\frac{1}{4}})$ when the cones undergo multiple covering. For larger ϵ the jets seem to break down. For certain angular frequencies ω_0, a low-order inertial mode of the rotating cylinder can be directly forced. Nonlinear triadic resonances between inertial modes are then observed and make the flow become quasi-periodic with frequencies ω_0, ω_1 and ω_2 such that $\omega_1 + \omega_2 = \omega_0$. The higher-order triads lead to oscillatory jets with two different orientations, corresponding to inertial wave packets of frequencies ω_1 and ω_2. Another kind of parametric instability, based on linear coupling of inertial modes by the piston motion, also arises above a given threshold. It induces a subharmonic response of the system at half the piston frequency [1].

*Department of Mathematics, University of Bristol, Bristol, BS8 1TW, UK
†LMFA, Ecole Centrale de Lyon, 36 Avenue Guy de Collongue, 69134 Ecully Cedex, France
[1] Duguet & al., *Phys. Fluids* **17**, 054110 (2005).

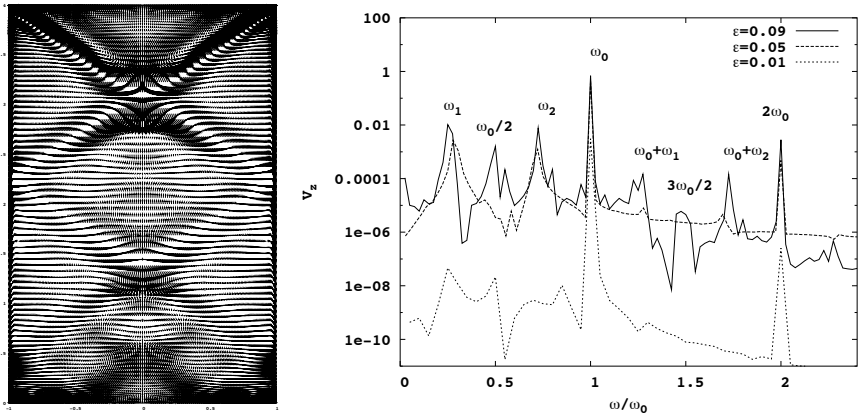

Figure 1: Basic flow (V_r, V_z) for $\epsilon = 10^{-3}$, $h_0 = 4$, $E = 10^{-4}$, $\omega_0 = 0.74$ (left); Frequency spectrum of V_z for $\omega_0 = 0.775$ and different values of ϵ (right).

The influence of centrifugal buoyancy in rotating convection.

F. Marques*, J. M. Lopez†, O. Batiste* and I. Mercader*

Rotating thermal convection is a paradigm problem that incorporates fundamental processes of great importance to atmospheric and oceanic circulations, as well as of astrophysical importance. We analyze rotating convection in a simple geometrical setting, consisting of an enclosed circular cylinder of depth-to-radius ratio $\Gamma = d/R = 1.0$, rotating at an angular rate ω, with the bottom endwall at temperature $T_0 + \Delta T$ and the top endwall at T_0. The nondimensional parameters are the Coriolis parameter $\Omega = \omega d^2/\nu$, the Rayleigh number $Ra = \alpha g \Delta T d^3/\nu\kappa$, the Prandtl number $\sigma = \nu/\kappa$ and the Froude number $Fr = \omega^2 R/g$. Three-dimensional numerical simulations using a spectral code have been made in this geometry.

Traditionally, density variation was only incorporated in the gravitational buoyancy term and not in the centrifugal buoyancy term. In this limit, corresponding to $Fr \to 0$, the governing equation admit a trivial conduction solution, resulting in important simplifications of the problem. Linear stability analysis neglecting centrifugal buoyancy in an enclosed rotating cylinder finds that typically the onset of thermal convection from the conduction state is to a so-called wall mode which consists of alternating hot and cold thermals rising and decending in the cylinder boundary layer[1]. Experiments to test this linear theory have needed to be carefully designed in order to minimize the effects of the neglected centrifugal buoyancy, and have found good agreement with the theory for the onset of convection[2].

The presence of centrifugal buoyancy changes the problem in a fundamental manner. The buoyancy force has a radial component that destroys the horizontal translation invariance assumed in the unbounded theoretical treatments of the problem. Furthermore, the Z_2 reflection symmetry about the cylinder mid-height is also destroyed. The centrifugal buoyancy drives a large scale circulation in which the cool denser fluid is centrifuged radially outward and the hot less dense fluid is centrifuged radially inward[3]. This large scale circulation exists for any $\Delta T \neq 0$, and so there is no trivial conduction state when the centrifugal buoyancy is incorporated.

For small Froude numbers the transition from the base axisymetric state to 3D flow happens around $Ra \approx 7.500$. We have found that for moderate Froude numbers ($Fr \geq 4$) the centrifugal buoyance delays this transition to much larger Rayleigh numbers, $Ra \approx 50.000$. At intermediate Fr the transition to 3D flow happens via four different Hopf bifurcations, with complex interactions between the bifurcated states,resulting in different coexisting branches of 3D solutions. How the centrifugal buoyancy and the gravitational buoyancy interact and compete, and the manner in which the flow becomes three-dimensional is different along each branch. The main conclusion is that centrifugal buoyancy changes quantitatively and qualitatively the flow dynamics, and should not be neglected in rotating convection problems.

*Departament de Física Aplicada, Univ. Politècnica de Catalunya, Barcelona 08034, Spain.
†Department of Mathematics and Statistics, Arizona State University, Tempe AZ 85287, USA.

[1] Goldstein et. al., *J. Fluid Mech.* **248**, 583–604 (1993).
[2] Zhong et. al., *Phys. Rev. Lett.* **67**, 2473–2476 (1991) and *J. Fluid Mech.* **249**, 135–159 (1993).
[3] Barcilon & Pedlosky, *J. Fluid Mech.* **29**, 673–690 (1967); Homsy & Hudson, *J. Fluid Mech.* **35**, 33–52 (1969).

Actual performance of improved WENO schemes on a selection of test cases

I. Fedioun*, L. Gougeon*, I. Gokalp*

Due to its simplicity, Monotone Integrated Large Eddy Simulation (MILES) has become a standard way of LES. This form of LES is intended to capture the correct flow energy up to some scale in the inertial range and then dissipate this energy at a non linear rate depending on the numerical dissipation of the scheme. Very long time simulations should then use highly accurate schemes in conjunction with a fine enough grid to ensure that the results are not affected by the numerics[1]. From our experience on Kelvin-Helmholtz instabilities[2], WENO schemes are good candidates for MILES but, in their initial form [3], they still suffer from a relatively poor resolution of contact discontinuities (with smearing for larger time) and may not always preserve monotonicity. Recent works [4] [5] allowed to fix these two key points, leading to a nearly optimal numerical scheme. We analyse the actual performance of this kind of modified WENO schemes and present an extension to multi-fluid simulations. This analysis is performed on several test cases sorted by order of complexity : (i) asymptotic analysis of the effective modified wave number, (ii) mono and multi-fluid shock tube problem, (iii) IWPCTM8's test cases[6] #2 (Rayleigh-Taylor) and #3 (Kelvin-Helmholtz) in 2D, (iv) 2D H_2/air reacting jet with detailed chemistry and variable transport coefficients (Figure 1).

*Laboratoire de Combustion et Systemes Reactifs, C.N.R.S., 1 C avenue de la Recherche Scientifique, 45071 Orleans cedex 2, FRANCE

[1] Fedioun et al., *Journal of Computational Physics* **174**, 1 (2001).
[2] Lardjane, *These de l'Universite d'Orleans* (2002).
[3] Shu, *ICASE Report*, **97-65** (1997).
[4] Balsara et al., *Journal of Computational Physics*, **160**, 405 (2000).
[5] Xu et al., *Journal of Computational Physics* **205**, 458 (2005).
[6] IWPCTM8's test problems; http://www.llnl.gov/iwpctm/html/test.htm

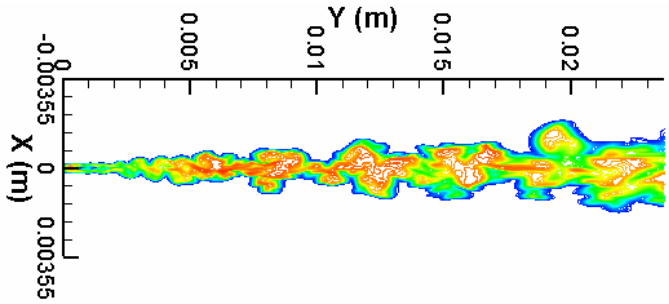

Figure 1: MILES of a subsonic H_2/air reacting jet: instantaneous contours of H_2O mass fraction.

Prediction of wall bounded flows using LES, DES and RANS

T. Persson[a], M. Liefvendahl[b], R.E. Bensow[a] and C. Fureby[a,b]

In the marine industry Computational Fluid Dynamics (CFD) is an important tool for resistance prediction and hull optimization, while methods for the simulation of propulsion, manoeuvring and cavitation are under development. These applications result in complicated unsteady flow fields and the codes used to solve these problems are often based on the Reynolds Average Navier-Stokes (RANS) equations[1]. Although RANS correctly models the mean flow in many cases, it often fails when facing more complex flows, or when applied to flows dominated by unsteady effects. Therefore it is important to investigate alternatives to RANS. The main candidates are Detached Eddy Simulation (DES)[2], and Large Eddy Simulation (LES)[3]. Both DES and LES are based on the idea of separating scales, splitting the flow into two regimes by which all scales larger than the grid are resolved using a space/time accurate algorithm, and only the effects of the subgrid scales on the large scales are modeled. The objective of this paper is to provide a systematic comparative study of DES, LES and RANS for three selected cases of particular interest. The first case consists of the fully developed turbulent channel flow at the friction velocity based Reynolds number (Re) of Re=395, 595, 1800 and 10,000, respectively. The second test case consists of the flow over a surface mounted axisymmetric hill at Re=130,000[4]. The final test case of interest to this study consists of the flow past an axisymmetric hull with an elliptic forebody and a smoothly tapered stern – the DARPA Suboff model AFF-1[5]. The computational results, in particularly for the axisymmetric hill, show that the LES and DES models give better agreement, with the experiments for the time-averaged data, than RANS.

---

[a] Chalmers, Shipping and Marine Technology, SE-412 96 Göteborg, Sweden.

[b] FOI, Div. of Weapons & Protection, Warheads & Propulsion, SE-147 25 Tumba, Sweden.

[1] Wilcox, D.C. (1993) DCW Industries

[2] Spalart P.R. *et al.* (1997) 1st AFSOR Int. Conf. On DNS/LES, Greyden Press, Columbus Oh.

[3] Sagaut P. (2001) Springer Verlag.

[4] Simpson R.L., Long C.H. & Byun G. (2002) Int. J. Heat & Fluid Flow, **23**, p 582.

[5] Huang T.T., Liu H-L., Groves N.C., Forlini T.J., Blanton J. & Gowing S. (1992) Proc. 19th Symp. on Naval Hydrodynamics, Seoul, Korea.

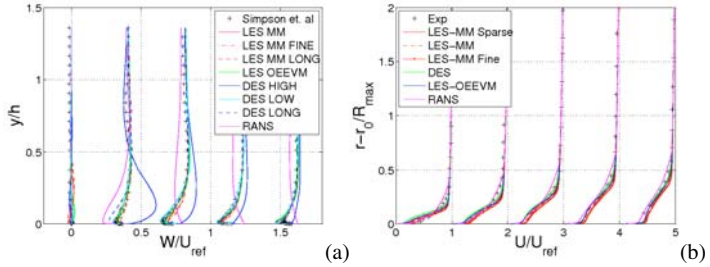

Figure 1: (a) Cross-stream velocity profiles in the wake of the axisymmetric hill and (b) stream-wise velocity components in the DARPA Suboff AFF-1 case.

Large eddy simulation of the turbulent field in a channel with oscillating walls

D. Tordella*, P.R.Bailey†, M. Iovieno*

Large eddy simulation of the incompressible Navier-Stokes field are employed to study the turbulent stresses in a channel flow forced by longitudinal sinusoidal oscillations of the walls, which is a kind of flow forcing not yet considered in literature. The two walls move in phase. The aim is the production of a friction reduction database which can be associated to the spanwise wall oscillation data base, which gathers numerical and laboratory results[1]. The calculations are performed at a Reynolds number $Re_\tau = 590$, based on the friction velocity u_τ of the unforced case, and on h, half the channel width. In this condition, we compute a maximum drag reduction of 12% for a dimensionless oscillation period of about half viscous units, $T^+ = Tu_\tau/h \approx 0.5$, and an amplitude equal to the friction velocity.

The instantaneous wall boundary conditions we recently proposed for resolved large scale simulations that extend inside the viscous sublayer are used[2]. These conditions transfer the physical no-slip and impermeability conditions, which can only be rigorously applied to the unfiltered variables, to the filtered variables. Since the filter scale close to the wall is increasing with the distance from the wall, this bondaury condition is used together with the explicit noncommutation procedure[3]. The subgrid turbulence model employed is the differential Intrinsic Angular Momentum model[4], which, being based on the representation of the turbulent viscosity through a vectorial quantity – the moment of momentum vector – may reproduce the anisotropic non-equilibrium near wall turbulence. The wall function model is not employed. A comparison with both experimental and numerical spanwise oscillation results will be given.

*Politecnico di Torino, DIASP, Cso Duca Abruzzi 24, 10129 Torino, Italy.
†Politecnico di Torino, Scuola di Dottorato, Cso Duca Abruzzi 24, 10129 Torino, Italy.

[1] see e.g. Iuso et al., *Phys. Fluids* **15**, 9 (2003), Quadrio and Ricco, *J. Fluid Mech.* **521**, 251 (2004)
[2] Iovieno et al., *Phys. Fluids* **16**, 10 (2004)
[3] Iovieno and Tordella, *Phys. Fluids* **15**, 7 (2003)
[4] Iovieno and Tordella, *Phys. Fluids* **14**, 2673 (2002)

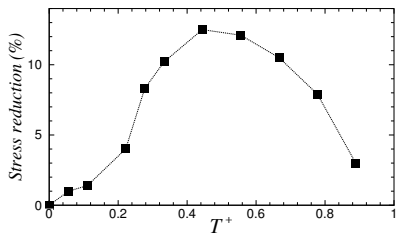

Figure 1: Stress reduction (L^∞ norm) as function of the dimensionless period.

Uncertainty Quantification in Large-Eddy Simulation

J. Ko*, D. Lucor* and P. Sagaut*

We present a recent path of research that attempts to model from first principles the various uncertainties associated with the numerical simulations of turbulent flows. Computational fluid dynamics (CFD) simulations such as Large-Eddy simulations (LES) have reached some degree of maturity today, but the new question is how to construct simulation error bars that reflect the uncertainties associated with the physical problem, in addition to those associated with the usual numerical inaccuracies due to the subgrid modeling and the numerical scheme.

In our approach, the quantification and propagation of the uncertainty in the system is captured spectrally by the generalized Polynomial Chaos functionals[1]. This method allows for random inputs with gaussian or non-gaussian distributions; the choice of the optimal functional depending on the type of random distribution considered. The stochastic algorithm is efficiently coupled to a deterministic parallel LES solver. An *intrusive* approach, where the governing stochastic equations are formulated by employing Galerkin projections, is presented. This leads to a coupled system of stochastic differential equations for the flow, a computationally prohibitive task at first glance. A *non-intrusive* approach, that does not required the modification of the deterministic LES solver, is also discussed. Both approaches are compared in terms of accuracy, efficiency and computational cost for different applications.

Those algorithms are applied to flow-structure interaction problems [2], decaying homogeneous isotropic turbulence and developing turbulent mixing layer subject to uncertainties. Comparisons with spectral stochastic DNS results are also presented. The isotropic turbulence case results are compared to a database of decaying homogeneous isotropic turbulence that was constructed including reference deterministic direct numerical simulations at two different Reynolds numbers and a large number of corresponding deterministic large-eddy simulations at various subgrid resolutions [3]. Errors in large-eddy simulation as a function of physical and numerical parameters (such as the Smagorinsky constant) are investigated. In particular, employing the Smagorinsky subgrid parametrization, the dependence of modeling and numerical errors on simulation parameters is quantified.

*Laboratoire de Modélisation en Mécanique, Université Pierre et Curie, Paris 75252, France.

[1] Ghanem and Spanos *Stochastic Finite Elements: A Spectral Approach* Springer, (1991).
[2] Lucor and Karniadakis *Phys. Rev. Lett.* **92**, 15 (2004).
[3] Meyers et al. *Phys. Fluids.* **15**, 9 (2003).

Large eddy simulation of impinging jets with focus on the inflow boundary conditions

T. Hällqvist *and L. Fuchs†

This paper deals with Large Eddy Simulation (LES) of submerged circular impinging jets. The main objective is to study the influence from the imposed inflow conditions. The outcome of a numerical simulation depends strongly on the discretization scheme, the computational grid and the type of modeling. However, in case of unsteady simulations the inlet velocity field may be just as important for the quality and relevance of the results. The benefits having an accurate scheme, a fine grid and a sophisticated SGS model may not be sufficient if not the appropriate inlet conditions are provided. In some applications, where the inflow is laminar or has limited influence on the region of interest, the simplest type of velocity data may be considered, i.e. a mean velocity profile with or without superimposed random perturbations. The major drawback with random perturbations is that there are no correlations in time or space. Furthermore, the energy distribution among the different scales is constant. The consequence is that the applied disturbances will quickly dissipate.

The most correct method is to use the velocity field from a precursor simulation. By doing this the correct correlations and spectrums are achieved. There are some drawbacks with this method though, namely the needed amount of storage capacity and the high cost for the precursor simulation. This method is also relatively inflexible as an additional calculation must be performed if modifications to the velocity field is wanted. Within the present work pipe flow simulations have been conducted with the prescribed Reynolds number, which is $Re_D = 20000$. The data from this simulation has then been supplied at the inlet of the impinging jet. The impinging jet has a nozzle-to-plate spacing (H/D) of 2 and 4 jet diameters. Results on mean velocities and mean scalar concentration as well as higher order statistics are presented for different type of inflow conditions (see figure 1).

*Scania CV AB, SE-151 87 Södertälje, Sweden.
†KTH Mechanics TR 8, SE-100 44 Stockholm, Sweden.

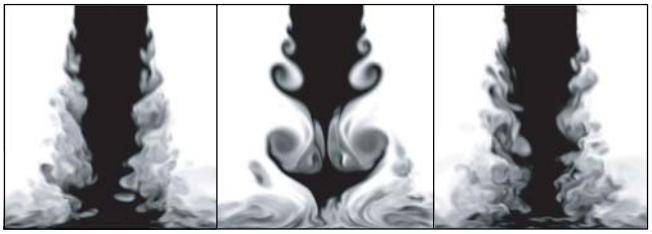

Figure 1: Influence from boundary conditions on the instantaneous scalar field for $H/D = 4$. Left picture: randomly perturbed top-hat profile, middle picture: randomly perturbed mollified profile, right picture: turbulent inflow conditions.

Stratified turbulence

G. Brethouwer*, P. Billant† and E. Lindborg*

Stratified fluids have been investigated in many theoretical, experimental and numerical studies owing to its importance for understanding geophysical flows. It remains a topic of dispute if the dynamics of stratified turbulence at low Froude number Fr (strong stratification) is essential two-dimensional with a inverse cascade of energy or three-dimensional with a forward cascade. The problem we are facing in laboratory and numerical experiments is that it is impossible to reach the same combination of Re (Re is the Reynolds number) and Fr as in geophysical flows. Stratified flows studied by laboratory and numerical experiments are perhaps not fully representful for the flows found outdoors.

When $Fr \ll 1$ and $ReFr^2 \gg 1$, analysis of the governing equations suggests the scaling $l_v \sim U/N$ for the vertical length scale l_v (U is a horizontal velocity scale and N is the Brunt Vaisala frequency) if the dynamics of the flow imposes the vertical length scale and not any other externally imposed condition [1]. Because of the sharp vertical gradients in stratified flows implied by this scaling, the advection terms involving the vertical velocity are of the same order as the other terms, although the vertical velocity is much smaller than the horizontal velocity, implying three-dimensional dynamics in strongly stratified fluids. Lindborg [2] adopted the scaling $l_v \sim U/N$ in his theoretical work which led him to the hypothesis of three-dimensional turbulence in strongly stratified fluids, but with a highly anisotropic forward cascade of energy. The scaling $l_v \sim U/N$ was confirmed by numerical simulations of strongly stratified fluids in very shallow boxes and computed transfer functions of spectral energy convincingly showed a forward cascade. The scaling $l_v \sim U/N$ exist only if $ReFr^2 \gg 1$. A different scaling exist if $ReFr^2 \ll 1$, a case which is often considered in laboratory experiments. Further analysis suggests that the dynamics is two-dimensional and strongly affected by viscosity if $ReFr^2 \ll 1$.

The aim of our study is to investigate systematically the influence of Re and F_h on the dynamics of strongly stratified fluids, in particular on turbulence, length scales and instabilities using and direct numerical simulations (DNS) and validate our scaling analysis with the DNS. In this way, we want to contribute to a better understanding and a clearer interpretation of the dynamics of strongly stratified fluids. DNS of homogeneous turbulence with a linear stratification are carried out. Energy is injected at the large scales by means of a forcing technique. Consequently, the flow attains a statistical stationary state. A series of DNS is performed at a fixed Re and with varying Fr at the moment with resolutions up to $1024 \times 1024 \times 192$ grid points. The parameters will be chosen so that both regimes, $ReFr^2 > 1$ but and $ReFr^2 < 1$, are covered by the DNS. Preliminary results reveal the existence of anisotropic three-dimensional turbulence with a forward cascade of energy if $ReFr^2 > 1$ and viscously dominated, predominantly horizontal turbulence with large pancake-like structures and with almost no overturning of the density field if $ReFr^2 < 1$.

*KTH Mechanics OB 18, SE-100 44 Stockholm, Sweden.
†LadHyX, Ecole Polytechnique, F-91128 Palaiseau Cedex, France.

[1] Billant & Chomaz *Phys. Fluids* **13**, 1645 (2001).
[2] Lindborg, *J. Fluid Mech.*, In press

Beta-plane turbulence in a basin with no-slip boundaries

W. Kramer*, H.J.H. Clercx* and G.J.F. van Heijst*

On a domain enclosed by no-slip boundaries, two-dimensional, geostrophic flows have been studied by numerical simulations of the Navier-Stokes equation with the beta-plane approximation at intermediate Reynolds numbers and a range of values for beta[1]. While most of the results are in agreement with other studies which use different boundary conditions, some aspects show a different and unexpected behavior. Without the beta-plane the flow is characterized by the formation of a single domain-sized coherent vortex due to the inverse energy cascade. From the simulations with the presence of the beta-effect it can be observed that the inverse cascade is clearly impeded by the presence of a beta-plane. This leads to a refinement of the flow structures (Figure 1a), which scales are in agreement with the Rhines scale. When the growing flow scales reach sizes comparable with the Rhines scale, the beta-effect becomes dynamically more important than advection and, consequently, the Rossby wave mechanism takes over from the inverse cascade. The arrest of the inverse cascade is visible as a plateau for wave numbers smaller than the Rhines wave number (Figure 1b). On a closed domain Rossby waves are described by basin modes, which are solutions of the inviscid flow equation on a bounded domain with free-slip boundaries. Frequency spectra of the flow profoundly exhibit the existence of basin modes, which excitation is favoured above the formation of vortices. The presence and apparent stability of basin modes on a domain with no-slip boundaries is a rather surprising observation, because these modes are solutions of the inviscid equations. The time-mean flow in forced simulations shows a zonal band structure (Figure 1c) which resembles the flow on a periodic domain (although the kinetic energy of the mean flow represents only 2-4% of the kinetic energy of the turbulent flow field itself). This a rather surprising result as numerous other simulations show a mean flow consisting of a dual gyre on a closed domain. The difference can be subscribed solely to the applied no-slip boundary conditions.

*Fluid Dynamics Laboratory, Eindhoven University of Technology, The Netherlands.

[1] W. Kramer et al., *Phys. Fluids*, accepted for publication.

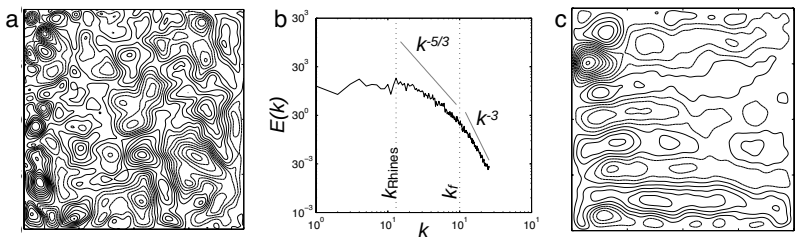

Figure 1: The stream function for the time dependent flow field (a) the 1D Chebyshev spectrum of the kinetic energy (b) and the time averaged stream function (c) .

Investigations of turbulence statistics in the laboratory model of an atmospheric cloud

P. M. Korczyk[a], F. Lusseyran[b], T. A. Kowalewski[a], Sz. P. Malinowski[c]

Interaction between small-scale turbulence and cloud particles is a key issue in warm rain formation mechanism, which is an important meteorological and climatological challenge[1,2]. We investigate this interaction observing motion of cloud droplets in a glass walled chamber 1m deep, 1m wide and 1.8m high, described elsewhere[3]. Cloudy air containing water droplets enters the main chamber forming the negatively buoyant, turbulent plume, mixing with unsaturated air in the main chamber and producing additional turbulence by evaporative cooling of droplets. The plume is illuminated with a 1.2mm thick sheet of laser light, forming the vertical cross-section through the central part of the chamber. Images of flow are recorded by a high-resolution CCD cameras placed outside the chamber.

Long sequences of images are collected to evaluate small scale turbulence statistics of the flow. The spatial flow characteristics are obtained using two- and three-component (Stereo-PIV) setup and double pulsed 35mJ Nd:YAG laser. The setup permits to record only few image pairs per second. Therefore, for temporal turbulence statistics long sequences of images (1000 and more) are acquired using high-speed CCD camera (PCO1200HS) and CW 5W Argon laser for illumination.

Droplets visualized in the chamber differ from typical PIV images with uniformly distributed tracers. Chaotic dynamics of mixing observed in the experiments makes images of flow complex and not easy to process. Therefore, standard PIV algorithms have to be used with care to avoid artefacts in the velocity field. Four different PIV evaluation methods are applied and tested on our experimental data: ILA OFS PIV algorithm[4], two *in house* developed multi-scale dynamic widow and image deformation based PIV codes, and Optical Flow evaluation method[5]. Statistical quantities and decompositions of vector fields are evaluated to check advantages of different evaluation methods. It was found that image deformation approach and in some sense equivalent Optical Flow methodology are the most reliable for our purpose.

The retrieved turbulence statistics exhibit significant anisotropy in accordance with preliminary numerical findings[6]. Three components PIV measurements confirm enhanced fluctuation amplitude for vertical velocity component. An attempt is made to correlate droplets distribution statistics and the measured velocity fields.

---

[a] IPPT PAN, Department of Mechanics & Physics of Fluids, PL 00-049 Warszawa, Poland.
[b] LIMSI-CNRS, 91403 Orsay, France.
[c] Warsaw University, Institute of Geophysics, Warszawa, Poland.

[1] Vailancourt and Yau, *Bull. Am. Meteorol. Soc.* 81, 285 (2000).
[2] Shaw, *Annu. Rev. Fluid Mech.* 35, 183 (2003).
[3] Malinowski et al., *J. Atmos. Oceanic Technol.* 15, 1060 (1998).
[4] ILA GmbH Optical Flow Systems, Germany.
[5] Quenot et al., *Exp Fluids*, 25, 177 (1998).
[6] Andrejczuk et al., *J. Atmos Sci.*, 61, 1726 (2004).

Differential diffusion in stratified sheared turbulence

H. Hanazaki*

Dirrefential diffusion of a passive scalar and and an active scalar/density in stratified shear flow is considered when both the density and the passive scalar have a mean vertical gradient. Extending the solution obtained by the rapid distortion theory for stratified sheared turbulence[1], vertical diffusion of the passive scalar (represented by eddy diffusivity coefficient $K_C = -\overline{cu_3}(t)/(dC/dx_3)$) and its difference from the vertical density diffusion K_ρ has been obtained. For inviscid flow, the results show a dependence on initial conditions similar to the unsheared stratified flow[2]. Namely, passive scalar flux $\overline{cu_3}$ has a 'slow mode' oscillating at the half frequency of the density flux $\overline{\rho u_3}$ only if there is initial potential energy due to density fluctuations ($PE_0 \neq 0$). Figure 1 shows the difference between the correlation coefficients of density ($R_{\rho 3}$) and passive scalar (R_{c3}) at the Richardson number of $Ri = N^2/S^2 = 1$ (N:Brunt-Vaisala frequency, $S = dU/dx_3$: mean vertical shear). This figure illustrates the 'period doubling' in the passive scalr flux due to the slow mode. In addition, we have found that there is another type of slow mode which exists only when the fluid is intrinsically viscous/diffusive (i.e., $Pr \neq Sc \neq 1$). This mode does not exist in the previous DNS where $Pr = Sc = 1$, but exists in the actual fluids, and explains the transient difference between K_C and K_ρ observed in the laboratory experiments. We will show how the molecular diffusion and the initial conditions lead to the difference in the turbulent fluxes of passive and active scalars, which are often assumed to be the same in many applications.

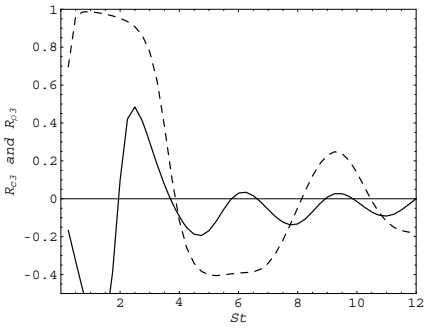

Figure 1: Time development of the correlation coefficients of density ($R_{\rho 3} = \overline{\rho u_3}/\rho' u_3'$: solid line) and passive scalar ($R_{c3} = \overline{cu_3}/c' u_3'$: dashed line) when the initial condition is the almost 'fossil' turbulence, i.e. $PE_0/KE_0 = 10000 (\gg 1)$ (PE_0: initial potential energy of turbulence due to density fluctuations, KE_0: initial kinetic energy). Time is scaled by the mean vertical shear S.

*Kyoto University, Kyoto 606-8501, Japan

[1]H. Hanazaki and J. C. R. Hunt, *J. Fluid Mech.* **507**, 1 (2004).

[2]H. Hanazaki, *Phys. Fluids* **15** , 841 (2003).

Coupling weather-scale flow with street scale computations

Zhengtong Xie* and Ian P. Castro*

Understanding the mechanisms by which the urban boundary layer and regional weather are coupled aerodynamically and thermodynamically is known to be vital but is still in its infancy. For the former, unsteadiness of a large scale (periodic) driving flow is known to have a significant impact on the turbulent flows[1]. One might anticipate similar effects in the urban boundary layer. For the latter, one could note that the temperature in cities has been found to be up to ten degrees higher than the surrounding rural areas and to cause large increases in rainfall amounts downwind[2]. In operational regional weather models the horizontal grid is no less than 1km, which eliminates most of the turbulent fluctuations. To investigate turbulent flows in an urban area down to a resolution one meter, small-scale computational fluid dynamics will inevitably have to be applied. Our objective is to develop tools for implementing unsteady spatial boundary conditions derived from the output of much larger-scale computations (UK Met Office's Unified Model) with a large-eddy simulation code for computing the street-scale flow. Flow over groups of cubes mounted on a wall provides an excellent test case for validation of LES. In order to avoid massive precursor computation, an efficient quasi-steady inlet condition has been developed and implemented with carefully designed artificially imposed turbulence fluctuations with prescribed integral length scales and intensities.

As an initial validation for unsteady large-scale driving flow, oscillatory throughflow over cube arrays was simulated, imposing quasi-steady inlet conditions. It was assumed that at the inlet the turbulent fluctuations, e.g. u_{rms}, v_{rms} and w_{rms}, are in phase with the mean streamwise velocity. Figure 1 is a typical plot, showing velocities sampled at the height $2h$ (h is cube height). The talk will provide more details and describe how more realistic unsteady large-scale driving flows (obtained from UM code) are being implemented.

*School of Engineering Sciences, University of Southampton, Southampton SO17 1BJ, UK.

[1]Sleath J.F.A, *J. Fluid Mech.* **182**, 369-409 (1987)

[2]Collier C.G. *RMetS Conf., Exeter* (2005)

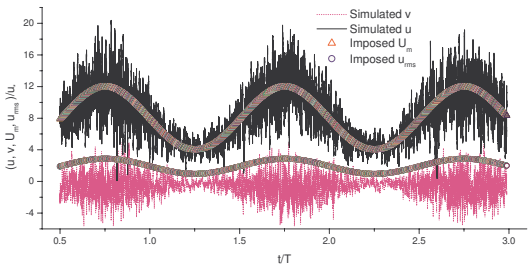

Figure 1: Times series of simulated streamwise and vertical velocities, and the imposed mean velocity and velocity $r.m.s$ at inlet. T, time period; u_*, friction velocity.

Mesoscopic Modelling of a two phase flow in presence of the boundaries

M. Sbragaglia*, L. Biferale†, R. Benzi † and S.Succi ‡

We present a mesoscopic model, based on the Lattice Boltzmann Equations [1], for the interaction between a solid wall and a non-ideal fluid. We study the dependency of the wetting properties on the free parameters of the model, i.e. the equivalent of the wall density and of the wall-fluid potential in Molecular Dynamics studies. We compare our model with some exact results based on the Navier-Stokes equations for a single-phase fluid with suitable boundary conditions [2][3]. Finally, the onset of dewetting transitions [4] on micro-corrugated surfaces is investigated.
The robustness of this approach over a wide range of scales, makes it a suitable tool to investigate various boundary condition problems including capillary effects coupled to rough surfaces and non-slip boundary conditions.

*Department of Applied Physics, University of Twente, 7500 AE Enschede, The Netherlands
†Department of Physics, University of Rome 'Tor Vergata', I-00133 Rome, Italy
‡Istituto per le applicazioni del calcolo CNR-IAC, I-00161 Rome, Italy
[1]Chen et al., *Annu. Rev. Fluid. Mech.* **30**, 329 (1998)
[2]Lauga et al, *J. Fluid. Mech.* **489**, 55 (2003)
[3]Philip, *Z. Angew. Math. Phys.* **23**, 353 (1972)
[4]Cottin-Bizonne et al. *Nature Materials* **2**, 237 (2003)

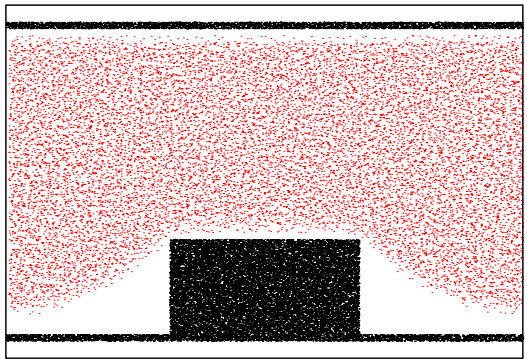

Figure 1: Onset of dewetting transitions in a Lattice Boltzmann Model. The critical interplay between a rough surface (black) and surface tension effects produce a dewetted state with gas pockets (white) on which the liquid (red) can slide producing enhancement of the effective slip properties.

Flow Separation from a Free Surface Dominated By Surface Tension

I. R. Williams*

An experiment is currently underway where the flow past capillary surface profiles is investigated. The range of surface shapes that are possible is of considerable interest. The experiment consists of a fully wetted upper reservoir with an adjustable aperture at its base. The aperture can be circular or linear. Fluid falls a distance of the order of the capillary length (4mm) into a lower reservoir. The Reynolds number, aperture size and jet length are varied. Profiles are possible where high surface curvature occurs or where thickness of the jet becomes of the order of the viscous length scale. Numerical results for the flow past the same two-dimensional surface profiles are calculated using the adaptive mesh refinement Navier-Stokes solver.

Boundary layer theory has mainly found application for flow past no-slip surfaces with very little attention being given to free-surface problems. Early work by Moore[1]. and Harper[2] looked at boundary layer flow past ellipsoidal bubbles and showed that the flow can detach from the surface of the bubble if the aspect ratio is sufficient. More recent numerical work (see Magnaudet and Eames review[3]) confirms flow separation from bubbles and shows that separation only occurs for a certain range of Reynolds number. This experiment aims to provide further details of flow separation from free surfaces. Also, by using an adaptive mesh Navier-Stokes solver[4], details of the boundary layer can be resolved within reasonable computational time.

*Department of Mathematics, University of Bristol, U.K.

[1]D.W.Moore, *J. Fluid Mech.* **23**, 749-766 (1965).
[2]J.F.Harper, *Adv. Appl. Mech* **12**, 59-129 (1972).
[3]Magnaudet and Eames, *Annu. Rev. Fluid Mech.* **32**, 659-708 (2000).
[4]Popinet, *J. Comput. Phys.* **190**, 572-600 (2003).

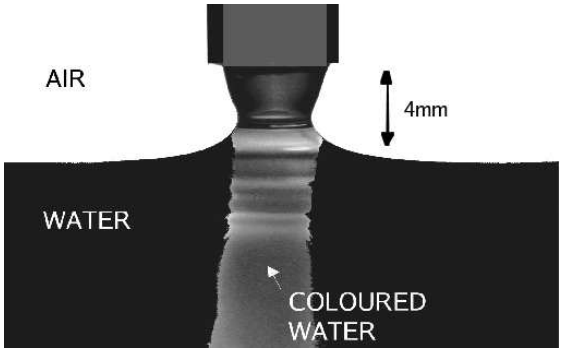

Figure 1: Photograph from a preliminary experiment showing flow separation from an axi-symmetric surface profile. Reynolds Number 300, Weber Number 0.5

Dynamic wetting transition: avoided critical behavior

G. Delon*, J.H. Snoeijer*, B. Andreotti* and M. Fermigier*

A solid surface can be coated by a thin film when the solid is withdrawn at constant speed out of a bath of liquid. This dip coating process was analyzed initially by Landau-Levich.

In a partial wetting situation, there is a threshold velocity below which the meniscus is steady and the solid remains dry. We investigate the dynamic wetting transition between the two states : at low velocity, a stable meniscus, at high velocity, an entrained film.

It has been shown that a receding contact line becomes unstable when the capillary number exceeds a critical value Ca_c [1]. In our experiments, liquid entrainment occurs at a capillary number Ca^* which is lower than Ca_c. The critical behavior expected at Ca_c is thus avoided. The threshold velocity coincides precisely with the contact line velocity above the transition. We explain the occurence of an early transition by the nucleation of a a capillary ridge (see fig.) which moves ahead of the thin film. The characteristics of this ridge determine the threshold velocity for liquid entrainment.

We discuss also the influence of the curvature of the solid surface on the wetting transition.

*PMMH,ESPCI, 10 rue Vauquelin, 75005 Paris, France.

[1] J. Eggers *Phys. Fluids* **17**, 082106 (2005).

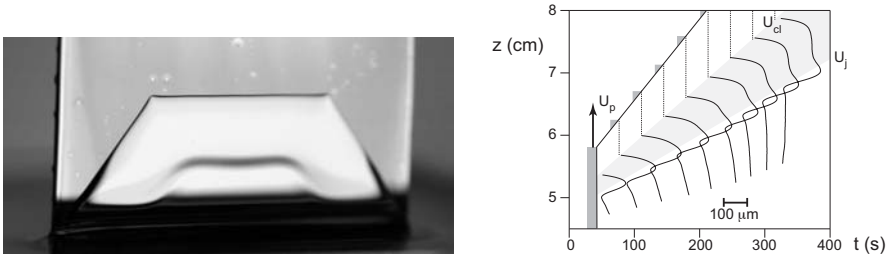

Figure 1: (Left) Liquid film (brighter part) entrained by a vertical plate pulled out of bath of silicone oil. (Right) Time evolution of the ridge profile (vertical cross sections in the middle of the liquid film. The three oblique lines in this space-time diagram represent the velocity of the solid plate, the velocity of the contact line and the velocity of the front between ridge and thin film.

Phase-Field Simulations of Free Boundary Flows

W. Villanueva*, and G. Amberg†

In this talk we present numerical simulations of free boundary flows using the phase-field method. We model the interface separating two different phases to have a finite thickness. The dynamics of the interface are governed by the convective Cahn-Hilliard equation which is coupled with the Navier-Stokes equations for the fluid motion with added surface tension forcing and forces due to gravity. A dimensionless system is derived and dimensionless parameters are identified, namely the Reynolds number, Capillary number, Bond number, Peclet number, equilibrium contact angle and the Cahn number.

Two types of problems are tackled: capillary-driven flows such as the wetting of a drop on a solid surface, sintering-like flows and imbibition, and second, the deposition of microdroplets under a liquid medium. In the capillary-driven flows, surface tension forces dominate and the effect of gravity can be neglected. With the basic wetting of a liquid drop on a solid surface, we found that the dynamic contact angle is fairly independent of the interface thickness. Moreover, the dependence of the dynamic contact angle on the Capillary number agrees favorably with known experimental data. Next, the model is applied to generic sintering-like flows where an aggregate of immobile solid particles and liquid drops are considered. The drops soften and rapidly wets the solid surfaces, see Figure 1. Important microstructural features of the actual liquid phase sintering such as precursor films, coalescences, breakups, pore movement and pore elimination are observed. The model is also applied to microstructural imbibition of a liquid under a porous medium. The amount of liquid imbibed into the porous medium depends on the equilibrium contact angle of the liquid on the solid surface and the pore channel's topological configuration.

The other problem of interest is the investigation of the factors affecting reproducibility of depositing microdroplets on a cylindrical anchor under a liquid medium. Experimental investigation has been carried out by J. Sjödahl, M. Kempka, J. Roeraade, of the Analytical Chemistry, KTH. We found that the volume deposited is affected by the height at which to deposit the droplets, the wetting properties of the system and the aspect ratio between the diameters of the anchor and the capillary tube that is used to deposit the droplets.

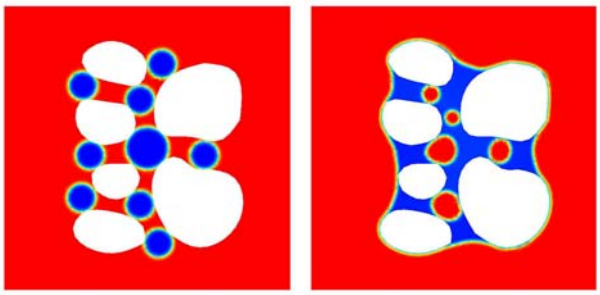

Figure 1: Generic sintering flow with a fixed matrix. Concentration field at $t = 0, 500$.

*KTH Mechanics OB 18, SE-100 44 Stockholm, Sweden.
†KTH Mechanics OB 18, SE-100 44 Stockholm, Sweden.

Error Estimation and Application of Different Volume of Fluid Implementations for Non-Newtonian Flows with Free Surfaces

A. Rudert*, R. Schwarze*, F. Obermeier*

Injection molding is an important processing technology for very different types of molding materials. Systematic improvements of the injection process are developed in model experiments and with numerical simulations. Therefore it is important to have efficient numerical models in order to describe the transient flow in the mold. Characteristic features of this flow are (i) a free surface is formed by the molding materials and (ii) the molding materials obey a non-Newtonian law of viscosity. In this paper, the injection of a Herschel-Bulkley fluid into a cavity is investigated. This problem demonstrates the same features which are characteristic for the injection molding. Model experiments of the injection process are performed with the fluid. The surface of the fluid within the cavity is mapped out in order to visualize the filling process. Filling times are deduced from several experimental observations and corresponding numerical simulations.

The numerical model is based on the finite-volume-method. The Volume of Fluid method is employed in order to describe the free surface flow of two incompressible phases. The interface between the phases is resolved by various methods. The governing equations of the flow are solved with different commercial and Open Source CFD packages on corresponding grids and with identical boundary conditions to estimate the efficiency and accuracy of the surface capturing methods. The results are compared to experimental data.

This comparison shows good agreement between the different surface capturing methods and the experiment in the filling time. Shapes and the position of the free surfaces are qualitatively comparable but vary to a certain extent, see figure 1. Though the numerical resolution of the free surface varies only slightly between the different methods, there are considerable differences in the computation time. In order to estimate the discretization error of both codes and the order of the different numerical schemes a method proposed by Perić and Ferziger [1] is used. Since the schemes differ only in the way the free surface is captured it is possible to decide which method is the more accurate one.

*Institut für Mechanik und Fluiddynamik, Technische Universität Bergakademie Freiberg, Lampadiusstr. 2, 09596 Freiberg

[1] Perić M. and Ferziger J. H. (2002) *Computational Methods for Fluid Dynamics* (Heidelberg: Springer-Verlag)

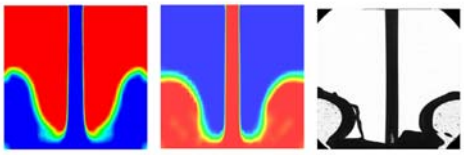

Figure 1: Phase distribution at the same time in first two from different numerical models and experiment.

Evaluation of a universal transitional resistance diagram for pipes with honed surfaces

J.J. Allen[a], M.A. Shockling[b] and A.J. Smits[b]

A method for evaluating a universal transitional resistance diagram for pipes that relates the pressure drop in the pipe to Reynolds number, as a function of relative surface roughness, is presented. The method assumes a universal wake function coupled with a logarithmic overlap region and a power fit in the viscous and buffer layer. Estimates can be made of the friction factor-Reynolds number relationship for arbitrary relative roughness. The method is illustrated for a pipe with a honed surface finish. The size of the non-dimensional velocity shift as a function of roughness Reynolds number comes from the honed pipe data of Shockling[1] which had a ratio of pipe diameter to roughness height of $40x10^3$. Honed roughness demonstrates an inflectional behavior in the transitionally rough regime, much like sandgrain roughness[2], but the method proposed here applies to any given roughness behavior. Figure 1(a) shows a compliation of mean velocity profiles from[1] over the Reynolds number range $57x10^3$ - $21x10^6$ and figure 1(b) shows the associated friction factor-Reynolds number relationship for this surface and predictions for a series of geometrically similar surfaces.

It is also suggested that the critical parameter that determines whether the resistance diagram for a honed pipe shows inflectional characteristics is the relative roughness, that is, the ratio of roughness height to outer layer scale. Based on analysis of data from previous researchers it is suggested that if the relative surface roughness k_{RMS}/D <0.005, where k_{RMS} is the RMS amplitude of the roughness and D is the pipe diameter, then inflectional relationships should be observed.

---

[a] Department of Mechanical Engineering, New Mexico State University, NM, USA..

[b] Department of Mechanical and Aerospace Engineering, Princeton University, NJ, USA.

[1] Shockling M.A. Shockling, *MSE Dissertation, Princeton University*, (2005).

[2] Nikuradse, *VDI Forschungsheft*, **361**, (1933).

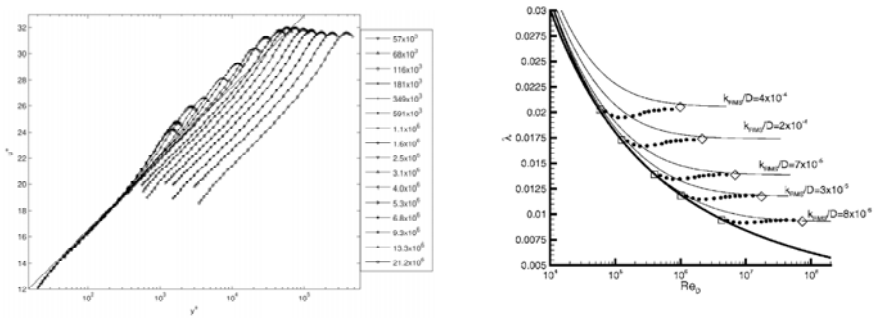

Figure 1: (a) Mean velocity profiles (b) Friction factor–Reynolds number results and predictions.

A general asymptotic description of turbulent boundary layers

B. Scheichl *, A. Kluwick*

A comprehensive rational theory of incompressible nominally steady and two-dimensional turbulent boundary layers (TBLs) is developed by adopting a minimum of assumptions regarding the flow physics and properly investigating the Reynolds-averaged equations of motion in the limit of high Reynolds number, denoted by Re. The logarithmic law of the wall is established and shown to be associated with an asymptotically small rotational streamwise velocity defect with respect to the external potential bulk flow on top of the viscous wall layer. Consequently, the classical scaling of two-tiered TBLs provides the simplest feasible flow structure. It is, however, possible to extend this concept and to formulate a three-tiered splitting of TBLs having a slightly larger, i.e. a 'moderately' large, velocity defect. This allows for, amongst others, the prediction of the in previous studies intensely discussed phenomenon of non-unique equilibrium flows for a prescribed pressure gradient[1].

Most important, it is observed that all commonly employed closures contain small numbers which are seen to be independent of Re and may serve as a perturbation parameter measuring the slenderness of the shear layer. Exploiting this characteristic finally leads to a fully self-consistent asymptotic description of TBLs which exhibit a velocity defect of $O(1)$ and a slip velocity of $O(1)$ at their bases by considering the formal limit $Re^{-1} = 0$. In turn, they closely resemble turbulent free shear layers and can even undergo marginal separation. This situation is accompanied by the occurrence of a weak singularity in the solutions of the boundary layer approximation. The analysis then reveals the necessity to adopt a viscous/inviscid interaction technique in order to capture the feedback of the pressure induced by the local boundary layer displacement in the external flow[2], also see figure 1. Additionally, we will outline, how the underlying asymptotic concept allows for further analytical and numerical progress and, amongst others, provides the adequate basis to tackle the extremely challenging problem of turbulent gross separation. First investigations indicate that, in contrast to the laminar case, here the Brillouin–Villat condition is not met.

*Institute of Fluid Mechanics and Heat Transfer, Vienna University of Technology, Resselgasse 3/E322, A-1040 Vienna, Austria.

[1]Scheichl and Kluwick, *Theor. Comput. Fluid Dyn.*, submitted in revised form.

[2]Scheichl and Kluwick, *AIAA paper 2005-4936* (2005).

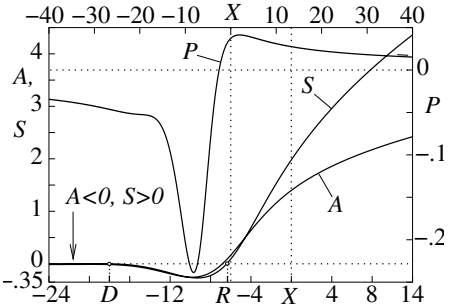

Figure 1: Typical solution of the interaction problem using suitably rescaled local variables: The streamwise coordinate and the locations of flow detach- and reattachment are denoted by X, D, and R, respectively. The top abscissa refers to the induced pressure P, the one at the bottom to the surface slip velocity S and the local boundary layer displacement $-A$.

Computations of turbulent boundary layers with streamwise and spanwise pressure gradients

A. Jammalamadaka[a], H. Nagib[a] and K. Chauhan[a]

The performance of four popular turbulence models, namely, Spalart-Allmaras, k-ε, SST and RSM, is evaluated for prediction of turbulent boundary layers subjected to streamwise and spanwise pressure gradients. The computations are made at one to one scale for a recently completed 2-D turbulent boundary layer experiment[1,2] and a previously measured 3-D turbulent boundary layer[3]. Both experiments were carefully documented with the aid of independent measurement of skin friction. The 2-D boundary layer comparisons are made for adverse (APG) and favorable pressure gradients with Re_θ in the range 10,000 to 50,000. The two-equation models fared better than the one-equation model when the mean velocity and skin friction coefficient are compared. Overall, the models fail to replicate the non-universal behavior of the Kármán *coefficient* κ, seen in experiments[1], although they exhibit considerable variation in it, as shown in Fig. 1(a). In the more complicated 3-D flow through an S-duct, with simultaneously varying streamwise and spanwise pressure gradients, the computations compare well for pressure gradient and skin-friction coefficients. However, the computations deviate significantly from the experiments where strong reversal of spanwise pressure gradient occurs and beyond; e.g., Fig 1(b). In both of these test cases, the Reynolds stress model suffers from lack of well-defined boundary conditions for $\overline{u_i u_j}$ resulting in poor agreement with experiments.

[a] Illinois Institute of Technology, Chicago, USA.

[1] Chauhan et al., Proceedings of iTi Conference on Turbulence, Germany, Sept. 2005.

[2] Nagib et al., IUTAM Symp., One Hundred Years of Boundary Layer Research, Germany, Aug. 2004.

[3] Bruns et al., *J. Fluid Mech.* **393**, 179, (1999).

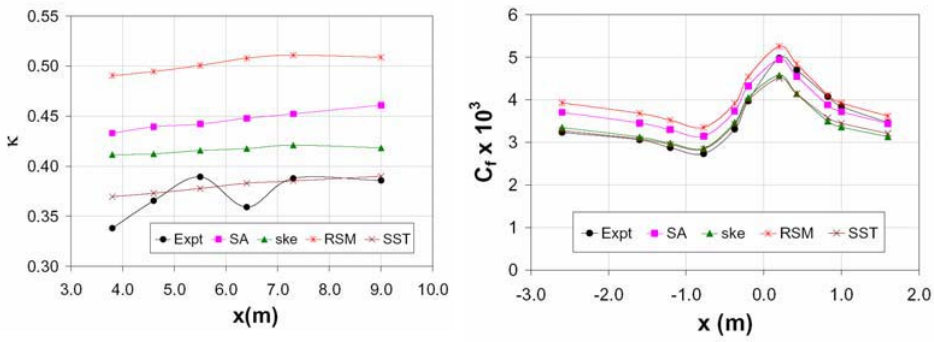

(a) (b)

Figure 1: (a) Downstream variation of κ in a 2D TBL (APG at U_{ref} = 40 m/s), and (b) Skin friction coefficient comparisons for 3D TBL.

Equilibrium boundary layers revisited

Y. Maciel[a]

The purpose of this presentation is to clarify some aspects of the similarity theory of the outer region of turbulent boundary layers (TBL), as well as concepts that are related to it, and to bring new ideas on the subject. The similarity analysis of the outer region of TBL is presented in a general form and in a manner which is consistent with the asymptotic theory for most pressure gradient conditions (assuming a two-region structure of the TBL). In this general form, the outer scales are not determined *a priori* and it is not assumed that the mean velocity defect and the three Reynolds stresses share a common velocity scale. This similarity analysis therefore encompasses all the various similarity analyses found in the literature. It is shown that in the limit of an infinite Reynolds number, the use of different scales for mean velocity defect and Reynolds stresses, as was done by Castillo and George[1], is unnecessary. In the asymptotic limit, the Reynolds normal stresses do not intervene, even in strong adverse-pressure-gradient (APG) flows, and self-similarity leads to a common velocity scale for the velocity defect and the Reynolds shear stress. The only necessary condition for self-similarity is, not surprisingly, a constant ratio of the turbulent and streamwise time scales.

At a finite Reynolds number, if multiple scales are assumed, then there exist five conditions for self-similarity. If a single turbulent velocity scale is assumed instead, then there exist three conditions for self-similarity at finite Reynolds number. These are two conditions on any two of the characteristic turbulent scales (length, time and velocity) and a corollary condition on the streamwise evolution of the freestream velocity. As a consequence of the multiple conditions necessary for self-similarity at a finite Reynolds number, turbulent boundary layers found in the real world are almost never in a state of equilibrium, although they might closely approach it, contrarily to what has been claimed in some recent papers.

It is also argued that the most appropriate turbulent (outer) velocity scale for all TBL is the Zagarola-Smits velocity and not the friction velocity or the freestream velocity for ZPG and mild PG and not the scales proposed by Mellor and Gibson[2] or Perry and Schofield[3] for strong APG. The ZS velocity scales correctly the mean velocity defect and all the Reynolds stresses in all pressure gradient and roughness conditions while all the other proposed scales do not. For ZPG and mild PG flow cases, if one accepts the ZS velocity as the turbulent velocity scale, then it should also be the inner velocity scale. Experimental evidence suggests that it is indeed a proper inner velocity scale for ZPG and mild PG flow cases, like the friction velocity. For strong APG flows, the ZS velocity cannot be used in the inner region and has to be replaced by the viscous/pressure-gradient velocity, $u_p = (-\nu U_e dU_e / dx)^{1/3}$.

---

[a] Mechanical Engineering Dept., Laval University, Quebec city, G1K 7P4, Canada.

1Castillo and George, *AIAA Journal*, **39**, 1 (2001).
2Mellor and Gibson, *J. Fluid Mech.*, **24**, 2 (1966).
3Perry and Schofield, *Phys. Fluids*, **16**, 12 (1973)

Flow Developments in Smooth Wall Circular Duct Facility

E.-S. Zanoun*, F. Durst†, C. Egbers*, L. Jehring*, and M. Kito*

The fully developed turbulent pipe flow represents the state of well-defined flow that has been the subject of numerous investigations of engineers and scientists interested in its basic properties and in understanding fully developed turbulence. Recently, a number of publications[1,2,3,4] resulted out of studies of fully developed turbulent pipe flows, yielding general conviction that the mean flow properties of this flow are fully understood. This is not the case, since a controversy discussion regarding the frictional loss and normalized form of the mean velocity distribution of fully-developed turbulent pipe flow still exists. For instance, it was pointed out[5] that many of the assumptions made in deriving the Moody Diagram as an engineering guide are not correct. The main aim of the present paper is therefore to provide a good basis for assessing questions regarding turbulent flow development length of the mean and fluctuating velocities as well as frictional loss along a smooth pipe flow test section. A new circular duct test rig is therefore setup at the Department of Fluid Mechanics and Aerodynamics (LAS) of BTU Cottbus to investigate the fully developed turbulent pipe flows at relatively high Reynolds number ($\mathrm{Re_m}$). The research program is designed mainly into two different phases. Phase I covers the application of some advanced measuring techniques for better understanding and quantitatively evaluating the mean flow characteristics and turbulence statistics for $\mathrm{Re_m} \leq 6 \times 10^5$. For the sake of comparison against the most recent pipe flow data from different experiments, the second phase focuses on extending the Reynolds number range to $\mathrm{Re_m} \leq 1.2 \times 10^6$. In addition, the results obtained from Phase I and Phase II are used to validate some recently developed theoretical investigations [6,7,8].

*LAS BTU Cottbus, Siemens-Halske-Ring 14, 03044-Cottbus, Germany.
†LSTM Erlangen, Cauerstr. 4, D-91058 Erlangen, Germany.

[1]Barenblatt, *J. Fluid Mech.* **248**, 513 (1993).
[2]Zagarola & Smits, *J. Fluid Mech.* **373**, 33 (1998).
[3]Wei et al. *J. Fluid Mech.* **482**, 51 (2005).
[4]Zanoun et al., *HEFAT* (2005).
[5]Smits, *Midwest Mechanics Seminar Series* (2005-2006).
[6]Wosnik et al. *J. Fluid Mech.*, **421**, 115 (2000).
[7]Oberlack, *J. Fluid Mech.*, **299**, 51 (2001).
[8]Monkewtiz & Nagib, *IUTAM* (2004).

Secondary Flow Measurement of an Outlet Guide Vane Cascade at Low and High Inlet Turbulence Intensities

S. Kennedy[a], V. Chernoray[b], J. Hjärne[b]

The aim of this project is to investigate the secondary flow pattern downstream of a low pressure turbine/outlet guide vane (LPT/OGV) cascade. These vanes are found downstream of the low pressure turbine in turbojet engines, and are responsible for turning the inlet swirling flow from the low pressure turbine into an axial outflow, whilst minimising pressure losses. This is of prime importance with both cost and weight being reduced in modern turbojets resulting in a reduced amount of stages in the LPT which in turn increases the loading on the OGV's.

The experiments were carried out at Chalmers in Sweden, using a low speed linear cascade. This paper presents the experimental results carried out using a cross wire probe at various downstream positions at 30 degrees inlet flow angle, which is the on-design point. Both low and high turbulence intensity cases have been investigated at one Reynolds number. As shown in figures 1a and 1b, the main characteristics of the flow include the passage vortex, the trailing edge vortex sheet and the boundary layer on the sidewall. The results also show the interaction of these structures and how they evolve as they move downstream. The effect of increased turbulence will be seen to play an important role in the diffusion of the vortical structures as well as their interactions. These findings are then related to the main flow characteristics, including velocity, pitch angle, losses, turbulence intensity and Reynolds stresses. This will result in an understanding of the significance of the secondary flows and how they affect the efficiency of turning the flow. The results from the cross wire probe will also be compared to those obtained from an earlier investigation using a five hole probe.

[a] Queens University of Belfast, Aeronautical Engineering, BT9 5AG Belfast, N. Ireland.
[b] Chalmers University of Technology, Applied Mechanics, SE-412 96 Göteborg, Sweden.

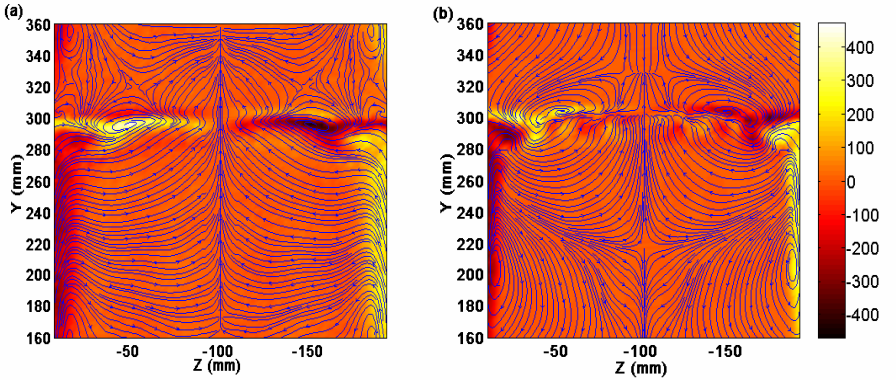

Figure 1: Streamwise vorticity distribution with superimposed streamlines in *yz* plane downstream of the mid vane of the cascade (a) at 5% turbulence intensity (Tu) and (b) at 0.5% Tu.

Super-late stages of boundary-layer transition and deterministic post-transitional turbulence

V. I. Borodulin[a], Y. S. Kachanov[a] and A. P. Roschektayev[a]

The paper is devoted to an experimental study of super-late stages of laminar-turbulent transition in a boundary layer with a streamwise adverse pressure gradient with Hartree parameter $\beta_H = -0.115$. The experiments were performed at controlled disturbance conditions in a low-turbulence wind-tunnel T-324 of ITAM SB RAS. The measurements were carried out by means of a hot-wire anemometer in a broad spatial region starting with stages of small-amplitude instability waves, developing in the laminar boundary layer, and ending with the post-transitional turbulent flow. The 'deterministic noise' method and a universal disturbance source of instability waves[1] were used in these experiments to excite the flow. The transition was initiated by a mixture of a quasi-2D Tollmien-Schlichting (TS) wave and 3D broadband perturbations (a "noise" of TS-waves). The broadband perturbations were random within 20 periods of the fundamental TS-wave but then repeated periodically at very large time scales, during which the flow passed the model several times. Thus, the "noise" was random from the viewpoint of the flow but it was deterministic (even periodic) from the viewpoint of data processing giving us the possibility to perform ensemble averaging of hot-wire signals.

It is found that the instability waves leaded to transition with formation of characteristic vortical structures. Father downstream formation of post-transitional turbulent boundary layer was observed. At this stage the mean velocity profiles, the profiles of rms velocity fluctuations, and the disturbance spectra corresponded to those observed in developed turbulent boundary layers. At the same time it was found that the flow remained deterministic to a considerable degree. The coherence coefficient, determined as a ratio of the rms intensity of the ensemble-averaged (deterministic) and total (non-averaged) velocity fluctuations, remained very large even in the post-transitional flow (between 80 and 60%). This circumstance gave us the possibility to obtain instantaneous velocity and vorticity fields in the (x, y, z, t)-space and to perform a computer-aided, quantitative visualization of the instantaneous flow structure in the post-transitional turbulent boundary layer both in near-wall and in the outer region. It is found that the structures resemble very much the vortical structures found earlier at later stages of transition[2], as well as the coherent vortical structures observed in developed turbulent boundary layers. A conclusion is made that the post transitional turbulent flow is mainly deterministic and can be simulated (modeled) experimentally. Such model turbulence can possess all main average statistical properties characteristic of the wall turbulence but, simultaneously, the instantaneous structure of this turbulence can be deterministic and reproducible.

This work is supported by Russian Foundation for Basic Research.

---

[a] Institute of Theoretical and Applied Mechanics of SB RAS, 630090, Novosibirsk, Russia.

[1] Borodulin et al., *Proc. Intl. Conf. Methods. Aerophysical. Research.* Novosibirsk: ITAM, Part **2**, 39 (1996).

[2] Borodulin et al. *Thermophysics and Aeromechanics*. **10**, 1 (2003).

Experimental and Theoretical Investigation into the Development of Turbulent Spots under Varying Pressure Gradient

D. M. Hernon[a], E. J. Walsh[a], D. M. McEligot[b]

Recent DNS studies on zero pressure gradient flow have elucidated the precursors to turbulent spot production; however, experimental and analytical techniques are not capable of reproducing such detailed results. The capability of DNS to trace back in time to the exact initiation of a turbulent spot can not be achieved in practice. Therefore, in order to gain a similar level of insight into the transition process the experimenter has to take a considered approach to the methodology of testing. Furthermore, within the literature little information exists on the generation of turbulent spots in both positive and adverse pressure gradients.

It is postulated that negative spikes observed in the outer portion of the boundary layer, Fig. 1 at $y/\delta=1$, are the receptivity sights where low speed streaks lift up and couple to high frequency disturbances from the freestream, see recent DNS results on the formation of negative jets[1,2]. A correlation between the frequency of the negative spikes upstream of transition onset in the outer layer and the development of the turbulent spots in the near wall region, Fig. 1 at $y/\delta=0.3$, is achieved for zero pressure gradient flow giving further insight into the transition process.

Variable pressure gradient and turbulence intensity is imposed on a flat plate on which a 32 element hotfilm array with 2.3mm element spacing is placed. The hotfilm array is located within the transition region. The objective of this experimental set-up is to gain further insight into the development of turbulent spots and spot production rates in both positive and adverse pressure gradients under the influence of varying freestream turbulence scales and intensity. Following this a theory relating the forcing frequencies in the freestream and boundary layer to the initiation of transition will be developed.

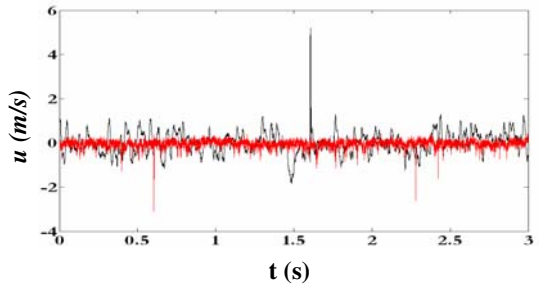

Figure 1. Perturbation velocity traces at transition onset, Re_θ=577 and %Tu=1.3. Black Line, $y/\delta=0.3$; Red line, $y/\delta=1$.

a Stokes Research Centre, University of Limerick, Ireland.

b Idaho National Laboratory (INL), Idaho Falls, Idaho 83415-3885, U.S.A.

1 Jacobs and Durbin, *J. Fluid Mech.* **428**, 185 (2001).

2 Brandt et al, *J. Fluid Mech.* **517**, 167 (2004).

Low-speed streaks developing at the laminar-turbulent interface of turbulent wedge

A. Inasawa[a], Y. Yokosawa[a] and M. Asai[a]

Development of low-speed streaks in lateral turbulent contamination in a flat plate boundary layer is examined experimentally by means of PIV and flow visualization. We focus on the lateral scale of low-speed streaks successively generated at both sides of turbulent wedge.

The experiment is conducted in a low turbulence wind tunnel with free-stream velocity 4 m/s, and turbulent wedge is generated by hairpin eddies introduced through a wall orifice[1]. Figure 1 illustrates the instantaneous streamwise velocity field near the wall, showing low-velocity streaks (black-coloured regions) inside the turbulent wedge. Figures 2(a) and (b) illustrate histograms of the lateral spacing of the low-speed streaks obtained from PIV data in the centre region and around the laminar-turbulent interface of turbulent wedge, respectively. In Fig. 2(a), the log-normal distribution, which is typical for the developed wall turbulence, is found with the mean spacing of 9mm (130 wall units). This value is slightly larger than the typical values (100 wall units) in the developed wall turbulence because the measurement is made in the buffer region. Around the laminar-turbulent interface, in Fig. 2(b), on the other hand, the histogram exhibits a sharp peak. Both the mean and the most-probable values are around 6 mm (85 wall units), which is smaller than the streak spacing in the centre region at this x-location. Interestingly, this value (85 wall units) is almost the same as the most-probable value in wall turbulence. Further details are presented at the conference.

[a] Tokyo Metropolitan Univ., 6-6 Asahigaoka, Hino, Tokyo, 191-0065, Japan

[1] Asai et al., *Fluid Dyn. Res.* **18**, 151 (1996).

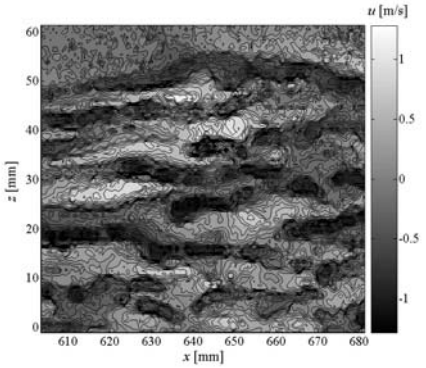

Fig. 1: Instantaneous streamwise velocity field at y = 2 mm ($yu_\tau/\nu \approx 30$). z = 0 is the spanwise centre of turbulent wedge.

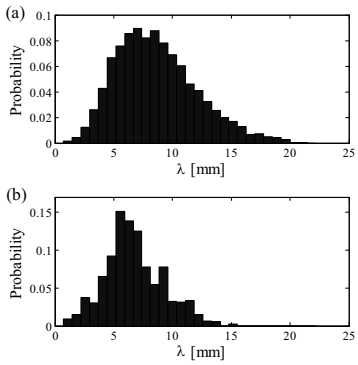

Fig. 2 : Histogram of streak spacing λ obtained from PIV data. (a) centre, (b) interface (x = 620 mm, y = 2 mm).

Large-Eddy Simulation of Bypass Transition

P. Schlatter*, L. Brandt* and D. S. Henningson*

In flat-plate boundary layers with ambient free-stream turbulence intesities above 1%, laminar-turbulent transition occurs rapidly, bypassing the classical scenario of exponentially growing TS waves. The former scenario, denoted bypass transition, is characterised by the appearance of streamwise elongated structures (streaks or Klebanoff modes) inside the boundary layer, which eventually undergo wavy motions and break down into turbulent spots. Detailed experimental data for bypass transition induced by free-stream turbulence are available due to several groups (e.g. Ref.[1]), however, only few fully-resolved direct numerical simulations (DNS) have been performed (e.g. Ref.[2]). These numerical studies are very expensive in terms of computational effort. Consequently, so far no detailed numerical parameter studies of important characteristics have been published, e.g. concerning the influence of both low (approx. 1%) and high ($\geq 6\%$) free-stream turbulence intensities.

In this paper, we focus on the applicability of large-eddy simulation (LES) to model the evolution and effect of the smallest transitional and turbulent spatial scales. LES requires only a fraction of the computational cost compared to DNS. The success of an LES is crucially dependent on the quality of the subgrid-scale (SGS) model, which are traditionally designed to produce accurate results in fully-developed turbulent flows, and their extension to transitional flows requires special care. Specifically, we apply the ADM-RT model[3] and the dynamic model[4] and compare their accuracy to DNS[2] and experimental data. Both of these models have been shown to be applicable to transitional flows, and, in particular, the ADM-RT was able to reproduce the dominant three-dimensional transitional vortical structures in forced transition[5]. However, the present case also requires to faithfully predict the receptivity of the boundary layer to the free-stream disturbances in addition to the streak breakdown.

The simulation results show that a no-model LES (i.e. a DNS without model at reduced spatial and temporal resolution) is not able to correctly predict neither statistical data nor the typical flow structures during breakdown. This is in agreement with Ref.[2] noticing that an accurate prediction of bypass transition requires very fine numerical resolution to correctly capture both receptivity and breakdown. On the other hand, applying the above mentioned SGS models a much more accurate prediction of important flow quantities is achieved. In particular, the ADM-RT model is able to reproduce the instability observed on the streaks prior to breakdown (varicose and sinuous instability). Moreover, statistical quantities during transition and in the turbulent boundary layer after breakdown are in very good agreement with DNS.

The final contribution will include parameter studies of several important quantities like the variation of the turbulence intensity and the influence of different energy spectra (integral length scales and shape) of the incoming free-stream turbulence.

*KTH Mechanics OB 18, SE-100 44 Stockholm, Sweden.

[1]Fransson et al., *J. Fluid Mech.* **527**, 1 (2005)
[2]Brandt et al., *J. Fluid Mech.* **517**, 167 (2004)
[3]Schlatter et al., *Int. J. Heat Fluid Flow* **25**, 3 (2004)
[4]Germano et al., *Phys. Fluids A* **3**, 7 (1991)
[5]Schlatter et al., *Laminar-Turbulent Transition*, Sixth IUTAM Symposium 2004, Bangalore, India

Direct Numerical Simulation of Laminar Heat Transfer to a Flat Plate affected by Free-Stream Fluctuations

J. G. Wissink*and W. Rodi*

Free-stream turbulence in incoming flow can influence strongly heat transfer to turbine blades. The physical mechanisms involved are only just beginning to be understood[1]. From experiments[2], we know that 1) the affected laminar boundary layer flow needs to be accelerating in order to observe a significant increase in "laminar" heat transfer - that is: the heat transfer in regions where the boundary layer is laminar - and 2) the increase in laminar heat transfer depends on the integral length scale of the incoming free-stream turbulence.

To further inverstigate this phenomenon, it was decided to perform a series of Direct Numerical Simulations (DNS) of an accelerating flat plate boundary layer flow with incoming free-stream turbulence. By varying both the Reynolds number Re and the integral length scale Λ of the free-stream turbulence, we aim to elucidate the physical mechanisms involved. The simulations are performed on the HP-XC1 cluster of the Scientific Supercomputing Centre in Karlsruhe (SSCK) using up to 64 processors and 135.8 Mio. grid points.

Figure 1(a) shows a cross-section of the computational domain. The contoured upper wall induces an accelerating boundary layer flow. At the inlet, free-stream turbulence ($Tu = 2.5\%$) - which stems from a separate simulation of isotropic turbulence in a box - is superposed on a Blasius velocity-profile. So far, two different Reynolds numbers, $Re = 100\,000$ and $Re = 200\,000$, both based on the free-stream inlet velocity u_e and the length-scale L - see Figure 1(a) - were employed. As shown in Figure 1(b), at $Re = 200\,000$, a significant increase in laminar heat transfer is obtained in the presence of free-stream turbulence with an integral length-scale of $\Lambda = 0.0830L$. A similar figure (not shown here) at $Re = 100\,000$ shows an increase in heat transfer which is located much farther downstream. This clearly illustrates a Reynolds number dependence. Further studies - varying both Re and Λ - are currently performed. We aim to present the results at the conference.

*Institute for Hydromechanics, University of Karlsruhe, D-76128 Karlsruhe, Germany.

[1]Mayle et al, *J. Turbomachinery* **120**, 402 (1998).

[2]Junkhan and Severoy, *J. Heat Transfer* **17**, 171 (1994).

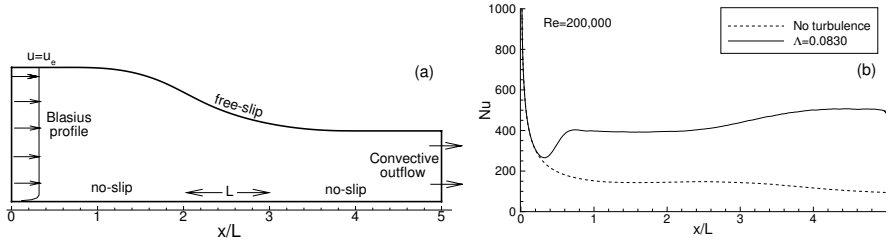

Figure 1: (a) Spanwise slice through the computational domain. (b) Local Nusselt number along the flat plate at $Re = 200\,000$.

Session 2

Axisymmetric absolute instability of swirling jets

J. J. Healey*

The linearized stability, and propagation characteristics, of disturbances to a family of simple models for swirling jet flow will be presented. Although non-axisymmetric waves are known to produce absolute instability (AI), and have been successfully related to helical modes of vortex breakdown, a difficulty in the application of Briggs' method to axisymmetric waves in swirling jets has been noted by several authors. The 'pinch-point' can cross the imaginary axis of the complex wavenumber plane, leading to the appearance of eigenfunctions that grow, instead of decay, with distance outside the shear layer. The same problematic behaviour of the pinch-point was recently found by the author in the rotating disk boundary layer, and the physical consequences were studied in detail in that context.

Our understanding of this behaviour in the rotating disk problem has been used to help us to calculate for the first time AI of inviscid axisymmetric waves in swirling jets. It is found that these waves can grow with distance in the radial direction outside the jet, and that the addition of a bounding cylinder far from the jet converts this spatial growth into an AI. As the distance from the jet to the outer cylinder reduces, the AI increases, and less swirl is needed to produce AI, see figure 1(a). It is interesting to note that many experiments on axisymmetric vortex breakdown involve swirling flows in pipes, and it may be that the presence of the pipe is instrumental in creating the AI, which perhaps leads in turn to vortex breakdown. Following previous studies, the model profiles have uniform axial flow, and constant angular velocity, within the jet and both velocity components drop discontinuously to zero outside the jet. A more realistic family of profiles with finite thickness smooth shear layers at the jet edge has also been studied. It is found that increasing the shear layer thickness produces AI, even in the unconfined jet, via an enhancement of the centrifugal instability, see figure 1(b). For a given swirl, the shear layer at the jet's edge thickens with downstream distance, causing the flow to change from CI to AI at a critical distance from the jet nozzle, possibly providing the location for axisymmetric vortex breakdown.

*Department of Mathematics, Keele University, Keele, Staffs. ST5 5BG, UK

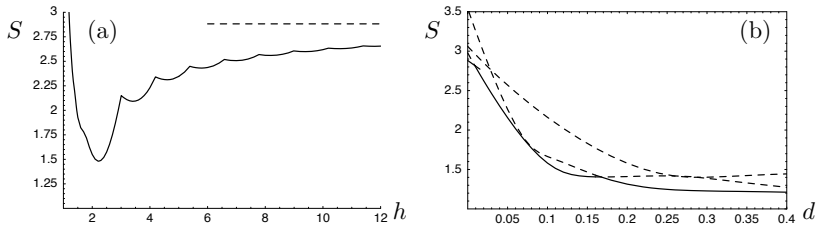

Figure 1: Neutral curves for axisymmetric AI. (a) Confined jets: swirl vs. outer cylinder radius (dashed line is limit as $h \to \infty$). (b) Smooth jets: swirl vs. shear layer thickness (dashed lines are non-pinching saddles).

The effect of confinement on the stability of two-dimensional jets and wakes

M. P. Juniper*

It has been shown recently[1] that a two-dimensional wake becomes more unstable when it is confined in the transverse direction by two flat plates. Confinement causes the transition from convective to absolute instability to occur at lower values of shear. This effect is examined comprehensively in this study for both jets and wakes. It is found to be caused by the constructive interaction of modes with zero group velocity in the central flow and modes with zero group velocity in the surrounding flow. Maximum instability occurs when the wavenumber of the fundamental mode in the central flow matches that of the fundamental mode in the surrounding flow. Other regions of high instability occur when the harmonics of one mode interact with the fundamental of the other.

The aim of this study is to isolate the effect of confinement on a shear flow rather than to include all the details of a realistic flow. Consequently the model comprises two inviscid fluids with plug velocity profiles. A linear spatio-temporal stability analysis is performed in order to identify the absolute/convective instability transition. Such linear analyses have proved to be very successful in predicting the onset of global modes in these flows[2] so a non-linear analysis is not attempted here. The advantage is that the dispersion relation can be derived analytically to give an explicit expression for the permissible complex angular frequency, ω, in terms of the complex wavenumber, k. Consequently it is very easy to plot contours of ω_i in the k-plane and to track saddle points as parameter values are varied. The parameters are (a) the density ratio between the two fluids, (b) the velocity difference between the flows and (c) the ratios of the thicknesses of the flows, which is known as the confinement. One can observe the interaction between saddle points that are associated with the inner flow and saddle points that are associated with the outer flow. This gives a good physical understanding of the effect of confinement on the combined flow.

Engineers have consistently found through trial and error that confined shear injectors cause good mixing with a low pressure drop[3]. It is likely that this is because they contain regions of absolute instability that stimulate an unstable global shear mode whose large scale flapping or spiralling motion enhances mixing. In this study the density ratio is varied from 0.001 to 1000. At each density ratio the confinement that causes maximum absolute instability is predicted. This gives a useful indication of the optimal injector geometry for a given pair of fluids if one wishes to promote mixing by stimulating an absolute instability in the injector.

*Cambridge University Engineering Department, Trumpington Street, CB4 1PZ, UK

[1] Juniper and Candel, *J. Fluid Mech.* **482**, 257 (2003).

[2] Delbende and Chomaz, *Phys. Fluids* **10** (11), 2724 (1998).

[3] Barrère *et al.*, Rocket Propulsion, Elsevier (1960)

Stability of the flow past a freely moving disk

G. Forlano[1] and P. Luchini[1]

Experiments on the stability of the wake of a freely moving disk were performed in 1964 by Willmarth[a]. In his experiments the freely falling circular disks are dropped in a liquid in broadside-on orientation. For small values of the Reynolds number, the falling disk retains this initial orientation and a steady axisymmetric recirculating wake is visualized behind the body. For sufficiently large values of the Reynolds number, the disks fall erratically with both a translating and a tumbling motion.

Similar experiment are presently underway at IMFT (Institute of Fluid Mechanics of Toulouse) by a group of researchers with the aim to investigate, in grater quantitative detail, the stability of freely moving disk. In coordination with this group we have undertaken a theoretical and numerical study of this instability problem.

Natarajan and Acrivos[b] studied the instability of the steady axisymmetric base flow past a fixed disk (oriented broadside-on to the incoming flow). A Finite-Element approach, based on non-uniform grid, was used to compute the steady axisymmetric flow, and examine its linear instability.

The stability of a disk free to oscillate, including the mutual interactions between the body and flow field around it, does not appear to have been studied before.

In this presentation we will discuss the properties of an unstable global mode as obtained through linear stability analysis. The axisymmetric base flow is obtained through the numerical solution, based on a finite difference method, of the stationary incompressible Navier-Stokes equations. The instability problem is formulated by simultaneously linearizing the Navier-Stokes equations and the rigid-body equations. Using a normal mode expansion of the linear equations we obtain an eigenvalue problem, that is solved numerically to evaluate the critical Reynolds number. We will show the influence of the body motion on the stability characteristics of the flow.

---

[1]DIMEC, University of Salerno, Via Ponte Don Melillo, 84084 Fisciano (SA), Italy.

[a]Willmart, W. W. Hawk et al., *Phys. Fluids* **7**, 197 (1964).
[b]R. Natarajan and A. Acrivos, *J. Fluid Mech.* **254**, 323 (1993).

Generalized energies for stability analysis: application to plane Poiseuille flow

A. Nerli*, S. Camarri† and M.V. Salvetti†

The classical energetic stability theory fails to predict the critical Reynolds number (Re_E) for several reference flows, such as, for instance, the plane Poiseuille flow. Possible explanations of this failure have been given in the literature. First, the classical energetic stability theory requires that the disturbance energy monotonically goes to zero. However, the non-normality of the linearized Navier-Stokes (NS) operator leads to the well known transient growth of the disturbance energy, which eventually can decrease to zero. Second, the non linear part of the NS operator does not play a role in the computation of Re_E and, thus, the amplitude of the disturbance does not enter in the problem.

The aim of the present work is to investigate whether the predictions of the energetic theory may be improved if the problems related to the non-normality of the linear operator are by passed and the amplitude of the disturbance is taken into account in the problem. To this aim, generalized energies (norms) are defined through a perturbations of the L^2 metric. Thus, the generalized energy is defined as:

$$\mathcal{F}(u) = \mathcal{E}(u) + \mathcal{P}(u)$$

where $\mathcal{E}(u)$ is the classical L^2 disturbance energy and $\mathcal{P}(u)$ is the perturbation term, which is computed in order to eliminate the transient growth due to the linear part of the NS operator. Hence, for Reynolds numbers lower than the one obtained by the linear stability analysis, the time derivative of the generalized energy is given by:

$$\frac{d\mathcal{F}(u)}{dt} = \mathcal{L}(u) + \mathcal{N}(u)$$

where $\mathcal{L}(u)$ is a quadratic form negatively defined by construction and $\mathcal{N}(u)$ a cubic form due to the non-linear part of the NS operator. This leads to the following criterion for conditional stability: $\frac{d\mathcal{F}(u)}{dt}$ must be negative if $\sqrt{\mathcal{F}(u)} < \mathcal{A}$, $\mathcal{A}$ being the critical amplitude. Thus, by numerically solving a maximum problem in the disturbance space, both the shape and the amplitude of the most critical disturbance can be obtained at each Reynolds number.

Although the proposed criterion can be applied to the whole NS operator, this requires huge computational resources. The criterion has, thus, been applied to reduced order models, previously proposed in the literature for the stability analysis of the plane Poiseuille flow. In particular, the model proposed by Waleffe (1995)[1] and a model very similar to that by Bergstrom (1999)[2] are considered. Preliminary results obtained for this latter model show that the proposed criterion gives the correct scaling of the critical amplitude with the Reynolds number. A more detailed analysis of the results obtained for both models will be reported in the final paper.

*Scuola Normale Superiore di Pisa, P.zza Cavalieri, 7, 56127 Pisa (Italy)
†Dip. Ingegneria Aerospaziale, Università di Pisa, Via G. Caruso, 56122, Pisa (Italy)

[1] Waleffe F., *Phys. Fluids*, **7**, 3060 (1995).
[2] Begström L., *Phys. Fluids*, **11**, 590 (1999).

Interaction of acoustic disturbances with a hypersonic shock layer on a flat plate

S. G. Mironov[1], A. N. Kudryavtsev[1], T. V. Poplavskaya[1], I. S. Tsyrjulnikov[1]

The problem of receptivity and evolution of disturbances in a shock layer on a temperature-controlled flat plate at zero angle of attack subjected to a hypersonic nitrogen flow with a Mach number equal to 21 and the Reynolds number based on the free-stream parameters and on the plate length $Re_L = 1.44\ 10^5$ has been solved for the first time by methods of direct numerical simulation on the basis of two-dimensional Navier-Stokes equations. The temperature factor of the surface is 0.25. Interaction of the shock layer with external acoustic slow-mode disturbances propagating in the streamwise direction is considered. The results of simulations are the mean flow field and the field of fluctuating parameters.

Simulations are compared with the mean density and Mach number measured in the shock layer, which displays good qualitative and quantitative agreement in the entire shock-layer flow. The computations also show that there are two maximums of density fluctuations in the shock layer; one of them (with a higher amplitude) is located on the shock wave, and the other (with a lower amplitude) is located in the region of rapid variations of the mean temperature and density across the shock layer. The phases of density fluctuations in these maximums are shifted by 180° relative to each other. Electron-beam measurements confirm the presence of these maximums of density fluctuations and reveal good qualitative and quantitative agreement with computations in terms of intensity of density fluctuations on the shock wave.

Visualization of the numerical vector field of velocity fluctuations displays pairs of counterrotating vortices between the shock wave and the region of rapid variations of density and temperature. The presence of two maximums of density fluctuations and the magnitude of the phase shift between them can be attributed to the dominating effect of vortex disturbances on the mean flow in the shock layer. To check this hypothesis, it was demonstrated within the framework of the linear theory of interaction of acoustic waves with the shock wave that the conditions of existence of acoustic disturbances behind the shock wave are not satisfied for all angles of interaction of acoustic waves with the bow shock wave, which are observed in experiments and numerical simulations. On the other hand, entropy-vortex disturbances can arise and propagate behind the shock wave for all angles of interaction, which is actually observed in direct numerical simulations of interaction of external acoustic disturbances with the shock layer on a flat plate.

This work was supported by the Russian Foundation for Basic Research (Grants 04-01-00474 and 05-08-33436).

[1] Institute of Theoretical and Applied Mechanics SB RAS, 630090, Novosibirsk, Russia

Application of the ray-tracing theory to the stability analysis of three-dimensional compressible boundary layers

R. S. Donelli*, G. Mazzotti*, P. Luchini†

The traditional approach to transition prediction is based on the linear stability analysis of viscous flows, generally treated as thin shear layers, consisting in determining the evolution, in space or in time, of small perturbations superimposed to a basic flow field[1], [2]. The transition location is individuated by using the e^N method[3]. The disturbance growth rate is computed in the hypothesis of constant spanwise wavenumber and frequency, then it is, traditionally, integrated along an assigned path, generally coincident with the chordwise flow direction, allowing the computation of the N factor curves.

The analysis is repeated for a wide range of spanwise wavenumbers (or wavelengths, depending on the approach) and frequencies to select the most amplified disturbances. Laminar turbulent transition is assumed to take place where the most unstable disturbances are amplified by a factor e^N, with N determined by correlation with experiments.

In the present work, a different approach has been introduced to individuate the transition location. The linear instability of steady compressible laminar boundary layers, developing on 3D tapered swept wings, has been approached in the framework of the theory of ray tracing in non-homogeneous anisotropic dispersive wave systems[4],[5]. The stability analysis permits, with this approach, to take into account three-dimensional effects because the N factor curves are, here, the result of the integration of the disturbance growth rate along the ray of propagation of the disturbances. The stability analysis is performed starting from points located on the neutral curve, changing initial spanwise wavenumbers and frequencies. The aim is to search the directions that show the maximum amplification of the disturbances. This investigation allows to build iso-N factor curves on the wing surface. As result of this analysis a map of the transition locations on the wing will be achieved. A second map built starting from a given N factor at transition will show the upstream regions that strongly affect the transition. The knowledge of this type of maps allows to individuate regions of the wing particularly critical for the transition of the boundary layer from laminar to turbulent because particularly sensitive to disturbances. This information is extremely important for the design and construction of a laminar wing since these critical regions require particular care if laminar flow is desired.

*CIRA Centro Italiano Ricerche Aerospaziali, 81043 Capua, Italy
†Dipartimento di Ingegneria Meccanica, Universita di Salerno, 84040, Fisciano.

[1]Mack, *AGARD* **709**, 51 (1984).
[2]Schlichting, *McGraw-hill Book* 7^{th} **ed.**, (1979).
[3]Van Ingen et all, *Douglas Aircraft Co. rept. Es 26388*, (1956)
[4]Donelli et all, *AIDAA proceeding* **vol. 2**, 1, (1995)
[5]Grea et all, *Phis. Rev. E.* submitted (2005)

Stability, transition and flow control of supersonic boundary layer on swept wing

N.V. Semionov [a], A.D. Kosinov [a], Yu.G. Yermolaev [a]

The paper is devoted to an experimental study of disturbances evolution in linear and non-linear areas of development and transition control in a three-dimensional supersonic boundary layer on swept wing. The problem of transition to turbulence in 3-D boundary layers is very important and very complicated. In a 3–D case exist along with the well–known Tollmien–Schlichting waves, which development results to the turbulent transition in the 2–D boundary layers, stationary vortexes with axes directed along the outer streamlines and some traveling waves (not T–S waves). Development of all instability disturbances and their relative role in transition strongly depend on the environmental conditions.
The experiments were made in a supersonic wind tunnel T-325 of the ITAM with test section dimension 200×200×600 mm at Mach numbers M=2.0 and 3.5. In experiments the models of swept wing with subsonic or supersonic leading edge were used. The disturbances were measured by constant temperature hot-wire anemometer. To measure a transition position the pneumometric or hot-wire methods were used.

As a result of researches the key difference of a nature of instability in pressure gradient flat and spatial supersonic boundary layers was revealed. The transition takes place as a result of interaction of stationary and traveling disturbances. Is shown, that the main mechanism of turbulence beginning in supersonic boundary layer on a swept wing - secondary instability of cross-flow.

A technique of control of laminar - turbulent transition on swept wing at supersonic speeds of flow was designed. The research of disturbances development in artificial laminarizated supersonic boundary layer on model of a swept wing from area of a linear stage of development up to area of transition was executed.

This work has been supported by the RFBR grant 05-01-00176.

[a] Institute of Theoretical and Applied Mechanics, Novosibirsk, Russia

Leaky Waves in Supersonic Boundary Layer Flow

J. O. Pralits*, F. Giannetti* and P. Luchini*

Linear stability analysis of compressible boundary layer flow is commonly investigated by solving the Orr-Sommerfeld equations (OSE), either in a temporal or spatial framework. The mode structure of the OSE is in both cases composed of a finite number of discrete modes which decay at infinity in the wall-normal direction y, and a continuous spectrum of propagating modes behaving as $\exp(\pm ky)$ when $y \to \infty$, with k being real. The number of discrete modes changes with the Reynolds number (Re) and they further seem to disappear behind the continuous spectrum at certain values of Re. This behaviour can be visualised by tracing the trajectory of the damped discrete modes as Re is decreased. In certain problems, such as e.g. leading-edge receptivity of the boundary layer to external disturbances, it is of importance not only to capture the evolution of the least stable mode as the Reynolds number is decreased, but also of the additional damped discrete modes. This is especially important in supersonic boundary layers where a number of modes become neutral at nearby locations. In order to enable such computation it is of interest to investigate if an all-discrete representation of the solution is possible.

This is here done solving the response of the boundary layer forced instantaneously in space and time. Since the solution of the forced and homogeneous Laplace transformed problem both depend on the free stream boundary conditions, it is shown here that an opportune change of variables can remove the branch cuts in the complex frequency plane. As a result integration of the inversed Laplace transform along the new path corresponding to the continuous spectrum, equals the summation of residues corresponding to new discrete eigen values. These new modes are computed accounting for solutions which grow in the y-direction, and a similar problem is found in the theory of waveguides, e.g. optical fibers, where so called *leaky waves*[1] are attenuated in the direction of the wave-guide, while they grow unbounded perpendicular to it.

The above analysis was previously performed for incompressible flat plate boundary-layer flows[2 3]. There it was shown that a discrete representation of the solution of the OSE is possible accounting for solutions which grow in the wall-normal direction to the flat plate, and that an analytical continuation in the complex frequency plane of the damped discrete modes is obtained. The all-discrete representation obtained here from the study of supersonic boundary layers can be used to clarify some mechanisms proposed by past authors[4 5 6 7] to explain the receptivity of supersonic boundary layers to acoustic disturbances.

*DIMEC, Universitá di Salerno, 84084 Fisciano (SA), Italy

[1] Marcuse, *Theory of dielectric optical waveguides, Academic press, inc.* (1991).
[2] Pralits and Luchini, *Proc., XVII AIMeTA Congress of Theor. and Appl. Mech., Firenze* (2005).
[3] Pralits and Luchini, *APS, Division of Fluid Dynamics, Chicago, IL* (2005).
[4] Fedorov and Khokhlov, *Fluid Dyn.* No. 9, 456 (1991).
[5] Fedorov and Khokhlov, *ASME Fluid Eng. Conf., Washington* FED-Vol. 151, 1 (1993).
[6] Fedorov, *J. Fluid Mech.* **491**, 101 (2003).
[7] Ma and Zhong, *J. Fluid Mech.* **488**, 31, and 79 (2003).

The Parabolised Stability Equations for 3D-Flows: Implementation and Numerical Stability

M. S. Broadhurst*, S. J. Sherwin*

The numerical implementation of the parabolised stability equations (3D-PSE) using a substructuring solver - designed to take advantage of a spectral/*hp*-element discretisation - is considered. Analogous to the primitive variable form of the two-dimensional PSE [1], the equations are ill-posed [2]; although choosing an Euler implicit scheme in the streamwise z-direction yields a stable scheme for sufficiently large step sizes ($\Delta z > 1/|\beta|$, where β is the streamwise wavenumber). Neglecting the $\frac{\partial \hat{p}}{\partial z}$ term relaxes the lower limit on the step-size restriction. The θ-scheme is also considered, and the step-size restriction is determined. Neglecting the pressure gradient term shows stable eigenspectra for $\theta \geq 0.5$. For $\theta = 0.5$, the formulation corresponds to the second order Cranck-Nicholson scheme. Consequently, for identical step-sizes in the streamwise direction, the truncation error will be lower than the Euler implicit scheme, and this can be taken advantage of when solving the 3D-PSE. Figure 1 illustrates how the absolute value of the most unstable eigenvalue varies with θ, where $|G| < 1$ corresponds to a stable scheme, for (a) the full 3D-PSE operator, and (b) the reduced 3D-PSE operator, where $\frac{\partial \hat{p}}{\partial z}$ is neglected. The motivation behind implementing the 3D-PSE comes from the recent application of a BiGlobal stability analysis to vortical flows [3], which has demonstrated a relationship between instability and breakdown. Direct numerical simulation of an unstable vortex indicates that as an instability develops, a loss in axial velocity is initiated. Consequently, this suggests a requirement for a stability analysis technique that will allow axial gradients to develop. It is proposed that the 3D-PSE is a suitable method.

*Department of Aeronautics, Imperial College London, London. SW7 2AZ. UK

[1] Li and Malik, *Theoretical and Computational Fluid Dynamics.* **8**, 253-273 (1996).

[2] Andersson, Henningson and Hanifi, *J. Eng. Math.* **33**, 311-332 (1998).

[3] Broadhurst, Theofilis and Sherwin, *IUTAM Symposium on LTT.* Kluwer (In Press).

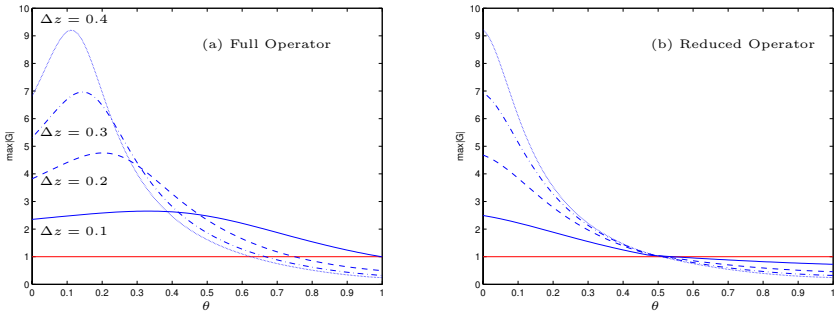

Figure 1: Influence of θ on the numerical stability of the θ-scheme

Solving turbulent wall flow in 2D using volume-penalization on a Fourier basis

G.H.Keetels*, H.J.H. Clercx* and G.J.F. van Heijst*

The volume-penalization method proposed by Angot et al.[1] allows the use of fast Fourier pseudospectral techniques to simulate turbulent wall flows (where periodic boundary conditions are absent). Convergence checks with respect to spatial resolution, time stepping and the penalization strength are presented where a challenging dipole-wall collision simulation serves as a benchmark (which is obtained by high-resolution simulations with a 2D Chebyshev pseudospectral method). In this numerical experiment thin boundary layers are formed during the dipole-wall collision, which subsequently detach from the boundary and (eventually) roll up and form small-scale vortices. In particular, the vorticity filaments and small-scale vorticity patches in the near wall region can possibly deteriorate the flow computation yielding a flow evolution deviating from the benchmark solution[2]. The complexity of such flows can be observed in figure 1 where vorticity contour plots are displayed of a dipole collision with the no-slip boundary near the upper right corner of a square domain. It is found that Gibbs oscillations have a minor effect on the flow dynamics. As a consequence it is possible to recover the solution of the penalized Navier-Stokes equations acceptably accurate using a high-order postprocessing technique [3]. Note that it is possible to capture all the small-scale features in the vorticity field of the oblique collision. Increasing the penalization strength results in a natural convergence scenario in terms of vortex trajectories which is demonstrated for a normal collision in figure 1. Solving the penalized Navier-Stokes equation on a Fourier basis is computationally much cheaper than the classical Chebyshev Navier-Stokes solvers. Therefore the potential of the approach is further examined by considering the statistical properties of fully developed 2D turbulence in bounded domains with Reynolds numbers substantially larger than previously possible.

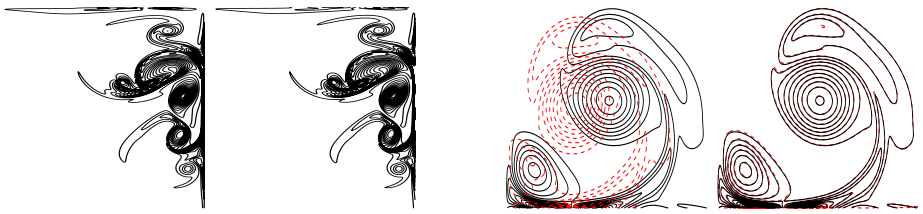

Figure 1: Vorticity contour lines of an oblique collision computed with the penalization method (left) and Chebyshev solver (right). Convergence in terms of increasing penalization strength (from left to right) for a normal collision, penalization computation (dashed) and Chebyshev result (solid).

*Department of Physics, Eindhoven University of Technology , P.O. Box 513, 5600 MB Eindhoven, The Netherlands

[1]Angot et al, *Num. Math*, **81**, 497 (1999).
[2]Clercx and Bruneau,*Comp. Fluids* **35**, 245 (2006).
[3]Tadmor & Tanner, *Found. Comp. Math.*,**2**, 155 (2002)

3D numerical simulation of Batchelor vortices

J. Ortega-Casanova* and R. Fernández-Feria*

A new numerical technique to simulate three-dimensional (3D) incompressible flows based on the potential vector formulation is developed. The numerical technique combines finite differences on a non-uniform grid in the axial direction (n_z nodes), a Chebyshev spectral collocation technique in the radial direction (n_r nodes), and a Fourier spectral method in the azimuthal direction ($2n_\theta + 1$ modes). The technique is adapted to simulate 3D vortices, and we have tested it by solving the 3D rotating flow in a circular pipe, and comparing the resulting nonlinear travelling and stationary waves with previous stability[1] and numerical results.[2] Then, we used the numerical code to characterise the nonlinear stability properties of Batchelor's vortex. Several Reynolds number (Re), based on the maximum axial velocity and the radius of the core, and swirl paramenter (q), defined as the ratio between the maximum of the swirl and axial velocity, have been analysed in a domain which extend 200 core radius in the axial direction and 40 core radius in the radial one. The results found are in good agreement with previous ones from linear stability analysis.[3] As an example, figure 1 shows the axysimmetric streamlines ($n_\theta = 0$) for $Re = 200$ and $q = 0.3$. This axisymmetric solution is used as the base flow to simulate the 3D flow ($n_\theta \neq 0$). The perturbation of the velocity is shown in figure 2 ($n_\theta = 5$). The contour lines show a travelling wave from which we characterise the nonlinear instabilities properties of the base flow.

*E.T.S. Ingenieros Industriales. Universidad de Málaga (Spain)

[1] del Pino et al. *Fluid Dyn. Res.* **32**, 261–281 (2003)

[2] Barnes and Kerswell, *J. Fluid Mech.* **417**, 103–126 (2000)

[3] Mayer and Powell *J. Fluid Mech.* **245**, 91–114 (1992)

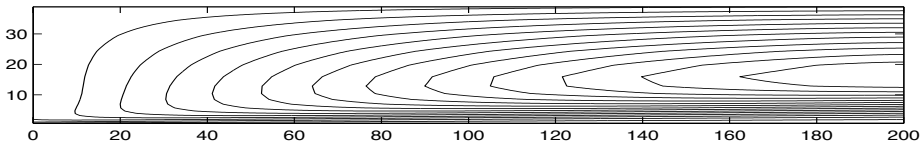

Figure 1: Contours of the stream-function for $Re = 200$ and $q = 0.3$ ($n_r = 30,\ n_z = 600,\ n_\theta = 0$)

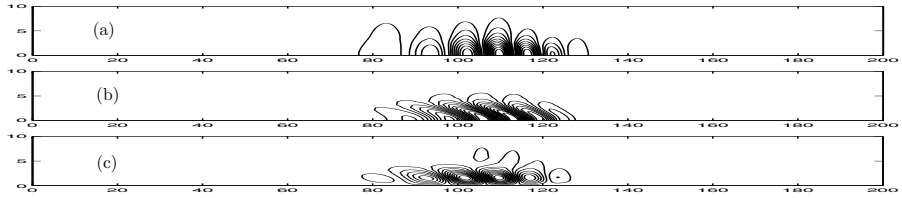

Figure 2: Perturbation of the velocity vector for $Re = 200$ and $q = 0.3$ ($n_r = 30,\ n_z = 600,\ n_\theta = 5$): (a) radial, (b) azimuthal and (c) axial velocity components.

Development of a 3D transient incompressible Navier-Stokes solver

N. Suresh Kumar[a], Anoop K. Dass[a] and Manmohan Pandey[a]

This work is concerned with the development of a 3D transient Navier-Stokes solver through finite difference method. The solver is based on the fractional step method proposed by Choi and Moin[1]. The spatial discretization of the convective fluxes is carried out through Kuwahara's third order upwind scheme[2] and viscous fluxes through a fourth order central difference scheme. In the fractional step method of Choi and Moin[1], every time step is advanced in four substeps. The method requires the solution of pressure Poisson equation in only one substep. In this method, continuity equation is satisfied only at the final substep. In the present code, the pressure Poisson equation is solved through a multigrid procedure with flexibility in choosing the number of levels to accelerate convergence. As the code is third order accurate in space and second order accurate in time, and multigrid accelerates its rate of convergence, it has DNS potential. However, the results presented here are for the steady state laminar flow in a 3D cubical cavity for Re=1000 on a 129×129×129 staggered grid, which have been obtained through the code in a time-marching fashion. Figure 1(a) shows the projection of streamlines on the cavity mid-plane and Figure 1(b) compares the centreline x-velocity with those of Renwei et al.[3] and 2D results produced on a 129×129 grid. Our results compare well with those of Ref. 3 and deviate from the 2D results, as expected.

---

[a] Indian Institute of Technology Guwahati, Guwahati 781039, India

[1] Choi and Moin, *J. Comp. Physics,* **113,** 1 (1994)
[2] Kawamura and Kuwahara, AIAA-85-0376 (1985)
[3] Renwei et al., *J. Comp. Physics,* **161,** 680 (2000)

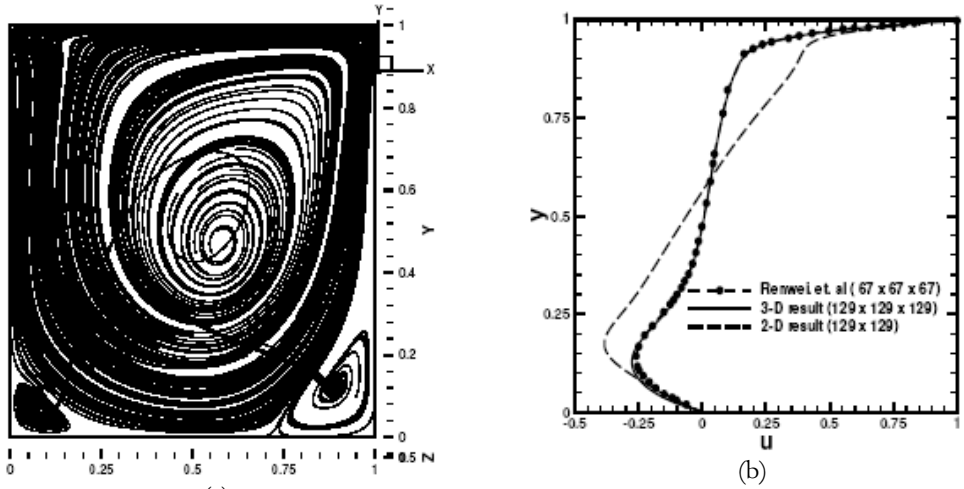

(a) (b)

Figure 1: (a) Projection of streamlines on the mid-plane, (b) Comparison of centreline x-velocity, for Re=1000

Flow inside a precessing cylinder

Christophe Eloy*, Patrice Meunier* and François Nadal†

The flow inside a precessing container is primarily interesting because it is found inside the liquid core of the Earth, where it may be responsible for the geodynamo, but also because it is found in the reservoir of rotating spacecrafts. Previous experiments in precessing cylinders have shown that this flow is unstable for strong precession[1] and several instability mechanisms have been proposed. But so far no quantitative experiment have been carried out in the regime of low Reynolds number and low angle of precession in order to characterise the instability.

Here, we report results of an experiment in which a cylinder rotating around its axis is mounted on a rotating turntable, with a small angle between the two axis (between 0.5 and 4 degrees). Visualisations are performed by adding Kalliroscope particles and illuminating a vertical plane. The flow is also analysed through velocity measurements in an horizontal plane using Particle Image Velocimetry (PIV).

At low angles of precession, the flow is stable and is composed of several Kelvin modes, stationary in the frame of reference of the rotating platform. Their amplitudes depend on the aspect ratio of the cylinder, and diverge when the height of the cylinder equals an odd number of half-wavelengths. These amplitudes are well predicted by the linear theory. But, at higher angle of precession, the flow can no longer be described by a linear theory. Depending on the aspect ratio, it can become periodic or exhibit strong geostrophic behaviour. These observed motions are analysed in the framework of interacting Kelvin modes.

At even higher angles of precession, the flow is found to destabilise, giving rise to a very disordered motion, which can sometimes relaminarize, leading to intermittent breakdown of the flow. This is similar to what has been observed for the elliptic instability inside a cylinder[2].

*IRPHE, CNRS, Univ. Aix-Marseille I & II, BP 46, F-13384 Marseille Cedex 13, France.
†CEA/CESTA, BP2, 33114 Le Barp, France
[1]Manasseh, *J. Fluid Mech.* **315**, 151–173 (1996). Kobine, *J. Fluid Mech.* **319**, 387–406 (1996).
[2]Eloy et al., *J. Fluid Mech.* **476**, 357–388 (2003).

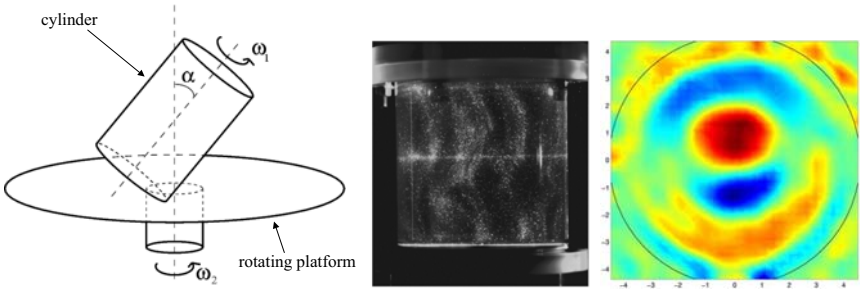

Figure 1: Left: Principle of the experiment. Middle: Visualisation of the flow using Kalliroscope particles. Right: PIV measurement of the vorticity field.

Buoyant control of nonaxisymmetric instabilities during spin-up of rotating stratified fluid

S. A. Smirnov[a] and D. L. Boyer[b]

An experimental study was conducted to elucidate the influence of a sloping bottom boundary on global stratified spin-up. The system consisted of a rotating continuously stratified fluid confined in a domain which has a shape of an inverted round cone with the upper surface being free. It is shown that under similar flow conditions (the same absolute values of the Rossby and Burger numbers) the spin-up flow remains stable and axisymmetric, while the spin-down flow undergoes a transition from axial symmetry to the formation of a system of anticyclonic eddies.

The stratified spin-up flow was found previously to be susceptible to nonaxisymmetric instabilities in the case of a horizontal bottom boundary[1]. Azimuthal asymmetry is manifested in the form of cyclonic and anticyclonic eddies with a practically vertical axis of rotation. These eddies develop at the density front formed by the corner regions near the sidewalls, where the isopycnals experience the largest deformations as a result of the Ekman meridional transport. The latter makes the corner regions grow until they reach a quasi-equilibrium height determined by the relative values of the Rossby and Burger numbers. The density structure of the corner regions after completion of the Ekman transport process was found to be a key factor in determining the stability of the stratified spin-up flow[2]. The corner regions are characterized by a weak density gradient. The presence of a higher density gradient above the weakly stratified corner regions suggests that in this part of the flow domain the isopycnals may reach steep slopes relative to the horizontal boundary.

The absence of nonaxisymmetric instabilities under similar flow conditions during stratified spin-up in a conical geometry suggests that a sloping wall plays a crucial role in flow control by altering the density structure of the corner regions. Asymmetry between stratified spin-up and spin-down is also manifested in a qualitatively different behavior of the bottom boundary layer. The density at a fixed location close to the slope increases monotonically in the case of stratified spin-up demonstrating smoothness of the upslope flow at all times. On the contrary, in the case of stratified spin-down the density field in the downslope flow shows high-frequency fluctuations at early times after the beginning of transition, suggesting the turbulent nature of the bottom boundary layer. These results may be found useful in interpreting in-situ measurements of upwelling- and downwelling-favorable oceanic flows in the coastal regions.

---

[a] Mechanical Engineering Department, Texas Tech University, Lubbock, TX 79409, USA.
[b] Department of Mechanical and Aerospace Engineering, Arizona State University, Tempe, AZ 85287, USA.

[1] Smirnov et al., *Phys. Fluids* **17**, 016601 (2005).
[2] Smirnov et al., *Phys. Fluids* **17**, 104111 (2005).

Upper bounds for the long-time averaged buoyancy flux in plane stratified Couette flow subject to a mixing efficiency constraint

C. P. Caulfield*, W. Tang†, & R. R. Kerswell‡

We derive non-trivial upper bounds for the long-time averaged vertical buoyancy flux $\mathcal{B}^* := \langle \rho u_3 \rangle g/\rho_0$ (where u_3 is the vertical velocity, g is the acceleration due to gravity, and angled brackets denote volume and time averaging) for stably stratified Couette flow: i.e. the flow of a Boussinesq fluid (with reference density ρ_0, kinematic viscosity ν, and thermal diffusivity κ) confined between two parallel horizontal plates separated by a distance d, which are driven at a constant relative velocity ΔU, and are maintained at a constant (statically stable) temperature difference leading to a constant density difference $\Delta\rho$.

We construct the bound by means of a numerical solution to the "background method" variational problem[1] using a one dimensional, uni-directional background. We require that the mean flow is streamwise independent and statistically steady. Furthermore, we impose the plausible coupling constraint that a fixed fraction of the energy input into the system by the driving plates (above that required to maintain a purely laminar flow) leads to enhanced irreversible mixing within the flow, i.e. we require a coupling such that that $\mathcal{B}^* = \Gamma_c(\mathcal{E}^* - \mathcal{E}^*_{\mathsf{L}})$, where $\mathcal{E}^*$ is the total mechanical energy dissipation rate, and $\mathcal{E}^*_{\mathsf{L}}$ is the total mechanical energy dissipation rate associated with a purely parallel, laminar flow. We calculate this bound up to asymptotically large Reynolds numbers for a range of choices of coupling parameters Γ_c and bulk Richardson numbers $J = g\Delta\rho d/(\rho_0 \Delta U^2)$ of the flow.

For all values of Re, we find that the calculated upper bound increases with J. However, there is always a maximum possible value of $J_{\max}(Re, \Gamma_c)$, at which it becomes impossible to impose the new constraint, and the density field and velocity field become decoupled. $J_{\max}$ increases with Re, but is a non-monotonic function of Γ_c, with for a given Re, a maximum apparently at $\Gamma_c = 1$. The value of the bound on the buoyancy flux at $J_{\max}$ is also a non-monotonic function of Γ_c, with $\Gamma_c = 1/2$ leading to the largest possible values as $Re \to \infty$, consistently with the upper bound presented previously,[2] where this coupling constraint was not imposed. The asymptotic scaling of the new coupled bound is the same as the previously calculated value, with dimensionally $\mathcal{B}^*_{\max} = \mathcal{O}(U^3/d)$, independent of the flow viscosity. At any particular value of Re, the previously calculated bounding solution may be associated with a specific value of Γ_c. Imposing the coupling constraint with that value of Γ_c, as $J \to J_{\max}$, the new bound approaches from below the previously calculated bound exactly. The predicted bounds are compared with the results of direct numerical simulations.

*BP Institute and Department of Applied Mathematics & Theoretical Physics, University of Cambridge, Madingley Rd, Cambridge CB3 0EZ, U.K. *c.p.caulfield@bpi.cam.ac.uk*

†Department of Mechanical & Aerospace Engineering, Jacobs School of Engineering, University of California, San Diego, U.S.A.

‡Department of Mathematics, University of Bristol, U. K.

[1] Doering & Constantin *Phys. Rev. Lett.* **69** 1648 (1992)

[2] Caulfield et al. *J. Fluid Mech.* **498** 315 (2004)

Plumes with time dependent source conditions in a uniformly stratified environment

M. M. Scase*, C. P. Caulfield†*, S. B. Dalziel* and J. C. R. Hunt‡

Motivated by Hunt[1] *et al.*, the classical bulk models for isolated jets and plumes due to Morton, Taylor & Turner[2] are generalised to allow for time dependence in the various fluxes driving the flow. These new systems model the spatio-temporal evolution of both Boussinesq and non-Boussinesq jets and plumes in uniformly stratified fluids. Separable time-dependent similarity solutions for plumes and jets are found. These similarity solutions are characterized by having time-independent plume or jet radii, with appreciably smaller spreading angles than either constant source buoyancy flux pure plumes or constant source momentum flux pure jets.

If the source buoyancy flux (for a plume) or source momentum flux (for a jet) is decreased generically from an initial to a final value, numerical solutions of the governing equations exhibit three qualitatively different regions of behaviour. The upper region remains largely unaffected by the change in buoyancy flux or momentum flux at the source. The lower region is an effectively steady plume or jet based on the final (lower) buoyancy flux or momentum flux. The intermediate transition region, in which the plume or jet adjusts between the states in the lower and upper regions appears to converge very closely to the newly identified stable similarity solutions. In figure 1, we consider an unstratified ambient fluid. Figure 1(a) shows the well-known conical plume shape established by Morton *et al.*[2]. In figure 1(b) we show the shape of a plume which has been convecting steadily for some time and then has its source buoyancy flux rapidly reduced. The spreading angles and velocities of the plumes are considered with a view to predicting pinch-off.

*DAMTP, University of Cambridge, CMS, Wilberforce Road, Cambridge CB3 0WA, UK.
†BP Institute, University of Cambridge, Madingley Road, Cambridge CB3 0EZ, UK.
‡CPOM, University College London, London WC1E 6BT, UK.

[1]Hunt, J. C. R., Vrieling, A. J., Nieuwstadt, F. T. M. & Fernando, H. J. S., *J. Fluid Mech.* **491**, 183–205 (2003).
[2]Morton, B. R., Taylor, G. I. & Turner, J. S., *Proc. Roy. Soc. Lon. A* **234**, 1–32 (1956).

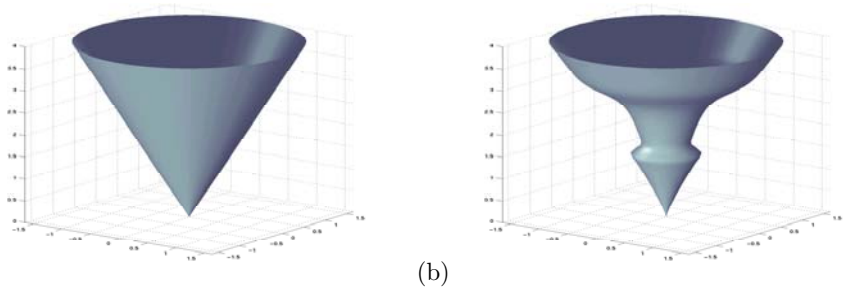

(a) (b)

Figure 1: (a) The 'well-known' steady Boussinesq plume shape. (b) Boussinesq plume that at some time t_0 has had its source buoyancy flux reduced.

Numerical Simulations of Rigid Fiber Suspensions

K. Gustavsson*, A.-K. Tornberg†

In this talk, we present a numerical method designed to simulate the dynamics of slender, rigid fibers immersed in an incompressible fluid. Fiber dynamics is of fundamental importance for understanding many flows arising in physics, biology and engineering. One typical example is paper-pulp, where the micro-structure of the suspension is made up of many fibers in a fluid. Here, we consider microscopic fibers that sediment due to gravity.

Our numerical algorithm is based on a non-local slender body approximation that yields a system of coupled integral equations, relating the forces exerted on the fibers to their velocities, which takes into account the hydrodynamic interactions of the fluid and the fibers. The system is closed by imposing the constraints of rigid body motion. The fact that the fibers are straight have also been exploited in the design of the numerical method [1].

Numerical simulations performed on a microscale offers the ability to obtain detailed information regarding the microstructure including interactions of individual fibers. It is well known that the shape of the particles have a large influence on the macroscopic properties of the suspensions and when the suspended particles are slender their orientation strongly affect the rheological properties of the flow. During sedimentation, a forming of clusters of fibers (flocculation) occurs which enhance the settling velocity to a value larger than the maximum speed of a single and vertically aligned fiber.

We present results from simulations including a large number of fibers in a periodic box and discuss averaged quantities such as mean sedimentation speed and fiber orientation and how these quantities are affected by cluster formation and vertical alignment of the fibers. We also present a more detailed study of how the sedimentation process depends on cluster size, cluster density and the orientation of fibers within the clusters.

*Royal Institute of Technology (KTH), Nada, S-100 44 Stockholm, Sweden
†Courant Institute of Mathematical Science, NYU, New York, USA
[1] Tornberg A.-K. and Gustavsson K., *J. Comput. Phys.* To appear (2006).

DNS of moving solids in viscous fluid : Application to rheology of complex fluids

P. Laure*, G. Beaume†‡ and T. Coupez‡

The orientation of long bodies (one dimension is much prevailing upon the other two) in liquids of different nature is a fundamental issue in a many problems of practical interest. In particular for composite material, the addition of spherical particles, short or long fibers to polymer matrix is well known to enhance the mechanical properties of composite material. The degree of enhancement depends strongly on the orientation of the fibers and the distribution or agregation of various particles in the final product. Then, a better knowledge of the motion of solid particles in polymer liquids is important for the design of molding equipment and determining the optimal processing conditions.

We propose a method to simulate fiber motions in flow by using finite element method with a multi-domain approach of two phases (namely a viscous fluid and rigid bodies). One must simultaneously solve the Stokes equations (governing the motion of the fluid having very high viscosity) and the equations of rigid-body motion (governing the motion of the particles). These equations are coupled through the no-slip condition on the particle boundaries. The rigid-body motion constraint is imposed by using a Lagrangian multipliers[1]. The main interest of this approach is that it is not necessary to give an explicit form of drag and lubrication forces acting between fibers.

However, it is not possible to simulate the motion of even a moderately dense suspension of particles without a strategy to handle cases in which particles touch. A collision strategy is a method for preventing near collisions by defining a security zone around the particle such that when the gap between particles is smaller than the security zone a repelling force is activated. Different repelling forces are proposed for spherical particles, but it is more complicated to express it for long fibers[2]. Our repelling force is based on the physics of elastic collisions occurring in the security zone[3].

Finally, computation are made for a large population of particles (fibers alone, fibers and spheres with different sizes). We point out that it is possible to get informations on macroscopic properties of fiber suspensions by averaging numerical results on an elementary volume. In this way, the influence of particle concentration and fiber aspect ratio on the "average" viscosity is analyzed.

*INLN, UMR 6618 CNRS-UNSA, 06560 Valbonne, France.
†Schneider Electric-Technocentre 38 TEC Grenoble
‡CEMEF, ENSMP-UMR 7635 CNRS, 06904 Sophia Antipolis, France

[1]R. Glowinski et al., *Int. J. Multiphase Flow* **25**, 755 (1999)
[2]Y. Yamane et al., *J. Non-Newtonian Fluid Mech.* **54**, 405 (1994)
[3]P. Laure et al., *Proc. of Computational Methods for Coupled Problems in Sci. and Eng.* (2005)

On the translational and rotational motion of ellipsoidal particles in a turbulent channel flow

P. H. M. Mortensen*, H. I. Andersson*, J. J. J. Gillissen†
and B. J. Boersma†

The translational and rotational motion of ellipsoidal particles suspended in a turbulent channel flow is being studied. The continuous fluid phase is solved by means of direct numerical simulation and a Lagrangian description of the dispersed particle phase is used to track the particle paths. In the particle translational equation of motion, the force acting on the particles is the steady Stokes drag. The rotational motion of the particles is achieved by solving the three Euler equations expressed in a coordinate system fixed to and rotating with the particles' mass center. The axes of this system are along the ellipsoids' principal directions of inertia. The complete orientation of the particles is described by the three independent Euler angles, but due to singularities for certain orientations, four dependent Euler parameters or quaternions are used for the orientational description [1] [2].
In the present case, the behavior of small ellipsoidal particles with an aspect ratio of 10 and non-dimensional momentum response time $\tau_p^+ = 0.18$ is investigated. It is well accepted that particles tend to accumulate in the viscous sublayer due to the action of near-wall coherent structures[3]. Figure 1(a) verifies this trend for small-inertia ellipsoidal particles where it is observed a peak in the instantaneous probability density function of particle position close to the wall. Figure 1(b) shows the mean orientation of the ellipsoids, i.e., the absolute values of the mean direction cosines of the particles' semi-major axis to the fixed wall-normal axis. It is observed that the particles tend to orient more towards the wall in the center of the channel. Close to the wall, the particles are more aligned with the wall.
The effect of varying the momentum response time, and also the inclusion of the hydrodynamic Saffman lift force, will be also be addressed in the presentation. The outcome of these effects will be compared and analyzed.

*NTNU Energy and Process Engineering, 7491 Trondheim, Norway.
†TU Delft J.M. Burgers centre, 2628 Delft, The Netherlands
[1] Goldstein, *Classical Mechanics*,2nd Ed., Addison-Wesley, Reading, Ma (1980).
[2] Fan and Ahmadi, *J. Aerosol Sci.* **31**, 1205 (1999).
[3] Marchioli and Soldati, *J. Fluid Mech.* **468**, 283 (2002).

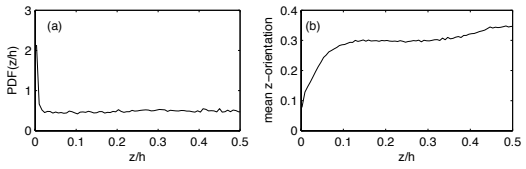

Figure 1: (a) Probability density function of particle position. (b) Mean direction cosine of particle semi-major axis to channel wall-normal axis.

Modelling Shear Flow Effects on the Fibre Orientation Distribution Function in a Planar Contraction

M. Hyensjö*and Anders Dahlkild†

The effect of turbulence generating vanes and its location in a planar contraction on fibre orientation anisotropy was studied by mathematical modelling. We use single phase CFD modelling as an input for the fibre orientation dispersion model to study the effect of shear flow and turbulence in an accelerated fluid flow on fibre orientation anisotropy. The fibre dispersion model is based on a Fokker-Planck equation[1], which describes the evolution of the fibre orientation probability distribution function in a flow field. We consider a plane case, for one orientation angle in the symmetry plane[2] of the contraction, and also the case of a 3D fibre orientation described with two orientation angles. The rotational angular velocities are based on the flow around a fibre with high aspect ratio, but without spatial extension[3]. The two models have been compared to experimental data[4]. For different streamlines in the contracting channel, the fibre orientation distribution function is obtained numerically, and the fibre orientation anisotropy could be studied along streamlines near the vane wall and vane tip and further away downstream. In figure 1 (a), (b) and (c) example on outlet fibre orientation distributions are shown for a wake, a undisturbed region and a wall boundary layer respectively. A higher degree of orientation can be seen in the undisturbed region, i.e. cf. figure 1 (b). In the wake region, cf. figure 1 (a), for a plane γ=0, the preferred orientation angle is shifted towards β values smaller than π /2, i.e. fibres are oriented upwards, the opposite effect is shown for the wall boundary layer, cf. figure 1 (c). For the wake region of the outlet profile of the contraction the fibre orientation anisotropy was decreased by moving the vane tip closer to the outlet.

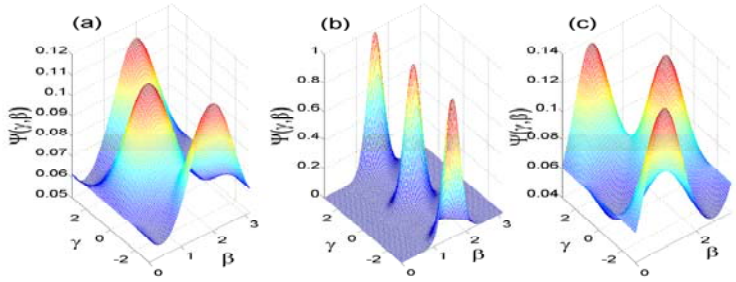

Figure 1: (a) The wake region. (b) The undisturbed region. (c) The boundary layer

*Metso Paper Karlstad AB, SE-651 15 Karlstad, Sweden.
†KTH Mechanics OB 18, SE-100 44 Stockholm, Sweden.
[1]Advani and Tucker, *Journal of Rheology*, 31(8) (1987).
[2]*Hyensjö*, Krochak, Olson, *Hämäläinen* and Dahlkild, *In Proc. ICMF'04, Yokohama*, (2004).
[3]Jeffrey, *Proc. R. Soc.*, 102(A) (1922).
[4]Asplund and Norman, *Journal of Pulp and Paper Science*, 30(8) (2004).

A Shell-Model Study of Turbulent Drag Reduction by Polymer Additives

Emily S.C. Ching[a]

The addition of long-chain polymers to turbulent flows can result in a significant reduction of the friction drag. This intriguing phenomenon was discovered more than fifty years ago but many fundamental aspects remain poorly understood. Recent direct numerical simulations of the finitely extensible nonlinear elastic-Peterlin (FENE-P) model equations of viscoelastic flows demonstrated that drag reduction also appears in homogeneous and isotropic turbulence. The FENE-P equations were further simplified to a shell model of viscoelastic flows. Using this shell model, we understand[1] two main features observed in experiments, namely, the onset of drag reduction and the maximum drag reduction asymptote. Moreover, we are able to recapture[2] the essence of the phenomenon of drag reduction by replacing the polymers with an effective scale-dependent viscosity.

This work is supported by the Hong Kong Research Grants Council (CUHK 400304).

[a] Department of Physics, The Chinese University of Hong Kong, Shatin, N.T., Hong Kong.

[1] Benzi et al., *Phys. Rev. Lett.* **92**, 078302 (2004).

[2] Benzi et al., *Phys. Rev. E* **70**, 026304 (2004).

Scale energy budget for a viscoelastic wall-bounded flow

E. De Angelis*, N. Marati, C.M. Casciola, R. Piva.

In isotropic conditions polymers affect the turbulent cascade of kinetic energy and deplete the inertial transfer below Lumley scale [1]. In the context of drag reduction, anisotropy and inhomogeneity can be included in the analysis by extending to drag-reducing viscoelastic flows the scale energy budget for a Newtonian channel flow [2],

$$\frac{\partial\langle\delta q^2\delta u_i\rangle}{\partial r_i} + \frac{\partial\langle\delta q^2\delta U\rangle}{\partial r_x} + 2\langle\delta u\delta v\rangle\left(\frac{dU}{dy}\right)^* + \frac{\partial\langle v^*\delta u^2\rangle}{\partial Y} = -4\langle\epsilon^*\rangle +$$
$$2\nu\frac{\partial^2\langle\delta q^2\rangle}{\partial r_i\partial r_i} - \frac{2}{\rho}\frac{\partial\langle\delta p\,\delta v\rangle}{\partial Y} + \frac{\nu}{2}\frac{\partial^2\langle\delta q^2\rangle}{\partial Y^2} + 4\frac{\partial\langle T^*_{ij}\delta u_i\rangle}{\partial r_j} + \frac{\partial\langle\delta T_{i2}\delta u_i\rangle}{\partial Y} - 4\langle\epsilon^*_P\rangle\,,$$

where $\langle\delta q^2\rangle = \langle\delta u_i\delta u_i\rangle$ is the scale-energy as a funtion of the separation vector r_i and of the mid-point $X_i = x_i + r_i/2$, the asterisk denote a mid point average and ϵ and ϵ_P are the Newtonian and polymer dissipations. According to the equation, the local conservation of scale-energy implies that the local source of scale energy – the sum of local production and the amount intercepted from the spatial flux – feeds the inertial cascade and the transfer towards the microstructure, see fig. 1. In the Newtonian plug of mildly drag-reducing flows the behavior is easily explained given the budget in the log-layer of Newtonian flows[2] and the effect the polymers have on the cascade[1]. Closer to the wall the polymers are much more active and directly interfer with the production process. As will be discussed in detail, in this elastic layer an entirely different picture emerges consistent with the alteration of the energy containing scales of the flow which entails dramatic consequences for the drag experienced at the wall.

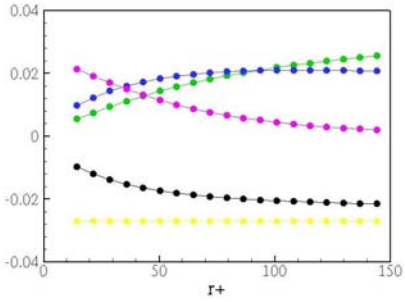

Figure 1: Scale-energy budget in the Newtonain plug: Force-velocity correlation —, inertial and polymer transfer (—, —), viscous diffusion —, polymer and Newtonian dissipation (—, —).

[1] De Angelis E., Casciola C.M., Benzi R., Piva R., *J. Fluid Mech* **476**, 105-114 (2003).
[2] Marati N., Casciola C. M., Piva R. (2004), *J. Fluid Mech* **521**, 191-215 (2004).

*Dip. di Meccanica e Aereonautica, "La Sapienza", via Eudossiana 18, 00184, Roma, Italy

Using CSP for Modeling Burgers-Turbulence

B. Müller*, D. A. Goussis† and B. Rogg *

The usual way to get results with sufficient accuracy by solving the Burgers-equation is to apply LES. In our work we investigated the *Computational Singular Perturbation*-method (CSP) for reducing stiff ODE- systems, which occur by the simulation of chemical elementary-reactions. It works *without* filtering and grid-coarsening. The CSP-algorithm not only simplifies Chemical Kinetics, but its data can give insights into the physics and chemistry of the elementary- reactions as well. Thus it is possible to detect the occurence of radicals by the so called *Radical pointer*. [1] CSP transforms the ODE-system to a new set of basis-vectors $\mathbf{a}_i$ that it can be expressed by $d\boldsymbol{\eta}/dt = \sum_{i=1}^{N} \mathbf{a}_i f^i$, where $\boldsymbol{\eta} = [\eta_1, ..., \eta_N]$ is the vector of the chemical species and f^i a "transformed" netto-reaction rate, called *amplitude*. Then every mode $\mathbf{a}_i f^i$ represents a timescale. Our aim was to simplify the ODE-system of the discretized Burgers-equation by using the CSP-algorithm. For that we translated the concept of the *Radical pointer* for the fastest mode ($i = 1$) ($RP(1)$) into the turbulent system. $RP(1)$ is given by the diagonal-elements of $\mathbf{a}_1\mathbf{b}^1$, where $\mathbf{b}^1 \odot \mathbf{a}_1 = 1$. It is a projection from each of the N velocity nodes into the fastest mode. Fig. 1 (left) shows that the maximum of $RP(1)$ is exactly on the place where $\partial v/\partial y$ *and* $\partial v/\partial t$ have their maximal values. During the first timesteps this peak tapers off and increases but at a certain timepoint ($t \approx 0.3$) it remains quasi constant until $t \to \infty$. The temporal evolution of $RP(1)$ indicates that since this timepoint the nodes with *non-negligible* $\partial v_i/\partial t$ are concentrated *only* in the shock-region. Then we can choose a (small) limit-value of $RP(1)$ and set at this limit right and left from the peak $\partial v_i/\partial t = 0$. Fig. 1 (right) shows the solution of the ODE-system simplified in this way. We can conclude that $RP(1)$ not only is a tool for simplifying, but also its shape and length give insights in the spatial distribution of the smallest turbulence structures.

*Ruhr-Universität Bochum, Lehrstuhl für Strömungsmechanik IB 6/145, Universitätsstrasse 150, D-44780 Bochum, Germany.

†Department of Mechanical and Aerospace Engineering, University of Patras, Patra, Greece.

[1] Lam and Goussis, *Int. J. of Chemical Kinetics* **26**, 461-486 (1994).

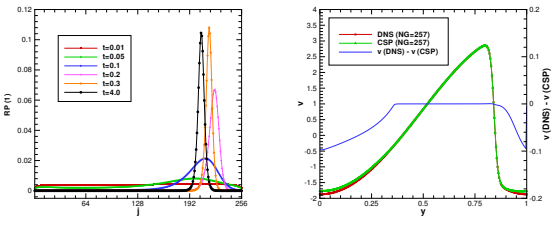

Figure 1: left: Temporal evolution of the Radical pointer into the fastest mode by DNS. right: Differences in solution between DNS and CSP-Modeling at $t = 0.3$.

A Leray Type Regularization for Low-dimensional POD-Galerkin Systems

F. Sabetghadam*, S. Sharafatmandjoor†

In recent years, Leray regularization of the Navier-Stokes equations has been used fairly extensive to manipulating the energy spectrum and improving the dissipation characteristics in the turbulent flow simulations. The main advantage of the method is that the resulting equations, usually called the Navier-Stokes-α equations, preserve the structures and statistics of the large scales without need to fully resolve the fine scales [1].

On the other hand, one of the most popular low-dimensional modelling of turbulent flows is the POD-Galerkin method. However, in many cases in the turbulent flow simulations, the resulting POD-Galerkin ODE systems have been observed to be unstable or , in the stable cases, can converge to wrong attractors. To improve the behavior of these low-dimensional models, a variety of methods have been suggested and tested. Methods like definition of the POD modes in H^1 Sobolev space instead of L^2 space, optimization of the POD eigenmodes[2], non-linear Galerkin projection and introducing the eddy viscosity or spectral vanishing viscosity[3].

In this article, inspired by the Leray regularization, a new method of improving behavior of the POD-Galerkin systems is suggested and assessed. The method consists of replacement of the non-linear terms, in the Galerkin projection of the Navier-Stokes equations, by their filtered ones. Because of using a filter with an α width, the method can be called the POD-α modelling. The method is assessed for a two-dimensional turbulent flow and the primary results show steeper decreasing in the energy spectrum for high wave numbers in comparison to the classical POD-Galerkin model and more stability of the model for a variety of chosen snapshots.

*Assistant Prof., Science & Research branch, IAU, Tehran, Iran.
†PhD student, Science & Research branch, IAU, Tehran, Iran.

[1] Chen etal, Physica D 133 (1999) 66-83.
[2] Couplet etal, Journal of Computational Physics 207 (2005) 192-220.
[3] Sirisup and Karniadakis, Journal of Computational Physics 194 (2004) 92-116.

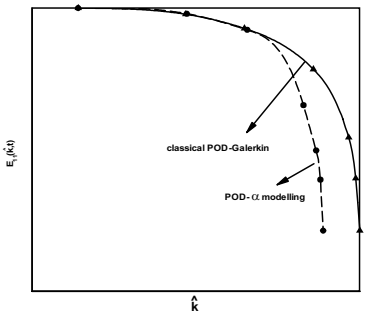

Figure 1: comparison of the energy spectrums for the POD and POD-α models

High Spatially Resolved Velocity Measurements of Turbulent Flows with a Fiber-Optic Velocity-Profile Sensor

K. Shirai[a], C. Bayer[a], T. Pfister[a], A. Voigt[a],
L. Büttner[a], J. Czarske[a], H. Müller[b], G. Yamanaka[c],
S. Becker[c], H. Lienhart[c], F. Durst[c]

In turbulent flows, choice of measurement techniques with a sufficient temporal and/or spatial resolution is important to resolve the scale of interest in the flow. Hot-wire (HWA) and laser Doppler anemometries (LDA) have been most commonly used for the measurement of turbulent flows, due to their advantage of relatively high temporal /spatial resolution. However, the spatial resolutions are restricted to their finite size of the measurement volumes. The velocity information is spatially averaged over the measurement volume and it hinders smaller scale motions compared to the volume and variation of velocity inside the volume. This occurs either when the flow Reynolds number increases and smaller the turbulence scale becomes or/and when there is a steep velocity gradient in the flow.

The laser Doppler velocity-profile sensor was proposed to overcome this problem[1,2]. It utilizes two optical fringe systems (e.g. diverging and converging). The measured two Doppler frequencies determine the position as well as velocity of single tracer particles passing through the measurement volume. Hence, it has a high spatial resolution inside the measurement volume and the velocity profile is obtained without traversing the measurement head many times. The technique was successfully applied to laminar boundary layers[3].

The profile sensor has a potential to be applied to challenging investigations of turbulent flows where a high spatial resolution is required. In this paper we will report on the development of a profile-sensor system and its application to turbulent boundary layers.

A fiber-optic heterodyne laser-Doppler velocity-profile sensor is developed with the aim of measuring turbulent statistics with a high spatial resolution. It has a spatial resolution of about 10 micrometers inside the measurement volume of about 1 mm length. It has already been successfully applied to resolve the velocity profile of a laminar boundary layer close to the wall, and also to a fully developed turbulent channel flow with low Reynolds number.

Currently we are working on the second generation sensor. Refined optical system and signal processing techniques will enable precise measurements of particle velocity with a high spatial resolution. Highly spatially resolved turbulent statistics will be provided in a fully developed turbulent flow with a moderately high Reynolds number condition. Measurements in a free shear flow from a jet are also going to be carried out to provide the statistics of the two-point correlation of streamwise velocity.

---

[a] Dresden University of Technology, Helmholtzstraße 18, 01069, Dresden, Germany
[b] Physikalisch-Technische Bundesanstalt Braunschweig, Bundesallee 100, 38116, Braunschweig, Germany
[c] Institute of Fluid Mechanics, Cauerstr. 4, 91058, Erlangen, Germany

[1] Czarske, *Meas Sci Technol* **12**, 52 (2001).
[2] Czarske et al., *Meas Sci Technol* **13**,1979 (2002).
[3] Shirai et al., *Flow Meas Instrum* **16**, 221 (2005).

Combined Velocity and Temperature Measurement in a Buoyancy Induced Ring Vortex

S.M.M. Salim[a], J.G.C. Kunnen[a], C.C.M. Rindt[a] and A.A. v. Steenhoven[a]

A combined velocity and temperature measurement in a buoyancy induced vortex ring was conducted. The vortex ring was produced by a droplet of Rhodemine B solution falling into a small tank filled with a solution of equal concentration but higher temperature. The main target was to test the accuracy of a combined velocity and temperature measurement technique using a pulsed laser. Additionally, a dye-visualization was conducted to understand the formation process of the ring vortex.

The experimental setup consists of a small tank filled with a Rhodamine B solution (1.0×10^{-4}mol/m^3) seeded with hollow spherical 10μm particles. A 29 Hz single pulsed Nd:YAG laser (532nm wavelength) was used as a lightsource. A 1.0 mm thick light sheet was created. Two 10-bit CCD cameras were used to capture the PTV and LIF images. A high pass filter of 532nm was put in front of the camera which captures the LIF signal emitted by the Rhodamine B (wavelength around 575nm) in order to block the light intensity scattered by the particles.

To obtain the temperature field an innovative correction method was developed to correct for the spatio-temporal variations of the Nd:YAG laser intensity. The correction is local and based on a correction line by line. The method requires knowledge of the temperature field in part of the image.

The velocity field is measured to see if the flow field could be resolved in the vortex cores which have a maximum outer diameter of 20mm. Figure 1(a) and (b) show the vorticity field as derived from the measured velocity field and the vorticity distribution along a line through the vortex cores. It can be concluded that the flow field can be resolved with high accuracy. Figure:1(c) shows the temperature field as measured in a different realization using the correction method. The result clearly shows the low-temperature vortex cores (Note different scale). The present method will be used for investigation of the 3D wake behaviour behind a heated cylinder[1].

---

[a] Energy Technology Group, Mechanical Engineering Department, Technische Universiteit Eindhoven, The Netherlands

[1] Ren et al., *Physics of Fluids* **16** (8): 3103 – 3114 (2004)

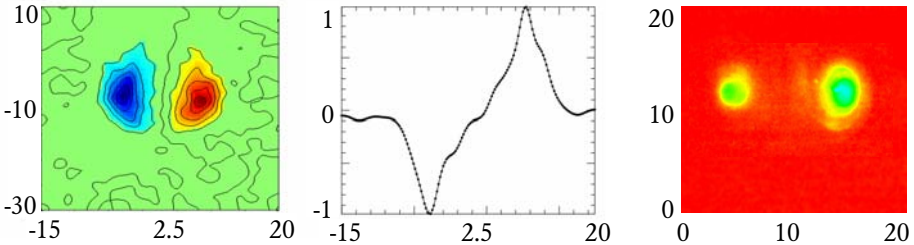

Figure1: (a) vorticity field (b) one line vorticity (c) temperature distribution

LOCAL HIGH-RESOLUTION WALL-SHEAR-STRESS MEASUREMENTS IN A TURBULENT BOUNDARY LAYER USING A MICRO-PILLAR BASED SENSOR CONCEPT

S. Große[a], Chr. Brücker[b], W. Schröder[a]

Local high-resolution wall-shear stress measurements in a turbulent boundary layer on a flat plate were carried out using a new MEMS-based sensor concept[1]. The micro-fabricated film-type sensor consists of flexible micro-pillars, which protrude from the wall into the viscous sublayer and bend in reaction to the applied fluid forces and the internal elastic strain. The wall-shear-stress distribution is determined by optical detection of the pillar bending in magnitude and direction and by applying the relation of the wall shear as a function of the mean velocity gradient at the wall. The pillars with diameters of a few micrometers are manufactured from elastomers (poly-dimethylsiloxane, PDMS) such that they are very flexible and easily deflected by the fluid forces.

In a recently performed feasibility study a single micro-pillar was mounted on the channel wall, so that the local shear stress could be detected. The experiments were carried out in the low-speed wind-tunnel facility of the Laboratoire de Mécanique de Lille. Local Reynolds numbers based on the momentum thickness Re_θ during the measurements reached from 6800 to 17800.

The data presented below was recorded with 20.1 Hz (1024 samples) to allow the calculation of averaged wall-shear-stress values. The experimental results are in very good agreement with theoretically predicted values for the wall-shear-stress in a turbulent boundary layer (figure 1). Figure 2 exemplarily shows the highly turbulent character of the wall-shear stress for 10 m/s freestream velocity.

In upcoming experiments a row of sensor elements will allow the simultaneous measurement of the wall-shear-stress distribution along a streamwise line parallel to the wall. Measurements with an array of pillars in channel flow are also under preparation enabling very high spatial resolution of the planar wall-shear-stress distribution.

---

[a] Institute of Aerodynamics, RWTH Aachen University, 52062 Aachen, Germany
[b] Institute of Mechanics and Fluid Dynamics, TU Bergakademie Freiberg, 09596 Freiberg, Germany
[1] Brücker, Spatz, Schröder, *Proc. 10th European Turbulence Conf.*, 040H, (2004)

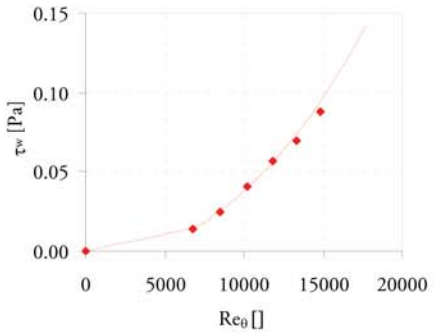

Figure 1: Wall shear stress as a function of the Reynolds-number based on the friction velocity. Experimental (♦) and analytical (-) wall shear stress.

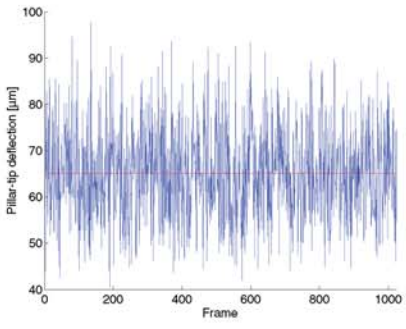

Figure 2: Pillar-tip displacement in pixels at 10 m/s freestream velocity. Recording of 1024 frames with a recording frequency of 20.1 Hz.

Dynamic Lift of Airfoils

R. Grüneberger, T. Bohlen, S. Barth and J. Peinke *

For airfoils it is known that the lift coefficient c_L depends not only on the angle of attack α but also on the steadiness of the flow. Varying the angle of attack with an angular velocity $\omega = \partial\alpha/\partial t$ the lift force for angles larger than the steady stall angle clearly depends on ω, too, i.e. $c_L = f(\alpha, \omega)$. Variations of α and ω can be either due to different pitch angles of the airfoil or due to fluctuations of amplitude and direction of the flow as it is the case for wind turbines in atmospheric boundary layers.

We present wind tunnel measurements. In order to quantify the dynamic stall effect, the lift of an FX79-W-151A airfoil, which is for use on wind turbines, is determined by the integral pressure distribution at the wind tunnel walls while rotating the airfoil with defined angular velocities ω. The rotation speed is varied by numeric control. The pressure measurement is performed by two sets of 40 pressure sensors at each side wall of the wind tunnel. The temporal resolution of the pressure measurement is in the range of milliseconds. For stochastic analysis the experiment is repeated several hundred times. In contrast to static lift values, there is an increase (overshoot) of lift before flow separation on the suction side occurs, dependent on ω, see Fig 1.

This knowledge of the maximum lift forces is relevant for the estimation of extreme mechanical loads on wind turbine blades and therefore of special interest for wind turbine manufacturers.

*ForWind - Center for Wind Energy Research - University of Oldenburg

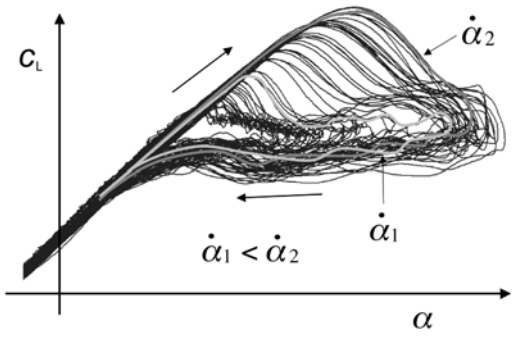

Figure 1: Increase of the maximum lift coefficient c_L with increase of the angular velocity $\omega = \dot{\alpha}$.

Session 3

Experimental study on the boundary layer transition induced by a shallow 3D roughness element

I. B. de Paula*†, M. A. F. de Medeiros*, W. Würz†, M. T. Mendonça‡

The influence of shallow 3-D roughness element on the evolution of a 2-D Tollmien-Schlichting wave was studied experimentally. The current measurements were carried out in a Blasius boundary layer. The cylindrical roughness element used was oscillated slowly as a quasi-steady disturbance. Therefore, the hot wire signal could be ensemble averaged in order to reduce the experimental noise. In the present work the 2-D wave was excited artificially with 2 different amplitudes. These amplitudes were selected according with numerical simulations provided by a PSE code. Thus, it was possible to select previously the bandwidth of oblique waves amplified by the fundamental resonance mechanism. Using this approach was possible to check how shallow roughness elements can affect the boundary layer transition. For roughness heights below $0.25\delta^*$, the bandwidth of amplified oblique waves observed downstream was in good agreement with the one predicted by secondary instability theory. For roughness higher than $0.25\delta^*$ the distribution of oblique modes amplitudes and growth started to deviate significantly from prediction. The results show that the value of critical roughness height which can affect the boundary layer transition is dependent of the threshold for self sustained k-type transition. These observations suggests that critical roughness height which can affect the boundary layer transition is dependent not only of the boundary layer thickness but also of TS wave amplitude.

Figures (a) and (b) show the comparison between theoretical and experimental normalized amplitude distribution of oblique modes. The comparison was made considering the amplitudes 105mm downstream the roughness. In figure (a) the TS amplitude at the roughness was adjusted to 0.45% and in figure (b) to 0.75%. This project was supported by CAPES and FAPESP from Brazil.

*Universidade de São Paulo - EESC, São Carlos, Brazil
†Universität Stuttgart - Institute für Aerodynamik und Gasdynamik IAG, Germany
‡Instituto Técnico Aeroespacial ITA - IAE, São José dos Campos, Brazil

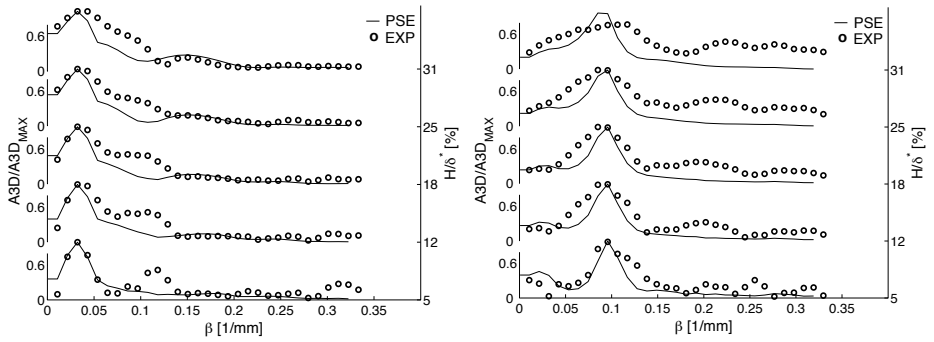

Flow visualization of relaminarization in a two-dimensional channel flow

M. Matsubara*and T. Matsuzawa*

In viscous flows, there exists the minimal Reynolds number at which flow sustains turbulent state against viscous dissipation. Around this Reynolds number the Kolmogorov scale is in same order of the large structure of turbulence correspond to flow geometry so that, in a sense, it is more facile to observe turbulent structure and sustain mechanism in experimental methods though there is no inertial subrange at all. On the other hand, a great deal of research effort has been put on seeking periodical solutions at relatively low Reynolds number in canonical flows such as channel or pipe flows.

In this research we focus on experimental observation of relaminarization from fully developed turbulence to laminar by the viscous effect in a two dimensional channel flow. In previous experiments the minimal Reynolds number based on the maximum velocity as in Poiseuille profile and half channel width has already been estimated at about 2100 by extrapolation of decay of Reynolds stress[1]. There is another estimation of 1000 to be determined observing turbulent spot generation with large point-like initial disturbance[2]. Our experiment attempt to decide the minimal Reynolds number in the channel flow and investigate disturbance structures at such low Reynolds number.

A 2 m length test cannel with 5 mm width and 260 mm span is following a 1 m expansion channel and a 1m pre-developping channel with tripping wires at its inlet. The expansion channel has 2 degree diffuse angle at the end walls so that the Reynolds number is reduced 2/3 of the inlet value. Flow visualization (figure 1) shows that at Reynolds number of 1340 the flow state is turbulence with relatively large spanwise scale of streaky structures. Around Reynolds number is 1100, the flow undergoes relaminarization with characteristic structures of disturbance that elongate in the streamwise direction with forming a cluster. Downstream of the cluster a new elongated structure is generated one after another and its upstream the structures are disappearing. For Reynolds number less than 960 flow becomes complete laminar, so that the minimal Reynolds number is between 960 and 1340

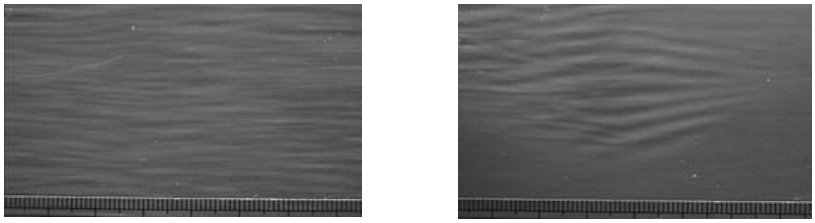

(a) Re=1340 (b) Re=1100

Figure 1: Flow visualization of relaminarization in two dimentional channel flow.

*Shinshu Univ. Mechanical systems engeneering, Wakasato 4-17-1, 380-8553 Nagano, Japan.

[1]M. A. Badri Narayanan, *J. Fluid Mech.* **31**, 609 (1968).
[2]D. R. Carlson et al., *J. Fluid Mech.* **121**, 133 (1982).

Natural sinuous and varicose breakdown during bypass transition

J. Mans*, H.C. de Lange and A.A. van Steenhoven

It is well known that in boundary layers exposed to high levels of free-stream turbulence (>5%), as for instance present in gasturbines, transition occurs rapidly bypassing the natural transition mechanism. The breakdown to turbulence is initiated by a secondary instability on low- and high-speed streaks. This natural (non-triggered) secondary instability has been studied using a water channel. The visualization results reveal the presence of a sinuous and varicose secondary instability mode[1].

In this contribution the main features in the development of the natural sinuous and varicose secondary instabilities are determined. Therefore, velocity and visualization fields are measured using a combined PIV-LIF technique mounted on a traversing system. By setting the translation speed of the traversing system approximately equal to the group velocity of the natural instability the developments in a 'contained' fluid area around an instability are determined. The measurement results show that in the sinuous secondary instability mode multiple low- and high-speed streaks are involved, which interact with each other in spanwise direction. In the varicose case only two streaks are active, a streamwise interaction is present between a high-speed streak which frontally runs into a low-speed streak. Both instabilities show a clear resemblance with the numerical result from the KTH[2]. In addition, the results show that in both instabilities discontinuities occur in the streak configuration. A strong interaction between the local low- and high-speed streaks appears at the discontinuity locations. Vortices appear in the vicinity of these locations during the development of the streaky base flow in streamwise direction. The vortices result in the presence of the typical sinuous (staggered vortex configuration) or varicose motion (symmetrical vortex configuration), see figure 1. The experiments are the first to show the development of the spatial structure during breakdown.

From the preceding transition 'mechanism' it is clear that the strong streak interactions at the discontinuities play an important role in the transition process. Ongoing stereo PIV measurements will elucidate the character of the discontinuity phenomena which may possibly identify the 'key initiation' factor of bypass transition.

*Technische Universiteit Eindhoven, P.O.Box 513, 5600 MB Eindhoven, The Netherlands.

[1]Mans et al., *Exp. Fluids.* **39(6)**, 1071 (2005).

[2]Brandt et al., *J. Fluid Mech.* **517**, 167 (2004).

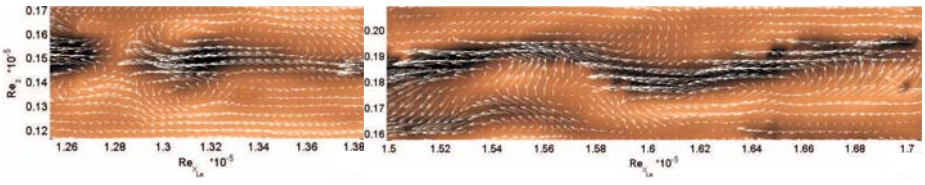

Figure 1: The varicose (left) and sinuous (right) velocity fields during breakdown.

Spot-like structure in freestream induced transitional flow

A. C. Mandal*, L. Venkatakrishnan†, J. Dey*

At high freestream disturbance levels, the breakdown process begins with the appearence of spanwise streaks [1, 2, 3], and finally spots originate near the boundary layer edge [3]. We report the spot-like structure inferred from our particle image velocimetry (PIV) measurements in a grid-induced transitional flow in a constant pressure boundary layer. The measurements are made on a flat plate with a black sticker stuck to it to avoid reflection. The PIV data here are for the wall normal plane. 532 PIV realizations were collected.

Figure 1a shows the breakdown feature at 1 % flow intermittency; the vectors here are the fluctuating velocity field in the background of v disturbance; darker region: $v < 0$, light white: $v > 0$.

The contours of the streamwise fluctuating velocity component (u) in figure 1b shows a layer of negative u sitting on a layer of positive u in $7 \leq x_1/\delta^* \leq 12$. This feature is seen in artificial turbulent spots[4, 5]; the calm region of positive u upto $x_1/\delta^* \approx 0$ is also similar to that in a turbulent spot[5]. This breakdown scenario is similar to a turbulent spot. However, it is not clear at this stage, whether it represents a single spot or parts of multiple spots. This similarity with an artificial turbulent spot observed here in an actual transition has not been reported in the available literature.

*Department of Aerospace Engineering, Indian Institute of Science, Bangalore-560012, India.
†EAD, National Aerospace Laboratories, Bangalore-560012, India.

[1] Kendal, *AIAA paper* 85-1695 (1985).
[2] Matsubara and Alfredsson, *J. Fluid Mech.* **430**, 149 (2001).
[3] Jacobs and Durbin, *J. Fluid Mech.* **428**, 185 (2001).
[4] Wygnanski et al., *J. Fluid Mech.* **123**, 69 (1982).
[5] Singer, *Phys. Fluids* **8**, 509 (1996).

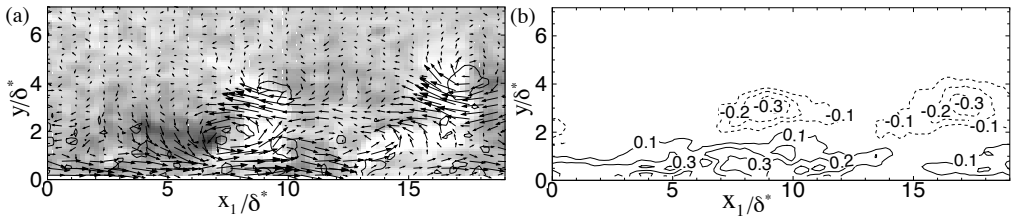

Figure 1: (a) Fluctuating velocity vectors in the background of v: dark- $v < 0$; light white- $v > 0$. Line contour: swirl strength. (b) u/U_0 contours.

Disturbance growth in boundary layer subjected to anisotropic free stream turbulence

T. Kenchi*and M. Matsubara*

In a flat plate boundary layer subjected the isotropic free stream turbulence of few percents turbulence intensity, the streaks, which streamwisely elongated regions of high and low streamwise velocity, form in the boundary layer and then break down to turbulent spots. Experiments[1] [2] and DNS[3] have revealed that the profile of the streamwise fluctuation energy has a peak at the middle of boundary layer and that the disturbance grows in proportion to the streamwise distance from the leading edge. These results are in good agreement with the non-modal theory[4]. However, which directional component of free stream turbulence dominates the growth of boundary layer disturbance has not been obvious. The present experiment focused on revealing effect of directional components of free stream turbulence on the boundary layer transition by means of hot-wire measurements and smoke visualization. An anisotropic free stream turbulence generated by a static turbulence grid placed at the inlet of the contraction has 0.7 % turbulence intensity comparatively smaller than in a isotropic turbulence generated by a grid at the contraction exit. In order to reach the same turbulence intensity as the isotropic case jets were emitted upstream from small holes on turbulence grid bars.

In both of the isotropic and anisotropic free stream turbulence cases, disturbance energy growth is proportion to the streamwise distance from the leading edge, correspond with non-modal growth. The growth rate is well normalized by wall normal components so that disturbance energy growth is dominated by wall normal components of free stream turbulence. In a case of weak and anisotropic free stream turbulence, however, new phenomenon that the peak value in the velocity fluctuation suddenly shifts close to the wall and increase up to more than 10 % is observed before the non-modal growth reach the break down intensity. Λ shape structures conformed in flow visualization at the same Reynolds number where the phenomenon is observed seems to play an important role in the final stage of the transition.

Figure 1: Smoke visualization for weak anisotropic case. $3.6 \times 10^5 \leq Re_x \leq 4.3 \times 10^5$

*Shinshu University. 4-17-1 Wakasato, Nagano, 380-8553, Japan

[1]M. Matsubara and P. H. Alfredsson, *J. Fluid Mech.* **430**, pp.149-168 (2001).
[2]J. H. M. Fransson et al., *J. Fluid Mech.* **527**, pp.1-25 (2005).
[3]R. G. Jacobs and P.A.Durbin., *J. Fluid Mech.* **428**, pp.185-212 (2002).
[4]P. Luchini, *J. Fluid Mech.* **404**, pp.289-309 (2000).

Numerical simulation of the three-dimensional fluid-structure interaction of a bileaflet mechanical heart valve

A. Cristallo*, R. Verzicco* and E. Balaras†

The complex turbulent flow patterns downstream of mechanical bileaflet valves are to a large extent responsible for the thromboembolic complications that remain a major concern after surgery. High levels of shear stresses are generally accepted as responsible of hemolysis and platelet activation. To illuminate the detailed dynamics of the flow in the vicinity of such valves we have performed Direct Numerical Simulations of the flow in a mechanical heart valve. The selected shape and size of the leaflets roughly mimics the SJM Standard bileaflet valve and the overall set-up resembles the one commonly used in in-vitro experiments. A three-dimensional unsteady flow analysis is performed using an Immersed Boundary approach[1] at physiological Reynolds numbers. A fluid structure interaction algorithm is also developed to achieve the leaflet motion. The forces exerted by the fluid on the leaflets are computed at each time step and applied to the leaflet equation of motion in order to predict the new leaflet position. Several complete cycles, including opening and closing phases, are simulated; the valve opens at the beginning of the systole and closes before the beginning of the diastole[2]. In figures 1(a) and (b) two instantaneous snapshots of the flow during the closing phase are shown while figure 1(c) reports the angular position of one of the leaflets in time together with the typical physiological aortic flowrate. Relatively large velocities are computed in the valve clearance region between the valve housing and the leaflet edge with the resulting relatively large wall shear stresses measured during the closing and leaking phases. Indeed, during the opening and fully open phases, the vortices originating from the leaflets and the housing dominate the flow in the downstream proximal area and are responsible for most of the production of turbulent stress.

*DIMeG & CEMeC Politecnico di Bari, Via Redavid 200, 70125 Bari, Italy.
†Dept. of Mechanical Engineering, University of Maryland, College Park, MD 20742.

[1] Cristallo A. and Verzicco R., Combined Immersed Boundary/Large-Eddy-Simulations of Incompressible Three Dimensional Complex Flows *FTaC* 2005 in press.

[2] Yoganathan A.P., He Z. and Jones C., Fluid Mechanics of Heart Valves *Annu. Rev. Biomed. Eng.* **6**, 331-62 (2004).

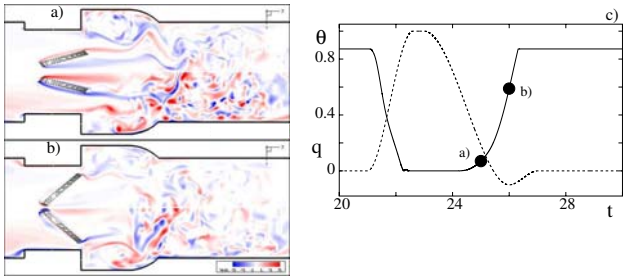

Figure 1: (a) and (b) Instantaneous snapshots of azimuthal vorticity on meridional sections during the closing phase. (c) Time evolution of the upper leaflet angular position (solid) and of the flowrate (dashed).

Experimental investigation of vitreous humour dynamics

C. Cafferata*, R. Repetto† and A. Stocchino *

The vitreous chamber is the region of the eye comprised between the lens and the retina. This portion of the eye globe is filled by a viscoelastic material, the vitreous body, the characteristics of which are significantly variable with age. In young people the vitreous is a gel like material and, with ageing, it typically deteriorates, losing its elastic properties and showing areas of partially or totally liquefied vitreous. During saccadic eye movements the vitreous body exerts a time dependent shear stress on the eye wall. This action, associated to retinal breaks or tears, is a possible cause of retinal detachment. We present experimental results on the vitreous dynamics, achieved employing a magnified model of the vitreous chamber. The model consists of a cavity carved in a perspex cylindrical container, which is filled with a highly viscous Newtonian fluid, i.e. pure glycerol. Two different sets of experiments have been performed: in the first one the cavity was perfectly spherical while in the second set the sphere was deformed by a protrusion that simulates the presence of the lens in the anterior region. The eye model has been mounted on the shaft of a computer controlled motor which rotates with a prescribed time law. We first modelled the eye movements with a sinusoidal time law and then with a more complex time law reproducing real saccadic movements. Measurements of the two-dimensional flow field on the equatorial plane have been carried out through the PIV technique. For the spherical model, theoretical results based on a simplified solution [1] are in fairly good agreement with experimental findings as reported in Repetto et al. (2005)[2]. In the present work we focus our attention on the effect of the presence of the lens on the flow field. The experimental measurements show that the velocity fields are strongly influenced by the deformed geometry of the domain. In particular, the formation of a vortex in the neighbourhood of the lens, which migrates toward the center of the domain, is invariably observed regardless the amplitude and the frequency of the prescribed oscillation. Starting from the two dimensional flow fields, the vortical structure is tracked during a period of oscillation by means of a vortex identification technique. Moreover, we calculate the tangential and normal stresses acting on the rigid boundary of the domain. We observe regions along the boundary with a higher concentration of stresses with respect to the spherical case, where the stresses are uniformly distributed. Finally, the existence of a secondary circulation induced by the deformed geometry is enlightened by calculating particle trajectories starting from the measured flow fields. Such a secondary motion may play an important role on the mixing processes that take place inside the eye globe.

*Diam, via Montallegro 1, 16145 Genova, Italy.
†Disat, Monteluco di Roio, 67040 L'Aquila, Italy.
[1] David et al., *Phys. Med. Biol.* **43**, (1999).
[2] Repetto et al., *Phys. Med. Biol.* **50**, (2005).

Effects of the flexibility of the arterial wall on the wall shear stresses in Abdominal Aortic Aneurysms

A. V. Salsac[a], M. Fernández[b], P. Le Tallec[c] and J. M. Chomaz[d]

As an abdominal aortic aneurysm forms and develops, large changes occur in the composition and structure of the arterial wall, which result in its stiffening. So far, most studies, whether experimental or numerical, have been conducted assuming the walls to be rigid. A numerical simulation of the fluid structure interactions is performed in different models of aneurysms in order to analyze the effects that the wall compliance might have on the flow topology and on the dynamics of the wall. The goal of the study is to quantify the changes induced by the wall compliance on the spatial and temporal distributions of wall shear stresses. Of interest is also the evaluation of the distribution of wall tension, which cannot be estimated in a rigid-wall configuration. The results of the numerical simulations are compared with measurements obtained experimentally in rigid models of aneurysms, which serve as the reference case.

The numerical code couples a fluid solver (resolution of the incompressible Navier Stokes equations in a ALE configuration) and a solid one (arterial wall modeled as a non-linear shell) with a message passing library. Both symmetric and non-symmetric models of aneurysms are considered, all idealistic in shape. The mechanical properties of the aneurysm wall are varied in order to simulate their progressive stiffening. The wall is fixed at its extremeties, preventing any displacement or rotation. A physiologically correct flow rate is imposed at the inlet cross-section and the normal stress at the outlet.

In the case of compliant walls, it is essential to reproduce a physiological pressure field. The pressure within the model is shown to be strictly governed by the oulet pressure condition, the flow dynamics having only a negligible effect. When using a 0D model for the outlet boundary conditions, we show that the wall elasticity leads to a decrease in the mean value of the wall shear stresses that depends on the coefficient of elasticity.

[a] Mechanical Engineering Dept., University College London, London WC1E 7JE, England.

[b] INRIA Rocquencourt, 78153 Le Chesnay Cedex, France.

[c] LadHyX, Ecole Polytechnique, 91128 Palaiseau Cedex, France.

[d] LMS, Ecole Polytechnique, 91128 Palaiseau Cedex, France.

The influence of gravity on the propagation of an air finger into a fluid-filled, elastic-walled channel

A. L. Hazel*, M. Heil*

Airway closure occurs when the gas-conveying vessels of the lung collapse and become occluded by the liquid normally present in a thin lining film. Closure of the larger airways occurs only under certain pathological conditions; and if the vessels remain closed for the majority of the breathing cycle, lung function is severely compromised. The aim of any clinical treatment is to reopen the closed airways as rapidly as possible, but without damaging the lung tissue.

Previous two-[1] and three-dimensional[2] theoretical studies of the system have neglected gravitational effects, an assumption justified by the relatively small size of the terminal airways (diameter $\approx 0.25mm$) and, hence, small values of the Bond number (ratio of gravitational forces to surface-tension forces). Recent bench-top experiments[3] have demonstrated, however, that gravity may yet play an important role in the reopening process. In particular, the internal pressure of the air finger measured experimentally was consistently greater than that predicted by a three-dimensional, theoretical model in which gravitational forces were absent.[2]

We model the reopening of an isolated, collapsed airway by considering the steady propagation of an inviscid air finger into a flexible-walled, two-dimensional channel initially filled by an incompressible viscous liquid. This fluid-structure-interaction problem is solved numerically using a fully-coupled, finite-element method. The motion of the fluid is described by the Navier–Stokes equations and the channel walls are modelled as two pre-stressed elastic beams supported on elastic foundations. We present results from simulations that include the effects of gravity and fluid inertia. The results indicate that modest values of the Bond and Reynolds numbers, the latter being the ratio of inertial to viscous forces in the fluid, lead to macroscopic changes in the geometrical configuration of the system near the finger tip and to significant increases in the pressure required to drive the air finger at a given speed.

*School of Mathematics, University of Manchester, U.K.

[1] Gaver et al. *J. Fluid. Mech.* **319**, 25 (1996)

[2] Hazel & Heil *ASME J. Biomech. Eng.* accepted

[3] Heap & Juel *J. Fluid Mech.* submitted

Wave forerunners of longitudinal structures on straight and swept wings

V. N. Gorev[a], M. M. Katasonov[a] and V. V. Kozlov[a]

In recent years the longitudinal localized vortex disturbances, so called "streaky structures", or "puffs" appearing in boundary layers under the effect of external flow turbulence are of much interest. Once these disturbances are generated, they amplify downstream, turn into the incipient spots, and finally, result in laminar-turbulent transition "1, 2". In the present work wave packets (forerunners) occurring in the regions preceding a drastic change of flow velocity inside the boundary layer at the longitudinal structures fronts are in focus. Their characteristics and dynamics have been studied experimentally in straight and swept wing boundary layers.

The investigations were carried out in the subsonic low-turbulent wind tunnel T-324, ITAM SB RAS. Free stream velocity was in the range $4 \le U_o \le 8$ m/s at the turbulence level smaller than 0.04%. One model was a straight wing of 1000 mm span with the chord of 450 mm, an other model was a swept wing with sweep angle 43º, chord of 730 mm and the same span. The models were set vertically at positive angle of attack of 5º. The disturbances (streaky structures) were generated via blowing (suction) through a thin slot arranged in the surface parallel to the leading edge.

In the present experiments the high-frequency perturbations, i.e. forerunners, at the leading and back fronts of the longitudinal structures evolving in the laminar boundary layer have been found. Their characteristics affected by the external-flow pressure gradient, the way of the longitudinal structures generation, and velocity gradients induced by the latter were investigated. In particular, it was observed that the forerunners are strongly amplified in the adverse pressure gradient flow being much influenced by local velocity gradients. The results of the study make reason to consider the forerunners as wave packets of 3D instability waves. It was found that at downstream development of the forerunners they transform into the Λ-structures.

The work was supported by the Russian Foundation for Basic Researches (grant No. 02-01-00006), President's Foundation for the support of the leading scientific schools of Russian Federation (grant No. SS-964.2003.1), President's Foundation for the support of the young Russian scientists (grant MK-1655.2005.1) and by project of the Ministry of Education and Science of Russian Federation (No. 8292).

---

[a] ITAM SB RAS, Institutskaya 4/1, 630090, Novosibirsk, Russia.

[1] Kozlov, *EUROMECH Colloquim 353: Booklet of summaries. Karlsruhe,* (1996).

[2] Boiko et al,. *Berlin; Heidelberg; New York: Springer Verlag,* (2002).

Features of laminar-turbulent transition of adverse pressure gradient flows at low and high Reynolds numbers

V.G. Chernoray[a], V.V. Kozlov[b], L. Löfdahl[a], G.R. Grek[b]

Recent experimental studies of laminar-turbulent transition are presented with focus on adverse pressure gradient flows. New developments in secondary instability of streaks and separation control are reported. In the first part of the presentation the studies of laminar-turbulent transition in non-swept and swept wing boundary layers are discussed, and in the second part the investigations of separated flows on wings with ordinary (plain) and modified (wavy-shaped) surfaces are considered. The role of three-dimensional velocity perturbations such as streamwise vortices and streaks in the laminar-turbulence transition process is demonstrated, and the importance of secondary instability mechanisms is outlined. For a straight wing, the experimental studies of the nonlinear varicose secondary instability are compared at zero and adverse streamwise pressure gradients. Results obtained testify to the strong influence of the pressure gradient upon the breakdown of streaks with developed instability[1]. For the swept wings, the stationary vortex packets are most likely to be generated under natural flight conditions and transition to turbulence is known to be the quickest within these disturbances. Two modes of the secondary instability are found to develop and the preferred mode is dependent on the properties of the primary stationary disturbance. The instability modes studied are the 'y' and 'z' high-frequency secondary instability modes, which are investigated separately and also their interaction under fully controlled experimental conditions[2]. Furthermore, the influence of wing surface modifications on the wing performance and drag is studied. The results testify that for the low-Reynolds-number flow conditions the critical angle of attack of a wing with a wavy-shaped surface can be up to 1.5 times or more than that of a similar plane-surface-wing, and for the attack angles in the range between 5 and 20 degrees the wing with a modified surface reveal higher aerodynamic quality owing to decreased size of the separated zones[3].

[a] Chalmers University of Technology, Applied Mechanics, SE-412 96 Göteborg, Sweden.
[b] ITAM SB RAS, 630090 Novosibirsk, Russia.

[1] Litvinenko et al., *Phys. Fluids* **17**, 118106 (2005).
[2] Chernoray et al., *J. Fluid Mech.* **534**, 295 (2005).
[3] Kozlov et al., *Proc. EUCASS Conf.* Moscow, Russia, Paper 2.11.07 (2005).

Stability and sensitivity analysis of separation bubbles.

L.Marino*, P.Luchini†

In the present contribution the linear stability of an incompressible flow in the presence of a recirculating bubble is considered.

The problem is relevant to aeronautical applications; in fact separation bubbles can arise near the leading edge of airfoils, under particular flight conditions, and can dramatically change their performance (lift and drag).

The stability properties of separation bubbles on flat plates have been studied by past authors through an approach based on parallel and weakly non-parallel approximations[1], or by direct numerical simulation[2]. In both cases the separation bubble has been induced by giving a predefined adverse pressure gradients to boundary-layer velocity profiles.

Here the analysis is carried out both in a flat geometry with a prescribed external pressure gradient and in the case of flow over a curved surface.

The properties of the ensuing global instability are obtained without any parallel-flow approximation; we remind that the term "global" is here referred to instabilities not amenable to the quasi-parallel approximation[3]. Consequently, the problem is studied by solving the complete Navier-Stokes equations.

The critical Reynolds number and the structure of the possible instability of the flow are the main topics of the present investigation. Moreover the sensitivity characteristics are determined, by an adjoint analysis of the relevant eigenvalue problem. In particular the effects of inflow disturbances and of structural perturbations (which comprise base flow and boundary conditions changes) are analysed and discussed.

A general three-dimensional perturbation is assumed, with a sinusoidal dependence on the spanwise coordinate. Such a formulation leads to a large-scale eigenvalue problem which is then solved by an inverse-iteration algorithm.

A particular attention was given to the boundary conditions necessary in order to achieve an asymptotic behaviour of both base flow and perturbation at the upper computational boundary. The influence of different choices of such conditions will also be discussed.

*Dipartimento di Meccanica e Aeronautica, Universitá degli studi di Roma "La Sapienza", Via Eudossiana 18, Roma, I-00184.

†Dipartimento di Ingegneria Meccanica, Universitá di Salerno, Fisciano (SA), I-84084.

[1]D.A. Hammond, L.G. Redenkopp, Local and global properties of separation bubbles, Eur. J. Mech. B/Fluids, **17**,1998.

[2]U. Rist, U. Maucher, Investigations of time-growing instabilities in laminar separation bubbles, Eur. J. Mech. B/Fluids, **21**,2002.

[3]J. -M. Chomaz, Global instabilities in spatially developing flows: Non-normality and nonlinearity, Ann. Rev. Fluid Mech., **37**,2005.

DNS of a Long Laminar Separation Bubble

O. Marxen* and D.S. Henningson*

A *laminar separation bubble* (LSB) can originate if an initially laminar boundary layer is subject to a sufficiently strong adverse pressure gradient, and transition occurs in the detached shear-layer. Further downstream, the turbulent flow often reattaches in the mean, forming a closed bubble. LSBs can occur on slender bodys and may adversely affect their performance in terms of lift and drag.

Owen and Klanfer[1] were the first to distinguish between *short* and *long* laminar separation bubbles. Tani[2] introduced a classification of long and short LSBs depending on whether their influence on the pressure distribution is local or global. Under certain conditions, for slight changes in the flow conditions short bubbles can break-up into long ones. Gaster[3] carried out a detailed investigation to settle characteristics of short and long bubbles, and to establish parameters that govern the bursting process.

While numerous studies, including DNS, exist on short LSBs[4,5], flow dynamics of long bubbles are not well understood on a fundamental level. Up to now, investigations of long LSBs were almost exclusively based on experiments. Baragona et al.[6] carried out RANS simulations of long LSBs and bubble bursting, but concluded that DNS is required to obtain reliable results. Past investigations of long LSBs and bubble bursting indicate that the transition process plays a major role in the flow dynamics.

Here, results from a DNS of a long LSB shall be reported. The underlying potential flow field resembles the one created by a cylinder (i.e. a dipole) above a wall, resulting in a strong acceleration of the boundary layer followed by a strong deceleration. At the inflow a Blasius profile is prescribed ($Re_{\delta^\star}$=1000) and the pressure gradient is induced via the streamwise velocity at the upper boundary. Transition is triggered by blowing and suction at the wall upstream of separation.

DNS results show that in contrast to what is known from short LSBs, the saturated disturbances are not able to reattach the flow soon after transition. Instead, reattachment occurs only considerably downstream of the transition location. If the triggering amplitude is chosen to be fairly large, a separation bubble forms that appears to be more comparable to short LSBs. This underlines the important role of the transition process. Furthermore, it strongly indicates that the disturbance content in the flow (turbulence level) is an important parameter to consider in investigations of bubble bursting. Future simulations shall investigate possible mechanisms leading to bubble bursting.

*KTH Mechanics OB 18, SE-100 44 Stockholm, Sweden.

[1] In: *A.R.C. Technical Report* **CP–220** (1955).
[2] *Prog. Aerosp. Sci.* **5**, 70 (1964).
[3] *AGARD* **CP–4**, 813 (1966).
[4] Häggmark et al., *Aerosp. Sci. Technol.* **5** 317 (2001)
[5] Marxen, Dissertation, Universität Stuttgart (2005)
[6] *AIAA J.* **41**(7) 1230 (2003)

Stability of reacting gas jets

Joseph W. Nichols*, Peter J. Schmid*, Patrick Huerre*
and James J. Riley†

The stability of a viscous, reacting, variable-density jet is analyzed by means of linear stability analysis and direct numerical simulation (DNS). The spatial branches of the transformed linearized low Mach number equations are solved using a matrix method to obtain a complete spectrum of eigenmodes. The effect of reaction is isolated by comparing results from the reacting jet to those from a non-reacting jet with the same mean profiles (in which the density is lowered in the region where the flame would otherwise be). Linear analysis shows that the non-reacting case is most unstable with respect to disturbances of azimuthal wavenumbers $n = \pm 1$, whereas the reacting case is most unstable to axisymmetric disturbances. This theoretical result is confirmed by DNS of the fully nonlinear problem, as shown in figure 1. Also, in order to understand the effect of streamwise development of the jet on its stability, linear analysis is applied to mean profiles measured from DNS at various axial locations. Finally, motivated by the fact that non-reacting, low-density jets transition from convective to absolute instability as the density ratio $S = \rho_j/\rho_0$ decreases past a threshold value of 0.72[1], reacting jets of differing fuel-to-air density ratios are considered in order to investigate how reaction affects this transition.

*LadHyX, CNRS-École Polytechnique, Palaiseau, France.
†University of Washington, Seattle, Washington, USA.
[1]Monkewitz and Sohn, *AIAA J.* **26**, 51(1988).

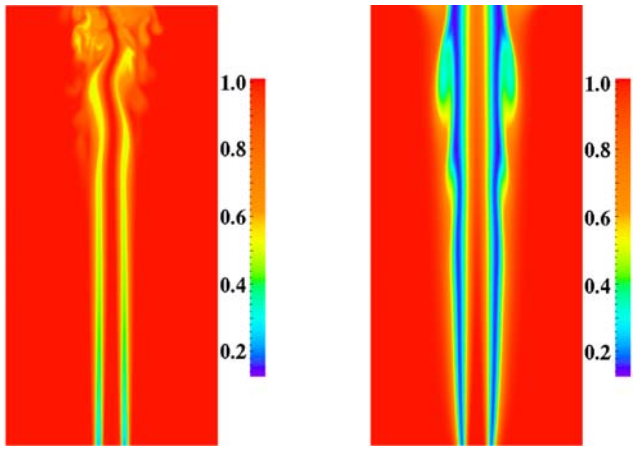

Figure 1: Contours of normalized density on axial cross sections taken from DNS results. (a) Non-reacting case, exhibiting $n = \pm 1$ modes. (b) Reacting case, exhibiting an axisymmetric mode.

Double Diffusive Instabilities of Statically Stable Chemical Fronts

A. Zebib[a] , J. D'Hernoncourt[b] & A. De Wit[b]

Gravitational Hele-Shaw fingering of an autocatalytic reaction diffusion interface is investigated theoretically. Dimensional analysis based on reaction diffusion length, time, and velocity scales reveal the dependence on the Lewis number Le, and thermal and concentration Rayleigh numbers R_T and R_c. Linear stability analysis of a planar upward propagating (against the gravitational acceleration) interface results in an eigenvalue problem for each wavenumber k which we solve using a Chebyshev pseudospectral method. Novel light over heavy instabilities were found when $Le>1$. One instability branch corresponds to an upward endothermic front that is equivalent to a downward propagating exothermic wave. Nonlinear second-order Crank-Nicolson, finite volume simulations are in agreement with linear theory and also show the docile nature of the interface breakup. A displaced particle argument confirms that this unexpected instability is local, that it is subdued by a region of local stability behind the front, and elucidates its dependence on the underlying reaction diffusion mechanism. A second branch of statically stable systems corresponds to an upward exothermic reaction. Displaced particle argument also explains this instability that takes place ahead of the front. This is confirmed by nonlinear computations with interface fingering much larger than that of the former branch.

[a] Mechanical & Aerospace Engineering, Rutgers University
[b] Service de Chimie Physique, Université Libre de Bruxelles

Elastocapillarity in wet hairs

J. Bico*, C. Py*, B. Roman*, S. Neukirch†, A. Boudaoud‡, C. Baroud§

The hairs of a dog coming out of a pond assemble into bunches giving it a spiny appearance. What is the number of hairs in a clump? The answer relies on a balance between capillary forces and elasticity of the hairs. From a practical point of view, the sticking of flexible elements dramatically damages mechanical microsystems or lung airways, but also allows the self-organization of the hairs of nanotube carpets into well defined structures. Experiments performed with macroscopic brushes teach us that the bundles results from a self-similar cascade of sticking events, which leads to an original form of coalescence process (figure 1). Preliminary results obtained with 1D brushes of parallel strips[1] will be completed by recent experiments involving 2D brushes of fibers. Other configurations involving self-crumpling of elastic sheets by capillarity and the fate of a flexible strut pushed through an interface will be finally discussed.

*PMMH-ESPCI, 75231 Paris, France
†LMM-UPMC, 75252 Paris, France
‡LPS-ENS, 75230 Paris, France
§LadHyx-École Polytechnique, 91128 Palaiseau, France
[1]Bico et *al,* Nature **432**, *690 (2004).*

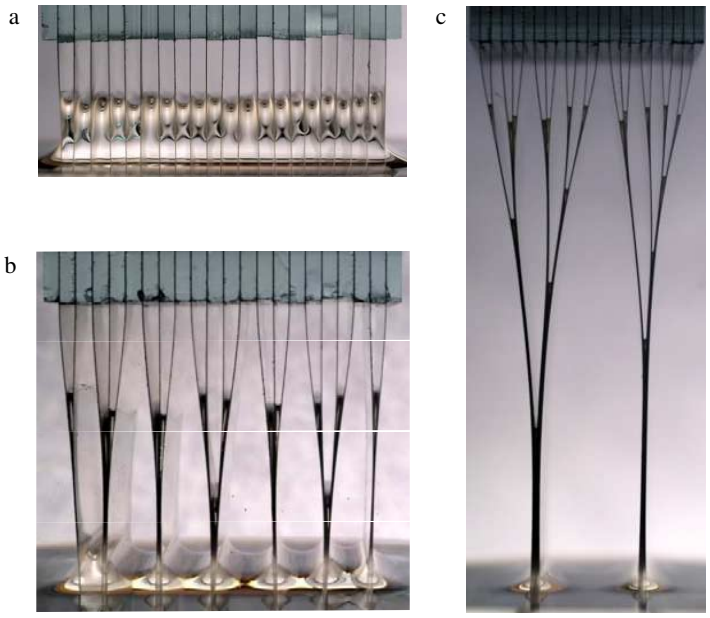

Figure 1: Brush of parallel strips progressively withdrawn from a liquid bath: a cascade of sticking events leads to a hierarchical structure

Capillary Rise between Heated Parallel Plates

J. Gerstmann*and M. E. Dreyer*

Within this study we investigated the rise behavior of a liquid meniscus between heated parallel plates (plate distance: 5 mm, plate breadth: 20 mm) at compensated gravity conditions (figure 1(a)). The aim was to identify the influence of the non-isothermal boundary condition on the dynamic contact angle (γ_d) and the rise behavior of the liquid meniscus. The situation is similar to the capillary transport of propellant along vanes in tanks of spacecrafts. The onset of Marangoni flow in the vicinity of the contact line changes the flow behavior.

Experiments have been carried in the drop tower Bremen. Microgravity conditions were obtained within milliseconds after the release of the drop capsule. Two digital high speed cameras was used to record the meniscus rise as well as the behavior of the dynamic contact angle. Digital image processing techniques were applied to detect the contour of the free surface and determine the dynamic contact angle.

It was found that the Marangoni flow has a significant influence on the dynamic contact angle and on the rise behavior. The change of the dynamic contact angle, compared to the isothermal case, shows a clear dependence on the thermocapillary Weber number, $\mathrm{We}_M = \Theta\sigma_T/\sigma$, where Θ is the characteristic temperature difference, σ_T is the surface tension gradient and σ is the surface tension. With increasing We_M the shift of the contact angle (γ_{shift}, figure 1(b)) increases. γ_{shift} describes the apparent static shift of the contact angle due to the Marangoni effect. The meniscus height decreases compared with the isothermal case.

The dynamic contact angle model by Jiang[1] was modified by replacing the static contact angle γ_s with γ_{shift}. A relation for the dynamic contact angle including the non-isothermal effect was determined. The relation can be used as necessary boundary condition for a mathematical model for the liquid rise between heated parallel plates with a non-isothermal boundary condition.

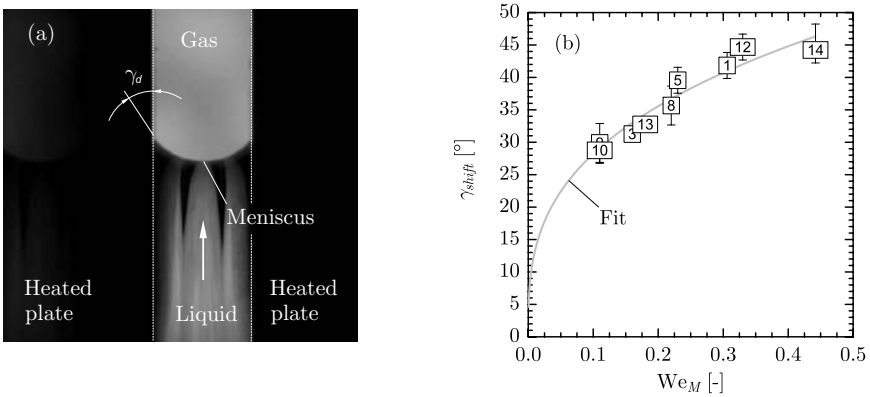

Figure 1: (a) Rising meniscus between heated parallel plates. (b) γ_{shift} vs. We_M.

*ZARM - University of Bremen, Am Fallturm 28359 Bremen, Germany.

[1] Jiang et al., *J. Colloid Interface* **69**, 1 (1979).

Open Capillary Channel Flows (CCF): Flow Rate Limitation in a Groove-Channel

D. Haake*, U. Rosendahl*, A. Grah* and M.E. Dreyer*

In the present study forced liquid flows through open capillary channels are investigated experimentally and numerically under reduced gravity conditions. An open capillary channel is a structure that establishes a liquid flow path at low Bond numbers. Thereby the capillary pressure caused by the surface tension force dominates in comparison to the hydrostatic pressure induced by gravitational or residual accelerations. The investigated capillary channel is a so called groove, which consists of two parallel plates with a free surface at one side and a closed geometry at the other side (see figure 1). In case of steady flow through the channel the capillary pressure of the free surface balances the differential pressure between the liquid and the surrounding constant pressure gas phase. Due to convective and viscous momentum transport the pressure along the flow path decreases and causes the free surface to bend inwards. The maximum flow rate is achieved when the free surface collapses and gas ingestion occurs at the channel outlet. This critical flow rate depends on the channel geometry and the liquid properties. Similarities exists to compressible gas flows in ducts and open channel flows under terrestrial conditions. Each of these flows is governed by similar equations. The flow rate of these flows is limited due to choking. The theory of choked flow predicts a limiting velocity corresponding to a characteristic signal velocity of the flow. In principle this velocity cannot be exceeded, thus the flow is limited to a certain value[1].

The experimental investigations of the open capillary channel flows were performed in the drop tower of Bremen. For the prediction of the critical flow rate an one dimensional theoretical model is developed taking into account the entrance pressure loss and the frictional pressure loss in the channel. We will introduce the experimental setup and present comparisons of the numerical as well as experimental critical flow rates and surface contours for different flows.

*ZARM, University of Bremen, Germany.

[1]Rosendahl et al., *J. Fluid Mech.* **518**, 187-214, (2004).

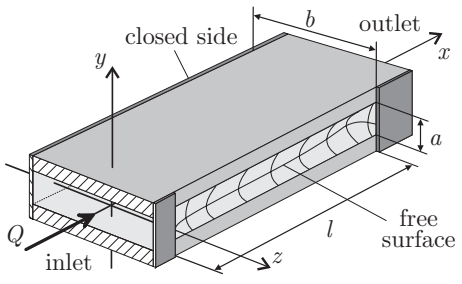

Figure 1: Groove-channel of length l, width b and gap distance a with flow rate Q.

On “fakir” drops

M. Reyssat[a], D. Quéré[a]

Hydrophobic surfaces can be made super-hydrophobic by creating a texture on them. This effect, sometimes referred to as the “fakir effect”, is due to air trapping in the structure, which provides a composite surface made of solid and air on which the deposited drop sits. Here we give evidence for this effect using forests of micro-pillars, made by photolithography and deep etching (cf. figure 1). This allows us to control the density of solid and air under the drop, and thus the degree of super-hydrophobicity. However, the “fakir state” is not always the most stable situation for a drop on a hydrophobic surface. The drop may instead fill the microstructure and this other state, called the “Wenzel state”, has very different properties. We show how to observe transitions between these two states.

We also achieve materials with a density gradient of micropillars, and discuss the possibility of inducing spontaneous drop motion on such surfaces (cf. figure 2).

[a] PMMH, ESPCI, 10 rue Vauquelin, 75005 Paris, France.

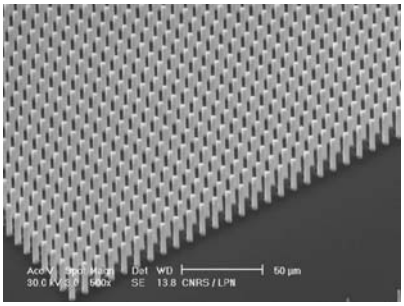

Figure 1: SEM image of a surface decorated with a forest of micropillars.

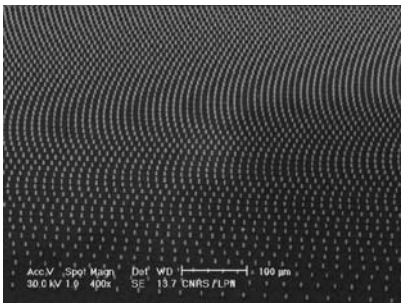

Figure 2: SEM image of a surface decorated with a gradient of micropillars density.

Stick-slip motion of droplets of colloidal suspension

E.Rio*, Adrian Daerr †, F. Lequeux ‡and L.Limat†

A dried coffee drop is surrounded by a ring more concentrated in coffee particles[1] (figure (a)). Evaporation indeed deverges at the contact line which makes the particles flow toward the contact line during the drying. The presence of a static contact line then accounts for this accumulation of particles at the surrounding. A dynamic contact line is often involved in coating processes, sometimes in presence of particles. We can wonder how the presence of these particles will modify the contact line behavior and what will be the consequences what concerns the deposition of a thin and homogeneous layer of particles.

To study such a problem we have set up an experiment allowing a drop of colloidal suspension to advance at different velocity. We observe a competition between drying which tends to accumulate particles and to pine the contact line and the liquid flow. At high velocity, the drop advances continuously with respect to the solid. But at small velocity the motion of the contact line becomes to stick-slip.

This pecular motion is shown on figure (b): on the 6 first pictures, the contact line is pinned on the substract and follows its motion (the solid is moving from the left to the right). On pictures 7 and 8, the contact line slips on the solid. This stick-slip is very regular and periodic. A simple model comparing the evaporation and the liquid flow allows to exhibit the critical velocity below which this behavior is observed.

*PMMH ESPCI, 10 rue Vauquelin, 75 005 Paris, France
†Laboratoire Matire et Systmes Complexes, UMR CNRS 7057, France
‡PPMD ESPCI,10 rue Vauquelin 75005 Paris, Frances

[1]Deegan, *Nature*, **389, 827 (1997).**

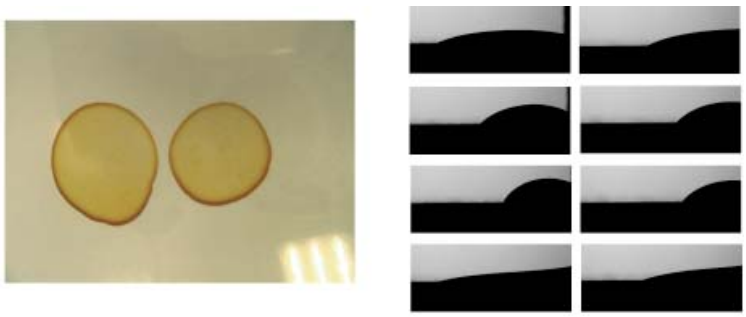

Figure 1: (a) Picture of a dried coffee drop surrounded by a darker ring . (b) Stick-slip motion of a drop of colloidal suspension. The solid is moving from left to right and the contact line advances by pinning-depinning with respect to the solid.

Drops on natural (super)-hydrophobic surfaces

S. Saint-Jean*†, M. Reyssat* and D. Quéré*

Wettability properties of plant leaf surfaces may be of great agronomic importance such as contamination and propagation of pathogens and for managed pesticide application. Most plant leaves are hydrophobic and few of them are super-hydrophobic owing to wax crystal presence and textured pattern of cuticular cells. Here we discuss some characterisations of plant surfaces in terms of contact angles and micro-textures observed on Scanning Electron microscope (Figs. 1 and 2). Then the stability of drops deposited on tilted surfaces is presented.

*Physique et Mécanique des Milieux Hétérogènes, ESPCI; 10, rue Vauquelin, Paris, France
†Environnement et Grandes Cultures, INRA; Thiverval - Grignon, France

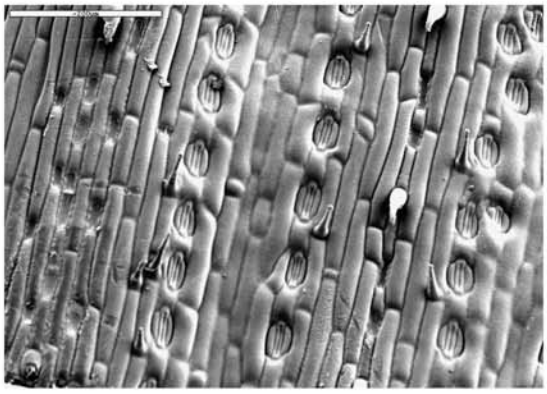

Figure 1: Details of a wheat leaf under scanning electron microscope

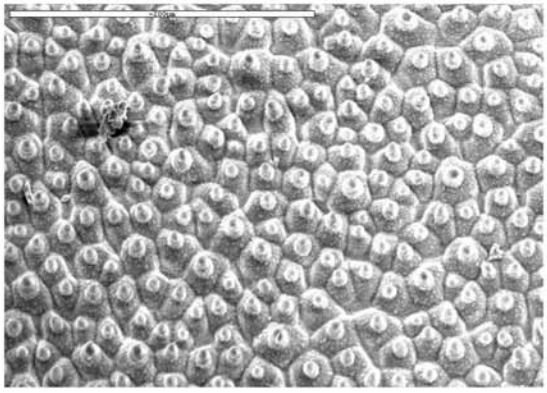

Figure 2: Details of lotus leaf under scanning electron microscope

Monochromatic internal waves from oscillating objects

B. Voisin*

Realization that mixing in the ocean owes much to the generation of internal tides by the ebb and flow of the surface tide over continental slopes[1], on one hand, and advent of the synthetic schlieren method for the measurement of internal waves in the laboratory[2], on the other hand, have led to a regain of interest in the generation of monochromatic internal gravity waves. This problem is tackled here in two parts.

First, the structure of the waves from an arbitrary monochromatic source term is investigated. Waves are radiated along beams, of inclination to the vertical determined by the frequency, while the structure of the waves inside the beams is determined by additional phenomena such as the size of the forcing and the viscosity of the fluid[3]. Transitions take place, between regions where each phenomenon dominates in turn (figure 1a). Near-field effects are prominent in three dimensions, and are proposed as an explanation for the discrepancy between experiment and existing, far-field, theories[4].

Secondly, the determination of the source terms equivalent to oscillating circular cylinders and spheres is considered. The variations of their added mass with frequency is predicted, and is shown to coincide with experiment[5]. Taking these into account, the radiated energy is shown to exhibit a maximum at a practically constant fraction of the buoyancy frequency, independent from the direction of oscillation (figure 1b). Implications for stratified turbulence are discussed.

*LEGI, CNRS–UJF–INPG, BP 53, 38041 Grenoble Cedex 9, France; Bruno.Voisin@hmg.inpg.fr

[1]St. Laurent and Garrett, *J. Phys. Oceanogr.* **32**, 2882 (2002).

[2]Dalziel et al., *Exp. Fluids* **28**, 322 (2000).

[3]Voisin, *J. Fluid Mech.* **496**, 243 (2003).

[4]Sutherland et al., *J. Fluid Mech.* **390**, 93 (1999); Flynn et al., *J. Fluid Mech.* **494**, 65 (2003).

[5]Ermanyuk and Gavrilov, *J. Fluid Mech.* **451**, 421 (2002), **494**, 33 (2003).

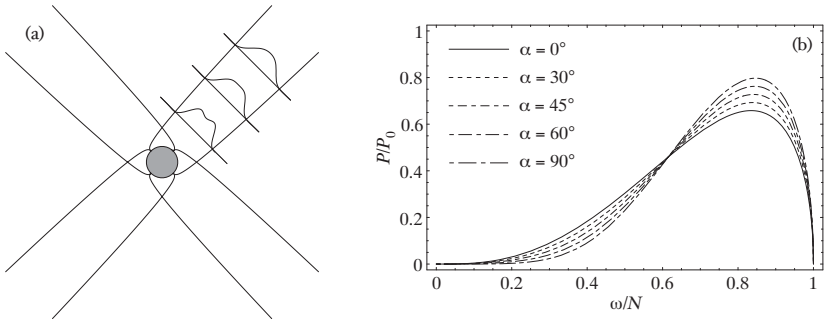

Figure 1: (a) Internal waves from a sphere, exhibiting the transition from a bimodal régime dominated by the influence of its size to a unimodal régime dominated by viscosity, as illustrated by the profile of wave intensity. (b) Radiated power from a sphere versus frequency ω, for different angles of oscillation α to the vertical, exhibiting a maximum at a practically constant fraction, between 0.83 and 0.85, of the buoyancy frequency N.

A general theory for stratified wakes

P. Meunier*, G. R. Spedding† and P. Diamessis†

The stratification of the ocean and the atmosphere plays a major role in geophysical flows (wakes of mountains, islands or sea-mounts) and in nautical applications (wakes of submarines) since it largely modifies the late stages of the wake. Although several experiments[1,2] and numerical simulations[3,4,5] described in detail the evolution of the wake and found empirical scalings for the decaying laws, there has been no theory predicting the characteristics of a stratified wake.

Here, we extend the model of a self-preserved non-stratified wake to the case of a stratified fluid, by assuming that the wake expands in the horizontal direction due to an eddy diffusivity (which was derived from experimental results) and in the vertical direction due to viscous diffusion. The mean characteristics of the wake (wake height and width, velocity defect) are derived analytically, and show a good agreement with the previous empirical results (see figure1). The three regimes from the literature are recovered and two new regimes are discovered. These results are valid for any bluff body once its momentum thickness is known, and can thus be directly applied to geophysical and nautical applications.

The support of ONR Grant no. N00014-04-1-0034 administered by Dr. R. Joslin is most gratefully acknowledged.

*IRPHE, CNRS, Univ. Aix-Marseille I&II, BP 46,F-13384 Marseille Cedex 13, France.
†AME Dept., Univ. Southern California, Los Angeles, California, USA.

[1]Spedding, *J. Fluid Mech.* **337**, 283 (1997).
[2]Bonnier and Eiff, *Phys. Fluids* **14**, 791 (2002)
[3]Gourlay et al., *Phys. Fluids* **13**, 3783 (2001).
[4]Dommermuth et al., *J. Fluid Mech.* **473**, 83 (2002).
[5]Diamessis et al., *J. Comp. Phys.* **202**, 298 (2005).

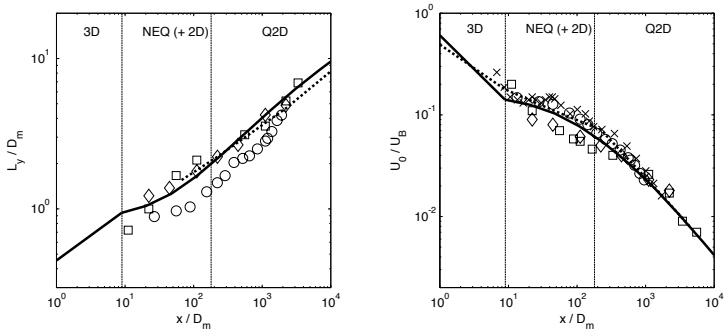

Figure 1: (a) Wake width and (b) velocity defect of a stratified momentum wake. The theoretical predictions (solid line) are compared with previous experimental results (dashed line[1] and crosses[2]) and numerical simulations (diamonds[3], squares[4] and circles[5]).

Turbulent Entrainment in Weak Fountains

G. R. Hunt*and N. B. Kaye*

Abstract

We determine analytically the initial rise height z_m of turbulent Boussinesq fountains for small and large source Froude numbers Fr_0. Our model uses a recasting of the plume conservations equations of Morton, Taylor & Turner (1956) in terms of the Richardson number (inverse square of Fr_0) and a local dimensionless fountain width. For highly-forced fountains (large Fr_0) the well-established linear increase of the rise height with Fr_0 is obtained, i.e. $z_m/r_0 \sim Fr_0$; r_0 denoting the source radius. In contrast, for small Fr_0 the fountain is 'weak' and the dependence $z_m/r_0 \sim Fr_0^2$ is predicted.

Experiments were conducted to establish the nature of the entrainment and rise height on the source Froude number. Based on our experiments and analytical solution we find that $\alpha_f \approx 0.058$ which is significantly closer to that of a jet than of a plume. We discuss this result in the context of existing variable entrainment models.

Morton, B. R., Taylor, G. I. & Turner, J. S. (1956), Turbulent gravitational convection from maintained and instantaneous sources, *Proc. Roy. Soc. A* ***234,*** *123.*

*Imperial College London, London, UK.

Analytical description of solidification processes of young sea ices in leads

D. V. Alexandrov*, A. P. Malygin* and I. V. Alexandrova*

Young sea ice plays a very important role in the surface heat and mass balance of the Arctic Ocean. This ice is formed, for example, due to the divergence of wind stress which is continually produces cracks in the perennial sea ice cover known as leads. These transient fissures attract scientific attention because they provide a thermal conduit through which heat and radiative transfer processes are enhanced tremendously, relative to the thick pack ice that surrounds them. The thermal importance of leads was put in context by Badgley, who showed that during winter the atmospheric heat flux from rapidly freezing leads can be several orders of magnitude larger than that over perennial sea ice. He emphasized the large-scale implications of leads by arguing that they need occupy only 1 percent of the area of the ice cover in order to dominate the exchange of heat from the ocean to the atmosphere. In order to describe these balances we develop theoretical approaches based on modern theories of nonlinear dynamics and differential series. We use previous results on highly resolved temperature data taken through the air/sea/ice interface during the transition from an ice-free to an ice-covered Arctic Ocean surface. Our detailed analysis is guided by recent theoretical and experimental advances in understanding the phase dynamics of directionally solidified systems. In particular, the temperature field and the rate of ice/sea interface are found analytically.

This work was made possible in part by Award No. REC-005 (EK-005-X1) of the U.S. Civilian Research and Development Foundation for the Independent States of the Former Soviet Union (CRDF) and due to the financial support of grants Nos. 05-01-00240, 04-02-96002 Ural, 04-01-96008 Ural (Russian Foundation for Basic Research). One of the authors, D. Alexandrov, is grateful to BRHE program (CRDF and Minobrnauka RF, grant No. Y1-PME-05-02).

*Department of Mathematical Physics, Urals State University, Lenin ave. 51, Ekaterinburg, 620083, Russian Fediration.

Flushing of buoyant fluid from a ventilated box

C. J. Coffey* and G. R. Hunt*

We consider the buoyancy-driven flushing of dense fluid from a box connected to a quiescent exterior environment of constant and uniform density. With connections at high and low levels and an interior environment initially stratified in two layers, the results of our experimental programme using saline solutions to produce density differences in water tanks show that a range of different flow patterns are possible. These include flows with and without significant interfacial mixing, and flows that exhibit either uni-directional or bi-directional flow through the lower openings. Restricting our attention to density differences that are small compared with the ambient density we develop simplified theoretical models of these different flows. These highlight the controlling parameters and enable us to predict the time-dependent stratification. Additionally, we consider the transitions between the different flows observed. Comparisons of our predictions with our experimental results show good agreement. An application of this work to the flushing of heat from ventilated buildings is considered.

*Imperial College London, London, UK.

The influence of the density maximum of water on free convection

P. A. Mooney[a], M. F. Cawley[a]

The density of water is known to exhibit a maximum at a temperature of 3.98°C at a pressure of one atmosphere. The presence of this anomalous property can be readily observed in the free convection of water at temperatures in the vicinity of the density maximum. A recent study of the convective flow in water near its density maximum shows that when water is cooled in a rectangular enclosure by subjecting it to a constant horizontal temperature gradient, the convective flow reverses its direction. During the reversal of the direction of flow, two counter rotating cells are observed and the transfer of heat through the fluid is considerable reduced.

In this study free convection is investigated numerically and experimentally in a rectangular enclosure of water subjected to a horizontal temperature gradient. The temperature profiles at set points along the central horizontal axis through the enclosure are presented. The rate of heat transfer through the enclosure and some sample velocity field plots are also presented. The study shows that the rate of heat transfer through the enclosure reaches a minimum in the vicinity of the density maximum.

[a]Department of Experimental Physics, National University of Ireland, Maynooth, Kildare, Ireland.

Core-annular flow through horizontal pipe: hydrodynamic counterbalancing of buoyancy force on core

G. Ooms* and C. Vuik*

In transporting a high-viscosity liquid through a pipe a low-viscosity liquid can be used as a lubricant film between the pipe wall and the high-viscosity core. This technique, called core-annular flow, is very interesting from a practical and scientific point of view. In a number of cases it was successfully applied for pipeline transport of very viscous oil. The low-viscosity liquid in these cases was water. The pressure drop over the pipeline was considerably lower for oil-water core-annular flow than the pressure drop for the flow of oil alone at the same mean oil velocity.

Much attention has been paid in the literature to core-annular flow. There are several review articles (see for instance Joseph et al.[1]). Most studies deal with the development of waves at the interface between the high-viscosity liquid and the low-viscosity one. These studies deal with axisymmetric vertical core-annular flow (the core has a concentric position in the pipe). It was shown experimentally and theoretically that both liquid phases can retain their integrity, although an originally smooth interface was found to be unstable.

For the transport of very viscous oil (or other liquids) it is also important to pay attention to core-annular flow through a horizontal pipe. Since the densities of the two liquids are almost always different, gravity will push the core off-centre in that case. However, experimental results suggest that under normal conditions a steady eccentric core-annular flow (rather than a stratified flow) is achieved. Relatively little attention has been paid in the literature to the question how the buoyancy force on the core, caused by the density difference, is counterbalanced. In this presentation a further development is made of the idea, that (eccentric) core-annular flow is possible due to hydrodynamic lubrication forces caused by the movement of waves at the core-annular interface with respect to the pipe wall. Contrary to earlier work the core is no longer assumed to be solid. The viscosity of the core liquid has a finite value although much larger than the viscosity of the liquid in the annulus. Using hydrodynamic lubrication theory (taking into account the flow in the core and annulus) the development of the waves is calculated. Also the force exerted on the core is determined, special attention being paid to the position of the core with respect to the pipe wall. It is found that when the pressure gradient over the pipe is sufficiently large, a balance exists between the buoyancy force and the hydrodynamic force on the core, that makes steady eccentric core-annular flow possible.

*J.M. Burgers Centre, Techn. Univ. Delft, Mekelweg 2, 2628 CD Delft, The Netherlands.

[1]D.D. Joseph, R. Bai, K.P. Chen and Y.Y. Renardy, *Ann.Rev.Fluid Mech.*, **29**, 65 (1999).

TRANSIENT DISPLACEMENT OF A NEWTONIAN LIQUID BY GAS IN PERIODICALLY CONSTRICTED CIRCULAR TUBES

Yannis Dimakopoulos[a], Maria Zacharioudaki[a], John Tsamopoulos[a]

We examine the displacement of viscous liquids by pressurized air from harmonically undulated tubes of finite length. This unsteady process gives rise to a long open bubble of varying radius, increasing length and surrounded by the liquid. In general, the thickness of the liquid film that remains on the tube wall is non-uniform. Under creeping flow conditions, it varies periodically, but with a phase difference from the tube radius. The liquid fraction remaining in each periodic segment of the tube increases as the ratio between the minimum and maximum of the tube radius, S, decreases, whereas it tends to the well-known asymptotic value for straight tubes (G.I. Taylor 1961), as $S \to 1$ or as the wavelength of the tube undulation increases, although here the flow is accelerating[1]. At high values of the Reynolds number, Re_p, the film thickness increases with the axial distance, and the periodicity of the flow field ahead of the bubble tip, which exists under creeping flow conditions, is broken. At even higher Reynolds numbers, recirculating vortices develop inside each tube expansion and when S also decreases significantly, nearly isolated bubbles are formed in each tube segment. Moreover, it is shown that monitoring the time variation of the pressure one can determine the location of the front of the penetrating gas and that this arrangement may provide a well-controlled method to produce a stream of bubbles of desired size and frequency.

---

[a] Laboratory of Computational Fluid Dynamics, Dep. Chem. Engin., Univ. of Patras, Greece 26500.

[1] Dimakopoulos, Y. & Tsamopoulos, J., *Phys. Fluids*, **15(7),** (2003).

(a)

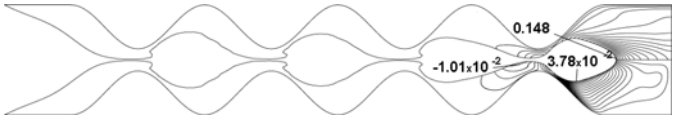

(b)

Contour lines of the axial and radial velocity component, upper and lower part of each figure, in undulated tubes with (a) S =0.7 for Re_p =0, at _=2.79, (b) S =0.2 for Re_p =1500, at _=76.37, where the dimensionless pressure difference, tube length, number of tube undulations, lengths of entrance and exit regions are: (P_{ext}, ε^{-1}, n, $\mathring{a}_i$, $\mathring{a}_e$) = (8333, 12, 4, 1.2, 1.2).

Influence of inlet conditions on flow patterns in oil-water flows in horizontal tubes at intermediate Eötvös number

B. Grassi*, P. Poesio*, E. Piana*, A. M. Lezzi* and G. P. Beretta*

Liquid-liquid flows have been used in many industrial applications: for instance, in petroleum industry water is added to oil to reduce the pressure drop in transportation pipelines. In that respect, one of the flow patterns which appears to be most attractive is the so called 'core-annular flow', in which a central core of more viscous fluid (oil) is surrounded by a thin annulus of less viscous one in contact with the pipe wall[1]. It is, therefore, of great importance to analyse the parameters to operatively create such configuration, and to evaluate the most efficient combination of all the variables (in particular the water holdup) in order to reduce the pressure drop as much as possible.

This paper focuses on the influence of inlet conditions on the development of core-annular flow for a two-phase oil-water flow in a horizontal tube in the case of $Eo \approx \mathrm{o}(1)$, where the definition of the Eötvös number $Eo = \frac{\Delta\rho \cdot g \cdot D^2}{c \cdot \sigma}$ for a liquid-liquid two-phase flow is given by Brauner[2] with $c = 8$.

From the viewpoint of the flow pattern maps, systems characterised by $Eo \ll 1$ resemble reduced-gravity systems[3], while systems with $Eo \gg 1$ show a behaviour which can be considered similar to that of gas-liquid systems. In the present work, two fluids with a consistent density difference and a small diameter (2.1 cm inner diameter) glass tube have been chosen for the experimental campaign, so that both the buoyancy and the superficial tension can have a strong influence on the establishing flow pattern.

For $Eo \approx \mathrm{o}(1)$, our experimental evidence shows that inlet conditions are crucial in the development of a core-annular configuration: as an example, it has been observed that a core-annular flow-pattern is promoted by injecting the oil into the water already in the desired configuration, that is, by guiding the oil flux through an internal tube concentric with the external glass pipe, while the water flows in the cavity between the two conduits, in the initial stretch of the system. The injection of oil in water can be realised in a number of ways, depending on which different results are obtained: in particular four different types of injection procedures are studied.

The tests provide information on oil and water flow rates which are necessary to generate a core-annular configuration (i.e., locus of core-annular existence on the flow pattern map expressed in terms of superficial fluid velocities), on oil-water interface, and on the pressure drop reduction with respect to the case of oil alone.

The present experimental investigation supports the conclusion that, for systems characterised by intermediate Eo, the interpretation of flow pattern maps should be related to the analysis of the inlet conditions, as speculated by Brauner[4].

*Università degli Studi di Brescia, Via Branze 38, 25123 Brescia, Italy.

[1] Joseph, *Powder Technology* **94**, 211-215 (1997).

[2] Brauner, *HEDU: The update journal of heat exchanger design handbook* **5-1**, 1-40 (1998).

[3] Andreini, Greeff, Galbiati, Kuklwetter and Sotgia, *International symposium on liquid-liquid two-phase flow and transport phenomena, Antalya, Turkey*, 3-7 (1997).

Experimental study of the effect of gas injection on oil-water phase inversion in a vertical pipe

M.Descamps*, R.V.A.Oliemans*, G.Ooms*, R.F.Mudde* and R.Kusters†

In the case of a single-phase (water) flow through a vertical pipe it has been shown that the efficiency of the gas-lift technique increases, when the bubble size of the injected gas is reduced [1]. It is not clear whether this also holds for an oil-water flow through a vertical pipe, as in that case phase inversion between the two liquids can occur. This is particularly relevant for the oil industry, since the gas-lift technique is widely used for oil (with water) production. The phase inversion phenomenon has been investigated by various authors both experimentally [2] and numerically [3], but very little is known about the influence of gas injection on this phenomenon.

Therefore, an experimental study has been made of the influence of gas injection on the phase inversion between oil and water flowing through a vertical pipe. Particular attention was paid to the influence on the critical concentration of oil and water at which phase inversion occurs and on the pressure drop increase over the pipe during phase inversion. By using different types of gas injectors also the influence of the bubble size of the injected gas on the phase inversion was studied. It was found that gas injection does not significantly change the critical concentration, but the influence on the pressure drop at the point of inversion is considerable (see figure 1). Local measurements of the phase concentration and bubble size may provide an explanation.

*J.M. Burgerscentrum for Fluid Mechanics, Delft University of Technology, Kramers Laboratorium, Prins Bernhardlaan 6, 2628 BW Delft, The Netherlands

†Shell International Exploration and Production B.V., Kessler Park 1, 2288 GS, Rijswijk ZH, The Netherlands

[1] Guet et al., *AICHE J.* **49**, 2242 (2003)

[2] Ioannou et al., *Exp. Therm. Fluid Sci.* **29**, 331 (2005)

[3] Brauner and Ullmann, *Int. J. Multiphase Flow* **28**, 1177 (2002)

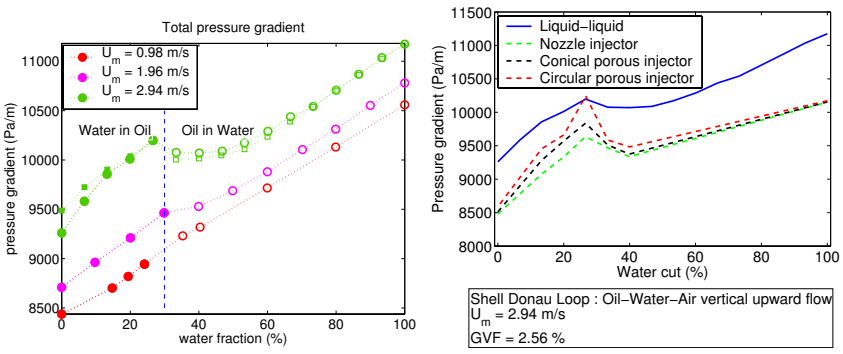

Figure 1: Pressure gradient as function of water volume fraction for an oil-water without (left) and with (right) gas injection.

Microbubble Drag Reduction in a Taylor-Couette System

K. Sugiyama *, E. Calzavarini* and D. Lohse*

We investigate the effect of microbubbles on a Taylor-Couette system by means of direct numerical simulations. In particular, the effect of axially rising bubbles on the modulation of the highly organized vortices in the wavy vortex flow regime (i.e. $Re = 600 - 2500$) is addressed. We employ an Eulerian-Lagrangian algorithm with a gas-fluid (*two-way*) coupling based on the point-force approximation[1]. Added mass, steady drag, lift, and gravity are taken into account in the modeling of the motion of the single bubble.

Our results show that microbubbles are responsible for a reduction of the torque exerted by the system, and therefore of the drag. In figure 1 we show the behavior of the normalized torque, as a function of Reynolds number, and a comparison with a recent series of experimental data obtained by Murai *et al.*[2]

Our analysis suggests that the physical mechanism for the torque reduction is due to the appearance of an axial flow, induced by rising bubbles, that is able to break the highly dissipative Taylor wavy vortices in the system. This effect is in principle similar to the one produced by an axial driving force applied to a single phase Taylor-Couette flow. However, we demonstrate that the bubble addition is more efficient in injecting energy into the flow. We finally show that the lift force acting on the bubble is crucial in this process. When neglecting it, the bubbles accumulate preferentially near the inner cylinder and the bulk flow is no longer modified.

*Department of Applied Physics, University of Twente, 7500 AE Enschede, The Netherlands.

[1]Mazzitelli, Lohse and Toschi, *J. Fluid Mech.* **488**, 283 (2003).

[2]Murai et al., *Proc. of 2nd Int. Symp. on Seawater Drag Reduction* (2005).

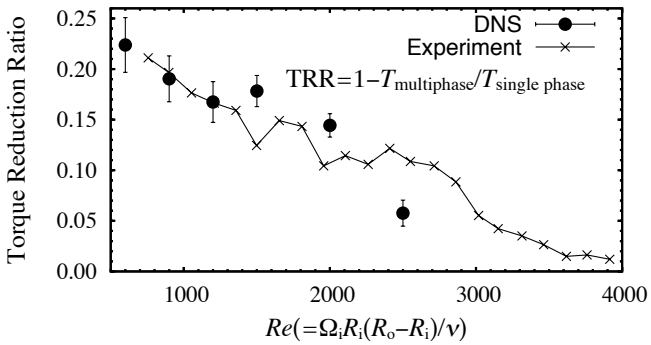

Figure 1: Torque reduction ratio, defined as the torque reduction due to the bubble addition normalized by the torque in the single phase flow, versus the Reynolds number for the Taylor-Couette system. The symbol • shows the present DNS. The symbol × shows the experimental data at the gas flow rate of $1.17 \cdot 10^{-6}\mathrm{m}^3/\mathrm{s}$ in Ref. 2. The inner and outer cylinder radii are $R_\mathrm{i} = 60\mathrm{mm}$ and $R_\mathrm{o} = 72\mathrm{mm}$, respectively.

Numerical modeling of heat transfer and fluid flow in rotor-stator cavities with throughflow

S. Poncet *, R. Schiestel *

The present study considers the numerical modeling of the turbulent flow in a rotor-stator cavity subjected to a superimposed throughflow with heat transfer. Numerical predictions based on one-point statistical modeling using a low Reynolds number second-order full stress transport closure (RSM) are compared with experimental data available in the literature. Considering small temperature differences, density variations can be here neglected which leads to dissociate the dynamical flow field from the heat transfer process. The turbulent flux is approximated by a gradient hypothesis with tensorial eddy diffusivity coefficient.

The fluid flow in an enclosed cavity with axial throughflow is well predicted compared to the velocity measurements performed at IRPHE [1] under isothermal conditions. When the shroud is heated, the effects of rotation Re and coolant outward throughflow C_w on the heat transfer have been investigated and the numerical results are found to be in good agreement with the data of Sparrow and Goldstein [2]. We have also considered the case of an open rotor-stator cavity with a radial inward throughflow and heat transfer along the stator, which corresponds to the experiment of Djaoui et *al.* [3]. Our results have been compared to both their temperature measurements and their asymptotic model with a close agreement between the different approaches (figure 1(a)). All the comparisons have been extended for a wide range of the Prandtl number Pr (figure 1(b)). The predictions can be correlated by the empirical correlation law: $Nu_{av} = 0.0044 \;\; Re^{0.8} \;\; (1000 + C_w)^{0.11} \;\; Pr^{0.5}$.

*IRPHE, Technopôle Château-Gombert, 13384 Marseille, France.

[1] Poncet *et al.*, *Phys. Fluids* **17 (7)** (2005).
[2] Sparrow and Goldstein, *J. Heat Transfer* **98**, 387 (1976).
[3] Djaoui *et al.*, *Eur. J. Mech. B - Fluids* **20**, 371 (2001).

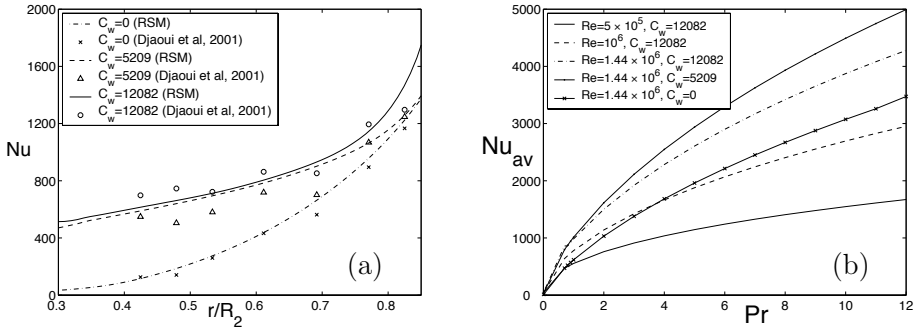

Figure 1: (a) Radial evolution of the local Nusselt number Nu for $Re = 1.44 \times 10^6$, $Pr = 0.7$ and three coolant flowrates. (b) Effect of the Prandtl number on the averaged Nusselt number Nu_{av} for five flow conditions (stator heated).

Turbulent scalar transport mechanisms in flows over a wavy wall

R. Rossi*

The analysis and prediction of turbulent flows inside complex geometries is still one of the most challenging issues in the field of fluid mechanics. Furthermore, the transport process of passive scalar within complex flow fields is of great interest for heat exchangers or chemical reactors design. In this work, the mechanisms of passive scalar transport in a turbulent flow over a wavy wall are investigated and discussed by a direct numerical simulation. The wave-like geometry has been choosen since the turbulence dynamics can be significantly altered by the presence of the wall while, under fully turbulent conditions, the flow field can be assumed periodic in both streamwise and spanwise direction and this greatly reduces the computational effort required to perform the simulations.

Figure 1(a) clearly shows higher values of predicted Nusselt numbers above the wavy wall than in the case of flat channels. This effect can be partly understood by the analysis of the turbulent scalar fluxes shown in figure 1(b). The computed vertical flux above the wavy wall is higher than the maximum value obtained for the flat case. Moreover, even if the streamwise component decreases, the mean scalar gradient in the streamwise direction induced by the wavy profile activates a further transport term which vanishes over a flat wall.

The analysis of the instantaneous flow and scalar field reveals the presence of large scale structures induced by the streamlines-curvature over the wavy wall. The role of these coherent turbulent structures on the transport of the passive scalar is finally discussed.

*Laboratorio di Termofluidodinamica Computazionale, Università di Bologna, Via Fontanelle 40, 47100 Forlì, Italy

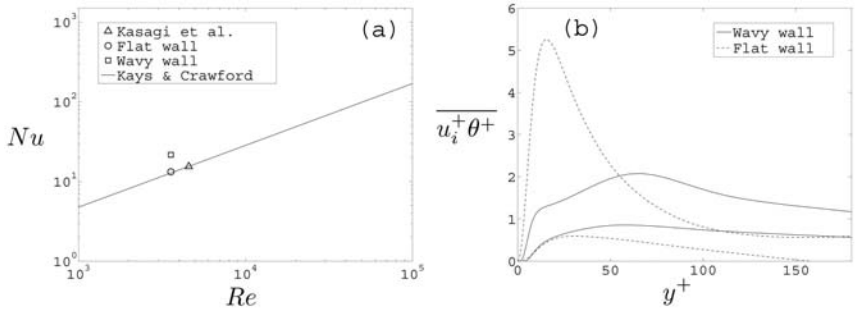

Figure 1: (a) Estimated Nusselt numbers compared to experimental and numerical predictions for flat channels. (b) Profiles of normalised turbulent scalar fluxes above the flat and wavy walls.

Turbulent thermal convection over grooved surfaces: effect of the finite thermal conductivity of the plates.

G.Stringano*, G.Pascazio* and R.Verzicco*

The effects of the finite thermal conductivity of the plates in turbulent thermal convection over grooved surfaces are investigated by direct numerical simulations of the Navier-Stokes equations with the Boussinesq approximation. The simulations are performed in a cylindrical cell of aspect ratio, diameter over cell height, $\Gamma = 1/2$ at Prandtl number $Pr = 0.7$. The cell is heated from below and cooled from above with an adiabatic sidewall. The plate geometry presents five axisymmetric V shaped grooves with the height of the tip over height of the cell, $H/h = 0.025$ and vertex angle equal to 90^o. The presence of grooves forces the formation of plumes over the tips, with a dynamics very similar to the 'wedge effect' in electrical problems[1] [2]. This effect, combined with a finite thermal conductivity of the plates, leads to a non isothermal fluid–plate interface and therefore to weaker wall normal temperature gradients thus reducing the overall heat flux. A comparison with ideal plates with infinite thermal conductivity, shows a decrease of the heat transfer, when the ratio between plates and fluid thermal resistance is smaller than a threshold value. This behaviour can be explained in terms of thermal energy balance: if the plates thermal conductivity is too low, the supplied heat flux can not balance the heat taken away by thermal plumes and the plate cools down below a developing plume. The different balance between the heat needed by an ascending plume and that supplied by the plate can alter the plume dynamics and consequently modify the heat transfer. Since regardless of the particular shape every non flat surface will have cusps and throats the main conclusion is that the tips of the rough elements represent a critical region for heat transfer. A detailed analysis of the plume dynamics and their role in the heat transfer will be presented at the conference.

*DIMeG & CEMEC Politecnico di Bari, Via Redavid 200, 70125 Bari, Italy.

[1]G.Stringano, G.Pascazio and R.Verzicco, Turbulent thermal convection over grooved plates, *J. Fluid Mech.* 2005 in press.

[2]Y.-B.Du and P.Tong, Turbulent thermal convection in a cell with ordered rough boundaries, *J. Fluid Mech.* 2000, *vol.* 407, *pp* 57-84.

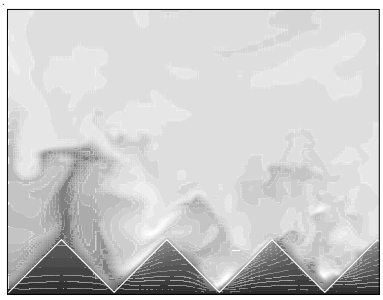

Figure 1: Temperature field at $Ra = 2 \cdot 10^{10}$ and $Pr = 0.7$ (closeup of the hot plate).

Comparative Study of Turbulence Modeling in variable density Jets and Diffusion Flames

F. Tabet-Helal[a], B. Sarh[a] and I. Gökalp[a]

In this study, the performances of the Reynolds Stress model (RSM) and the k-ε model with Pope correction in their turbulence dissipation rate equation, ε, are investigated in many configurations of variable density jet and non-premixed flames. The predictions are compared to the available experimental data.

It is known that the k-ε model and the RSM model over-predict the spreading and decay rate of the round jet flow by 40 %[1]. To improve the accuracy of these turbulence models for solving round jet flows and jet flames, the turbulence constants ($C_{\varepsilon 1}$ and $C_{\varepsilon 2}$) of the turbulence dissipation rate transport equation may be modified, as they are responsible for the generation/destruction of the turbulence energy dissipation. Modifications to the turbulence constants have been suggest in the past by McGuirk and Rodi[2], Morse[3], Launder et al.[4] and Pope[1]. All modifications involve the turbulence constants becoming functions of the velocity decay rate and jet width. For complex flows, a more convenient way is to introduce a correction like that proposed by Pope[1] taking into account the vortex stretching. Also, this modification is more generally applicable.

The variable density jets studied are respectively methane, air and CO_2. The corresponding density ratio between the jet flow and the air coflow are respectively 1.8, 1 and 0.66. The diffusion flames considered are respectively, H_2/Air, CH_4/Air and CH_4-H_2-N_2/Air flames. A flamelet library approach has been applied to account for chemistry and turbulence interaction effects. This work is focused on the applicability of Pope correction to a wide range of variable density jets and diffusion flames.

A Pope correction model is implemented in the commercial CFD code Fluent 6.1.22. User-define subroutine function of the flow variables is written for this purpose.

The results obtained compare favourably with the experimental data. The two turbulence models predictions including Pope correction in ε equation are, in general, very close in all the configurations considered. However, the RSM model calculations needs more refine mesh and consequently more computing time than the k-ε model.

---

[a] LCSR-CNRS, 1 C avenue de la recherché scientifique, Orléans 45071, France.

[1] Pope, AIAA *J*. **16**, 3 (1978).

[2] Mcguirk and Rodi, 1st Symp. *On Turbulent Shear Flows*,71-83, (1979)

[3] Morse, *PhD Thesis, London University*, 1977.

[4] Launder et al., *NASA SP*-311, 1972.

An explicit algebraic model for the subgrid passive scalar flux

L. Marstorp*, G. Brethouwer*, and A.V. Johansson*

Accurate descriptions of turbulent flows including scalar mixing are desirable in many engineering applications and geophysical situations. In Large Eddy Simulations, the eddy diffusivity model is a widely used model for the subgrid scalar field. It is simple and computationally cheap, but it has several known drawbacks. One example is its inability to predict the anisotropy of the subgrid passive scalar field as pointed out by Kang and Meneveau [1]. Recently Wikstrom et al.[2] proposed an explicit algebraic scalar flux model, EASFM, based on a modelled transport equation for the Reynolds averaged scalar flux. It predicts the scalar flux more accurate in shear flows than the eddy diffusivity model and it is computationally cheap. The objective of this study is to develop a new model for the subgrid scalar flux, by applying the same kind of methodology that leads to the EASFM for the Reynolds averaged scalar flux.

The new subgrid scalar flux model can be derived in the same manner as the EASFM of Wikstrom et al.[1], but with filtered quantities instead of Reynolds averaged quantities. It takes the form

$$q_i = -\tau_{sgs}(1-c_1)B_{ij}\tau_{jk}\frac{\partial\tilde{\theta}}{\partial x_k}$$

where $q_i = \widetilde{u_i\theta} - \tilde{u}_i\tilde{\theta}$ is the subgrid scalar flux, $\tilde{\theta}$ is the resolved scalar field, τ_{jk} is the subgrid stress, and τ_{sgs} is the time scale of the subgrid velocity field. B_{ij} depends on the resolved rate of strain and the rotation rate tensor. The performance of the new model was tested in rotating homogeneous shear flow, with a mean shear $U_i = Sx_3\delta_{i1}$ and a mean scalar gradient $S_i^\theta = \delta_{i3}$. The time scale τ_{sgs} was estimated using dimensional analysis and the model parameters were adjusted to produce the right amount of mean dissipation. These parameters may, however, not be optimal and they will be improved by a priori and a posteriori test with DNS data.

In the present test case, the new explicit model provides for a better description of the mean subgrid scalar variance dissipation than the eddy diffusion model. Moreover, it describes the anisotropy of the subgrid flux in a more realistic way than the eddy diffusivity model. Some results on the anisotropy of the subgrid dissipation will be presented. The new model also provides for backscatter of scalar variance. However, it is necessary to tune the model parameters and determine their dependence on the filter length scale. The DNS by Brethouwer and Matsuo[3] will be used for a priori and a posteriori tests.

*KTH Mechanics OB 18, SE-100 44 Stockholm, Sweden.

[1]Kang et al., *J. Fluid Mech.* **442** , 161 (2001)
[2]Wikstrom et al., *Phys. Fluids* **12**, 3 (2000).
[3]Brethouwer et al., *Proc. of TSFP* **4**, (2005).

Simulation and evaluation of mixing in a plane compressible wall jet

Daniel Ahlman*, Geert Brethouwer*, and Arne V. Johansson*

A plane wall jet is obtained by injecting fluid along a solid wall in such a way that the velocity of the jet supersedes that of the ambient flow. The structure of a developed turbulent wall jet can formally be described as two adjacent shear layers of different character. The inner layer, reaching from the wall up to the maximum mean streamwise velocity, resembles a thin boundary layer, while the outer part, positioned above the first layer and reaching out to the ambient fluid, can be characterized as a free shear flow. A consequence of this twofold nature is that properties such as mixing and momentum transfer exhibit distinctively different character in the two shear layers.

An increased understanding of the mixing properties close to a wall is of prime importance in connection to combustion. In all combustion applications some part of the mixing and reaction will take place close to a wall, with properties distinctively different from those further out in the mixture. How the mixing processes are affected by the proximity to the wall, and to what extent these are captured by present combustion models, is currently not fully understood, and it is of interest to add to this knowledge.

In the present study, we analyze the mixing processes in a plane compressible and turbulent wall jet, by means of three-dimensional direct numerical simulations. The wall jet mixing is characterized by the evolution of a conserved passive scalar, introduced in the jet in a non-premixed manner. The simulations are aimed at both investigating the dynamics of the plane wall jet and to provide mixing statistics useful for evaluation and model development. The developing wall jet provides an interesting test case since it contains inhomogeneous mixing.

The simulations are performed, using a compressible code based on a compact finite difference scheme of sixth order for the spatial discretization and a third order, low-storage, Runge-Kutta scheme for the temporal integration. The domain used in the simulations is rectangular with a no-slip wall positioned at the bottom. The physical domain size, in terms of the jet inlet height h, is $L_x/h = 47$, $L_y/h = 18$ and $L_z/h = 9.6$ in the streamwise, wall normal and spanwise directions respectively. The domain is discretized using $384 \times 192 \times 128$ nodes. The inlet of the jet is positioned directly at the wall with the flow directed along it. The Reynolds number based on the inlet height and velocity is 2000. Above the jet inlet a coflow of 10% of the jet inlet velocity is applied. The flow field is compressible with a moderate inlet Mach number of 0.5. The dynamic structure of the wall jet is investigated by averaged profiles, velocity fluctuations and Reynolds stresses. Comparisons are made with the experimental data of Eriksson et al.[1] and the LES data of Dejoan and Leschziner[2]. The mixing processes are investigated through scalar fluxes, turbulent Schmidt numbers and probability density functions of the passive scalar. Further statistics relating to combustion modeling, such as the scalar dissipation rate, are also evaluated.

*KTH Mechanics OB 18, SE-100 44 Stockholm, Sweden.

[1]Eriksson et al., *Experiments in Fluids* **25**, 50 (1998).
[2]Dejoan and Leschziner, *Phys. Fluids* **17**, 025102 (2005).

Modelling of optimal vortex ring formation using the Stokes approximation

F. Kaplanski*and Y. Rudi*

Previous studies show that vortex rings generated in the laboratory can be optimized for efficiency, based on the jet length-to-diameter ratio (L/D), with peak performance occurring $3.5 < L/D < 4.5$[1]. The objective of the present research is to develop predictive model of the optimal vortex ring formation. For this purpose we considered an analytical solution describing the evolution of a vortex ring from thin to thick-cored form in the Stokes approximation. The proposed model agrees with the reported theoretical and experimental results referring to the formation and to the decaying stages of ring development. The obtained class of rings can be classified in terms of the parameter τ, representing the ratio of the ring radius R_0 to the time-dependent core radius ℓ. The present contribution extends analysis reported in[2], which only considers the scale ℓ equal to $\sqrt{2\nu t}$, (ν is the kinematic viscosity). It is found new similarity variables and functional forms using the invariance of the governing equations, boundary conditions and vorticity impulse. The obtained circulation, kinetic energy and translation velocity are compared with the results for Norbury vortices and are used to give predictions for the normalized energy and circulation describing the flow behaviour near the experimentally discovered critical value of L/D ("formation number"). The predicted values match very well with the experimental data. The experimental results[1] indicate that the vorticity ω extends to the symmetry axis when L/D=4. This feature is employed for evaluating "formation number" parallel with the method of the entrainment diagrams[3]. The obtained results for both approaches are shown in figure 1(a) and (b).

*Tallinn University of Technology, Akadeemia tee 23A Tallinn 12618, Estonia.

[1]Gharib et. al, *J. Fluid Mech.* **360**, 121 (1998).

[2]Kaplanski and Rudi, *Phys. Fluids* **17**, 087101 (2005).

[3]Cantwell *J. Fluid Mech.* **104**, 369 (1981).

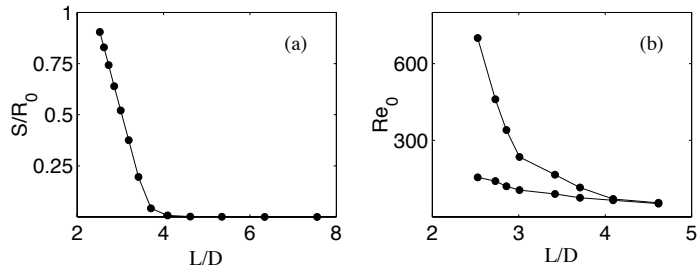

Figure 1: (a) Distance between the contour lines of vorticity 0.01 ω_{max} along a line connecting two cores of a vortex ring versus L/D. (b) Boundaries for the flows consisting of a wake and a vortex ring in the parameter space (L/D and Re_0).

Experiments on Vortex-Ring Dynamics in a Rotating Fluid

M. A. Brend[a], P. J. Thomas[a] and P. W. Carpenter[a]

We present results of our first experiments investigating the dynamics of vortex rings in a rotating fluid. The experiments are conducted in our new, unique large-scale rotating-tank facility (see Fig. 1). The rig (overall height $5.7\,\mathrm{m}$) was purpose-built for our study. It constitutes a water-filled tank (height $2.5\,\mathrm{m}$, diameter $1\,\mathrm{m}$) mounted on a computer-controlled rotating turntable. A piston-type, computer-controlled vortex-ring generator is located in the centre at the top of the tank. It is rigidly attached to the tank, rotates with it and injects vortex rings vertically downwards into the tank.

We summarise results from dye-visualisations and PIV measurements. We found that, in the rotating system, Coriolis forces induce several hitherto unknown flow phenomena absent for corresponding vortex rings in non-rotating flow. Coriolis forces induce, for instance, a cyclonic swirling flow in the vortex-ring wake. Additionally they establish a back flow, from the ring towards the generator nozzle. They induce shedding of secondary and, sometimes, tertiary rings from the primary ring - these have opposite vorticity in comparison to the primary ring. We further observed that background rotation decreases the translational velocity of the rings slightly and that it destabilises the rings substantially. The decay length of a ring, i.e. the distance that a ring can propagate until it has completely lost its entity, scales with a Rossby number based on the mean translational ring speed and the ring diameter. Finally, Coriolis induced secondary flows can suppress the well-known wavy Widnall instability[1] that is closely associated with vortex rings in non-rotating flow.

---

[a] School of Engineering, University of Warwick, Coventry CV7 7AL, United Kingdom

[1] Widnall and Tsai, *Phil. Trans. Roy. Soc.* **287**, 273 (1977).

Figure 1: Our rotating tank facility with members of the research team in foreground to illustrate the size of the rig.

The effect of a sphere on a swirling jet in an open flow

K. Atvars*, M. C. Thompson* and K. Hourigan*

This work presents the results of an investigation into the effects of a solid body placed along the central axis of a swirling jet in an open tank. The experiment was conducted in an open tank apparatus similar in design to that used by Billant et al.[1] which enables independent control over axial flow rate (Re) and roation imparted on the flow (ω_M). Previous work on controlling vortex breakdown in a swirling jet has focussed on the shear layer between the relatively stagnant tank flow and the swirling jet, and although a stagnation point has been noted as occuring in a particular place, its distance P from the nozzle as a function of the varying swirl parameters has not been fully investigated.

For the current preliminary investigation into vortex core obstruction, a sphere of diameter equal to that of the nozzle was placed on the vortex core centreline at one nozzle diameter downstream of the nozzle. As the rotation rate ω_M was increased, a stagnation point was observed to occur upstream of the sphere, in much the same way as Mattner et al.[2] observed in their experiments in a pipe. This stagnation point appeared to be much steadier in its position than in the unobstructed case. P then became smaller as ω_M was increased for a given Re. As expected, it was found that with increasing Re, ω_M also needed to be increased to maintain the same stagnation point location. However, once the data were replotted against swirl number $S = f(\omega/Re)$, it appeared as though there was in fact an Re dependence of the the swirl number S required to maintain a specific P. Furthermore, for a given Re, the variation in P with S had an almost logarithmic dependence. Further work on the effects of varying the sphere size as well as location away from the nozzle will also be presented, along with stereoscopic PIV results to verify the Re dependence.

*FLAIR, Dept. of Mechanical Engineering, Monash University, Melbourne, Australia.

[1]Billant et al., *J. Fluid Mech.* **376**, 183 (1998)

[2]Mattner et al., *J. Fluid Mech.* **481**, 1 (2003).

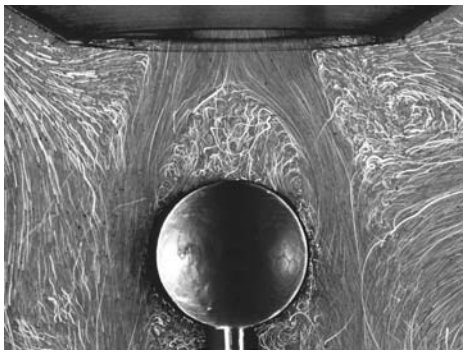

Figure 1: Processed image of flow visualisation showing the steady stagnation point upstream of the sphere surface.

The Kelvin waves and the singular modes of the Lamb–Oseen vortex *

David Fabre, †Denis Sipp ‡& Laurent Jacquin†

Columnar vortices are known to support a family of waves initially discovered by Lord Kelvin (1880) in the case of the Rankine vortex model. This paper presents an exhaustive cartography of the eigenmodes of a more realistic vortex model, the Lamb–Oseen vortex. Some modes are Kelvin waves related to those existing in the Rankine vortex, while some others are singular damped modes with a completely different nature. Several families are identified and are successively described. For each family, the underlying physical mechanism is explained, and the effect of viscosity is detailed. In the axisymmetric case (with azimuthal wavenumber $m = 0$), all modes are Kelvin waves and weakly affected by viscosity. For helical modes ($m = 1$), four families are identified. The first family, noted "D", corresponds to a particular wave called the displacement wave. The modes of the second family, noted "C", are cograde waves, except in the long-wave range where they become centre modes and are strongly affected by viscosity. The modes of the third family, noted "V", are retrograde, singular modes which are always strongly damped and do dot exist in the inviscid limit. The modes of the last family, noted "L", are regular, counterrotating waves for short-wavelengths, but they become singular damped modes for long wavelengths. In an intermediate range of wavelengths between these two limits, they display a particular structure, with both a wave-like profile within the vortex core and a spiral structure in its periphery. This kind of modes are called critical layer waves, and their significance is explained from both a physical and a mathematical point of view. Double-helix modes ($m = 2$) can similarly be classified into the "C", "V" and "L" families. Moreover, one particular mode, called "F", plays a particular role. For short wavelenghs, this mode corresponds to a helical flattening wave, and has a clear physical significance. However, for long wavelenghts, this mode completely changes its structure, and becomes a critical layer wave. Modes with larger azimuthal wavenumbers m are all found to be substantially damped.

*Fabre, Sipp & Jacquin, *J. Fluid Mech.*, in press (2006).

†IMFT, Allée du Professeur Camille Soula, 31400 Toulouse, France

‡ONERA, Fundamental and Experimental Aerodynamics Department, 8 rue des Vertugadins, 92190 Meudon, France

Three-dimensional stability of non-uniform vortex patches

D. Guimbard*, S. Leblanc*

The three-dimensional stability of a family of two-dimensional inviscid vortex patches discovered by Abrashkin & Yakubovich[1] is explored. Generally unsteady and non-uniform, these vortex patches evolve freely in surrounding irrotational flows. The family of solutions they discovered are exact solutions of Euler's equation described in Lagrangian representation and their corresponding complex trajectories are:

$$Z(t) = X(t) + iY(t) = G(\xi)e^{i(\omega+\Omega)t} + H(\bar{\xi})e^{i\Omega t}$$

where G and H are analytic functions, ω and Ω are real numbers.

Described in Lagrangian representation (ξ is the complex lagrangian variable), this family of solutions includes Rankine circular vortex, Kirchhoff's ellipse, and freely rotating multipolar vortices with hypocycloidal shape as special cases and weirdly Gerstner's waves.

Taking advantage of their Lagrangian description, the stability analysis is carried out with the local theory of short wavelength instabilities.

It is shown that, except Rankine vortex, these flows are generically unstable to three-dimensional disturbances. However, additional effects such as external rotation or density stratification may be stabilizing[2].

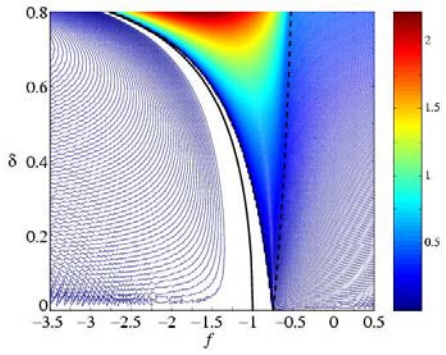

Figure 1: Instability map for vortex patches with $G(\xi) = \xi$ in a non-stratified flow. Level lines of the computed maximum dimensionless growth rate σ/ω of the disturbances as a function of the vortex deformation $\delta = |H'|$, and the rotation parameter $f = \Omega/\omega$. The solid line corresponds to stable trajectories with zero absolute vorticity. The dotted lines delimit the unstable region for vertical wave number.

*LSEET, Université du Sud Toulon-Var, France

[1] Abrashkin and Yakubovich, *Sov. Phys. Dokl.* **29**, 370–371 (1984)

[2] Guimbard and Leblanc *J. Fluid Mech.* submitted (2005)

Stability of a stratified tilted vortex

N.Boulanger, P.Meunier, S.Le Dizès*

The stability of a vortex tilted with respect to the stratification has been investigated theoretically and experimentally.
The basic flow solution has been obtained analytically in the limit of small inclination angles. The inviscid approximation of the solution exhibits a singularity where $N = \Omega(r)$, with N the Brunt-Väisala frequency and $\Omega(r)$ the angular velocity profile. This singularity can be smoothed by a viscous critical layer analysis. The solution corresponds to strong jets and strong density variations of order $O(Re^{\frac{1}{3}})$ localized in the critical layer of $O(Re^{-\frac{1}{3}})$ width . PIV measurements and shadowgraph visualization have been used to validate the theory (see figure 1a).
The basic flow has been observed to be unstable. A shadowgraph picture reveals the emergence of co-rotating structures in two distinct strips arranged symmetrically on either side of the vortex (see figure 1b). The evolution of the azimuthal vorticity has been obtained experimentally and show a reorganization of the vorticity from vertical homogeneous distribution toward ponctual and regularly spaced vortices. The unstable mode is not an helicoidal mode but instead localized on either side of the vortex as if it was due to a Kelvin-Helmholtz instability of the shear generated in the critical layer. This interpretation is discussed and validated by simple models.
The impact of this new and very general instability induced by tilting on mixing and internal waves generation are also considered.

This work has been supported by the french ministry of research and is part of the ACI " Dynamics of cyclonic vortices ".

*IRPHE, Marseille, France.

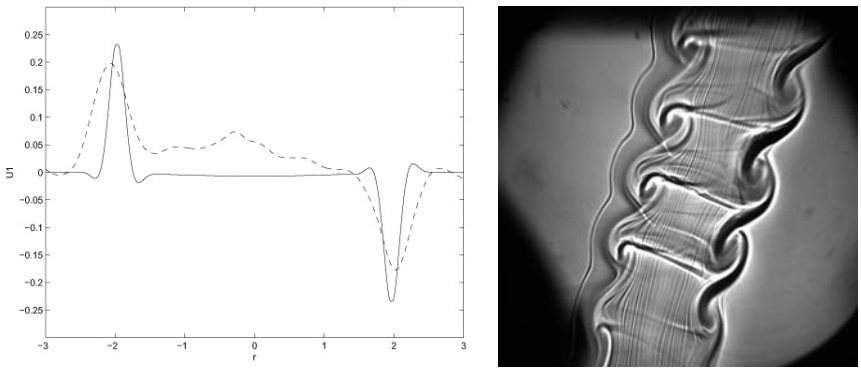

Figure 1: (a)Theoretical (solid line) and experimental (dashed line) radial profile of axial velocity . (b)Shadowgraph visualization of the instability of a tilted vortex.

Session 4

Dynamics of droplet deformation and break-up

L. Prahl*, J. Revstedt*, L. Fuchs*

Liquid sprays are modeled usually by assuming spherical non-deforming objects. The forces on each sphere is determined by the difference between the particle velocity and the surrounding flow. These forces rely heavily on the sphericity of the droplet. The individual droplets are tracked by using a Lagrangian Particle Transport (LPT) approach, assuming non-displacing particles and neglecting inter-particle interactions. The main purpose with this study is to extend the LPT models with respect to droplet deformation. The aim is to first account for non-uniformities in the flow around a droplet, which affects the droplet shape, and secondly, to introduce a more detailed droplet break-up model. Current models are based on linear models related to Kelvin-Helmholtz and Rayleigh-Taylor instabilities. The former approach is used in the TAB model and is controlled by the Weber number, We, whereas the latter approach is employed in the bag break-up model. Additionally, due to droplet deformation, the forces acting on the droplet differ also from that acting on a corresponding sphere.

The focus is on studying a single droplet as the Weber number along with the particle Reynolds number are varied in order to identify the features connected with droplet deformation and break-up. The Weber and Reynolds numbers are varied in the range of 0.01 to 100 and 0.01 to 200, respectively. Through these parametric studies a parametrization of the problem is obtained and thereby, drop deformation and break-up as well as the effects of droplet deformation on the forces acting on it can be accounted for. The deforming droplets are modeled using the Volume of Fluid (VOF) approach. The enclosed figures depict the flow past a droplet for two different We (0.1 and 10, respectively) and Re=100. It is experimentally established that droplets do deform for We > 6, thus for We $= 10$, the droplet shape is no longer spherical. Also, the drag (and in shear-layers also the lift) differ widely from the forces acting a corresponding spherical particle. For We $= 0.1$ the droplets behave very closely to a solid sphere and therefore current models behave reasonably well.

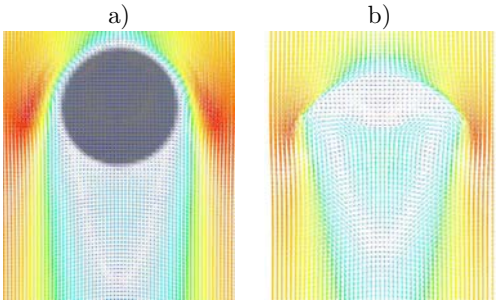

Figure 1: Velocity field at the droplet center plane for (a) $We = 0.1$ and $Re = 100$. (b) $We = 10$ and $Re = 100$.

*Div. Fluid Mech., LTH, SE-221 00 Lund, Sweden.

Modelling of the dynamics and break-up of jets and sprays

S. Sazhin[a], S. Martynov[a], C. Crua[a], E. Sazhina[a], M. Heikal[a], A. Chtab[b], M. Gorokhovskii[b] and D. Katoshevski[c]

This presentation is focused on modelling and experimental observations of the dynamics and break-up of jets and sprays, with particular emphasis on the applications to diesel engines.

The effect of flow in the injection nozzle on jet break-up is studied. A model for spray formation, which accounts for the spectra of perturbations generated by the flow inside the injector, is suggested. This model is based on the Taylor Analogy Break-up (TAB) model, and implemented into computational fluid dynamics (CFD) code KIVA-II.

The model is applied to predict deterministic regimes of disintegration of laminar forced-excited liquid jets, and realistic regimes of spray break-up in diesel engines. Calculations are performed based on the presumed spectrum of disturbances at the outlet of the injection nozzle. To validate the model, experimental observations of diesel spray from a common rail injector are studied. The measurements were performed for several injection pressures using a high speed video camera. Numerical results are compared with the measurements of macroscopic parameters of diesel fuel sprays (e.g. their cone angle and penetration length) and transverse oscillations of the diesel fuel jet.

The stochastical droplet break-up model has been incorporated into KIVA II code. Preliminary results of the comparison of predicted and observed characteristics of diesel fuel sprays are reported.

Analytical spray penetration models in the absence and in the presence of external turbulence are reviewed. These models are shown to be in good agreement with available experimental data referring to diesel fuel sprays.

Three modes of grouping of spray droplets in an oscillating flow are described using a qualitative model. These are: (1) stable grouping, (2) weak grouping, and (3) non-grouping. The model can predict grouping behavior depending on droplet size, velocity of flow, wave phase velocity and oscillation frequency. The numerical results are compared with measurements of the transversal oscillations of the liquid jet and history of variation of the dispersion angle of the jet over time.

[a] School of Engineering, Faculty of Science and Engineering, The University of Brighton, Brighton BN2 4GJ, U.K.

[b] CORIA UMR 6614 CNRS, University of Rouen, 76 801 Saint-Étienne du Rouvray, France

[c] Department of Environmental Engineering, Ben-Gurion University of the Negev, Beer-Sheva 84501, Israel

Dynamics of drop breakup in inhomogeneous turbulence

S. Galinat*, F. Risso†, O. Masbernat* and P. Guiraud‡

A drop may break under the action of the turbulent eddies. The Kolmogorov-Hinze theory[1] introduces the Weber number, $\langle We \rangle = \rho_c \langle \delta u^2 \rangle d/\sigma$ (ρ_c is the continuous phase density, σ the surface tension, $\langle \delta u^2 \rangle$ the variance of the velocity difference over the bubble diameter, d). It postulates that the breakup occurs when We exceeds a critical value. Because this approach ignores the dynamical response the drop, it is valid only when the residence time is short compared to the drop period of oscillation. For a single bubble in isotropic turbulence, it had been shown[2] that the deformation, A, is well described by a linear oscillator[3] forced by the instantaneous Weber number:

$$\frac{d^2A}{dt^2} + 2\frac{\beta}{\omega}\frac{dA}{dt} + A = We(t). \tag{1}$$

The dynamics of the interface is determined by the ratio of the damping rate, β to the frequency, ω. The goal of this work is to test the model when the turbulence is inhomogeneous and the volume fraction is large. The breakup of drops in a turbulent pipe flow downstream a restriction is investigated experimentally. The evolution of coloured drops is recorded by high speed video and the fluid flow is measured by PIV. Eq. (1) is solved numerically by using the measured Lagrangian $We(t)$. Breakup statistics are computed from many turbulent realisations by assuming that the drop breaks beyond a critical deformation A_c. Fig. 1 shows that the same value of A_c leads to a good agreement with experiments for contrasted fluid properties. Additional experiments show that the model remains valid for volume fractions up to 20%.

*LGC, UMR 5503 CNRS/INPT/UPS, 5 rue Paulin Talabot, 31106 Toulouse, France.
†IMFT, UMR 5502 CNRS/INPT/UPS, Allé Camille Soula, 31400 Toulouse, France.
‡LIPE, INSA, 135 avenue de Rangueil, 31077, Toulouse, France.

[1] Hinze, *AIChE J.* **1**, (1955).
[2] Risso and Fabre, *J. Fluid Mech* **372** (1998).
[3] Lamb, *Hydrodynamics*, Cambridge University Press (1932).

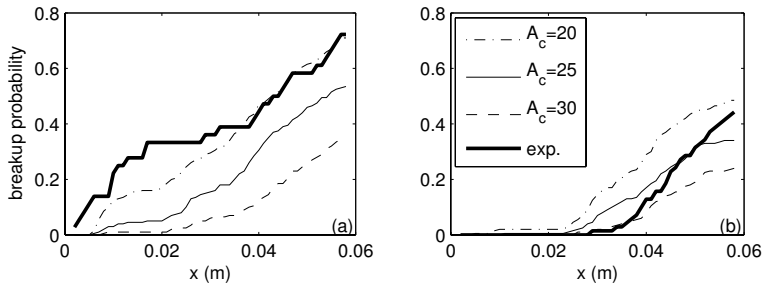

Figure 1: Breakup probability of a single drop against the distance, x, to the restriction. (a) $\beta/\omega = 0.15$ (b) $\beta/\omega = 0.7$.

Nonlinear long waves on an interface of steady-state flow of the two-layered viscous liquid in a horizontal channel

D. G. Arkhipov* and G. A. Khabakhpashev*

Problems for gravity waves on free surfaces of shallow liquid currents with a shear of the longitudinal velocity draw attention of specialists in the area of hydromechanics for a long time. Recently, however, an interest to the similar researches has increased noticeably (see, for example, [1]). In the paper[2] there was derived the evolution intergro-differential equation for long plane nonlinear interface perturbations which travelling in the direction of the two-layered laminar flow in a channel with the horizontal lid and bottom or opposite it.

In this paper it is allowed that the steady-state two-layered current of viscous incompressible liquids may be at an arbitrary angle of the wave propagation direction. There are assumed that liquids with arbitrary ratio of densities are incompressible and immiscible, their flows in a horizontal channel are laminar, amplitudes of perturbations are small but finite, characteristic horizontal lengths of disturbances are larger and thickness of unsteady viscous boundary layers are smaller than the fluid depths, and finally, capillary effects are moderate. Besides the vertical profiles of the normal velocity are accepted be linear. More general evolution equation for the interface disturbances η, which taking into account long-wave contributions of the layers inertias and the surface tension, a weakly non-linearity of perturbations, and nonstationary shear stresses at all boundaries of the system, was obtained. For the case when $\partial\eta/\partial y \sim \varepsilon\,\partial\eta/\partial x$ (ε is a small parameter) it has the following form:

$$\frac{\partial^2\eta}{\partial t^2} + u_{0i}\,(1+S_f)\frac{\partial^2\eta}{\partial t\partial x} + v_{0i}\,(1+S_f)\frac{\partial^2\eta}{\partial t\partial y} - (c_0^2 - S_f\,u_{0i}^2)\frac{\partial^2\eta}{\partial x^2} +$$

$$+\,2\,u_{0i}\,v_{0i}\,S_f\frac{\partial^2\eta}{\partial x\partial y} - C_d\,\frac{\partial^2 eta}{\partial t^2\partial x^2} - C_n\,\frac{\partial^2\eta^2}{\partial x^2} = \int\limits_0^t C_b\frac{\partial^2\eta}{\partial x^2}\frac{dt'}{\sqrt{t-t'}}.$$

Here the coefficients S_f, c_0^2, C_d, C_n, and C_b are depended not only on the geometrical (the layers depths) and the physical (the acceleration of the free fall, densities, viscosities, the surface tension) parameters of the problem, but on the liquids velocities components of the steady-state flow at the interface (u_{0i} and v_{0i}).

Allowing for dissipation the transformation of plane solitary waves of a various length were investigated numerically. It is shown the effect of value and direction of an unperturbed flow to amplitudes and profiles of disturbances.

If the initial spatial solitary waves were symmetric not only with respect to x but also with respect to y three-dimensional horseshoe-shaped perturbations were found after a time.

This work was supported by the Russian Foundation for Basic Research (Grant 04-01-00183) and by the Siberian Branch of the Russian Academy of Sciences (Basic Grant 4.2-04).

*Dept of Phys. Hydrodynamics, Institute of Thermophysics SB RAS, 630090 Novosibirsk, Russia.

[1] Grimshaw et al., *Nonlinear Processes in Geophysics* **9**, 221 (2002).

[2] Arkhipov and Khabakhpashev, *Fluid Dynamics* **40**, 126 (2005).

Experimental study of inclined film flow along periodic corrugations: The effect of wall steepness

K. Argyriadi[a], M. Vlachogiannis[a] and V. Bontozoglou[a]

Major questions arising in connection to film flow along corrugated walls are: (1) What is the morphology and structure of steady flow? (2) Under which conditions is the steady flow stable? (3) What are the characteristics of wavy, fully-developed flow under unstable conditions? The geometric characteristics of the corrugations are main input parameters, and the flat wall evidently serves as reference point for all other cases.

The present work considers flow of a film of water along rectangular corrugations of constant wavelength (L=12 mm) and varying height, B. Thus, main goal is the study of the effect of corrugation steepness, B/L (which dictates the extent of deviation from the flat wall) on the various flow phenomena outlined by the aforementioned questions. The conditions investigated correspond to the laminar, inertia-dominated regime, and include inclination angles 1º-15º and Re~10-450.

Steady flow leads to a static deformation of the free surface, of the same wavelength as the wall, which is interpreted in terms of a resonance interaction with maximum deformation at a peak Re[1]. The deformation is characterized by the steepness of the free surface and by its harmonic content (deviation from sinusoidal shape), of which the former is found independent of corrugation steepness and the latter strongly dependent on it.

Transition to a three-dimensional flow regime (consisting of transverse arrays of depressions along corrugation valleys) occurs beyond the peak Re, i.e. at the maximum steady, two-dimensional deformation, which notably is the same for all corrugation steepnesses and inclination angles tested. At lower Re, the steady two-dimensional flow becomes convectively unstable to streamwise disturbances that evolve into travelling waves. An interesting experimental finding is that the critical Re for stability increases drastically with corrugation steepness. This result, which was anticipated theoretically[2], proves that steep corrugations have a strong stabilizing effect on the steady flow.

Moving to fully-developed wavy flow under unsteady conditions, we find that the shape of travelling waves is dictated by a combination of near-solitary humps (steep front/gentle tail) with the small-scale deformation of steady flow. Steep wall corrugations appear to significantly regularize the frequency and increase the size of these travelling waves, in comparison to their counterparts along a flat wall. The difference is attributed to the continuous interaction of travelling pulses with the steadily deformed substrate.

---

[a] Dept. of Mechanical & Industrial Engineering, University of Thessaly, GR-38334 Volos, Greece.

[1] Bontozoglou, *CMES* 1, 129 (2000).

[2] Wierschem and Aksel, *Physica D* 186, 221 (2003).

Three-dimensional gravity-capillary interfacial solitary waves and related problems

E. I. Părău*, J.-M. Vanden-Broeck* and M.J. Cooker*

Fully localised three-dimensional gravity-capillary solitary interfacial waves, which travel on the interface between two superposed fluids, with a lighter fluid lying above a heavier one, are calculated. The fluids are assumed to be inviscid and incompressible and the flow is assumed to be irrotational. The fluid layers can be semi-infinite or of finite thickness. The three-dimensional problem is formulated as a nonlinear integro-differential equation by using the Green's identity in each layer and the dynamic boundary condition, which includes capillarity. These waves have damped oscillations in the direction of propagation, as in the two-dimensional case [1], and also decay in the transverse direction. When the density ratio is zero, the three-dimensional solitary interfacial waves reduce to free-surface solitary water waves which were studied in recent papers. [2] [3] [4] The stability of the solutions is discussed. A typical solution is presented in figure 1 for central-elevation and central-depression interfacial solitary waves.

The algorithm is modified to compute three-dimensional flows due to an immersed disturbance that propagates at a constant velocity U along the interface between the two fluids, and the effect of density ratio on the wave patterns is studied. Possible generalisations of the algorithm include the computation of waves when both on interface and an upper free-surface are present.

*School of Mathematics, University of East Anglia, Norwich, NR4 7TJ, UK.

[1] Dias and Iooss, *Eur.J. Mech./B Fluids*, **15**, 367(1996).
[2] Părău et al., *J. Fluid Mech.* **536**, 99(2005).
[3] Kim and Akylas *J. Fluid Mech.* **540**, 337(2005).
[4] Părău et al., *Phys. Fluids* **17**, 122101 (2005).

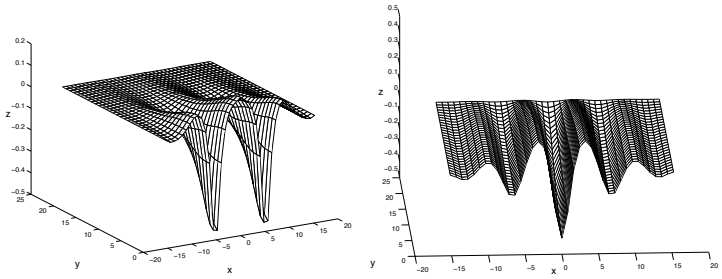

Figure 1: (a) Central elevation wave (b) Central depression wave. Only half of the each symmetric solution is shown. The waves propagate in the x direction.

Sounding rocket experiment on capillary channel flow

M. E. Dreyer*, U. Rosendahl* and C. Fechtmann*

We will report on the experimental procedure and the results of a sounding rocket experiment (TEXUS EML) on open capillary channel flows which was launched end of December 2005 from ESRANGE in North Sweden. The rocket provides 6 minutes of compensated gravity with the ability to communicate with the payload including the downlink of 2 S-VHS video channels.

The capillary channel consists of two parallel plates (25 mm breadth) mounted at a gap distance of 10 mm. The length of the open flow path, along which the test liquid (FC-72) is exposed to the ambient gas phase, is variable in-between 12 mm and 19 mm. Depending on the applied volumetric flow rate, the liquid pressure decreases in the flow direction due to flow losses. To achieve steady flow conditions the difference between the liquid pressure and the ambient pressure has to be balanced by the capillary pressure of the free liquid surfaces. A steady flow is only obtained for a flow rate below a critical value. If this value is exceeded, the liquid surfaces collapse at the channel outlet and the flow changes from steady single-phase flow to unsteady two-phase flow. The aim of the experiment is to determine the profiles of the free surfaces and to find the critical flow rate.

For this purpose the critical flow state was approached on one hand by increasing the flow rate and on the other hand by increasing the flow length. Additionally measurements of the flow velocity profiles were performed with a miniaturized Laser Doppler Veliciometer. The typical observation for a steady flow is shown in figure 1(a), while an unsteady flow due to overcritical flow rate is shown in figure 1(b). Due to total reflection of the back illumination the liquid surfaces appear dark. In order to predict the flow, a one-dimensional theoretical model was developed[1], and the critical flow rate and the surface profile data are in good agreement with the theoretical predictions.

*Center of Applied Space Technology and Microgravity (ZARM), University of Bremen, D-28359 Bremen, Germany.

[1]Rosendahl et al., *J. Fluid Mech.* **518**, 187–214 (2004).

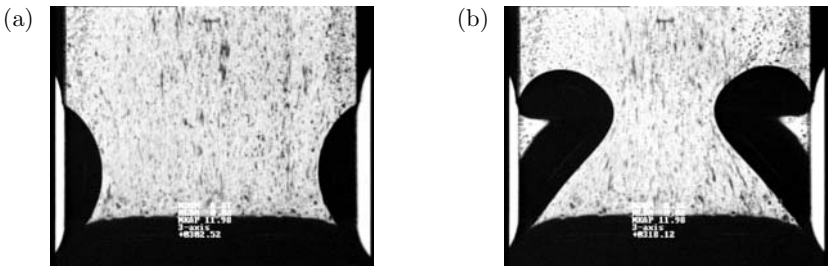

Figure 1: Front view of the capillary channel. (a) Stable flow. (b) Unstable flow.

Linear and non-linear theory of long wavelength Marangoni instability with Soret effect at finite Biot numbers.

A. Podolny*, A. Oron†, A. A. Nepomnyashchy‡

We consider a system which consists of a layer of an incompressible binary liquid with a deformable free surface, and a solid substrate layer heated or cooled from below. Surface tension σ is assumed to be linearly depend upon both temperarute and solute concentration. The Soret effect is taken into account. It is assumed that the layer is sufficiently thin, so the effect of buoyancy can be neglected as compared to the Marangoni effect. The Dufour effect is neglected.

We investigate the long wavelength Marangoni instability in the case of asymptotically small Lewis and Galileo numbers for finite surface tension and Biot numbers. We find both long wavelength monotonic and oscillatory modes of instability in various parameter domains of Biot and Soret numbers.

The weakly nonlinear analysis is carried out in the limit of the small conductivity of the solid substrate. In the leading order of the problem we consider a particular solution corresponding to a pair of travelling waves with complex amplitudes $H_{\pm}$, and angle θ between wave vectors. We obtain a set of two Landau equations that govern evolution of wave amplitudes:

$$\frac{dH_+}{d\tau} = \lambda H_+ + \alpha(X,Z)|H_+|^2 H_+ + \beta(X,Z,\theta)|H_-|^2 H_+, \tag{1}$$

$$\frac{dH_-}{d\tau} = \bar{\lambda} H_- + \bar{\alpha}(X,Z)|H_-|^2 H_- + \bar{\beta}(X,Z,\theta)|H_+|^2 H_-, \tag{2}$$

where $\alpha = \alpha_r + i\alpha_i$, $\beta = \beta_r + i\beta_i$, X is rescaled Galileo number, Z is rescaled squared wave number. In the case of small gravity ($X = 0$) the weakly nonlinear theory predicts the appearance of stable supercritical solutions if (i) $\max\beta_r(\theta) < \alpha_r < 0$ (travelling waves); this case takes place for $3.033 < Z < 4.756$ and $37.335 < Z < 44.892$; (ii) $\alpha_r < 0$, $\alpha_r < \max\beta_r(\theta)$, $\alpha_r + \max\beta_r(\theta) < 0$ (superposition of two waves with the angle θ_{max} between wave vectors, the angle θ_{max} corresponds to the maximum value of $\beta_r(\theta)$); this takes place for $1.632 < Z < 3.033$. In all other cases unstable subcritical solutions appear, hence the weakly nonlinear theory is not sufficient for finding stable solutions. It is shown that the two-wave solution with the angle θ_{max} between wave vectors, corresponding to the maximum of value $\beta_r(\theta)$, is linearly stable with respect to the excitation of new waves.

*Department of Mathematics, Technion, Haifa 32000 Israel.

†Department of Mechanical Engineering, Technion, Haifa 32000 Israel.

‡Department of Mathematics, Technion and Minerva Center for Nonlinear Physics of Complex Systems, Technion- Israel Institute of Technology, Haifa 32000 Israel.

Flow rate limitation in open capillary channels due to choking

U. Rosendahl*, M. E. Dreyer*, A. Grah* and A. Ohlhoff*

Our investigations are concerned with flow-rate limitations in open capillary channels under low-gravity conditions. An open capillary channel is a structure in which capillary forces enable a free surface flow and essentially influence the flow properties. Such channels are used in the space technology for positioning and transporting liquids.

The capillary channel we consider consists of two parallel plates that are connected to ducts of closed circumference. The open flow path is bounded by two free liquid surfaces at the sides. Depending on the applied volumetric flow rate, the liquid pressure decreases in the flow direction due to flow losses. A steady flow is obtained only for a flow rate Q below the critical value Q_{crit}. For $Q > Q_{crit}$, the liquid surfaces collapse at the channel outlet and the flow changes from steady single-phase flow to unsteady two-phase flow.

The aim of these investigations is to understand the mechanism of the flow rate limitation. Our thesis is, that the limitation occurs due to a 'choking-effect', which is known from compressible gas flows and open channel flows under normal gravity. The theory of choked flow predicts a limiting velocity corresponding to a characteristic signal velocity of the flow. Once that this critical velocity is reached the mass flow is maximum and cannot be increased further. For open capillary channel flows we expect a limiting velocity defined by the speed longitudinal waves.

The investigations are based on data achieved from sounding rocket experiments (TEXUS 41, TEXUS EML) which were launched from the ESRANGE in North Sweden. For the prediction of the flow an one-dimensional theoretical was developed[1]. The experiment evaluation yields the critical flow rate and the surface profiles in good accuracy with the theoretical predictions. We can show that the gained differential equation is of the same structure like the equations of similar compressible gas flows. Thus, in analogy to the Mach number we introduced a speed index defined by the ratio of the flow velocity and the speed of longitudinal capillary waves as the key parameter. The numerical computations show that the speed index always tends towards unity when the flow rate is increased which indicates the influence of choking. This trend is confirmed by the experimental results.

*Center of Applied Space Technology and Microgravity (ZARM), University of Bremen, D-28359 Bremen, Germany.

[1]Rosendahl et al., *J. Fluid Mech.* **518**, 187–214 (2004).

Surface oscillations of liquid nitrogen under microgravity

M. Stief* and M. E. Dreyer*

The free surface behavior has always been a matter of concern for space applications involving the handling of fluids. Special needs arise if the fluid handling involves large quantities of cryogenic fluids like liquid hydrogen or oxygen as used in the upper stage of rockets.

To overcome this lack of knowledge experiments have been performed at the drop-tower in Bremen to investigate the surface oscillations of liquid nitrogen (LN_2) upon sudden change of gravity acceleration. The oscillations were observed inside the axisymmetric configuration of a right circular cylinder with diameter D. The circular cylinder is filled with LN_2 up to the height h and the liquid is initially quiescent. The free surface forms a flat interface due to the initial acceleration of $k_{zi} = 9.81$ m/s^2 along the symmetry axis z of the cylinder. With the release of experiment setup inside the drop tower the whole system undergoes a sudden change of the acceleration from k_{zi} to $k_z \approx 1.0 \cdot 10^{-6}$ m/s^2 and the free surface is initiated to search its new equilibrium configuration.

To perform the experiment with LN_2 under isothermal and ambient pressure conditions the described experimental setup required to be at cryogenic temperatures in the range of 75-80 K. This was achieved by integrating the experiment inside a bath cryostat with two vacuum insulation shields.

For the surface oscillation upon sudden reduction of gravity two characteristic time domains can be identified. During the initial time domain a wave is traveling from the wall of the cylinder towards the center of the free surface. The influence of the first time domain can be shown by the MORTON number which expresses the ratio of the viscous time scale $t_{pvLc} = \nu\rho L_c/\sigma$ and convective time scale $t_{puLc} = \left(\sigma/\rho k_{zi}^3\right)^{1/4}$. This yields to a Morton number of $\mathrm{Mo} = \left(k_{zi}\mu^4/\rho\sigma^3\right)^{1/4}$.

The second time domain is characterized by the OHNESORGE number which is expressing the global behavior of the free surface oscillation. The OHNESORGE also derives from the ratio of convective to viscous time scale but in this case with the radius $R = D/2$ of the container as the characteristic length scale (where for the initial time domain the capillary length scale $L_c = (\sigma/\rho k_{zi})^{1/2}$ has been found). This leads to the expression $\mathrm{Oh} = \left(\nu^2\rho/\sigma L\right)^{1/2}$ for the OHNESORGE number.

With the use of liquid nitrogen we are able to investigate the free surface oscillation down to a OHNESORGE of $\mathrm{Oh} \approx 3.0 \cdot 10^{-4}$ where previous experiments[1] with conventional liquids could only cover the range down to $\mathrm{Oh} = 0.98 \cdot 10^{-3}$.

A series of experiments have been performed to investigate the main characteristic of the surface reorientation like maximum displacement z_{cp}, time for the first oscillation t_{cp} and the oscillation frequency ω. The optical observation of the free surface also revealed the feature of the formation of a liquid layer at the cylinder wall during the reorientation process.

*ZARM - University of Bremen, Am Fallturm, 28359 Bremen, Germany.

[1] M. Michaelis et al., *PAMM* (Proceedings in Applied Mathematics and Mechanics), **2**, (2003).

The effect of an electric field upon a pinched incompressible fluid

H. Gleeson*, J-M. Vanden-Broeck*, P. Hammerton* & D. Papageorgiou†

The influence of electric fields upon fluids is of considerable physical interest, particularly in applications such as coating and cooling, where liquid films are used to enhance mass or heat transfer; liquid jets and fluid sheet problems in printing, particle sorting, fuel injection and fibre formation.

We consider the dynamics of a two fluid liquid layer in the presence of a vertical electric field. The motion in the upper layer is neglected and the lower fluid is assumed to be a perfect conductor. Linear and weakly non-linear solutions have been calculated by Papageorgiou and Vanden-Broeck[1]. In this talk we present fully non-linear solutions computed using boundary integral equation methods. However, the main focus of this talk is the longwave problem when the thickness of the fluid layer is small compared with the length of the wave. By taking suitable scalings we derive an equation for the surface elevation $\eta(x,t)$,

$$2\eta_t + 3\eta\eta_x + \left(\frac{1}{3} - \tau\right)\eta_{xxx} + E_b\mathcal{H}[\eta_{xx}] = 0,$$

where E_b is the electric capillary number, τ is the inverse Bond number and $\mathcal{H}[\cdot]$ denotes a Hilbert Transform. When $E_b = 0$, we recover the Korteweg de Vries equation where analytic expressions exist for the travelling wave solution (for $\tau \neq 1/3$). For $E_b \neq 0$, numerical solutions for travelling waves will be presented. When the inverse Bond number reaches a critical value ($\tau = 1/3$), the dispersive term disappears and we recover the Benjamin-Ono equation. By looking at the diffusive term close to this critical value and considering $\tau = 1/3 + \varepsilon\tau_1$, ($\varepsilon << 1$), we introduce different scalings and derive a fifth order Korteweg de Vries equation,

$$2\eta_t + \frac{1}{45}\eta_{xxxxx} + 3\eta\eta_x - \tau_1\eta_{xxx} + \bar{E}_b\mathcal{H}[\eta_{xx}] = 0.$$

We look for solutions of the fifth order KdV equation, in particular for travelling wave solutions. We compare the solutions found to both problems with the fully non-linear solutions with a large wavelength to see when our solutions are valid.

*School of Mathematics, Univeristy of East Anglia, Norwich, NR4 7TJ, UK
†Department of Mathematical Sciences and Center for Applied Mathematics and Statistics, New Jersey Institute of Technology, Newark, NJ 07102, USA

[1]Papageorgiou and Vanden-Broeck, *J. Fluid Mech.* **508**, 71 (2004).

Waves above turbulence

R. Savelsberg*, G.J.F. van Heijst*, and Willem van de Water *

Surprisingly little is known about the statistical nature of the shape of a free surface above turbulence and how these statistics are connected to those of the sub-surface turbulence itself. Naively one would expect surface wrinkles to be primarily associated with low pressure in the cores of vortices attached to the surface.

We study this in a free surface water channel in which turbulence is generated by means of an active grid. The grid produces turbulence with a Taylor-based Reynolds number up to $Re_\lambda = 250$. The surface slope is measured in space and time by means of a novel technique, based on measuring the deflection of a laser beam that is swept along a line on the surface. By combining this with simultaneous Particle Image Velocimetry measurements of the sub-surface velocity field, we find that part of the surface shape is indeed correlated with large sub-surface structures. This is also clear from spectra of the surface slope in space and time. Such a spectrum, measured along a streamwise line, is shown in figure 1 (a). The structures directly connected to the turbulence are represented by a branch in this spectrum that corresponds to the mean-stream velocity. However, the same spectrum also shows the presence of gravity-capillary waves. Far more energy is present in a branch that corresponds to the dispersion relation for such waves, which in this streamwise spectrum is Doppler-shifted due to the mean stream velocity. The corresponding spectrum in the spanwise direction, shown in figure 1 (b), also shows the presence of gravity capillary waves.

These waves are radiated from the large scale structures attached to the turbulence and travel in all directions across the surface. As a consequence the wave-number spectrum of the surface slope is far steeper than the spectrum of the sub-surface turbulence. Furthermore, the anisotropy of the surface shape is directly connected to the anisotropy of the sub-surface turbulence.

*Eindhoven University of Technology, P.O. Box 513, 5600 MB Eindhoven, The Netherlands

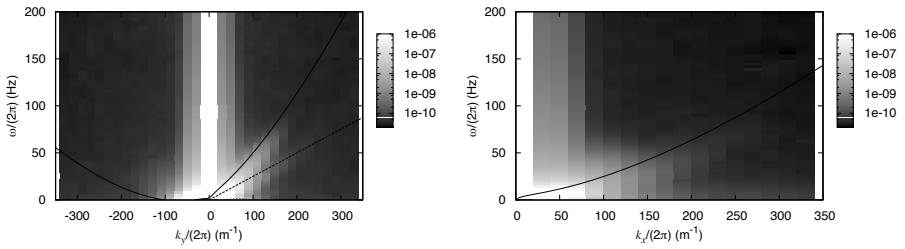

(a) (b)

Figure 1: (a) Wavenumber-frequency spectrum of the surface slope along a streamwise line and (b) the corresponding spectrum in the spanwise direction. The solid lines correspond to the dispersion relation for gravity-capillary waves. The dotted line corresponds to the mean-stream velocity in the water-channel.

Dynamic stall of oscillating NACA0012 airfoil

M.A. Ashraf[a], R. Elakoury[a], G. Martinat[a], Y. Hoarau[b], M. Braza[a] and G. Harran[a]

The unsteady turbulent flow around oscillating NACA 0012 airfoil is studied by means of numerical simulation and comparison with experimental data. Advanced statistical turbulent modelling closures (Organised Eddy Simulations) are used to capture the non-equilibrium turbulence character of the dynamic stall at high Reynolds number. The incompressible, unsteady turbulent flow aroud a static airfoil at 12° of incidence is studied at a Reynolds number of 10^5. The study is then extended to an oscillating NACA 0012 airfoil with following cases:

Oscillating NACA0012	Case 1	Case 2
Mean pitch angle α_0	12°	15°
Amplitude of pitch angle oscillation $\Delta\alpha$	6°	10°
Reynolds number	10^5	$0.98.10^6$
Mach number	0.18	0.072
Reduced frequency $k= \omega c/(2u_\infty)$	0,188	0,1

Three turbulence models in the context of the two-equation modelling approach are tested separately: the k- ε and k- ω models modified by the OES approach and the classical Menter's shear stress transport model.

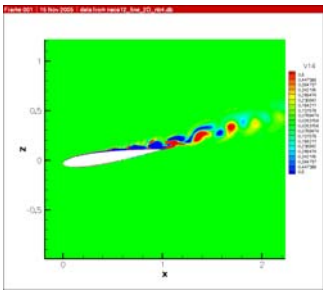

Figure 1 : Vorticity contours, Case 2, α=8.4°, pitching up, k- ε/OES model

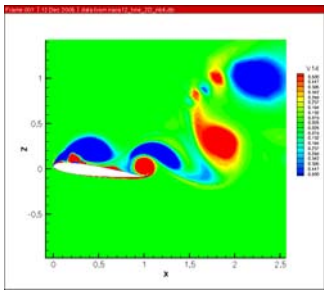

Figure 2 : Vorticity contours, Case 2, α=23.7°, pitching down, SST model

[a] Institut de Mécanique des Fluides de Toulouse, allée Camille Soula, 31400 Toulouse, France.

[b] Institut de Mécanique des Fluides et des Solides de Strasbourg, 2 rue Boussingault, 67000 Strasbourg, France.

Flow around a NACA 0021 airfoil at 60° angle of attack

R. El Akoury[a], M. Braza[a], Y. Hoarau[b], and G. Harran[a]

The flow around symmetric NACA 0021 airfoil at angle of attack 60°, is studied at the Reynolds number based on the chord length Re=(UC)/ν=2.7.10^5. Three dimensional simulations are carried out for a spanwise length of one chord using a 148x104x34 grid. k-ε model modified by the OES (Organised Eddy Simulation) approach, and three hybrid turbulence models DES (Detached Eddy Simulation) are tested separately. New turbulence length scale is used according to experimental results (Braza *et al.*[1]). Thus the URANS parts (Unsteady Reynolds Averaged Navier-Stokes) use a modified turbulence length scale (in the context of OES approach) based on the modification of the turbulence spectrum due to coherent-incoherent structures interaction in the inertial region. Time averaged pressure coefficient distribution ($C_p(x)$) and time averaged drag and lift coefficients (C_d , C_l) for the four turbulence models used are compared with experimental parameters[2].

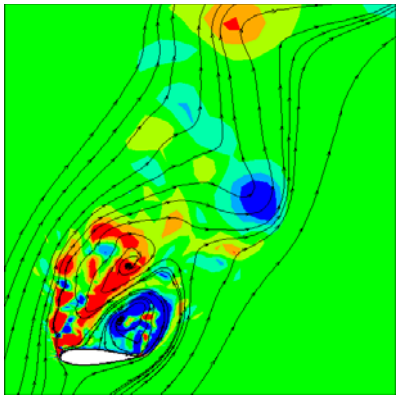

Figure 1 : Vorticity contours and streamlines

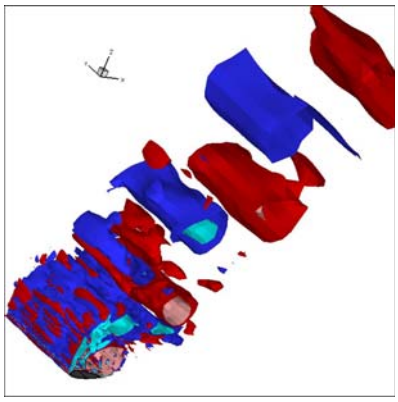

Figure 2 : 3D iso-vorticity surfaces

[a] Institut de Mécanique des Fluides de Toulouse, allée Camille Soula, 31400 Toulouse, France.

[b] Institut de Mécanique des Fluides et des Solides de Strasbourg, 2 rue Boussingault, 67000 Strasbourg, France.

[1] Braza et al., *BBVIV4, Santorini*, (2005).

[2] Swalwell et al., *21st AIAA Applied Aerodynamics Conference*, 2003-3416, (2003).

Global drag fluctuations of disks having different sizes in a turbulent jet : averaging effect of the turbulent scales

B. Thiria*, J. -F. Beaudoin†and O. Cadot*.

The fluctuating drag of a disk $\delta F(t)$ with a surface S (the corresponding diameter vary between $1cm$ and $5cm$) facing a turbulent jet (of radial size $10cm$, velocity $U = 10m/s$, Reynolds number $Re = 65000$) is measured with a piezoelectric transducer. A special care was taken in order to increase the frequency response of the drag fluctuations that crucially depends on the transducer holding stand. The transfer function is measured with a white noise electromagnetic excitation and shows the measurements to be reliable for frequencies up to 1Khz. The fundamental question is: how are the local turbulent fluctuations averaged in space and time to form the resulting global drag fluctuation on the disk ? As far as we know there are not much studies devoted to this while it is of great interest for industrial applications. In the present study, the experimental parameter being the disk surface S and the drag an extensive variable, we focus on the drag divided by S, say $\delta F(t)/S$. The first important result is that whatever the disk surface the standard deviation $\delta F^{rms}/S$ is constant. However, the skewness of the fluctuations are significantly reduced as the disk surface increases showing somehow a filtering effect. The filtering effect is confirmed by a cut-off at lower frequencies for larger disk's surface. The effect is also accompanied by an increase of energy contained at low frequencies. This redistribution of energy fluctuations is equivalent to the constancy of standard deviation.

*Unité de Mécanique, Ecole Nationale Supérieure de Techniques Avancées, Chemin de la Hunière, 91761 Palaiseau Cedex, France.

†Department of Research and Innovation, PSA Peugeot-Citroën, 2 route de Gisy, 78943 Vélizy-Villacoublay, France.

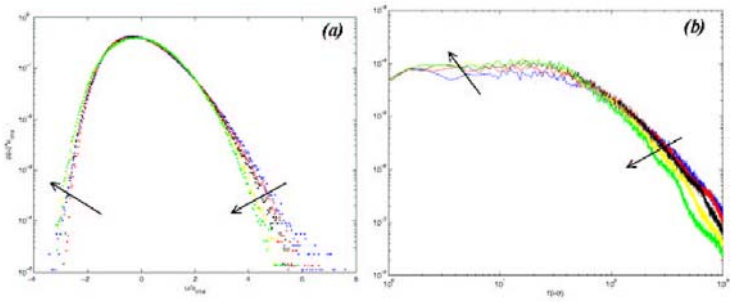

Figure 1: (a): Density probability function (PDF) of the drag reduced by its standard deviation. (b): power spectrum of drag fluctuations $\delta F(t)/S$. For both cases, the arrows signalize the increase of the surface S.

Investigation of flow structure upon new wing section for small UAVs and MAVs

V.V. Kozlov[a], I. D. Zverkov[a] and B.Yu. Zanin[a]

.

The report focuses on flow separation on airfoils and associated phenomena which are much important due to creation of modern small-scale aircrafts (small UAVs and MAVs) with improved aerodynamic characteristics. The data shown in what follows provide deeper insight into flow physics at separation and leading-edge stall at small Reynolds numbers as well as into new possibilities of flow control employing wings with wavy surface.

First, the separated flow structure is investigated on wings placed at zero angle of attack. The results are obtained using two experimental models with one and the same airfoil but different shape of the lifting surface, that is, the smooth (a) and the wavy one (b). By means of oil-film visualization the flow patterns are documented in both cases, see Figure 1, and compared with pressure data and results of hot-wire measurements. Thus, a correlation between three-dimensional flow structure and transition to turbulence was observed. It is found that on the wavy surface the separation region splits into several small-scale separation bubbles that affects the transition process.

Then, the flow over smooth and wavy wings is explored at variation of the angle of attack, Reynolds number and the free-stream turbulence level. Using flow visualization, hot-wire technique and measurements of aerodynamic forces some benefits of the wavy wing were found. In particular, the wavy wing has a critical angle of attack which is much higher than that of the smooth one and a larger lift-to-drag ratio at α = 5 to 20 degrees in a low turbulent stream. At examination of the effect of external turbulence on flow separation it was concluded that flight conditions can be reproduced perfectly in low-turbulent aerodynamic facilities.

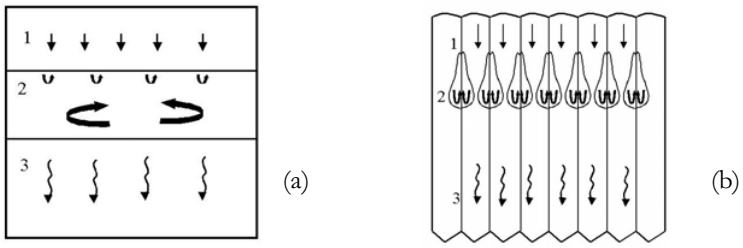

Figure 1: Flow patterns upon wings with smooth surface (a) and wavy surface (b), at angle of attack $\alpha=0^{O}$. 1 – laminar flow; 2 – separation bubble; 3 – turbulent flow.

[a] ITAM SB RAS Institutskaya str., 4/1 Novosibirsk, 630090 Russia.

Application of sound measurements to quantitative analysis of the parameters of concentrated vortical structures

S. I. Shtork[a, b], E. C. Fernandes[a]

Examples of the concentrated vortices include propeller tip vortices, trailing vortices behind the aircrafts, tip vortices above the delta wings, tornadoes, columnar vortices inside the cyclonic separators and swirl combustors. In case of the technological devices like gas-turbine combustors and cyclone dust cleaners a strong flow swirling associated with the high vorticity magnitude provides indispensable condition for their proper operation. On the other hand these vortices may generate disastrous vibrations and noise, demanding for exploration of ways to restrain the danger they pose. For these reasons this phenomenon attracts a permanent attention from the fluid mechanics research community.

Basically, access to the vortex dynamics implies determination of the main vortex characteristics such as vorticity distribution in the vortex core, the core size and total vortex intensity represented normally by the vortex tube circulation. As an alternative to expensive (in terms of the time consumption and high cost equipment employed) detailed flowfield examination, which conventionally used to characterize the vortex properties, the pressure detection can be considered. Previously this approach has been used for nonintrusive measurements of the size and intensity of vortices based on the pressure measurements at a vortex chamber bottom[1]. Static pressure difference across the vortex has been taken to characterize the flow regimes in a model gas turbine combustor[2]. Two-point acquisition of fluctuations of the instantaneous pressure has been also utilized to explore the unsteady vortex flow structure in a swirl-stabilized combustor under isothermal [3] and reacting[4] conditions. In present study an acoustic technique based on the specific local pressure probes will be applied to quantify characteristics of the precessing vortex generated in swirling jet flow over a model vortex burner[5] and the results will then be compared to the velocity data obtained with an LDV. Additionally a study will be carried out to assess the influence of the acoustic probe on the flow field as well aspects like: probe orientation, probe size and corresponding acoustic transfer function on the data interpretation.

The first author would like to gratefully acknowledge financial support from the Portuguese Science and Technology Foundation (Grant SFRH/BPD/1641/2000, Coordinator Prof. M.V. Heitor).

---

[a] Mechanical Engineering Department, Instituto Superior Técnico, Lisbon, Portugal
[b] Institute of Thermophysics SB RAS, Novosibirsk, Russia

[1] Alekseenko et al., *J. Fluid Mech.* **382**, 195 (1999).
[2] Anacleto et al., *Comb. Sc. Techn.* **175(8)**, 1369 (2003).
[3] Fernandes et al., *Exp. Fluids*, (2005) http://dx.doi.org/10.1007/s00348-005-0034-4
[4] Fernandes et al. In proc. *12th International Congress on Sound and Vibration*. 11-14 July, 2005, Lisbon, Portugal.
[5] Shtork et al., *Techn. Phys. Let.* **31(8)**, 660 (2005)

Simultaneous density and concentration measurements on hypersonic jets

M. Belan*, S. de Ponte*, and D. Tordella†

This work presents an experimental investigation on free hypersonic jets, travelling over a long scale, about 50 initial diameters. The jets under study are underexpanded (non-isoentropic), with barrel and normal shocks, in quasi-steady conditions. The facility is essentially made of a vacuum vessel with suitable nozzles for the gas inlet and a CCD camera; it makes use of the electron beam technique for the gas ionization [1] [2]. The system permits to use different gases for the jet and the external ambient, so that the density ratio (jet/external medium) may be adjusted in the range 0.04 to 10. Depending on the stagnation/ambient pressure ratio, the maximum value of the Mach number along the jet axis ranges from 5 to 30[3]. Besides visualizations and density measurements, in this experiment simultaneous density and concentration maps of the images are made possible by a new image post-processing method: this leads to direct measurements of the mixing layer thickness, and in general of the lateral spreading, giving more informations on the long term spatial evolution of the jets.

The results show that a heavy jet in a light medium has a small spreading angle and a simple structure, with a single normal shock along the axis. On the other hand, a light jet in a heavy medium has a larger spreading angle with a more efficient mixing with the ambient, and it exhibits a more complex structure, with multiple recompressions after the first normal shock. As an example, the figure shows a helium jet travelling in an argon ambient, and the relevant concentration curves taken at two different cross sections, before and after the first normal shock. In this example the long term density ratio is $\rho_{\rm jet}/\rho_{\rm amb} \simeq 0.11$, the maximum Mach number is $M_{max} = 17$.

*DIA, Politecnico di Milano, v. la Masa 34 - 20156 Milano, Italia
†DIASP, Politecnico di Torino, c. Duca degli Abruzzi 24, 10129 Torino, Italia

[1] Dankert, Bütefisch, *Engineering Research* **52** *(5)*, 1986
[2] Mironov, *Int. Conf. on the Methods of Aerophysical Research*, Novosibirsk-Tomsk, Russia, 2000
[3] Belan et al., *Astrophysics and Space Science* **293** *(1-2): 225-232*, 2004

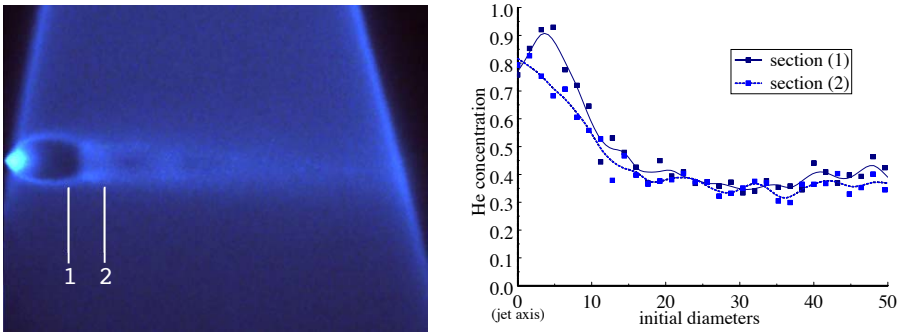

Figure 1: (a) Jet image; (b) He concentration along two cross-sections

APART: An MTV technique applicable in a large range of environments

J. Bominaar*, M. Pashtrapanska*, N. Dam*, W. van de Water*†and J. J. ter Meulen*

Molecular Tagging Velocimetry provides an interesting alternative to particle-seeded techniques for measuring flow velocities. Commercial techniques used nowadays require adding seed particles to the flow, which possibly perturb the flow, do not follow small scale turbulence very accurately and can not reach all regions of the flow. With the MTV technique used in our lab (APART; Air Photolysis And Recombination Tracking[1]) a line of NO molecules is created locally by focusing a 193 nm ArF excimer laser. An applied flow will change the characteristics and position of this line which can be monitored, after an adjustable delay, by imaging the fluorescence of NO induced by a 226 nm dye laser on a CCD camera. Figure 1 shows a schematic drawing of the setup.

We present experiments where the APART technique was applied to several environments including high temperatures and high pressures. Statistical data on the turbulent characteristics of a turbulent premixed methane-air flame has been gathered and compared to LDA measurements performed in a different lab. Another study was performed in a high pressure cell where the pressure was varied between 0 and 80 bar and the ratio of oxygen and nitrogen adjusted. The width and diffusion for the different compositions and pressures was examined.

*Radboud University Nijmegen, Institute for Molecules and Materials, Applied Molecular Physics, the Netherlands.
†Eindhoven University of Technology, Applied Physics, the Netherlands
[1]Dam *et al.*, *Opt Lett.* **26**, 36 (2001).

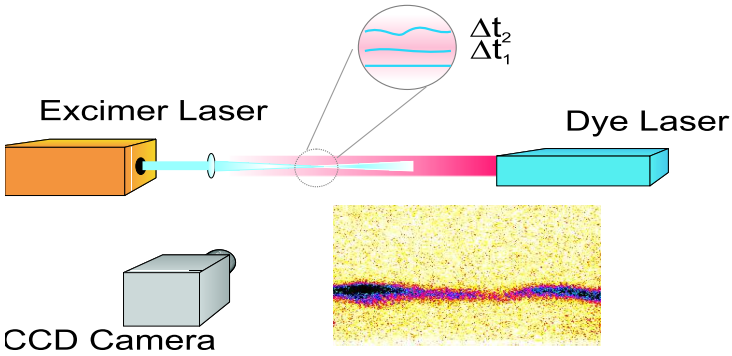

Figure 1: Schematic drawing of the APART setup; an ArF excimer laser is focused in a line creating nitric oxide molecules from the ambient air. The line of molecules will displace in the flow and can be visualized by imaging the fluorescence induced by a 226 nm dye laser on an ICCD camera. The inset on the lower left shows a typical image created by with this technique in a turbulent flame.

Introduction of newly developed towing wind tunnel facility

S. Yoshioka[a], T. Kato[a], Y. Kohama[a], F. Ohta[a], M. Tokuyama[a]

We have built 7 km long testing line in Sunrise beach research facility of Tohoku University in Hyuga city, Miyazaki, Japan in 2003. In the first 2 km out of total 7 km we constructed a testing track of the towing wind tunnel. A schematic of this facility is shown in Fig. 1. The first 910 m is accelerating region, the next 515 m is the measuring region, where is covered by acoustic material, see Fig. 2, and the final 475 m is the decelerating region. In this track an electrically driven vehicle runs. We named this facility as HART which stands for Hyuga Aerodynamic Research facility by Towing. We call the vehicle as HART vehicle.

As a first experiment we put a vertical flat plate, see Fig. 3, on this HART vehicle and tried to measure the boundary layer transition on this flat plate. Fig. 4 shows the obtained velocity signals. Signals in Fig. 4 are representative signals measured in laminar, intermittent and turbulent boundary layers. In the signals measured in the intermittent boundary layer, the passage of the turbulent spots is clearly observed as a positive spike. The transitional Reynolds number where intermittency factor falls to 0.5 was Re_{50}~4.0×10^6. This very high transitional Reynolds number shows very low free stream turbulence condition.

[a] Institute of Fluid Science, Tohoku University, Sendai, Japan

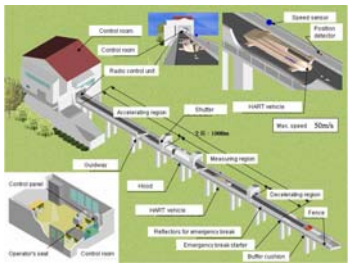

Figure 1: Schematic of HART facility

Figure 2: HART vehicle in measuring region

Figure 2: Vertical flat plate

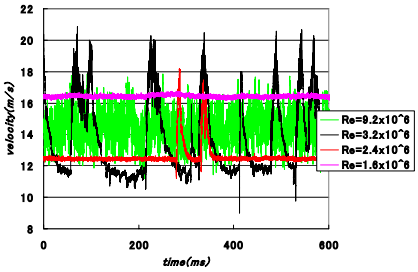

Figure 3: Velocity signals in boundary layer

Session 5

A Simple Model for Gas-Grain Two Phase Isentropic Flow and a High Resolution Scheme for the Numerical Solution of the Governing Equations

J. Hudson and D. Harris*

This contribution presents a simple model for the isentropic two phase flow of a solid granular material dispersed in a gas obeying the perfect gas law. The dispersed and continuous phases are both treated as continua and an Eulerian description of the flow is adopted.

The first key physical quantity in the model is the solids volume fraction and the model comprises continuity equations and balances of linear momentum for the gas and solid phases.

The second key physical quantity is the fluctuation energy for the solids phase, otherwise known as the granular temperature. The fluctuation energy arises in the theory of the statistical mechanics of granular materials and dense gases and was later introduced into continuum models. The model is complete by the fluctuation energy equation. The presence of the solids fluctuation energy gives rise to a solids pressure in the balance of momentum for the solids phase. We assume the simplest possible equation of state for the solids pressure, namely the analogy of the perfect gas law. In the absence of viscosity the classical equal pressures model is ill-posed, but we demonstrate numerically that the presence of the solids pressure due to the solids fluctuation energy gives rise to regimes in which the model is indeed well-posed.

The hyperbolicity of the system of equations is investigated numerically and the numerical solution of the equations in conservation form is accomplished using a high-resolution scheme[1] in the hyperbolic regime. Careful attention is given to the discretisation of the inhomogeneous terms. Three one-dimensional test cases are considered, namely a simple advection test problem, a square pulse test problem and a steady state problem and we use these to obtain quantitative and qualitative insight into the predictions of the model.

*School of Mathematics, University of Manchester.

[1]Hudson et al, submitted to *J. Comp. Phys.*

Experimental study of incipient motion and transportation of particles with various shape

K.J.A. Westin[a], F. Alavyoon[b] and M. Henriksson[a]

Objects (particles) entering the reactor pressure vessel in a nuclear power plant may cause damages to the fuel assemblies, with expensive production stops as a consequence. At present time there are intentions to increase the thermal power in many plants, which also implies increased flow rates. A question that has received attention lately is how the increased flow rate will affect the probability for particles entering the reactor pressure vessel.

The aim of the present study is to quantify the required flow velocity for transportation of particles with generic shapes (cylinders, washers, sphere). At first the drag coefficients for free falling particles were determined by measuring the terminal fall velocity in a test tank. These tests also demonstrated the inherently oscillating motion that is obtained with the washers and the low-aspect ratio cylinders. The incipient motion of the particles subjected to a slowly increasing flow rate was then studied in a horizontal pipe with a dimension similar to a feed water pipe (inner diameter 290 mm). The particle motion in a 90° bend and in a vertical pipe section was examined in order to determine the required flow rate to obtain a vertical transportation of the particles, and the particle behaviour near an obstacle was also studied. Besides video recordings, simultaneous measurements of flow rates and wall-shear stress (Preston tubes) were carried out.

The required flow rates to obtain a transportation of the particles along the vertical pipe were quantified, showing 1.2 to 5 times larger flow velocity than predicted by assuming a balance between the drag force (based on mean bulk velocity) and the gravitational force. It was also shown that the curvature of the pipe had a clear stabilizing effect on cylinders aligned with the flow, which significantly delayed the particle transportation along the horizontal pipe.

[a] Vattenfall Utveckling AB, SE-814 26 Älvkarleby, Sweden.

[b] Forsmarks Kraftgrupp AB, SE-742 03 Östhammar, Sweden.

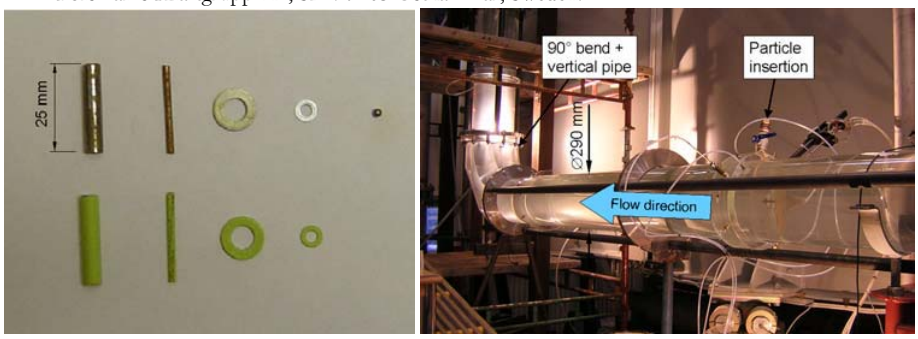

Figure: (Left) Test particles. (Right) Test rig for transportation tests (acrylic glass).

Dynamics of heavy particles near a helical vortex lament

R. H. A. IJzermans*, R. Hagmeijer* and P.J. van Langen*

The motion of small heavy particles near a helical vortex filament is investigated both numerically and analytically. We study the case of a helical vortex filament in unbounded space and the case of a helical vortex filament which is placed in a concentric cylindrical pipe. Potential flow is assumed which is not influenced by the presence of the heavy particles (one-way coupling). For both cases, the velocity field in a helical coordinate frame is described by a stream function [1,2]. In the equation of motion of the heavy particles, Stokes drag is taken into account.

Numerical results show that heavy particles may accumulate in a fixed point in the helical coordinate frame, near an elliptic region in the stream function. In physical space this corresponds to a helically shaped equilibrium trajectory. The relation between the topology of the carrier flow field and the phenomenon of particle accumulation becomes clear from figure 1, where the positions of a group of initially uniformly distributed particles are plotted after a long time. The particle accumulation is proven analytically by a linear stability analysis. In addition, a full classification of possible flow field topologies is presented.

These results can be useful in the design of gas-liquid separators, in which a helical vortex filament is used for the separation of small dust particles and/or very small droplets [3].

*University of Twente, P/O box 217, 7500 AE, Enschede, Netherlands.

[1] Hardin, *Phys. of Fluids* **25**(11), (1982).
[2] Alekseenko et al., *J. Fluid Mech.* **382**, 185 (1999).
[3] Hagmeijer et al., *Phys. Fluids* **17**, 056101 (2005).

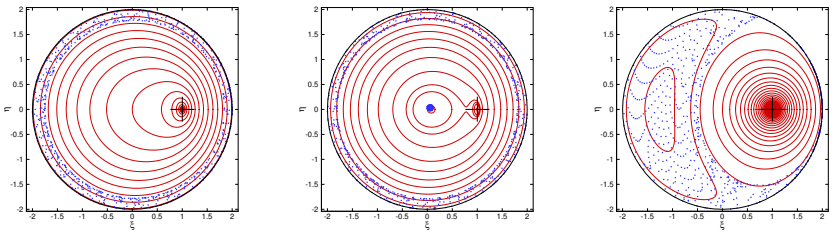

a) $\epsilon/a = 10^{-3}$, $l/a = 0.5$. b) $\epsilon/a = 10^{-2}$, $l/a = 1$. c) $\epsilon/a = 10^{-2}$, $l/a = 5$.

Figure 1: Positions of heavy particles (blue dots) after time $t\Gamma/a^2 = 100$, for three different values of the thickness of the vortex filament ϵ/a and the helix pitch $2\pi l/a$; the tube radius $R/a = 2$ and the particle relaxation time $\tau_p\Gamma/a^2 = 0.4$, where Γ is the vortex strength and a the radius of the helix geometry. For comparison, the streamlines of passive tracers are plotted in the background (red lines).

Dispersed phase subgrid models for Euler-Euler Large Eddy Simulation of turbulent gas-particle flows

M. Moreau*, E. Riber*†, B. Bedat* and O. Simonin*

A new challenge in the two-phase CFD field is the prediction of unsteady phenomena induced by the most energetic scales of turbulence. For example, cycle to cycle variations are a major concern in the design of car engines as they affect the pollutant emissions. Large Eddy Simulations (LES) approach allow to compute the large scales of a fluid turbulent flow and provide a well established powerfull tool. For gas-dispersed phase flow, this approach is classicaly coupled with Deterministic Particle Simulation ie. Lagrangian tracking of individual particles. However, processes involving a huge number of droplets, DPS are difficult to handled in industrial configuration. A promising alternative tool is Eulerian approach for the dispersed phase coupled with fluid LES.

As shown by Février et al. [1], in the case of inertial particles with response times larger than the Kolmogorov time scale, the Eulerian approach for particle phase must account specifically for the effects of a particle Random Uncorrelated Velocity, which can be derived in the frame of the Mesoscopic Eulerian Formalism. Eulerian equations of the dispersed phase (particle number density, momentum, Random Uncorrelated Energy (RUE)) are obtained by a conditional average for a given fluid turbulent flow realization. An attempt to directly simulate these equations has been done by Kaufmann et al[2] and shows the difficulty to capture smallest relevant scales of the flow.

By a spacial filtering procedure, particle large scales eulerian equations are obtained. Subgrid terms arise and need to be modeled. Particle subgrid stress models for momentum equation are derived from fluid compressible turbulence subgrid stress models[3]. Modeling of subgrid term in RUE is investigated. Model validation is performed thanks a-priori test using DNS+DPS results in homogeneous isotropic turbulence and a-posteriory test of gas-particle confined jet.

*IMFT, allée du Pr C. Soulas, 31400 Toulouse, France.
†Cerfacs, 42 Avenue Gaspard Coriolis. 31057 Toulouse Cedex 01, France.
[1]Février et al., *J. Fluid Mech.* **533**, 1-46 (2005).
[2]Kaufmann et al., *5th Int. Conf. on Multiphase Flow*, 443-ICMF'04 (2004).
[3]Riber et al., *11th Workshop on Two-Phase Flow Predictions*, (2005).

Stability of dusty gas flow in a vertical channel

S.A. Boronin[a], A.N. Osiptsov[a]

The problem of laminar-turbulent transition in 2D dusty-gas flows was considered in a number of studies using the Saffman[1] formulation or its small modifications[2], in which velocity slip of the phases in the basic flow was ignored. It was shown that the presence of even a small amount of particles can significantly change the limits of the laminar flow regime. In the present study, dealing with the stability of a vertical channel flow with inertial particles, we modify the Saffman formulation and focus on the role of phase velocity slip in the basic flow (caused by the gravity force) in laminar-turbulent transition.

We consider the linear stability of downward dusty-gas flow in a vertical channel within the two-fluid model[3] with Stokes particles. The basic carrier-phase flow is given by the Poiseuille velocity profile, with the particle velocity slip being equal to the gravitational settling velocity. The disturbances are specified in the form of travelling waves. After the linearization, the problem is reduced to a modified Orr-Sommerfeld equation with several extra terms. The eigenvalues are calculated numerically at high accuracy using an orthonormalization method.

The effect of the particles on the gas flow is described by three similarity parameters: Froude number (which determines the velocity slip in the basic flow), particle mass loading α, and inverse Stokes number β (ratio of the channel width to the particle velocity relaxation length). A parametric study of neutral curves was performed for fixed α=0.1. It was shown that: (i) for $\beta <$ 0.075 (high-inertia particles), the critical Reynolds number decreases as compared to horizontal channel flow and the effect of particles is most pronounced at small Froude numbers (high gravity). (ii) For $\beta \geq 0.075$, the instability region in the (Re, k) plane (Re – basic-flow Reynolds number, k – wave number) becomes bounded and reduces (tending to a point) as the Froude number decreases and tends to a threshold value Fr_0. Accordingly, for $Fr < Fr_0$ the flow is stable with respect to arbitrary small perturbations. The work was supported by the RFBR (project 05-01-00502).

---

[a] Institute of Mechanics Lomonosov Moscow State University, Michurinskii pr., 1 119899 Moscow, Russia

1 Saffman, *J. Fluid Mech*. 13, 120 (1962).

2 Asmolov and Manuilovich, *J. Fluid Mech*. 365, 135 (1998)

3 Marble, *Ann. Rev. Fluid Mech.* 2, 397 (1970)

Large Eddy Simulation of Horizontal Particle-Laden Channel Flows with Effect of Wall Roughness

A. Konan*, O. Simonin* and K. D. Squires†

Detailed analysis of the particle behaviour in horizontal channel in experimental works by Schade et *al.* [1], Sommerfeld et *al.* [2, 3] show that the wall roughness affects strongly the particle transport. They observed a modification of pressure loss, particle mass flux, particle mean and fluctuating velocities along a narrow channel, due to the roughness effect on the particle-wall interaction mechanism. Such an effect has been accounted for in several numerical studies based on RANS approaches [4, 5, 6, 7] leading to very convincing results. In particular, according to Sommerfeld, the roughness effect may be accounted for by assuming that any incident particle collides with a virtual wall with a random inclination obeying a given truncated Gaussian probability distribution function satifying the realisability of the particle bouncing angle.

We have carried out Large-Eddy Simulation (LES) of the carrier phase flow coupled with Discrete Particle Simulation (DPS) using the Sommerfeld's virtual wall model. Lagrangian particle tracking is computed by assuming only gravity and drag forces. Simulations are performed in the dilute limit in which particle-particle collisions are accounted for, using a deterministic approach (hard-sphere model), but neglecting the modification of the underlying carrier flow by momentum exchange with the particles. Computations were performed for spherical glass beads with diameters between $130\mu m$ and $195\mu m$ and different wall roughness standard deviations ($1.2°$ and $7.0°$). The numerical predictions (mass flux, mean and turbulent velocities) are compared with Sommerfeld's experimental results [8].

In addition, statistical properties of the incident and bouncing particle velocities are measured from the simulations and used for the theoretical derivation of particulate eulerian wall boundary conditions [9].

*Institut de Mécanique des Fluides, Allée du Professeur Camille Soula, 31400 Toulouse, France.
†Department of Mechanical and Aerospace Engineering, Arizona State University, Tempe, Arizona 85287, USA

[1] K.-P Schade and Th. Hädrich, *3th International conference on multiphase flow, ICMF'98, Lyon,France, June 8-12*,(1998).
[2] M. Sommerfeld and N. Huber, *Int. J. Multiphase Flow* **25**,(1999).
[3] J. Kussin and M. Sommerfeld, *Experiments in Fluids* **33**,(2002).
[4] Y. Tsuji, T. Oshima and Y. Morikawa, *KONA* **3**,(1985).
[5] M. Sommerfeld, *Int. J. Multiphase Flow* **18**,(1992).
[6] M. Sommerfeld and J. Kussin, *Powder Technology* **142**, 180-192 (2004).
[7] Xia Zhang and Lixing Zhou, *5th International conference on multiphase flow, ICMF'04, Yokohama, Japan, May 30 - June 4*, **162** (2004).
[8] Sommerfeld, *11th Workshop on two-phase flow predictions, Merseburg, Germany, April 5-8*,(2005).
[9] A. Konan, O. Simonin and J. Adou, *11th Workshop on two-phase flow predictions, Merseburg, Germany, April 5-8*, (2005).

Joint fluid-particle pdf modeling of a binary mixture of colliding particles falling across a turbulent homogeneous gas flow

P. Fede*, O. Simonin*, L. Zaichik†

The wide range of applications involving gas-solid turbulent flow leads to the strong development of modeling approach. Examples of applications are: pneumatic conveying, circulating fluidized bed and sediments motion as well. In such applications complex phenomena take place such as particle dispersion, particle segregation, turbulence modulation by particles, particle-particle collision, particle-wall interaction. In addition, the modeling approach has to take into account another level of complexity, namely the particle-size distribution. In particular, the non-uniqueness of particle diameter induces mean momentum and random kinetic energy transfers by collision between particle species.

A statistical description of the inter-particle collision effect, based on the joint fluid-particle probability density function (pdf) is proposed. Compare to the standard kinetic theory statistical description (i.e. using single particle velocity pdf and molecular chaos assumption), the joint fluid-particle pdf allows to take into account some specific effects occurring in gas-particle turbulent flows[1]. Especially, following Laviéville et al.[2] the collision kernel may be expressed with a closure accounting for the correlation between colliding particle velocities induced by the turbulence. Effective dispersed phase numerical modeling is carried out using the moment method (also called n-fluid model) consisting in the computation of transport equations for particle and fluid-particle pdf moments (number density, mean velocity, particle kinetic stresses, fluid-particle velocity covariance).

In the present work, we focus on the modeling of random kinetic energy transfers in binary mixture of particles falling in a homogeneous isotropic turbulent gas flow. The effects of the correlation induced by the turbulence and of the mean drift between particle species induced by the gravity are investigated. For validation, we compare the closure assumptions and model predictions with detailed numerical results from Large Eddy Simulation (LES) coupled with Discrete Particle Simulation (DPS).

*Institut de Mécanique des Fluides de Toulouse, Avenue Camille Soula, 31400 Toulouse, France.
†Institute for High Temperatures of the Russian Academy of Sciences, Krasnokazarmenaya 17a, 111250 Moscow, Russia

[1] O. Simonin, P. Février & J. Laviéville, 2002, "On the Spatial Distribution of Heavy-Particle Velocities in Turbulent Flow : from Continuous Field to Particulate Chaos", *Journal of Turbulence*, Vol. **3**, 040.

[2] J. Laviéville, E. Deutsch & O. Simonin, "Large Eddy Simulation of interaction between colliding particles and a homogeneous isotropic turbulence field", *6th Int. Symp. On Gas-Solid Flows*, 1995, Vol. **228**, pp 347-357, ASME FED.

Instability of an axisymmetric vortex in a stably stratified fluid

S. Le Dizès* P. Billant†

The stability of a vertical vortex in a stably stratified fluid is considered by analytical and numerical methods. We show, in a general setting, that a centrifugally stable vortex can be destabilized by gravity wave radiations when the Froude number is small. The analytical study is based on a large axial wavenumber asymptotic analysis[1,2] of the inviscid perturbation equations under the Boussinesq approximation. By matched asymptotic methods, we demonstrate the existence of unstable modes for all non-zero azimuthal wavenumbers m satisfying $|m| < N/\Omega_0$ where N is the Brunt-Väsäilä frequency and Ω_0 the angular velocity of the vortex on the axis. These modes are therefore unstable when the stratification is sufficiently large ($F = \Omega_0/N < 1$). The dispersion relation for these modes and a simple expression for their growth rate are obtained as a function of the angular velocity profile of the vortex. For the Lamb-Oseen vortex, the asymptotic results are compared to the instability modes computed numerically by a shooting method and a very good agreement is obtained (see figure). The asymptotic study also provides the radial structure of the unstable eigenmodes and hints for the instability mechanism. The unstable modes are made of two oscillating regions separated by a small interval in which is located a critical point (where $\omega = m\Omega(r)$, ω being the frequency of the instability wave) and which acts as a potential barrier. The first region plays the role of potential well for inertial-gravity waves and discretizes the frequencies of the modes. The second region is a radiating zone which extends to infinity. The instability mechanism is associated with the destabilizing "scattering" of the inertial-gravity waves from the first region toward the second region across the potential barrier.[3,4]

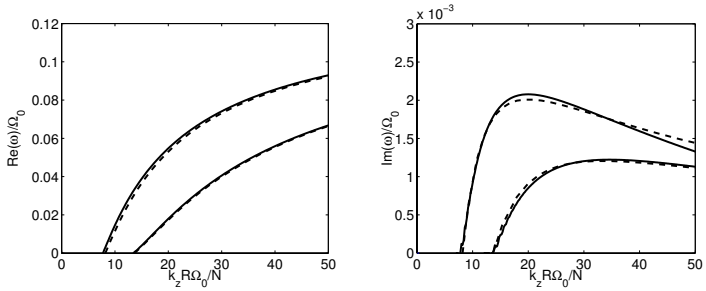

Figure 1: Frequency (left) and growth rate (right) of two unstable modes for $m = 1$ and small Froude Number for the Lamb-Oseen vortex. (−): Numerics; (−−): Theory.

*IRPHE, 49 rue F. Joliot Curie, BP 146, F-13384 Marseille cedex 13, France.
†LADHYX, Ecole Polytechnique, F-91128 Palaiseau cedex, France.

[1]Le Dizès and Lacaze, *J. Fluid Mech.* **542**, 69–96 (2005).
[2]Billant and Gallaire, *J. Fluid Mech.* **542**, 365–379 (2005).
[3]Ford, *J. Fluid Mech.* **280**, 303–334 (1994).
[4]Schecter and Montgomery, *Phys. Fluids* **16**, 1334–1348 (2004).

Three-dimensional stability of vortex arrays in a stratified fluid

Axel Deloncle*, Paul Billant and Jean-Marc Chomaz

The three-dimensional linear stability of classical vortex configurations (Von Karman street and double symmetric row) is investigated through a theoretical and numerical analysis in the case of a strongly stratified fluid.

For strong stratification, recent studies have shown that columnar vertical vortex pairs are subject to a 3D zigzag instability[1,2] which consists in a bending of the vortices (figure 1–left) and leads to the emergence of horizontal layers.

We demonstrate that both the Von Karman street and a double symmetric row of columnar vertical vortices are also unstable to the zigzag instability. By means of an asymptotic theory in the limit of long-vertical wavelength and well-separated vortices, the most unstable wavelength is found to be proportional to bF_h, where b is the separation distance between the vortices and F_h the horizontal Froude number ($F_h = \Gamma/\pi a^2 N$ with Γ the circulation of the vortices, a their core radius and N the Brunt-Väisälä frequency). The maximum growthrate is independent of the stratification and only proportional to the strain $S = \Gamma/2\pi b^2$. A numerical linear stability analysis fully confirms the theoretical predictions (figure 1–right).

The non-linear evolution of these vortices arrays as well as other random configurations shows that the zigzag instability ultimately slices the flow into horizontal layers. These results demonstrate that the zigzag instability is a generic instability. It may explain the observations of layered structures in experiments[3] and numerical simulations[4] of stratified turbulence.

*LadHyX, Ecole Polytechnique, CNRS, 91128 Palaiseau, France.

[1]Billant and Chomaz, *J. Fluid Mech.* **418**, 167 (2000).
[2]Otheguy et al., *J. Fluid Mech.* in press.
[3]Praud et al., *J. Fluid Mech.* **522**, 1 (2005).
[4]Waite and Bartello, *J. Fluid Mech.* **517**, 281 (2004).

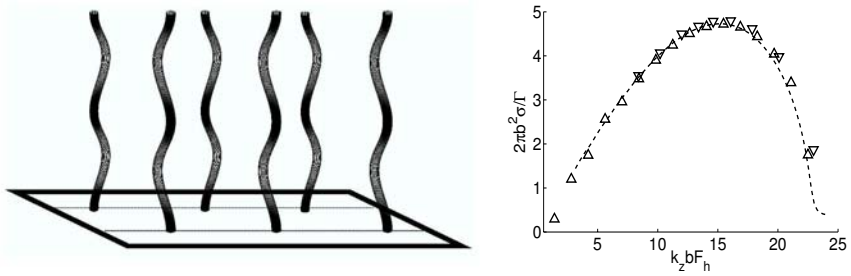

Figure 1: Von Karman street. (left) sketch of the zigzag instability. (right) growthrate $2\pi b^2\sigma/\Gamma$ of the zigzag instability versus the vertical wavenumber $k_z bF_h$. - - -: asymptotic theory; Numerics with a 256x640 resolution: $F_h = 0.2$ $\triangle$, $F_h = 0.4$ $\triangledown$

Scattering of internal gravity waves

A. Nye[a] and S.B. Dalziel[a]

Internal gravity waves are generated by disturbances to continuous stable stratifications such as those found in the deep ocean. While reflection from smooth boundaries (*i.e.* boundaries that appear flat on the scale of the wavelength) may be well modelled through simple ray tracing, the same is not true when the boundaries contain features of a scale comparable with the wavelength. In such cases incident wave energy flux may be 'scattered' amongst different wavenumbers at boundaries and even reflected back along the path of the incident wave beam. The amplitude and steepness of the scattered waves will also differ from that of the incident beam. Consequently, subsequent propagation of scattered waves can result in breaking, turbulence and mixing. Such mixing is associated with higher wavenumbers because the corresponding waves have small length scales and may develop shear instabilities.

This research aims to establish scattering behaviour of internal gravity waves incident on topography with length scales similar to those of incident waves. Numerical and experimental methods are used to investigate two-dimensional internal gravity waves with frequencies less than the buoyancy frequency interacting with topography.

A two-dimensional inviscid numerical model had been developed to describe internal gravity waves propagating in a stable linear stratification. Waves are generated by fluxes varying sinusoidally in time over the surfaces of a square 'source'. Structures of simulated wave beams are compared before and after incidence on various numerical topographies. Amplitudes of the scattered waves are used to determine the partitioning of incident energy flux between different wavenumbers and frequencies at the boundary. A complementing experimental investigation uses a "synthetic schlieren"[1] technique to observe scattering of internal gravity waves in a stable linear salt-stratified tank. Waves are produced by small amplitude vertical oscillation of axis-symmetric cylinders of circular and square cross-section. These studies are intended as a comparison to theoretical work currently in progress.

[a] DAMTP, University of Cambridge, U.K.

[1] Dalziel et al., *Exp. Fluids* **482**, 51 (2003).

Mixing by merging Kelvin-Helmholtz billows

M. D. Patterson*, J. N. McElwaine*, C. P. Caulfield†and S. B. Dalziel*

Quantitative time dependent measurements of the irreversible mixing caused by the development, saturation and turbulent breakdown of Kelvin-Helmholtz (KH) billows on an initially stable two layer stratification of miscible fluids are taken from a series of laboratory experiments. The experiments are carried out in a tilting tank similar to that used by Thorpe[1]. The initial conditions consist of a two layer stratification of fresh water, ρ_1, and a dyed saline solution, ρ_2, where $\rho_1 < \rho_2$. The evolution of the KH billows is recorded using a digital video camera. The results are post-processed using a light attenuation technique [Hacker et al.[2]]. The light attenuation technique relates the amount of light that passes through the dyed fluid directly and noninvasively to the spanwise-averaged time-dependent concentration field. Figure 1 shows four experimental snapshots that highlight the temporal evolution of the KH billows. The contours in the figures give an exact measure of the spanwise averaged density field. Using the available potential energy framework of Winters et al.[3], the time-dependent mixing associated with the billows as they develop streamwise secondary instabilities which trigger turbulence, are quantified. Two different types of KH development are identified quantitatively. Under certain circumstances, the billows merge in a largely symmetrical manner (shown below), having developed to an approximately equal saturated amplitude. However, it is also possible for the development of a billow to be stunted by more rapidly growing neighbours and the stunted billow is then absorbed by a larger neighbour. The mixing properties of these different life-cycles are qualitatively different, with the stunted billows leading to measurably more irreversible mixing due to the enhanced intensity of the transition to turbulence.

*DAMTP, Wilberforce Road, University of Cambridge, U.K.
†B.P. Institute and DAMTP, Wilberforce Road, University of Cambridge

[1]Thorpe, *J. Fluid Mech.* **46**,299 (1971).
[2]Hacker, Linden, and Dalziel, Dynamics of Atmospheres and Oceans **24**, 183 (1996)
[3]Winters, Lombard, Riley and D'Asaro, *J. Fluid Mech.* **289**, 115 (1995).

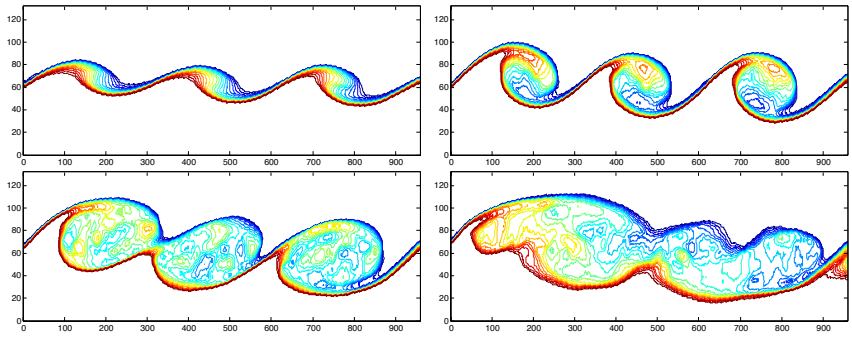

Figure 1: Density contour at t= 4, 5, 6 and 7 s after the initiation of the experiment

Scattering of linear Rossby waves by abrupt topography

Gareth W. Owen*, I. David Abrahams† and Andrew J. Willmott*

Planetary Rossby waves propagate across the world's ocean basins. They play a vital rôle in the long term distribution of ocean vorticity and to the oceans' rapid adjustment to atmospheric and climatic variability. Knowledge of the interaction between these waves and topography is crucial to a full understanding of this process, and hence to the transportation of energy, mixing and ocean circulation. Previously, the interaction of baroclinic Rossby waves with abrupt topography was modelled using barotropic or simple layered models. Here a more realistic model is employed, with a continuously stratified fluid of buoyancy frequency $N(z)$. The topographic variation consists of a 'top-hat' ridge of infinitesimal or finite width.

The quasi-geostrophic streamfunction, ψ, satisfies the linear Rossby wave equation

$$\frac{\partial}{\partial t}\left\{\frac{\partial^2\psi}{\partial x^2}+\frac{\partial^2\psi}{\partial y^2}+\frac{\partial}{\partial z}\left[\frac{f^2}{N^2}\frac{\partial\psi}{\partial z}\right]\right\}+\beta\frac{\partial\psi}{\partial x}=0.$$

The vertical modes satisfy a Sturm-Liouville eigenvalue problem, which predicts a qualitatively different modal structure than that of layered models. Applying a mode matching technique results in a singular algebraic system of equations. This is solved using a novel method in order to determine the scattering coefficients. In the case where this algebraic method breaks down we employ matched asymptotic expansions.

We consider two ideal stratifications: a constant buoyancy frequency[1] and a buoyancy frequency that decays exponentially with depth[2]. It is found that the scattered field depends crucially upon the stratification. When the density variation is confined to a thin thermocline a large amount of the incident wave energy is reflected by a small ridge. Appreciable energy conversion between the propagating modes takes place in this case and the scattered field differs markedly from the two-layer solution.

*Mathematics, Keele University, Keele, Staffs. ST5 5BG, UK.
†Mathematics, University of Manchester, Manchester M13 9PL, UK.
[1]Owen, Abrahams, Willmott and Hughes, *J. Fluid Mech.* **465**, 131 (2002).
[2]Owen, Willmott, Abrahams and Mansley, *Geophys. and Astrophys. Fluid Dyn.* **99**, 219 (2005).

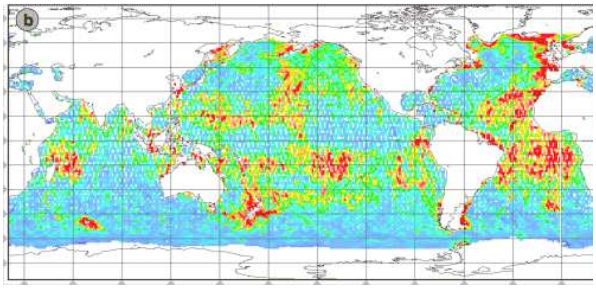

Figure 1: Satellite altimetry data reveals strong Rossby wave activity in regions close to ocean ridges. Phase shifts are consistent with conversion between baroclinic modes.

The new approach to the evolution description of moderately long planar nonlinear surface waves

D. G. Arkhipov* and G. A. Khabakhpashev*

In this paper there are assumed that liquid is incompressible, its stationary flow is absent, amplitudes of perturbations are small but finite, characteristic horizontal lengths of disturbances and the bottom topography are larger and the thickness of unsteady viscous boundary layer is smaller than the fluid depth, and finally, capillary effects are moderate. The input system of the hydrodynamics equations was reduced to one basic evolution equation for nonlinear perturbations of the free surface η

$$\frac{\partial^2\eta}{\partial t^2} - gh\nabla^2\eta - \frac{g}{2}\nabla^2\eta^2 - \frac{h}{2}\nabla^2\mathbf{u}^2 + \nabla\cdot\left(\mathbf{u}\frac{\partial\eta}{\partial t}\right) - g\,\nabla h\cdot\nabla\eta -$$

$$-h^2\left(\frac{1}{3}-\frac{1}{\mathrm{Bo}}\right)\nabla^2\frac{\partial^2\eta}{\partial t^2} + g\sqrt{\frac{\nu}{\pi}}\int\limits_0^t \frac{\nabla^2\eta\ dt_i}{\sqrt{t-t_i}} = 0 \qquad (1)$$

and two linear elementary auxiliary equations for a determination of the liquid horizontal velocity vector $\mathbf{u}$ averaged over the layer depth h which is contained in the equation (1) only in the terms of the second order of smallness:

$$h\,\nabla\cdot\mathbf{u} = -\partial\eta/\partial t, \qquad \nabla\times\mathbf{u} = 0. \qquad (2)$$

Here g is the free fall acceleration, the operator ∇ is defined in a horizontal plane, Bo is the Bond number, and ν is the kinematic viscosity of a fluid. The suggested model is suitable for nonlinear waves running on any angles. Even in case of an ideal liquid this approach is in essence easier than known systems of equations, in which all equations contain both linear and nonlinear items (see, for example, [1,2]). Some solutions of the equations (1)–(2) were found numerically. The results of calculation for initial perturbation "cross" on water with $h = 10$ cm are shown in Figure 1.

*Dept of Phys. Hydrodynamics,Institute ofThermophysics SB RAS, 630090 Novosibirsk, Russia.

[1]Peregrine, *J. Fluid Mech.* **27** 815 (1967). [2]Green and Naghdi, *J. Fluid Mech.* **78** 237 (1976).

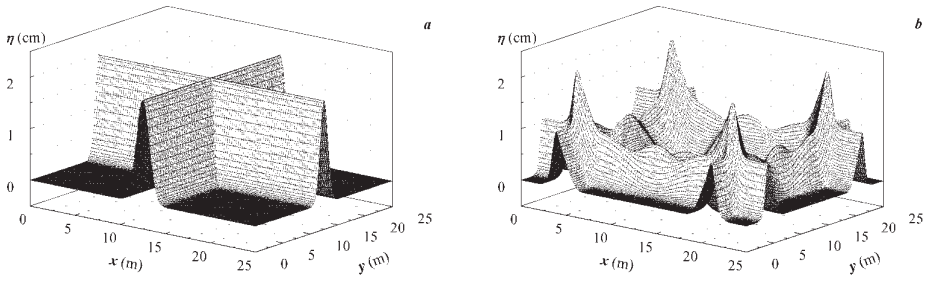

Figure 1: (*a*) Initial perturbation. (*b*) Shapes of 4 quasi-plane waves after 8 seconds.

Segregation of sinking particles of different densities in an oscillating velocity field of strongly nonlinear surface waves

N. Antipin[a], A. B. Ezersky[a], F. Marin[b] and O. A. Cheikh[b]

Arising of patterns at the bottom under the action of intense nonlinear waves – solitons – when particles of the same size but having appreciably different densities take part in pattern formation is investigated experimentally and theoretically. Experiments were carried out in the channel of the laboratory of the Le Havre University. The procedure of soliton excitation was described in the work[1]; the interaction of solitons with patterns at the bottom when there is only one type of particles in the bottom layer was studied in[2]. In this work we investigate features of bottom relief formed when nonlinear waves agitate the sand (size d ~ 160 μ, density ρ ~2.6 g/cm^3) and polyvinylchloride (PVC) balls (size d ~ 160 μ, density ρ ~1.26 g/cm^3) under the action of bottom turbulence. It was found that, after the external action exciting nonlinear waves has ceased and the particles have started sinking at the bottom, their concentration in the neighborhood of sand ripple crests increases as the waves and turbulence are damping. As soon as the motion in the liquid has ceased, one can visualize PVC particles localized in a narrow region of ripple crests (fig. 1). A theoretical model explaining such a density-dependent segregation of particles has been developed.

[a] Institute of Applied Physics RAS, 46 Ulyanov Str. 603950, Nizhny Novgorod, Russia.

[b] LPMG Universite du Havre, Place R.Schuman, B.P. 4006, 76610, Le Havre, France.

[1] Ezersky et al., *J. Phys. Fluids*, submitted for publication (2005).

[2] Marin et al., *J. Geophysical Research* **110**, accepted for publication (2005).

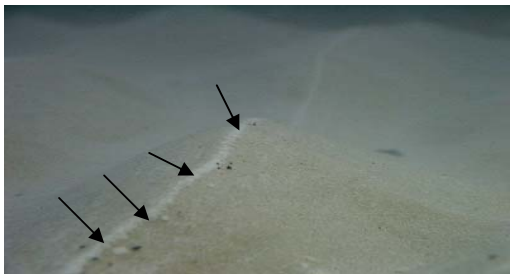

Figure 1: Particle segregation at sinking of a mixture of 95% of sand and 5% of PVC balls after excitation of nonlinear waves has ceased. The arrows mark the narrow region of concentration of PVC particles along the crests of sand ripples

Nonlinear Vorticity Waves Between Critical Layers

O.G. Derzho[a]

A new theoretical model for long vorticity waves propagating on a sheared background flow is developed. Undisturbed flow is assumed to be confined between two critical layers (i.e. layers where magnitude of the mean shear is equal to the velocity of the disturbance) located near lower and upper rigid boundaries. In such system even small disturbances will break and a zone filled with the mixed fluid may subsequently appear near the walls. A technique that explicitly resolves structure of the recirculation zones is developed using an approach similar to the described earlier[1].

This technique is applied to derive one nonlinear evolution equation for the amplitude of a wave-like disturbance of finite magnitude. Not surprisingly dispersion and temporal terms in this equation are the same as in the KdV theory while nonlinearity is shown to be drastically different. It comprises of the nonlinearity associated with nonlinear shear across the wave guide and the nonlinearity due to the flow over zones of mixing fluid. It is shown that the combined nonlinearity may change sign depending on the location of the mixing zone near upper or lower boundary of the waveguide. Furthermore, nonlinearity due to the flow over mixing zones may effectively cancel the nonlinearity associated with the shear flow within a certain interval of amplitudes; however outside this interval it doesn't take place. We examine stationary solutions of the obtained equations and show that there are no stationary vorticity waves in our geometry if fluid has a constant density. Weak effect of stratification which effectively adds a linear term in our resulting equation actually controls the existence of nonlinear stationary vorticity waves solely due to the specific structure of the nonlinearity that varies if the wave speed is changed. This specific nonlinearity gives rise to a number of new nontrivial wave-like structures, which include cnoidal and solitary waves and internal (generally asymmetric) bores. We anticipate that all these solutions essentially differ from typical vorticity waves or KdV-type solitary waves in stratified fluid with shear. Relevance of the obtained results to the formation of gravity currents will be discussed.

Next, an analogy between vorticity waves on a sheared stratified flow and vorticity inertial waves on a swirling flow in a tube with axial shear will be discussed based on the approach[2]. Using this analogy a mechanism of formation of the breakdown bubble between two critical layers (i.e. layers where the mean axial velocity is equal to the phase velocity of an inertial wave) can be proposed.

---

[a]Institute of Thermophysics, 630090, Novosibirsk, Russia

[1] Derzho and Grimshaw, *Phys. Fluids*, **9**, 3378 (1997)

[2] Derzho and Grimshaw, *J. Fluid Mechanics*, **464**, 217 (2002)

LES of a turbulent channel flow at streamwise rotation

N. A. Alkishriwi, M. Meinke, and W. Schröder *

In many engineering and industrial applications the investigations of rotating turbulent flows is of great interest. In this type of flow the Coriolis force has a strong influence on the turbulence. For instance, turbulent flows in a rotating channel are severely affected by this force, which is induced by the system rotation. It produces a secondary flow in the spanwise direction. Some research has been done for channel flows with a spanwise rotation axis [1]. However, up to now very few investigations have been done on channel flows with a rotation about the streamwise axis. Analyses of this type of flow based on Lie-group theory and DNS [2] suggest that a secondary flow perpendicular to the main flow direction is generated whose distribution strongly depends on the rotational speed [3]. In the present study an LES of a turbulent streamwise rotating channel flow at $Re_\tau = 180$ is performed using a moving grid method to predict the three-dimensional structures and secondary flows. Among different issues the impact of the formulation on the spanwise boundary condition is one of the major objectives of this study. That is, the question whether or not periodic boundary conditions in the spanwise direction allow to numerically reproduce the experiments conducted by Recktenwald et al. will be addressed. The simulations are carried out at rotation rates corresponding to Rossby numbers $R_o = u_b/Hf$ with H being half the channel height $R_o = \infty$, $R_o = 65.2$, and $R_o = 37.5$.

Results

First, the method of solution has been applied to compute the flow in a stationary channel ($R_o = \infty$) at the same Reynolds number. The turbulent statistics and the mean flow profiles are compared with the direct numerical simulations of Kim et al. [4]. Figure 1 shows the convincing comparison of the distribution of the LES based streamwise, spanwise, and normal Reynolds stresses with DNS findings. The final version of the study will focus on the detailed discussion of the flow field in the streamwise rotating channel. A first result of the averaged spanwise velocity profile is shown also in fig. 1.

*Institute of Aerodynamics, RWTH Aachen University, Wüllnerstraße 5 thr. 7, D-52062 Aachen, Germany.

[1] Kristofferson and Andersson, *J. Fluid Mech* **256**, 163 (1993).

[2] Oberlack et al., Proceedings of the Center for turbulence Summer Programm 221 (1998).

[3] Recktenwald et al., Proc. of the Tenth European Turbulence Conf., Trondheim, Norway 2004.

[4] Kim et al., *J. Fluid Mech* **177**, 133 (1987).

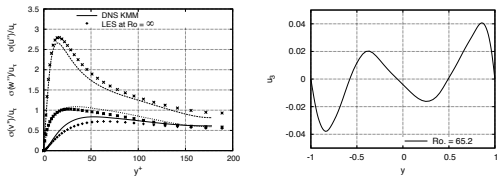

Figure 1: Distribution of the streamwise, spanwise, and normal Reynolds stresses (left), spanwise velocity distribution (right).

Direct numerical simulations of rotating channel flow at high rotation numbers

O. Grundestam*, S. Wallin* and A.V. Johansson*

Turbulent rotating channel flow subject to high rates of system rotation is studied through direct numerical simulations. The computational code is based on a pseudo-spectral method using fourier series in the periodic spanwise and streamwise directions and Chebychev polynomials in the wall-normal direction. A computational box with a size of $4\pi\delta \times 2\delta \times 2\pi\delta$ in the streamwise, wall-normal and spanwise directions, respectively, was used. Simulations have been performed for Reynolds number $Re_\tau = 180$, based on the wall-shear velocity and half the channel width, using a resolution of $192 \times 129 \times 160$ for rotation numbers $Ro = 2\Omega\delta/U_b = 0.98$, 1.07, 1.15, 1.21 and 1.27 where Ω is the system rotation rate and U_b the mean bulk flow.

In the present study, the increase in rotation clearly has a damping effect on the turbulence. This involves both the stable and unstable side of the channel as well as all components of the Reynolds stress tensor. The present trend is hence different compared to the behaviour for lower rotation numbers studied by Alvelius[1]. The system rotation also have a very strong stratifying effect on the velocity fluctuations which implies a significant difference in the turbulence levels in the stable and unstable side for all rotation rates studied. This is illustrated in figure 1 below in which an instantaneous yz-plane is shown for the wall-normal fluctuating velocity, v', at $Ro = 1.27$. The difference between the unstable and stable side is striking and the velocity fluctations are clearly restricted to the unstable side of the channel.

The slope of the mean velocity is close to 2Ω in the center of the channel. There is, however, a small but significant deviation from this for all rotation numbers. The present investigation confirms the trend of decreasing difference between the wall-shear velocities on the stable and unstable side with increasing Ro, suggested by Alvelius[1]. In fact, for the highest rotation number the difference is smaller than for the $Ro = 0.055$ case presented by Alvelius[1].

*KTH Mechanics, OB 18, SE-100 44 Stockholm, Sweden.

[1]Alvelius, *PhD-thesis*, KTH Mechnics (1999).

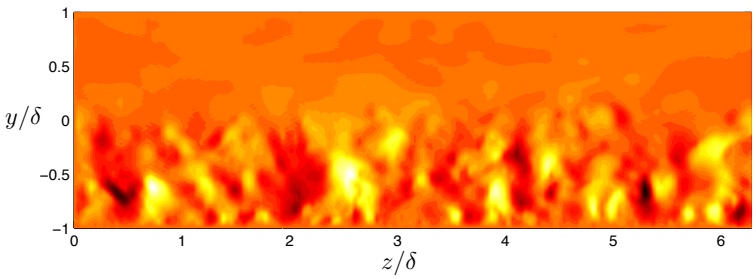

Figure 1: Wall-normal fluctuating velocity v' in an instantaneous yz-plane for $Ro = 1.27$. Dark/bright areas indicate positive/negative v'.

Heat Transfer in Turbulent Rotating Convection

R. P. J. Kunnen*, H. J. H. Clercx*, and B. J. Geurts*†

Rayleigh-Bénard convection is a classical problem in which a fluid layer enclosed between two parallel horizontal walls is heated from below. In a rotating frame of reference the dynamics can change considerably through the fundamental involvement of a combination of buoyancy and Coriolis forces. The rotating Rayleigh-Bénard (RRB) setting is important for many applications, *e.g.,* in engineering and climate modelling.

The dynamics of RRB convection can be characterised by three dimensionless parameters. The Rayleigh number Ra characterises buoyancy, the Taylor number Ta is associated with rotation, and the Prandtl number σ is a fluid property. Our aim is to gain a better understanding of the transport of heat across the layer that is described by the Nusselt number Nu, which is a function of Ra, Ta, and σ.

Direct numerical simulation (DNS) is used to calculate Nu at systematically varied Ta. The DNS code solves the incompressible Navier-Stokes equations in a rotating frame of reference, coupled to the heat equation within the Boussinesq approximation. Periodic boundary conditions are adopted in the horizontal directions and the vertical boundaries are treated as isothermal, no-slip walls.

The cyclonic thermal plumes that erupt from the thermal boundary layers are the dominant structures in turbulent rotating convection, as shown in figure 1(a). The Ta dependence of Nu is depicted in figure 1(b). At moderate Ta Nu increases, associated with Ekman pumping. At higher Ta a dominant geostrophic inhibition of vertical (convective) motion arises. This figure is for $Ra = 2.5 \times 10^6$ and $\sigma = 1$.

The velocity and temperature averages from this DNS will be compared to measurements in a water-filled cylindrical convection cell. Detailed velocity and temperature data will be obtained using stereoscopic particle image velocimetry and laser induced fluorescence, respectively.

*Department of Physics, Eindhoven University of Technology, P.O. Box 513, 5600 MB Eindhoven, The Netherlands

†Department of Applied Mechanics, University of Twente, P.O. Box 217, 7500 AE Enschede, The Netherlands

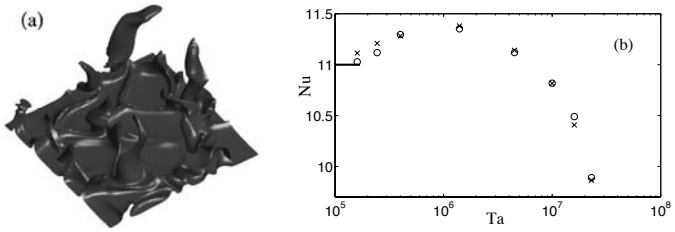

Figure 1: (a) Cyclonic thermal plumes as observed in a temperature isosurface plot. (b) Nu as a function of Ta. The line on the vertical axis indicates Nu at $Ta = 0$, crosses and circles are Nu calculated at top and bottom walls, respectively.

Study of anisotropy in purely stratified and purely rotating turbulence by orthogonal wavelets

Lukas Liechtenstein* and Kai Schneider†

Rotating or stratified turbulence develops coherent structures which are generally known as cigars and pancakes, respectively. This self organization of the flow is widely observed in direct numerical simulations of homogeneous anisotropic turbulence[1] as well as in laboratory experiments[2].

The iso-surfaces of vorticity for a stratified (left) and rotating flow (right) shown in Fig.1 illustrate the strongly anisotropic character of these coherent structures. A quantitative analysis of their anisotropy has up to now not been performed, partly due to the difficulty in defining a coherent structure. Attempts have been made by using statistical measures, such as directional correlation length scales or directional Rossby and Froude numbers [3]. However, a scaling law including the parameters determining the anisotropy, namely f the Coriolis parameter, N the Brunt-Vaisala frequency and ν the kinematic viscosity, have not been found.

An objective way to define coherent structures has been introduced[4] using an orthogonal wavelet decomposition of vorticity. The coherent flow is reconstructed from few strong wavelet coefficients, while the incoherent flow corresponding to the majority of weak coefficients is uncorrelated and noise like. In the present paper we apply the orthogonal wavelet decomposition to extract coherent vortices out of rotating or stratified turbulence calculated by decaying DNS with Reynolds numbers of $Re_\lambda \approx 150$. The orthogonal wavelet decomposition of a 3D-flow field creates by definition coefficients with seven pre-defined directions. Due to this characteristic of the coefficients, we then quantify the anisotropy of the coherent vortices by studying the energy distribution and higher order moments in wavelet coefficient space.

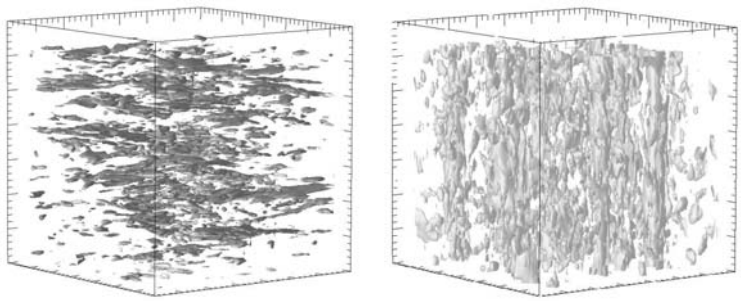

Figure 1: Iso-surfaces of coherent vorticity for $|\vec{\omega}| = 3.70, \sigma = 0.92$ computed at resolution 256^3. Left: stratified case, represented by 2.12 % of the wavelet coefficients. Right: rotating case, represented by 2.25 % of the wavelet coefficients.

*MSNM-CNRS, IMT Château-Gombert, 38 rue Joliot Curie, F-13451 Marseille, FRANCE
†MSNM-CNRS & CMI Univ.de Provence, 39 rue Joliot Curie, F-13453 Marseille, FRANCE

[1] see e.g. Liechtenstein *et al.*, *Journal of Turbulence* **6**, 24 (2005).
[2] see e.g. C. Morize *et al*, *Phys. Fluids* **17** 095105 (2005)
[3] Godeferd and Staquet, *J. Fluid Mech.*, **486**, 115 (2003)
[4] Farge *et al*, *Phys. Rev. Lett.*, **87(5)**, 054501-1 (2001)

Modelling anisotropic dispersion in rotating stratified turbulence

L. Liechtenstein, F.S. Godeferd & C. Cambon*

Direct numerical simulations (DNS) of homogeneous turbulence under the effect of rotation and stable stratification show a modification of the structure of the turbulent field with respect to the isotropic case, as well as a strong modification of the energy exchange processes. The structures length scale in the turbulent flow increase along the rotation axis ("vertical"), or perpendicular to the density gradient when stratification dominates (*i.e.* along the "horizontal"). Nonlinearity is unavoidable in the dynamics for constructing these anisotropic Eulerian one- or two-point statistics.

However, valuable information can still be obtained from linear approaches when considering Lagrangian statistics. It has been shown that the analytical solutions obtained from rapid distortion theory (RDT), limited to one-particle dispersion in the vertical and horizontal directions, compare well with results from DNS.[1] This is also true for anisotropic one-particle dispersion results obtained from a computationally efficient stochastic model called Kinematic Simulation (KS), provided care be taken about how the stratification and rotation effects are included in the model.[2] One shows that the inclusion of inertio-gravity waves is a key ingredient of these anisotropic KS simulations for rotating stratified turbulence. With respect to RDT, KS also permits to compute any time-dependent Lagrangian arbitrary-order correlations.

The first message conveyed in our work is that anisotropy has to be dealt with care when generating the random modes basis for the stochastic model. This point is supported by a poloidal-toroidal formalism for decomposing the velocity field, coupled with an original way of distributing the random inertio-gravity waves with a pdf-based method. Even for isotropic turbulence without waves, the new randomization of the wavevector yields significant improvements vs. previous standard methods.

We then tackle the paradox which consists in having a good prediction without nonlinearity for one-particle Lagrangian statistics, whereas for Eulerian ones, be they one- or two-point, linear models totally fail. A first element of answer is to be found in the two-particle Lagrangian statistics, which we investigate in this work, comparing what is obtained by KS, DNS and RDT. One discusses the respective influence of advection, anisotropy, and the topology of coherent structures on two-particle dispersion, trying to determine which mechanism is dominant.

Regarding two-particle dispersion, one observes three regimes: a small-time ballistic range, a long-time Brownian one, and intermediate regime of internal waves altering Richardson's law. The extent in time of each of them depends on timescales that are related to the strength of stratification and rotation, although no definite scaling can be satisfactorily proposed at the moment. These non-classical scalings, in both the horizontal and vertical directions, and the possibility of gathering two-particle dispersion under one unified description shall be discussed, especially contrasting with one-particle dispersion, for which the Lagrangian timescale is unambiguously defined.

*LMFA, École Centrale de Lyon, Écully F-69134 France

[1] Cambon et al., J. Fluid Mech., **499**, 231, (2004)

[2] Liechtenstein, Godeferd & Cambon, *J. of Turb.* **6(24)**, 1 (2005).

Direct numerical simulation of turbulent flow in a tilted rotating duct

G. E. Mårtensson*, G. Brethouwer* and A.V. Johansson*

Studying the effects of system rotation on turbulent flow is a most difficult and important area of turbulence research. This area is of fundamental academic interest, as well as of considerable industrial importance concerning applications such as centrifugal separators and turbines. In centrifugal separator applications, the flow is subjected to extremely high system rotation rates, the Rotation number being typically around or above one. At these high Rotation numbers, the flow field in a plane channel is strongly asymmetric and contains large zones of relaminarized flow on the stable side. Recent experimental[1] and numerical studies[2] of the turbulent flow in rapidly rotating square ducts have shown the importance of the specific geometric configuration.

In the present study, a direct numerical simulation of turbulent flow in a rotating tilted square duct is carried out to further probe these geometric effects. The rotation vector is in the (0,1,1) direction, see Figure 1. Simulations have been performed for a set of Rotation numbers between 0 and 1, where the rotation number is defined as $\mathrm{Ro} = \Omega\, d/U$, where U is the mean flow velocity, Ω is the magnitude of the rotation vector and d is a characteristic length of the duct. The Reynolds number, defined as $\mathrm{Re} = (\mathrm{U}\,\mathrm{d})/\nu$, where ν is the kinematic viscosity of the fluid, has been chosen to be 4400. The change of the boundary layers owing to rotation has a pronounced effect on the resistence in the duct, producing an increase compared to the non-tilted case. The boundary layer configuration, as well as mean and turbulent quantities will be presented, see for example Figure 1.

*KTH Mechanics, Osquarsbacke 18, S-100 44 Stockholm, Sweden.

[1]Mårtensson, G.E., Gunnarsson, J., Johansson, A. V. and Moberg, H. 2002 "Experimental investigation of a rapidly rotating turbulent duct flow", *Exp. Fluids*, **33**, pp. 482–487.

[2]Mårtensson, G.E., Brethouwer, G. and Johansson, A. V. 2005 "Direct numerical simulation of turbulent flow in a rotating duct", *Proceedings of TSFP-4, Williamsburg, VA, USA*, **3**, pp. 911–916.

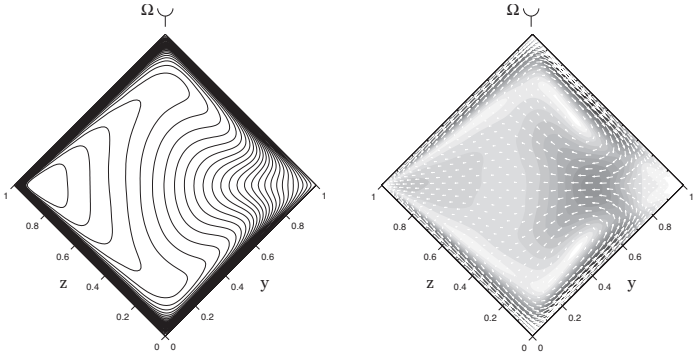

Figure 1: (a) Contour plot of the streamwise velocity u. (b) Combined contour and vector plot of the secondary flow, v and w.

Experiments on a swirling jet issued by a rotating pipe flow

L. Facciolo*

A swirling jet is generated by a fully developed, turbulent rotating pipe flow (6 m long, diameter 60 mm). The Reynolds number is 24000 and the swirl number S, defined as the ratio between the velocity at the pipe wall (V_w) and the bulk velocity in the pipe, is set to 0.5. Besides the experiments a DNS simulation is performed for a Reynolds number of 5000 at the same swirl number S=0.5.

The main characteristics of this experiment is that, due to the effect of the cross-stream Reynolds stress, the turbulent flow in a rotating pipe does not reach a solid body rotation and instead the azimuthal velocity component (V) lags behind it[1]. The jet issued at the pipe end preserves, as shown by both experiments and numerical simulations, the azimuthal velocity imposed by the pipe flow in the central region a few diameters downstream. Moving further downstream the azimuthal component decays until, in the core of the jet, it becomes negative and the flow actually rotates in the opposite direction with respect to the rotation of the pipe. The counter-rotating core covers a region of approximately the pipe diameter and its amplitude represents a few percent of the velocity at the pipe wall but is clearly detected in experiments and simulations.

Hot-wire and PIV data show the development of the jet flow field and confirm the counter- rotating core at a distance of approximately 6 diameters from the pipe outlet. Time and space resolved stereo PIV showed large scale structures of the counter-rotating core in the cross flow plane as well as in the axial stream-wise direction. The influence of these structures on the counter rotating core will be discussed in the presentation.

*KTH Mechanics, SE-100 44 Stockholm, Sweden.

[1]Luca Facciolo and P. Henrik Alfredsson, *Phys Fluids* **16**, L71-L73 (2004).

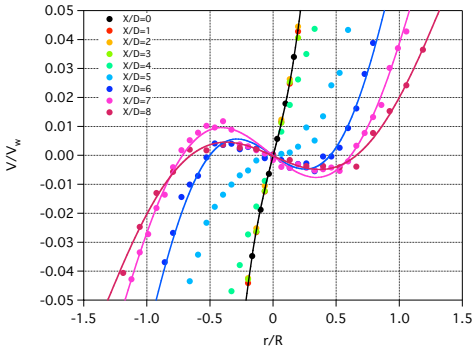

Figure 1: The counter rotating core of the swirling jet. LDV data

Assessment of a wavelet based coherent structure eduction technique in turbulent wall flows.

R. Camussi[a], W. Da Riz[a]

The aim of the work is to present an assessment of a wavelet based method for identifying coherent structures (CS) from 2D PIV data in turbulent wall flows.

The database used is provided by Adrian and co-workers (http://ltcf.tam.uiuc.edu/) and previously used in Adrian et al.[1] for high and low Reynolds number flows (Re_θ = 1015/7705, θ = 8.84/10.35 mm).

The algorithm is based on wavelet analysis of 2D PIV velocity field (Camussi[2]) and validated against a method based on the swirling strength (Zhou et al.[3]). An algorithm for the computation of the velocity gradient tensor at each point of the 2D PIV velocity field has been implemented: the CS has been identified as to be the area where the velocity gradient tensor has a pair of conjugate complex eigenvalues with squared imaginary part λ_{ci}^2 overcoming a fixed threshold equals to std(λ_{ci}^2). The algorithm for CS identification via wavelet analysis is based on the LIM indicator (Farge[4], Camussi and Guj[5]); here only the velocity component normal to the wall has been used. The CS has been identified as the point where the maximum value of LIM over all wavelet scales shows a relative peak. Statistics of CS identified by means of the two methods revealed no substantial differences for negative-vorticity structure, and a relationship between wavelet wavelength and vortex size has been carried out (Fig. 1-a). For positive-vorticity structures the analysis of results shown striking differences arising from the fact that the LIM based algorithm tends to identify negative-vorticity vortex packets (Fig. 1-b circled), which form a zone of local positive vorticity (Fig. 1-b red) along with positive-vorticity structures. Similarities and differences between high and low Re flows are also shown.

---

[a] Mechanical and Industrial Engineering Department, University "ROMA TRE", Rome, Italy.

[1] Adrian, R. J.,Meinhart C. D., Tomkins C., *J. Fluid Mech.* **422**, 1–53 (2000).
[2] Camussi R., *Exps. Fluids*, **32**, 76-86 (2002).
[3] Zhou, J., Adrian, R.J., Balachandar S., Kendall T.M., J. *Fluid Mech.* **387**, 353-396 (1999).
[4] Farge M., *Annual Review of Fluid Mechanics*, **24**, 395-457 (1992).
[5] Camussi R., Guj G., *J. Fluid Mech.* **348**, 177-199 (1997).

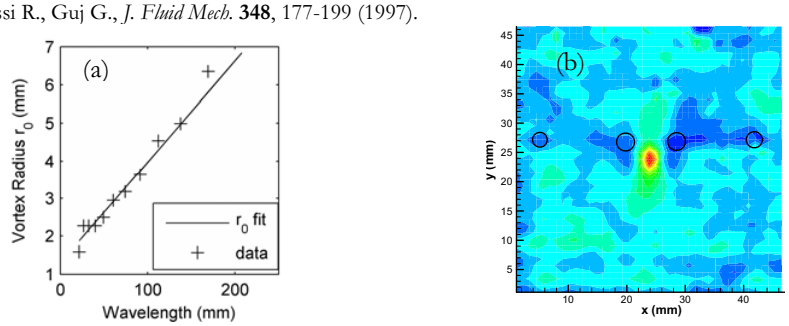

Fig. 1: (a) r_0 vs. wavelength. (b) Mean velocity field vorticity (wavelength = 26.6 mm)

Multi-scale exact coherent structures in channel flow

T. Itano*, F. Waleffe† and S. Toh‡

Recent discoveries of coherent solutions of the Navier-Stokes equations in channel and pipe flows are opening new avenues for understanding the dynamics of shear turbulence[1]. These discoveries have been made possible by a bifurcation method that leads to unstable saddle-node branches of solutions that do not bifurcate from the simple laminar solution[2].

Here, the method is applied to find another type of traveling wave solutions in channel flow, that contains not a single structure but several structures at different scales. This multi-scale structure is of great interest since it is similar to what is observed in wall-bounded shear flows. Our new solution contains two distinct types of structures simultaneously. One is a near-wall structure (NWS) located in the buffer-layer, consisting of wavy low-speed streaks flanked by staggered quasi-streamwise vortices. The other is a mean-flow perturbation with a spanwise wavelength that is twice that of the near-wall structure. The latter is suggestive of the large-scale structure (LSS) observed over the buffer layer in turbulent channel flow[3]. We call this new solution the "double-decker structure" (DDS).

The bifurcation diagram of these DDS in the (c_x, Re_P) space is shown in figure (a) below, where c_x is the streamwise phase speed of the solution normalized by the laminar centerline velocity. The near-wall structure previously obtained[1] is also calculated, which is shown as a reference by a curve with triangles in the figure. The second type of DDS is emerged at $Re_P = 1553$ in the diagram. It is clearly found that the existence of perturbation reduces the phase speed of the second type of DDS. In figure (b), the DDS is visualized by contours of the first and second Fourier components of streamwise velocity with respect to the spanwise wavenumber.

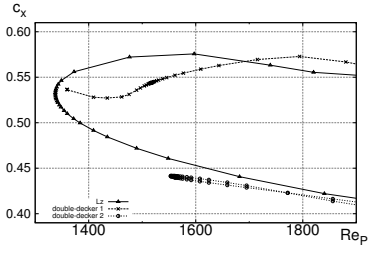

(a) The bifurcation diagram at the streamwise and spanwise wavelengths, $(\alpha, \gamma) = (1.00, 1.94)$.

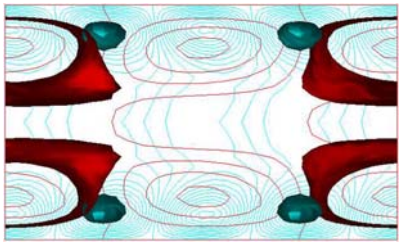

(b) The cross view of the second type of DDS at $Re_P = 1553$. $\hat{u}_{k_z=1}(y,z) = -0.01(red)$, $\hat{u}_{k_z=2}(y,z) = -0.1(cyan)$.

*Faculty of Engineering, Kansai University, Osaka, Japan
†Department of Mathematics and Engineering Physics, University of Wisconsin, Wisconsin, USA.
‡Department of Physics and Astronomy, Graduate School of Science, Kyoto University, Kyoto, Japan.

[1]Waleffe *Phys. Fluids* **15**, 1517 (2003), Wedin and Kerswell, *J. Fluid Mech.* **508**, 333 (2004)
[2]Nagata, *J. Fluid Mech.* **217**, 519 (1990)
[3]Toh and Itano, *J. Fluid Mech.* **524**, 249 (2005)

Numerical study of turbulence in a rotating pipe using Large Eddy Simulation

J. Revstedt*, C. Duwig*, L. Fuchs*

Today, many industrial devices are making use of swirling flows. The main advantages of adding swirl to, for example, a jet is to increase turbulence and mixing. Modeling and understanding the swirling flows is then a key issue. However, despite of more than 40 years of research, the mechanisms of vortex break down are only partially understood. The main difficulty of the problem is the unsteady behavior of this type of flow[1] : Large structures resulting from vortex breakdown and the swirling shear-layers, affect directly the flow.
In the present work, we consider an infinitely long rotating pipe. The rotation adds some swirl to the turbulent jet flow. Additional tangential shear is also added. It modifies the mean velocity profiles as well as the characteristic of turbulence. The present study aims to capture the large structures in a rotating pipe flow and understand how they are affected by swirl and Reynolds number.We use performed at three Reynolds numbers ($Re = 12000, 24000, 36000$) and at three rotational speeds (S= 0.2, 0.5, 1.0). The influence of these parameters on the mean velocity and mean turbulent stress fields is investigated. In addition vortex tubes visualization will be presented and turbulent energy spectra will be analyzed. Mean velocities and stresses are compared also to the experimental data[2]. LES captures well the shear-layers and the 'smoothing' effect of turbulence. Strong vortex tubes are visualized using the λ_2 technique. Figure 1 shows the instantaneous vortex stuctures using this technique.

*Energy Sciences/Fluid Mechanics, Faculty of Engineering, Lund University, P.O. Box 118, SE-221 00 Lund, Sweden

[1]Lucca-Negro and O'Doherty, *Progress in Energy and Combustion Science* **27**, 431 (2001).

[2]Facciolo, *TRITA-MEK Tech. Rep. 2003:15* KTH, Stockholm (2003).

Figure 1: Visualization of the vortex tubes using the λ_2 technique. $Re = 36000$, $S = 1.0$

Anisotropic fluctuations in a turbulent boundary layer

B. Jacob*, C. M. Casciola†, A. Talamelli‡and P. H. Alfredsson§

The aim of the present work is an experimental investigation of both *large-* and *small-*scale turbulent properties of the boundary layer over a flat plate at $Re_\theta \approx 15000$. We focus on the scaling behaviour of the two-points correlation tensor of order p, defined by: $S^{(p)}_{\alpha_1 \ldots \alpha_n}(\mathbf{r}) = \langle \delta u_{\alpha_1}(\mathbf{r}) \ldots \delta u_{\alpha_n}(\mathbf{r}) \rangle$, at different distances from the wall. By projecting each component of the tensor on the so-called *sectors* of the group of rotations SO(3), it is possible to extract the isotropic contribution and to distinguish between different kinds of anisotropies. The contribution from the isotropic sector is completely described throughout the entire inner region by two sets of *universal* exponents, pertaining respectively to the small- and the large-scale ranges[1]. Preliminary measurements[2] seem to suggest a similar behaviour also for the pure anisotropic terms of the correlation tensor, like $S_{111112}(r_3)$ or $S_{111222}(r_3)$. A first direct evidence is provided in Fig.1, which shows how the data in the upper part of the logarithmic layer can be exactly described by the same scaling exponents of the homogeneous shear flow. The behaviour in the buffer region, where the increase of the mean shear and the proximity of the wall are expected to drastically change the turbulence dynamics, will also be discussed in the presentation.

*INSEAN, Rome, Italy.
†DMA, University "La Sapienza", Rome, Italy.
‡DIEM, University of Bologna, Forlì, Italy.
§KTH Mechanics, Stockholm, Sweden.

[1]Casciola et al., *Phys. Rev. Letters* **95**, 024503 (2005).
[2]Jacob et al., *Phys. Fluids* **16**, 11 (2004).

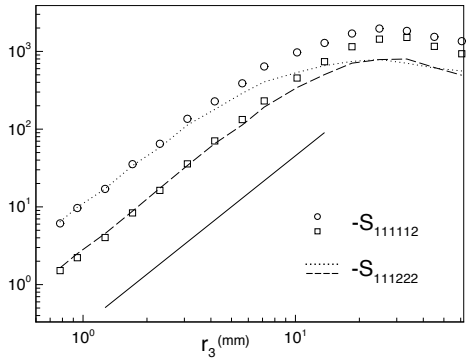

Figure 1: Scaling behaviour at two different wall-normal distances of the anisotropic components of the 6-th order correlation tensor. Squares and dashed line: $S_{111112}(r_3)$ and $S_{111222}(r_3)$ at $y^+ \approx 700$, respectively. Circles and dotted line: $S_{111112}(r_3)$ and $S_{111222}(r_3)$ at $y^+ \approx 300$, respectively. The solid line corresponds to the scaling $\sim z^{\zeta_{6,2}}$, with $\zeta_{6,2} = 2.2$ the exponent of the homogenous shear flow. The streamwise, wall normal and transverse directions are denoted by 1, 2 and 3 respectively.

Development of Sub-Layer Streaks in Two- and Three-Dimensional Turbulent Boundary Layers

K.L. Kudar[a], P.W. Carpenter[a] and C. Davies[b]

The results of a series of simple computational experiments will be presented. The focus of the study is on the sub-layer streaks found in turbulent boundary layers with emphasis placed on the effect of streamwise pressure gradient and also on the effect of sweeping the boundary layer.

To model the boundary-layer flow, the velocity-vorticity method of Davies & Carpenter[1] is used. Initially, as two-dimensional flows are studied the velocity profile of Spalding[2] and Coles[3] is used to approximate the complete, mean, turbulent velocity-profile and allows for the variation in streamwise pressure gradient. To generate the sub-layer streaks, a vorticity source is placed at an optimum position in the boundary layer to approximately model the hairpin vortices found in turbulent boundary layers. The sub-layer streaks subsequently generated are studied and the results are compared with the seminal experimental work of Kline *et al.*[4]. Owing to the nature of the direct numerical simulations, the strength and form of the vorticity source can be systematically varied providing an insight into the generation of sub-layer streaks that would be very difficult to gain from experimental studies.

In most cases, three-dimensional turbulent boundary layers are less efficient at generating turbulence than their two-dimensional counterparts. There is also experimental evidence that the behaviour of the sub-layer streaks is more complex in swept three-dimensional boundary layers. Following a previous computational study of analogous structures[5] (Klebanoff modes) in laminar three-dimensional boundary layers, the act of sweeping the boundary layer can have a very significant effect on their physical manifestation and also on their evolution. A similar study of the sub-layer streaks in three-dimensional turbulent boundary layers is to be presented.

[a] School of Engineering, University of Warwick, Coventry, England, CV4 7AL, U.K.
[b] School of Mathematics, Cardiff University, Senghennyd Road, Cardiff, Wales, CF24 4AG, U.K.

[1] Davies & Carpenter, *J. Computational Phys*., **172**, 119 (2001).
[2] Spalding, *J. Applied Mech.*, **28**, 455 (1961).
[3] Coles, *J. Fluid Mech.*, **1**, 191 (1956).
[4] Kline et al., *J. Fluid Mech.*, **30**, 741 (1967).
[5] Kudar et al., *Laminar-Turbulent Transition*, *IUTAM Symposium*, Bangalore, India, (2004).

Very-rough-wall boundary layers

Ian P Castro* and Ryan Reynolds*

Rough-wall boundary layers are ubiquitous. It is therefore striking that despite their practical importance a number of the most fundamental questions concerning the effects of surface roughness on the nature of the turbulent boundary layer remain unanswered. The classical view was expounded by Townsend[1], who argued that the major effect is simply to change the surface stress, altering the value of the constant in the usual log-law relation for the mean velocity profile, but without structural changes in the turbulence. This amounts essentially to the assumption that the inner and outer regions do not interact strongly. For small ratios of roughness height to boundary layer depth, $h/\delta < 0.03$, say, there is much evidence that this view is reasonable [2,3]. But it must inevitably become increasingly less so as h/δ rises and there is evidence that for large enough h/δ not only can structural features change *throughout* the flow, but also that these differences (from the smooth wall boundary layer) may depend on the topology of the roughness[4,5]. It remains generally unclear exactly how and under what circumstances the roughness effects extend throughout the flow.

In this presentation we will discuss these issues, provide further evidence that roughness effects on the outer flow depend on h/δ and highlight the current uncertainties about such flows. An example of current work is provided by figures 1(a) and (b), which show PIV data in the boundary layer flow over a staggered array of cubes (with $h/\delta = 14$). Such data yield turbulence structural information and differences from the usual smooth-wall behaviour will be emphasised.

*School of Engineering Sciences, University of Southampton, Southampton, UK

[1]Townsend AA, *The structure of turbulent shear flows*, CUP
[2]Jimenez J, *Ann. Rev. Fluid Mech.* **36**, 173-196 (2004).
[3]Raupach et al., *Appl. Mech. Rev.* **44**, 1-25 (1997).
[4]Krogstad P-A & Antonia RA, *Expts. in Fluids*, **27**, 450-460 (1999)
[5]Smalley et al., *Expts. in Fluids*, **33**, 31-37 (2002)

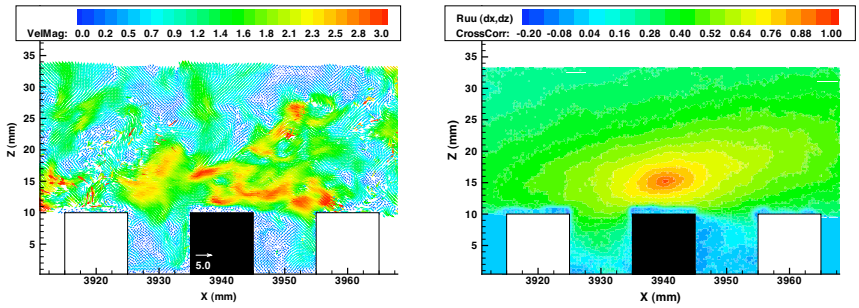

Figure 1: (a) PIV 'snapshot' of fluctuating velocity vectors behind cube in a staggered array; (b) Spatial correlation contours of the axial mean velocity - fixed 'probe' above centre of cube.

Flowcontrol with crosswise groves in diffusor flows

R. Meyer[a], W. Hage[a] and C.O. Paschereit[b]

Crosswise grooves can increase the efficiency of flows that are partially separated due to a high pressure gradient. In the present investigation the effect and mechanisms of such crosswise grooves are examined in detail on a simple diffuser geometry. A diffuser with smooth walls and without areas of flow separation surely exhibits the best efficiency. But with high pressure gradients and short overall lengths a separation-free diffuser is however, not attainable. By the implementation of orifice plates or crosswise grooves into the area of separated flow the efficiency of a Borda-Carnot diffuser can be improved from 28% to 75%. Pressure measurements within a Reynolds number range of 10,000 to 250,000 (related to the nozzle diameter) show that the orifice plates effectively obstruct pressurization between the small and the large cross section of the diffuser (see fig. 1). Particle Imaging Velocimetry (PIV) measurements (see fig. 2) and CFD calculations show clearly the differences in the flow field with and without orifice plates. In the second part of the investigation these principles will be exploited in the context of axial compressors from turbo machines. A large part of the compressor stage losses is caused by corner separations on the blades and the side walls (casing and hub). By flow control with crosswise groves these secondary flow losses should be decreased. Thus the efficiency of axial compressors and gas turbines could be improved.

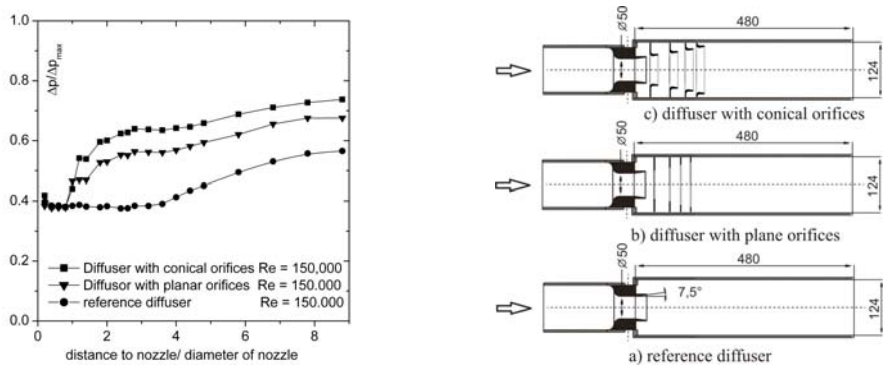

Figure 1: Efficiency of the different diffuser geometries; all dimensions in [mm]

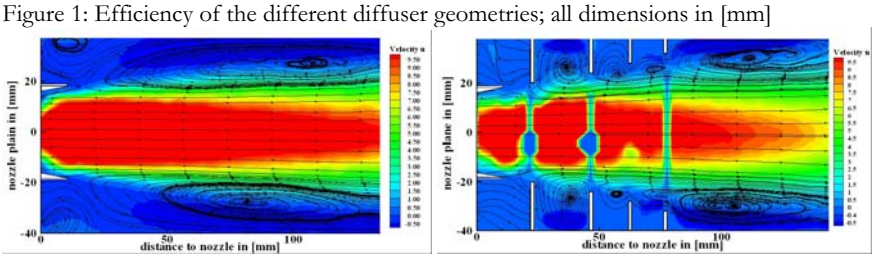

Figure 2: PIV-measurements of two different diffusor configurations. (Re =10,000).

[a] German Aerospace Center (DLR), Mueller-Breslau-Strasse 8, D-10623 Berlin, Germany.
[b] Technical University of Berlin, Hermann-Foettinger-Institute, Mueller-Breslau-Strasse 8, D-10623 Berlin, Germany

Numerical Simulations of Transient Turbulent Flows

Y. M. Chung*

A detailed numerical study of transient turbulent wall-bounded flow for investigating unsteady coherent near-wall structure are performed. Temporal acceleration (and also deceleration) of turbulent boundary layer is studied using DNS, LES and URANS. The main focus of the study is to develop a high-quality DNS database for transient turbulent flow, which is then used in testing and assessing popular turbulence models and LES wall models for unsteady turbulence for industrial use. The test cases described below have a high importance in engineering and will improve the understanding of the flow physics of transient turbulent flow.

Direct numerical simulations are performed for a temporally accelerating (and also deceleration) turbulent pipe flows. The calculations are started from a fully-developed turbulent pipe flow. For the acceleration cases, the Reynolds number increases due to flow acceleration from $Re_0 = 7000$ to $Re_1 = 45,200$, and the Reynolds numbers based on the friction velocity (u_τ) are $Re_\tau = 230$ and 1190, respectively. Preliminary LES simulations have been performed with a $128 \times 193 \times 256$ grid system[1] and DNS is also applied to a lower Re number.

The responses of the turbulence quantities (e.g., turbulence intensities, Reynolds shear stress, and vorticity fluctuations) and the near-wall turbulence structure to the pressure gradient change are investigated. It is found that there are two different relaxations: a fast relaxation at the early stage and a slow one at the later stage. The early response of the velocity fluctuations shows an anisotropic response of the near-wall turbulence[2]. Four turbulence models are tested in this study: the S-A model, the $k-\varepsilon$ model, the $k-\omega$ model, the Baldwin-Lomax model. The preliminary DNS results of transient channel flow are shown in Figure 1.

*School of Engineering, University of Warwick, Coventry CV4 7AL, U.K.

[1]Chung, *Workshop on Dynamics Systems, Fluid Dynamics and Turbulence* (2005).

[2]Chung, *Int. J. Num. Meth. Fluids* **47**, 925 (2005).

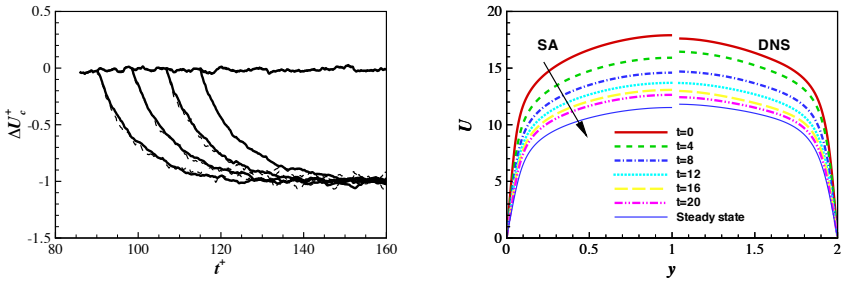

Figure 1: (a) Time history of the centreline velocity U_c using DNS. Symbols represents *steady* channel flow, solid lines represent transient cases. (b) Streamwise velocity at several time instants using DNS and the S-A turbulence model.

Experiments on the reverse Bénard-von Kármán vortex street produced by a flapping foil

R. Godoy-Diana*, J.L. Aider* and J.E. Wesfreid*

Control of wake vortices to generate propulsive forces is the everyday task of swimming fish and other animals. Many studies on actual flapping tails and fins have been motivated looking forward to gain a better understanding of this form of propulsion with the ultimate goal of enhancing man-made propulsive mechanisms (see e.g. Triantafyllou, et al. [1] for a review). A feature that is present in almost every configuration involving flapping foils is the generation of a wake vortex street with the sign of vorticity in the core of each vortex reversed with respect to the Bénard-von Kármán (BvK) street in the wake of non-flapping body. The goal of the present work is to study experimentally this *reverse BvK vortex street* in a simple configuration in order to identify basic dynamical mechanisms. The experimental setup consists of a high-aspect-ratio pitching foil placed in a hydrodynamic tunnel. The main control parameters on the experiment are the forcing frequency (f) and oscillation amplitude (A) of the foil and the flow velocity in the tunnel (U). In figure 1 we present visualizations of the wake of the foil obtained in two different parameter configurations by injecting two fluorescein dye filaments upstream at mid-height of the foil. In figure 1.a the flapping motion produces a typical example of a reverse BvK vortex street whereas in figure 1.b an asymmetric regime is established in the wake of the foil. Particle image velocimetry (PIV) measurements give access to the spatio-temporal characteristics of the vorticity field in the wake and allow for a calculation of the spatial distribution of velocity fluctuations as well as an estimate of the forces on the foil. We compare these results for reverse BvK vortex streets, with respect to those of a forced BvK wake produced by a cylinder performing rotary oscillations[2].

*PMMH-ESPCI, 10 rue Vauquelin, 75231 Paris Cedex 05, France

[1] Triantafyllou et al., *Annu. Rev. Fluid Mech.* **32**, 33 (2000).

[2] Thiria et al., *J. Fluid Mech.* to be published (2006).

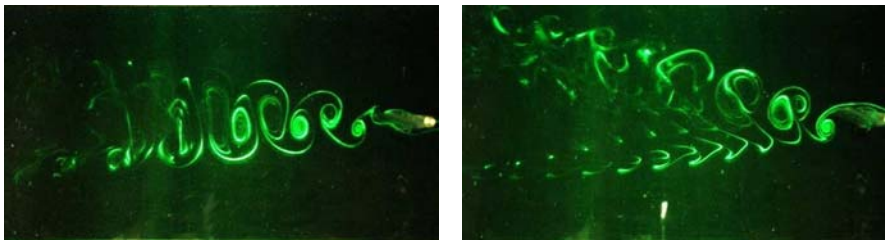

Figure 1: (a) Reverse BvK vortex street ($f = 0.75\text{s}^{-1}$); (b) Asymmetric wake ($f = 1\text{s}^{-1}$). In both cases the Reynolds number based on the width of the foil D is $Re = UD/\nu = 95$.

Decay or Collapse: Aircraft Wake Vortices in Grid Turbulence

M. Ren*, A. Elsenaar*, G. J. F. van Heijst* and A. K. Kuczaj†, B. J. Geurts*†

Trailing vortices are naturally shed by airplanes and they typically evolve into a counter-rotating vortex pair. Downstream of the aircraft, these vortices can persist for a very long time and extend for several kilometers. This poses a potential hazard to following aircraft, particularly during take-off and landing. Therefore, it is of interest to understand what effects control the decay rate in strength of the trailing vortices.

The decay of the aircraft wake vortices is strongly dependent on weather conditions. To simulate an environment of atmospheric turbulence, homogeneous isotropic turbulence is introduced next to localized vortical structure. In this contribution, the effect of external turbulence on the vortex decay will be investigated numerically, using a DNS method, and experimentally. Wind tunnel experiments are carried out using a smoke visualization technique, as shown in Figure 1 (a), and a Particle Image Velocimetry(PIV) method, Figure 1 (b).

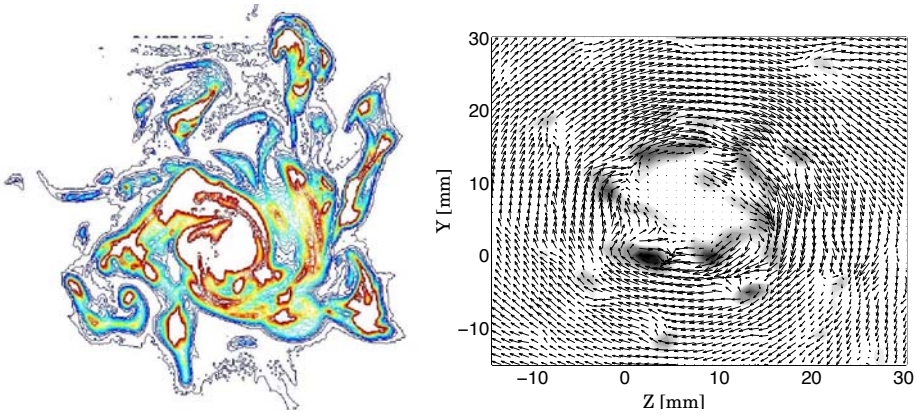

(a) (b)

Figure 1: Wing-tip vortex in grid turbulence at a cross-section well behind a wing (a) smoke visualization with main velocity $U_\infty = 2\,[\mathrm{m/s}]$ and (b) velocity field with main velocity $U_\infty = 13\,[\mathrm{m/s}]$ using PIV technique, color indicates the strength of the axial vorticity.

From the measurement observations, it appears that external turbulence accelerates the decay process of the vortex pair by increasing the diffusion of vorticity. This tends to destroy the wake by enhancing the mixing with the surrounding fluid. The aim of this contribution is to quantify the effect of external turbulence on the decay of the wing-tip vortices.

*Fluid Dynamics Laboratory, Applied Physics, Technische Universiteit Eindhoven, 5600 MB, Eindhoven, the Netherlands.

†Multiscale Modeling and Simulation, Applied Mathematics, Universiteit Twente, 7500 AE, Enschede, the Netherlands.

Kinematic-dynamic correspondence in flow-driven motion of a valvular leaflet

G. Pedrizzetti[a], F. Domenichini[b]

When the flow pushes onto the upstream face of a movable door, we think to the leaflet of a cardiac valve, this opens rapidly with the fluid making little resistance. A model of a fluid-leaflet interaction should be based on the equations of fluid mechanics coupled with those of solid mechanics for the structure[1]. A fluid is a simple (Newtonian) material that develops a complex behaviour due to vortices, boundary layer separation, and turbulence. On the opposite, a solid presents a simpler behaviour where complexity appears through the material properties that can be non-linear, time varying, and neither homogeneous nor isotropic. Approximate elastic structures are usually considered. In physiology, either the material behaviour of a cardiac valve and its parameters are unknown and difficult to assess. This makes the realistic study of physiological flows in presence of a moving leaflets often prohibitive.

An asymptotic model of the leaflets dynamics is presented here[2]. After assuming that vortex shedding can only occur from the trailing edge, we consider the limit when the leaflet moves with the flow such that shedding is inhibited. This kinematic (Kutta) condition does not depend on either the material structure and elasticity. The relation between asymptotic condition and actual torque on the solid element is carefully addressed to show the relation between kinematic condition and actual dynamic balance on the solid element.

A model problem, made of a leaflet in a two-dimensional channel, is here considered. The coupled flow-structure dynamics is first recalled in the irrotational scheme, then analysed numerically at finite Reynolds number (Fig.1). The objectives of this study are twofold: (*i*) the introduction of a technique that allows - asymptotically- a simple solution of the coupled flow-tissue dynamics, and (*ii*) the analysis of vortex generation from a freely or constrained moving leaflet.

[a] Dept. Civil Engineering, University of Trieste, Italy.
[b] Dept. Civil Engineering, University of Firenze, Italy.

[1] De Hart et al., *J. Biomech.* **36**, 103 (2003).
[2] Pedrizzetti, *Phys Rev Lett.* **94**, 194502 (2005).

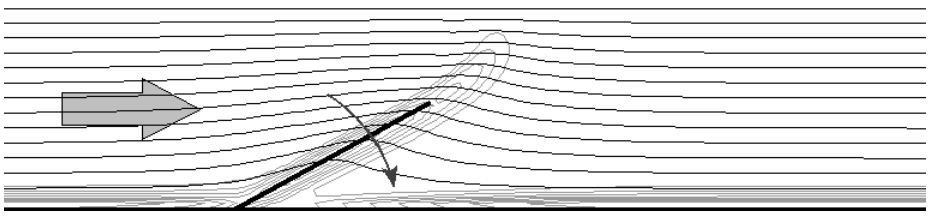

Figure 1: Streamlines and vorticity contours for an accelerated flow in presence of a freely moving plate. Numerical solution at Re=10[3].

Prandtl-Batchelor channel flows past plates at normal incidence

F. Gallizio*, L. Zannetti*, A. Iollo†

The classical problem of 2-D steady inviscid flow past bluff bodies is addressed. Prandtl-Batchelor flows are solution of the Navier-Stokes equations in the limit of the Reynolds number going to inifinity. In particular we consider the problem of the Prandtl-Batchelor[1] flow past wall-mounted plates in a channel. Inviscid separated flows may present multiple solutions according to multiple allowable values of vorticity inside the recirculating regions and of the Bernoulli constant jump on their boundaries. The Prandtl-Batchelor solution is one of these solutions with the property of being the limit of the viscous solution for the Reynolds number going to infinity. Briefly, the solutions here considered have zero Bernoulli constant jump, constant vorticity and are completely or partly embedded in an external potential flow. Their multiplicity is related to different allowable values of area and vorticity.

Particular cases of Prandtl-Batchelor flows are the Finite Area Vortex Regions (FAVR)[2]. If these vortex regions are stable, they don't change the shape within the flow-field in which they are introduced.

As an example, let consider the symmetric inviscid flow past a circular cylinder as studied by Elcrat *et al.*[3]. By examining the half plane problem, the simplest solution is offered by a standing point vortex. This solution is relevant to a vanishing area vortex region. There is an infinity number of possible standing point vortices and their locus is defined by the generalized Föppl curve[4]. Finite area solutions can be obtained as accretions of point vortex solutions.

Thus, the point vortex solution is interesting as a seed of FAVRs solutions. Moreover, there is the strong numerical suggestion that if there is not a point vortex solution, there is not a FAVR solution either.

These considerations can be extended to the flow inside a parallel wall channel. It can be shown that a flat plate orthogonal to the flow in a channel does not allow a standing vortex. This conjecture may explain the difficulties in reproducing Turfus' result[5] for the flow past a flat plate in a channel. Therefore several numerical and analytic evidences seem not to be in accordance with the solutions bifurcation branch hypothesis for the large Re wakes past an infinite row of flat plates[6].

*DIASP, Politecnico di Torino, Corso Duca degli Abruzzi 24, 10129 Torino, Italy
†MAB-INRIA, Université Bordeaux 1, 351 cours de la Libération, 33405 Talence, France

[1]Batchelor, *J. Fluid Mech.* **1**, 177 (1956).
[2]Deem and Zabusky, *Phys. Rev. Lett.* **40**, 859 (1978).
[3]Elcrat et al., *J. Fluid Mech.* **409**, 13 (2000).
[4]Zannetti, *J. Fluid Mech.* (submitted) (2005).
[5]Turfus, *J. Fluid Mech.* **249**, 59 (1993).
[6]Turfus and Castro, *Fluid Dynamics Research* **249(3)**, 181 (2000).

Three-dimensional structures in quasi-two-dimensional shallow flows

A.R. Cieslik*, R.A.D. Akkermans*, H.J.H Clercx* and G.J.F. van Heijst*

The dynamics of the Earth's atmosphere and oceans can be considered approximately as two-dimensional. Two-dimensionality is enforced by the presence of rotation of the Earth, the density stratification, and the geometrical confinement.

In order to validate ideas from two-dimensional turbulence many laboratory experiments have been performed, e.g. in rotating fluids[1], in stratified fluids[2], and in shallow fluid layers[3]. Our experimental setup (fig 1) is similar to Tabeling's[3] and consists of a 50cm× 50cm square tank with magnets below the bottom and two electrodes on opposite sides of the tank. A salt solution serves as the fluid. The flow is forced electromagnetically. The thickness of a fluid layer is a few millimeters.

It is tacitly assumed that shallow flows are quasi-two-dimensional, which means that three-dimensional motions are suppressed by geometrical confinement. Although it is important to realize that this type of flow is essentially three-dimensional due to the no-slip condition at the bottom. Consequently, vortices in shallow flows due to the shear in vertical direction possess secondary circulations[4]. The issue we want to address in this contribution is the extent of two-dimensionality in shallow flows, which has not yet been elucidated.

To investigate this, a Stereoscopic Particle Image Velocimetry (SPIV) technique has been developed that enables the measurement of the three component velocity field in a plane. The general idea of SPIV is depicted in fig 1. As a simple flow we produce a single dipole in the interior of the tank. We found significant vertical velocity components in the frontal region of the dipole, the so-called frontal recirculation. Measurements at different fluid heights revealed a Poiseuille-like velocity profile in vertical direction. The second flow situation is a dipole-wall collision where we study the influence of the wall on the flow. A key characteristic of such a collision is the vorticity production at boundaries. It is possible to make a distinction between pure two-dimensional dynamics and three-dimensional recirculating flows. In a third step we will elucidate the role of three-dimensional recirculation on decaying and on forced quasi-two-dimensional turbulence in shallow flows with no-slip boundaries.

*Fluid Dynamics Laboratory, TU/e, P.O. Box 513, 5600 MB Eindhoven, Netherlands.

[1]Van Heijst and Kloosterziel, *Nature* **338**, 369 (1989).

[2]Maassen et al., *Europhys. Lett.* **46**, 339 (1999).

[3]Tabeling et al., *Phys. Rev. Lett.* **67**, 3772 (1991).

[4]Satijn et al., *Phys. Fluids* **13**, 1932 (2001).

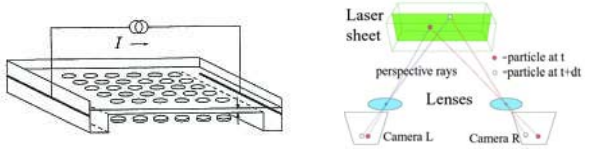

Figure 1: Left: The experimental setup, Right: The idea of SPIV

On the generation of diagonal 'rib' vortices in the braid region of a mixing layer

Jimmy Philip*and Jacob Cohen*

The three-dimensional (3D) structure of a plane turbulent mixing layer is characterized by the presence of secondary quasi-streamwise counter-rotating vortices (ribs), connecting the bottom of the primary upstream spanwise vortex (roller) with the top of the downstream one.[1] The flow region generated between the two rollers is that of a plane stagnation flow. A similar field has been also observed between the heads of two consecutive hairpin vortices in a turbulent boundary layer.[2] We show that a 3D localized disturbance embedded in this plane stagnation flow can develop into the rib vortices which have been widely observed in turbulent mixing layers. We use the fluid impulse (FI) of the disturbance to analytically predict its growth for an arbitrary initial amplitude. The predictions are confirmed by numerical simulations.

Accordingly, an initial dipole Gaussian vorticity distribution is placed in an external, unbounded, irrotational plane stagnation flow represented by $\mathbf{U} = (Ay, Ax, 0)$. The viscous disturbance vorticity equation is integrated analytically. The results show that the FI associated with such disturbances decays and grows exponentially along the principal axes $x = y$ (figure 1a) and $x = -y$ (figure 1b), respectively. Numerical simulations for both linear and nonlinear disturbances confirm the above predictions. The resulting structure is that of a counter-rotating vortex pair as seen in figure 1(c), which is similar to that of ribs vortices observed in turbulent mixing layers. Furthermore, it is shown that the FI, the disturbance kinetic energy and enstrophy follow the same trend, i.e. when the FI increases with time so does the kinetic energy and enstrophy, and vice-versa. The correspondence between them suggests the use of the fluid impulse to predict stability of plane stagnation flow to such localized disturbances.

*Faculty of Aerospace Engineering, Technion - Israel Institute of Technology, Haifa 32000, Israel.

[1] Bernal and Roshko, *J. Fluid Mech.* **170**, 499 (1986).

[2] Adrian *et al. J. Fluid Mech.* **422**, 1 (2000).

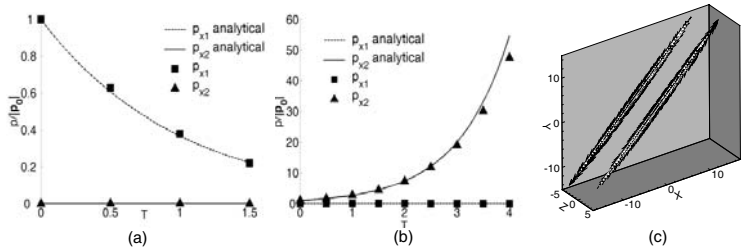

Figure 1: (a) Comparison between analytical solution and numerical simulation of the FI evolution: initial fluid impulse, $p_0 = p_{x_{10}}$ (b) initial FI, $p_0 = p_{x_{20}}$. (c) The evolved counter-rotating vortex pair shown by iso-surfaces of the vorticity magnitude.

Lagrangian (physical) analysis of coherent vortical structures

D. Doorly*, I. Motazavi†, and S. Sherwin*

One of the most helpful techniques to study two and three-dimensional vortex dynamics is the identification of the Coherent structures (CS). Coherent structures generally refer to the organised and concentrated rotational patterns within the flow and are a useful way to characterise flow evolution in time. An important feature of coherent structures identification is the reduction of a vector flow field into scalar quantity. Typically a specific isocontour value, or cutoff, of the scalar quantity is then chosen to identify the coherent structures. Whilst the original definitions[1],[2] defined exact values for the cutoff in numerical practise the cutoff value is varied to eliminate numerical noise.

In this work, we focus on the Lagrangian (physical) interpretation of a Coherent Structure (CS). A more physical understanding of the λ_2 criterion suggested by Jeong and Hussain can be gained by considering the motion of two adjacent points in a plane. Here, we shall show that if we ignore contributions from unsteady the strain and rotational tensor then the λ_2 criterion can be interpreted as requiring the inner product of the displacement between two material points with the acceleration of the two points, i.e.

$$\Delta_x \cdot \Delta_x'' < 0 \tag{1}$$

where the superscript prime denote time differentiation. When $\lambda_2 < 0$ we shall demonstrate that this can be interpreting as equivalent to requiring that the inner product (1) is satisfied for all points in one plane containing the point of interest.

Then, we study the cutoff (λ_2) choice for a CS and its effect on the identification procedure extending previous research[3] to three-dimensional flows. The results show that the exact application of the vortex identification approaches can generate noisy vorticity configurations[4]. Ranges of choice of cut-off values are extensively studied for laminar ($Re = 100$) and transitional ($Re = 500$) external and internal flows. As a procedure for choosing an appropriate cut-off the proportion of the enstrophy captured within the λ_2 coherent structure to the total enstrophy within the global flow domain is studied. We see that an appropriate value of λ_2 permits to capture the coherent vortices. Larger or smaller cut-off values, either generate large noise or miss the main informations on vortical structures. We propose that numerical application of the λ_2 to coherent structure identification criterion should be used in conjunction with an enstrophy capture analysis to determine a valid range of cut-off values.

*Department of Aeronautics, Imperial College London, London, SW7 2BY, UK.
†MAB UMR 5466, Université Bordeaux 1 and INRIA, 351 cours de la Libération, F-33405 Talence.
[1] Joeng and Hussain, *J. Fluid Mech.* **285**, 69 (1995).
[2] Weiss, *Physica D* **48**, 273 (1991).
[3] Creusé and Mortazavi, *Europ. J. Mech. B/Fluids* **20**, 603 (2001).
[4] Miliou, Mortazavi and Sherwin *Comptes Rendus Acad. Sc.* **333**, 211 (2005).

Session 6

The evolution of energy in flow driven through rising bubbles

Enrico Calzavarini*, Detlef Lohse†, Irene Mazzitelli‡and Federico Toschi§

We investigate by direct numerical simulations the flow that rising bubbles cause in initially quiescent fluid. We employ the Eulerian-Lagrangian[1] method and embody the two-phase coupling by retaining the bubbles like point sources (see figure 1(a)). The effects of added mass, buoyancy, drag and lift are included in the model equation for the bubble dynamics. The possibility of bubble-bubble interaction (*4-way* coupling) is analyzed in detail. Our analysis is confined to bubble of small Reynolds number, $Re_b \sim O(1)$, corresponding to micro-bubbles in water.
The present results suggest that a large scale motion is generated in the initial stages of the flow evolution, owing to an *inverse energy cascade* from the small to the large scale, later on the flow reaches a statistically steady condition where no relevant large scale fluctuations are present, see figure 1(b). Our analysis at relatively low gaseous volume fractions, $\alpha \simeq 1\%$, suggests that the vorticity induced by the gas on the liquid phase is not strong enough to enhance bubble accumulation in vortices and therefore bubbles remain spreaded. The lift force and collision term play a major role in reducing the degree of clusterization in the high vorticity regions of the flow.

*Department of Applied Physics, University of Twente, 7500 AE Enschede, The Netherlands.
†Department of Applied Physics, University of Twente, 7500 AE Enschede, The Netherlands.
‡Department of Applied Physics, University of Twente, 7500 AE Enschede, The Netherlands.
§Istituto per le Applicazioni del Calcolo, CNR, Viale del Policlinico 137, I-00161 Roma, Italy.
[1]I. M. Mazzitelli, D. Lohse and F. Toschi, *J. Fluid Mech.* **483**, 283 (2003) and *Phys. Fluids* **15**, L5-L8 (2003).

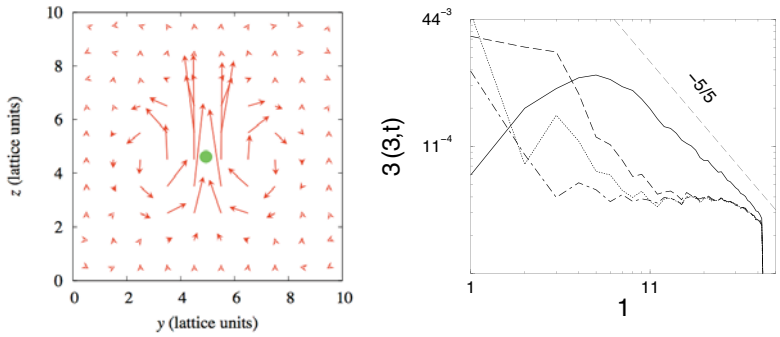

Figure 1: (a) Effect of the bubble feedback on still fluid, vertical section of the velocity field. (b) Evolution of the velocity spectra in a typical run, void fraction $\alpha = 0.016$, a transient characterized by relatively large velocity fluctuations (solid line) is followed by a state of almost equi-partition of energy (the time evolution is as follows: dashed, dotted and dot-dashed lines).

BUBBLE DYNAMICS IN A CYLINDRICAL LAMINAR COUETTE FLOW

Y. Juaneda, C. Colin[a]

Some results concerning bubble dynamics and migration at low and moderate bubble Reynolds numbers Re_B in a laminar shear flow are presented. Experiments are performed in normal gravity in laboratory and also in microgravity conditions in parabolic flights. An experimental device is especially designed to create a shear flow between two rotating horizontal cylinders of 12 cm and 20 cm diameter. Isolated bubbles of a few millimeters diameter are injected in the gap between the two cylinders. In normal gravity, the bubbles may have a stable equilibrium position, which is used to determine the drag and lift coefficients from a force balance on the bubble. The effect of bubble deformation and wall vicinity is highlighted. For spherical bubbles far from the wall, the experimental results (Figure 1) are in agreement with those of the litterature[1]. Near the wall of one cylinder, the lift coefficient drops. The experimental results are compared to the theoretical study of Magnaudet et al.[2] at low Re_B. For the drag coefficient a good agreement is found between theory and measurements even for Re_B values greater than 1. For the lift coefficients some discrepancies are oberved close to the wall with the theoretical results at low Re_B.

The bubble migration is also investigated. Experiments performed in normal and microgravity conditions with bubbles of different sizes cover a wide range of bubble Reynolds numbers Re_B from 0.001 to 10. The migration of the bubbles at low Re_B has been theoretically studied in a previous paper[3] and the experimental results are compared to this study.

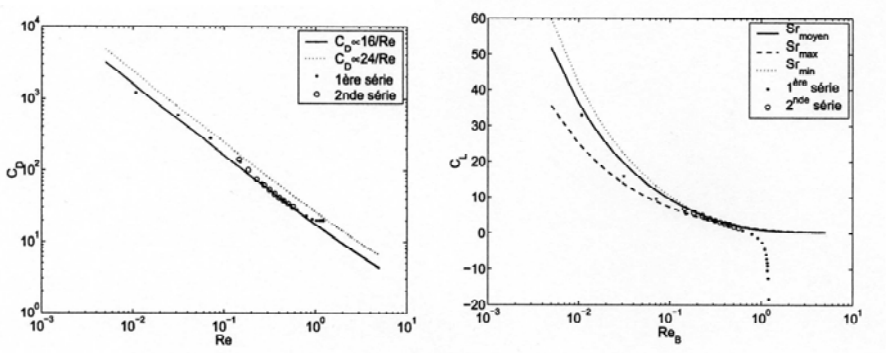

Figure 1: Drag coefficients (left) and Lift coefficients (right).

[a] Institut de Mécanique des Fluides de Toulouse, France

[1] Legendre, D., Magnaudet, J., *J. Fluid Mech.* **368**, 81 (1998).
[2] Magnaudet et al., *J. Fluid Mech.*, **476**, 115 (2003)
[3] Juaneda, Y., Colin, C., *Mécanique et Industries*, **5,** 565 (2004).

Levitation of small bubbles and droplets in a rotating liquid

F.Peters[a], S.Biermann[a], N.Fries[a]

The free rise of small air bubbles (smaller than 1.5 mm) in water is a classical problem in fluid mechanics which has not yet been resolved completly. Analytical and numerical approaches require sound boundary conditions which can hardly be warranted by experiments. Due to various effects the bubble rise is rather a transient than a stationary process. Among these effects are shape oscillations at the start, size variation due to diffusion and static pressure and, most importantly, ageing of the fresh interface present at the start. The ageing mechanism is not known in detail, however enrichment of surfactants is favoured by most researchers. In sum, the key problem of experimenting with rising bubbles is that a stationary state is difficult to achieve and that the observation time of a bubble rising at say 100mm/s is rather short.

Our approach is a new experiment that provides levitation of a bubble at stationary conditions associated with long observation times (minutes). The essential part is a glass walled cylindrical chamber filled with water as shown in Fig.1. This chamber revolves about its center as does the water after a starting phase. A small bubble injected into the water by a syringe rises against the downcoming water. At first the observer is surprised that the bubble finds a stable position at some radius corresponding to a certain rise velocity. At second thought it emerges that there exists a balance of different forces in two dimensions that hold the bubble in place. We apply different methods to investigate the bubble. First "Mie Scattering Imaging" is used to determine the size down to a micron[1]. As there is sufficient observation time the bubble shrinkage due to diffusion is resolved. The optical method allows also to determine the sphericity of the bubble. Knowing the rotational speed and the bubble position in the chamber the rise velocity can be plotted versus diameter, the most interesteing experimental value. A drag coefficient may be deduced from that result.

Of course, one must be aware of the fact that the bubble is exposed to a slight velocity gradient not present in the regular water tank experiment. Yet, this is also a benefit because it allows the direct determination of the lift coefficient in shear flow.
The bubble results provoke the question whether droplets can be investigated in the same manner. An silicon oil was found which shows levitation at very low speeds for droplets up to a few mm. Results for the flow field around the droplet were obtained by visualization as well as by the method of Particle Image Velocimetry (PIV).

[a] Fluid Mechanics, Ruhr-Universität Bochum
44780 Bochum, Germany
[1]S.Biermann, F.Peters13. Fachtagung der Deutschen Gesellschaft für Laser-Anemometrie
GALA e.V., GALA e.V. Cottbus 2005

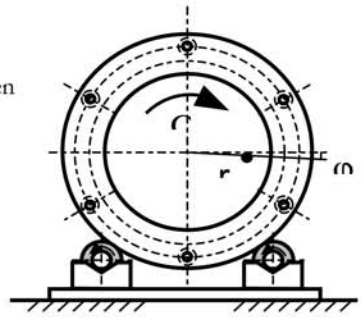

Fig.1: Rotating water chamber showing levitated bubble in stable position ready for investigation by optical methods

Modeling Cavitation on a Wing Section using LES

T. Persson[a], N. Berchiche[a], G. Bark[a], N. Wikström[b] and C. Fureby[a,b]

Cavitation can occur in a wide range of liquid flows, especially in marine applications e.g. around rudders and propellers and consequently cavitation research is a very important topic for the marine industry. To enable modelling of the complex behaviour of cavitating flow, time accurate, high resolution simulation of a two phase flow problem with mass transfer is required. Presently the flow dynamics is captured by employing Large Eddy Simulation[1] (LES) of the incompressible flow equations, whereas water and vapour is separated using an interface capturing two phase model.

The mass transfer model used is based on the work by Kunz et al.[2]. In this model proportionality between the liquid volume fraction and the amount by which the pressure is below the vapour pressure is used to model the transformation from liquid to vapour. The transformation of vapour to liquid is modelled using a simplified form of the Ginzburg-Landau potential.

The aim of this ongoing work is to study the possibility to simulate early and large scale developments that by experimental studies[3] are confirmed to result in cavitation erosion.

The proposed model is tested on the flow around a NACA0015 wing profile at 10° angle of attack. Two flow conditions are tested, cavitation number $\sigma = 0.69$ and $\sigma = 1.07$, giving different cavitation behaviour on the suction side of the wing. At $\sigma = 0.69$ a thick cavity is shed from the main sheet and a stable tip vortex cavity is present, see figure 1a. At $\sigma = 1.07$ a thinner sheet cavity, behaving differently, is located near the leading edge of the wing and only a very short tip vortex cavity is present. The instantaneous pressure coefficient for $\sigma = 1.07$ given at z/L=0.59, where L is the length of wing section and z=0 is at the tip of the wing, is shown in figure 1b.

[a] Chalmers, Shipping and Marine Technology, SE-412 96 Göteborg, Sweden.

[b] FOI, Div . of Weapons & Protection, Warheads & Propulsion, SE-147 25 Tumba, Sweden.

[1] Sagaut P. (2001) Springer Verlag.

[2] R. Kunz *et al.* (1997) 14th AIAA CFD Conference, Norfolk, June, 1999

[3] Berchiche et al. (2003), 5th Int. symp. on Cav., Nov. 1-4, 2003, Osaka, Japan

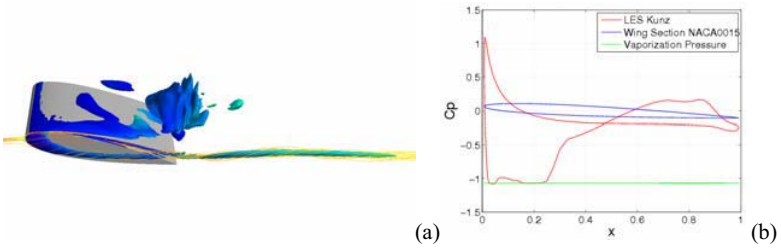

Figure 1: (a) Isosurface of the instantaneous volume fraction at $\sigma = 0.69$. (b) Instantaneous pressure coefficient on the surface of the wing section at $\sigma = 1.07$.

Mechanisms of gas migration through porous media

Michael Stöhr * and Arzhang Khalili *

The mechanism of buoyancy-driven gas flow in a porous medium has important implications such as gas scape from a seabed. The aim of this study is to characterize experimentally gas escape mechanism through a porous medium using the light transmission technique. The experimental setup is composed of a rectangular standing box filled with a saturted porous medium (natural sand or broken glasses) and an air flow through a nozzle placed at the container bottom. A series of experiments for different combinations of natural and artificial sediments were performed. Figure 1 shows the results for a combined study of gas injection into natural sand and granular broken glass with a gas flow rate of 2.5 ml/min. The temporal evolutions of pressure at the inlet show a number of similarities. The connection between the behavior of the gas in the sediment and the corresponding features of the pressure curve is then established by the analysis of the respective images of the transparent sediment.

Corresponding studies of gas injection into sediments with other mechanical properties reveal fundamentally different mechanisms. The results show that the amount of gas which has to build until it penetrates into the water column, i.e. the capacity of the sediment to retain the gas, varies strongly with the sediment type.

The detailed phenomenon is explained in a manuscript sbmitted[1].

*Max Planck Institute for marine microbiology, Celsiusstr. 1, 28359 Bremen, Germany.

[1]Stöhr and Khalili, *Submitted to Phys. Rev. Lett.* (2005).

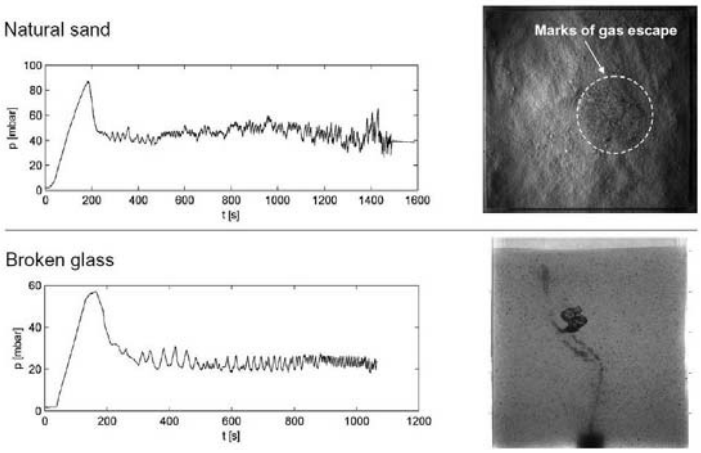

Figure 1: Comparison of gas migration in a natural and a transparent, artificialsediment. *Left images*: temporal evolution of inlet pressure. *Right image*: features of gas migration at the surface and inside the sediment, repectively.

Mass transfer and dispersion from a cylinder surface immersed in a granular bed in alignment with the fluid flow

J. M. P. Q. Delgado[a]

There are several situations of practical interest, both in nature and in man made processes, in which there is fluid flow through a bed of inert particles, packed against a mass of solid (or immiscible fluid) that dissolves in (or reacts with) the moving fluid. Examples may be found in diverse fields, such as dilute catalyst fixed bed reactors, fluidised bed combustion, ore leaching and water contamination by buried waste or NAPLs (non aqueous phase liquids).

The present work describes the mass transfer process between a moving fluid and a slightly soluble cylinder (with length L and diameter d_1) buried in a packed bed, in alignment with the direction of flow. The bed of inert particles (with diameter d) is taken to have uniform voidage.

The partial differential equation (PDE) was solved numerically using a finite-difference method. A second-order central differencing scheme was adopted for the discretisation of the diffusive terms and the convective term was discretised using the CUBISTA high-resolution scheme proposed by Alves et al.[1], which preserves boundedness, even for highly advective flows.

Numerical solution of the PDE describing mass conservation of the solute gave the concentration field near the soluble surface and the mass transfer flux was integrated to give values of the Sherwood number as a function of the relevant parameters. A mathematical expression is proposed that describes accurately the dependence found numerically between the value of the Sherwood number and the values of Peclet number, Schmidt number, d/d_1 and aspect ratio, L/d_1, of the cylinder. For large enough diameter of the cylinder, the problem degenerates into mass transfer from a plane surface and the same equation applies, with $L/d_1=0$.

The equation was tested through the measurement of diffusivity for different solutes released by slightly soluble solids, and the experimental values obtained were in excellent agreement with the values found in literature.

An important feature of the work is the detailed discussion of the finite differences method adopted, with emphasis on the high-resolution schemes used in the discretization of the convection term of the PDE.

---

[a] Dep. Engenharia Química, Faculdade de Engenharia-Universidade Porto, 4200-465 Porto, Portugal.

[1] Alves et al., *Int. J. Numer. Meth. Fluids* **41**, 47 (2003).

Surface waves in coupled channels and acoustic waves in coupled ocean layers

I. Yu. Popov **, L.V.Gortinskaya*, E.S.Tesovskaya*

The problem of surface water waves in the case of constant depth reduces to two-dimensional Helmholtz equation. The system of two channels laterally coupled through small windows is considered. We assume that the Neumann boundary conditions takes place. The existence of coupling window leads to the existence of quasi eigenvalue (resonance) near the second (and third, fourth, etc.) threshold. We construct the asymptotics (in the width of windows) of resonances for the Neumann Laplacian for this system. The cases of one coupling window, finite number of windows and periodic system of windows are considered. We use method of matching of asymptotic expansions of solutions of boundary value problems by A.M.Il'in. Also the scattering problem is considered for the case of one and two coupling windows.

The developed technique as been applied to the problem of acoustic waves in layered structures particularly in ocean. Propagation of acoustic waves in weakly coupled layers of water of different densities(typical ocean structure) is described. If the layers are coupled in small regions then resonant scattering of acoustic waves is observed. The direction diagrams for these waves are constructed.

**St.-Petersburg State University of Information Technologies, Mechanics and Optics, Kronverkskii 49, St.-Petersburg, 197101, Russia.

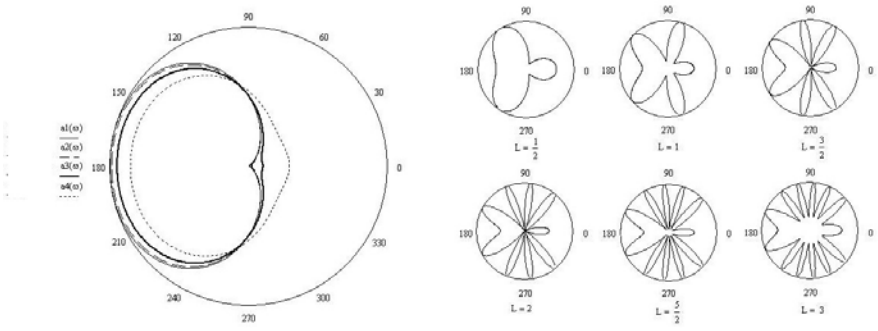

Figure 1: Direction diagrams for different angels of incoming wave (left picture) and different distance between regions of coupling (right picture)

Modelling buoyancy driven displacement ventilation

S. D. Sandbach[a]

Displacement ventilation driven by buoyancy is investigated using full-scale and small-scale laboratory models. A new transient displacement ventilation model (modelling buoyancy evolution over time) is also presented. The convective flow rising from the heat source is modelled using plume equations[1]. Once the hot air reaches the ceiling it spreads out and begins to fill the room. This process is modelled using an approach similar to Germeles[2] modified for displacement flow[3]. Conductive and convective heat transfer close to the surfaces is modelled in the normal way and radiative heat transfer is calculated using Gebharts[4] modified view factor. The model was used to investigate the configurations given in figure 1, these results were then compared with results from existing simplified mathematical models and experimental work. Full-scale results were obtained in an environmental chamber measuring 7.45 m by 5.5 m by 2.78 m high. It is located in a laboratory that is 7.5 volumes larger and of relatively constant temperature. There are two standard size doorway openings to the room (0.83 m by 2.05 m each) as well as ventilation openings. The chamber is equipped with 59 thermocouples located strategically around the chamber and heat sources (1.2 and 2.4 KW) at floor level. Small–scale results were obtained using a 1/15th scale replica of the chamber, modelling the heat input and buoyancy with dyed saline solution. The scaled model is housed in a larger tank of fresh water with transparent sides and a capacity 20 times that of the scaled model. Video footage of the ensuing flow was captured and analyzed using flow visualization software.

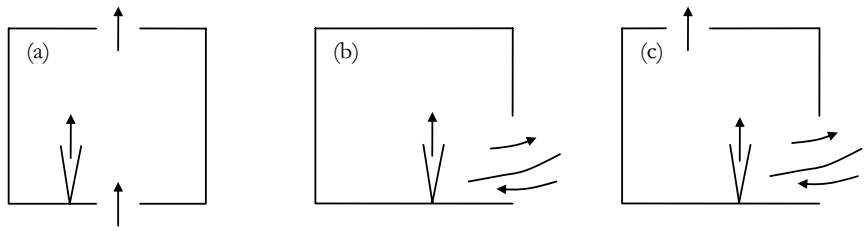

Figure 1: (a) Displacement flow. (b) Doorway Flow. (c) Doorway and vent

[a] School of Mechanical, Aerospace and Civil Engineering, The University of Manchester, UK.

[1] Morton et al, *Proc.of Royal Soc* **234**, 1 (1956).
[2] Germeles, *J. Fluid Mech.* **71**, 601 (1975).
[3] Linden et al, *J. Fluid Mech.* **212**, 309 (1990).
[4] Gebhart, *ASHRAE Trans* **65** 321 (1959)

Validation of urban dispersion simulations by comparison of simulations and measurements obtained around 2D and 3D building arrays in a wind tunnel

O. Parmhed*, and G. Patnaik†

The recent evolution in computer power has made it possible to perform Large Eddy Simulations (LES) for complex gemotries like e.g. submarine hydrodynamics[1]. Among the present uses is the simulation of urban dispersion of airborne hazardous materials. Such material may be accidentally released in e.g. accidents with transport of industrial chemicals or deliberately released by e.g. terrorists. As an example, Figure 1(a) shows the simulated concentration of some pollutant five minutes after an instantaneous release (bomb) in the Stocholm Old Town.

Although important, validation of such simulations is difficult. In this study we compare simulations to observations of the flow around building arrays in a windtunnel. As opposed to the case of the single building, there have been relatively fewer measurement campaigns of the flow around groups of buildings. For this reason, and to provide a data set suitable for the validation of Computational Fluid Dynamics (CFD) codes, Brown et al[2] conducted experiments of 2D and 3D building arrays in the U.S. Environmental Protection Agency's (USEPA) Fluid Modeling Facility wind tunnel. The building arrays consist of 7 or 7x11 rectangular blocks. Figure 1(b) shows the setup for the 3D case.

Here we present results from CFD simulations using LES. The simulations have been performed with various models for subgrid turbulence and with and without wall models. Two different CFD codes have been used, *FOAM* and *Fast3D*. We present here comparisons with both these codes and the measurements from the wind tunnel, Figure 1(c). In general, satisfactory results are obtained.

*FOI, Swedish defence research agency, Grindsjön Research Centre, SE - 147 25 Tumba, Sweden
†NRL, Navy Research Laboratory, Washington, DC 20375-5344, USA
[1]Grinstein and Fureby, Comp. Sci. Eng. **6**, 37 (2004)
[2]Brown et al., *Int. Soc. Environ. Hydraulics*, Tempe, AZ, 6 (2001)

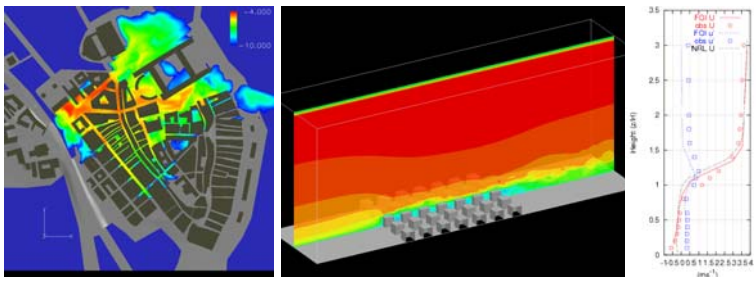

(a) (b) (c)

Figure 1: Simulated dispersion in the Stockholm old town (a). Along flow velocity in windtunnel validation simulation (b). Comparison of profiles (c).

Nonlinear interaction of a pair of sails in a flow: comparison between theory and observation

T. Sugimoto[a]

Many efforts have been introduced into the study of interaction between a sail and a viscous or inviscid flow in two- and three-dimensions. These problems are known to have multiple equilibria and hence hysteresis in aerodynamic and structural characteristics. But there are only a couple of studies on the interaction among a flow, jib and main sails. Also, the former studies could treat only special cases. The limitation is due to difficulty in finding a physically meaningful set of tensions in two structurally independent sails.

The present study deals with the problem by formalism of a two-dimensional inviscid flow. This offers quite tractable basic equations, that is, a couple of Fredholm integral equations of the second kind, accompanied by a couple of nonlinear integral constraints upon sail length.

We shall look for shapes of sails and tensions acting upon sails in equilibrium by giving the angle of attack, the stagger angle between sails, and sail length. The developed method of solution consists of a panel method as a flow-field solver and Newton-Raphson method for tensions search. This method is very robust and leads us to multiple solusions depending on initial guesses in terms of tensions.

Three types of configuration between two sails are studied: largely overlapping sails with the same size or different sizes; less overlapping sails with the same size. In each case there exist multiple equilibria and complex hysteresis in aerodynamic and structural characteristics. Too much overlap of sails is found to fail to obtain high lift that would be expectedly developed by the jib sail.

To verify the theory, we conduct experiments to observe shapes of sails by use of an upright wind tunnel. In case of the same-length sails for example, we observe three types of shapes as shown in figure 1: a pair of concave and convex sails; a pair of sigmoid and convex sails; a pair of convex sails. The theory exactly predicts these.

[a] Kanagawa University, 3-27-1 Rokkakubashi, Kanagawa Ward, Yokohama, Japan

(a) (b) (c)

Figure 1: In the circular window shapes of the same-length sails in a flow are shown; the stagger angle is 5 degrees; air blows from top to bottom. The angles of attack are -20, +6.0, and +20 degrees for (a), (b), and (c), respectively.

Numerical study of flow patterns in an automotive paint bath

Kitty Kui-Hua Sun*, Vijayan Murugaian, Alex Jouvray
International Automotive Research Centre, Warwick Manufacturing Group, University of Warwick, Coventry, CV4 7AL, UK.

In the e-coat process a thin layer of organic polymer is deposited on a conductive car body through application of an electric current. During the e-coating operation, the car body-in-white is first submerged at one end of a paint bath, coated as it travels along the bath and then exits from the bath opposite to the entry point. Paint circulation in the bath is maintained to prevent the precipitation of paint particles, to prevent contaminants (such as metal particles which have been brought into the bath by the car, aggregates of paint particles, and/or bubbles) from depositing on the surface of the car and to remove contaminants from the bath. Normally paint is injected through specially designed pumps called eductors (also known as Venturi pumps). A typical eductor and the flow surrounding an eductor are shown in Figure 1. During the electrodeposition treatment heat is generated and the local e-coating film temperature is increased, resulting in a lowered paint film resistance and thicker film at the outer surfaces. Therefore, the flow in the bath can also act as a control mechanism for the temperature of the coating film. Due to the large number of independent variables that need to be considered, for example, paint formulation and rheological properties, voltage zones, anode locations, body material, body design, etc., flow optimisation in the e-coating bath has largely been neglected until recently.

In this research a CFD numerical simulation has been carried out to study the flow patterns in an automotive e-coat paint bath. Sensitivity studies on the effect of numerical discretisation mesh size and turbulent models have been performed. Also, parametric studies have been conducted to identify potential problems and optimise the flow in the bath. The simulation results show that due to the scale of the bath, an uneven flow profile and channelling may occur. With the existing bath design, the velocity at the free surface is reduced in the downstream direction. Experimental validation of the simulation results has also been carried out. Agreement is obtained between numerical results and the experimental findings. Finally a range of practical options for improving the flow in the bath are discussed.

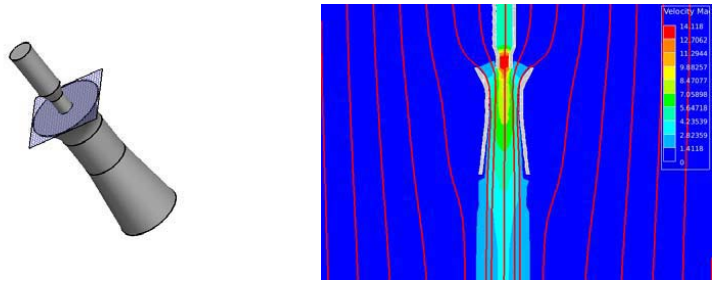

(a) (b)

Figure 1. (a) Eductor (b) Flow surrounding an eductor

* Corresponding author: Kitty Kui-Hua Sun, International Automotive Research Centre, Warwick Manufacturing Group, University of Warwick, Coventry, CV4 7AL, UK. Tel: +44 (0) 24765-75411 Fax: +44 (0) 24765-75403 Email: k.h.sun@warwick.ac.uk

Bubble interactions in Acoustic Fields fully accounting for viscous effects

N. Chatzidai[a] , J. Tsamopoulos[a]

The interaction of gas bubbles pulsating in a liquid is a well-known phenomenon, first analysed by Bjerknes: If the driving frequency lies between the two linear pulsation frequencies of the individual bubbles, they will repel each other; otherwise an attractive force arises. We have studied (a) the nonlinear interactions of two deforming bubbles subject to changes in the far-field pressure, ignoring viscous effects[1,2] and (b) the formation of acoustic streamers when viscous effects are small and the bubbles remain spherical[3]. In order to fully account for viscous effects and large bubble deformations, we have now developed a new Numerical method and solved the NS equations by a finite element/Galerkin method coupled with implicit Euler for time integration. The highly deforming interfaces are accurately computed by a block-structured mesh, which closely follows their surfaces. In every block we solve a set of partial, elliptic differential equations for the mesh nodes. At each time step, the flow equations are solved along with the mesh equations using Picard iterations. It is shown that the bubbles deform less, when viscous effects are properly accounted for. The attraction or repulsion of two gas bubbles depends on their relative size, their distance, the Re number and the pressure amplitude. Increasing the viscosity of the liquid increases the time required for two equal bubbles, subjected to a step change in the far-field pressure, to approach each other.

---

[a] Laboratory of Computational Fluid Dynamics, Dep. Chem. Engin., University of Patras, Greece 26500

[1] Pelekasis and Tsamopoulos, *J. Fluid Mech.* **254**, 467 (1993).

[2] Pelekasis and Tsamopoulos, *J. Fluid Mech.* **254**, 501 (1993).

[3] Pelekasis, Gaki, Doinikov and Tsamopoulos, *J. Fluid Mech.*, **500** (2004)

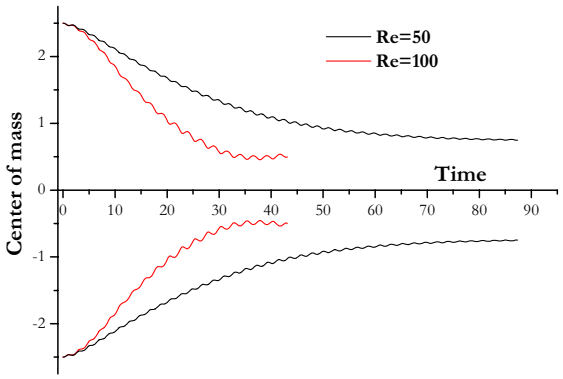

Figure 1: Evolution of center of mass of two bubbles with equal radius $R_1=R_2=1$, at an initial dimensionless distance D=5, and a step change of the dimensionless pressure at the far-field $P_\infty=2$.

Generation of metal nanodroplets and impact experiments

A. Habenicht*, P. Leiderer* and J. Boneberg*

Flat metal nanostructures on inert substrates like glass, silicon or graphite are illuminated by single intensive laser pulses with fluences above the melting threshold. The liquid structures produced in this way are far from their equilibrium shape and a dewetting process sets in. On a timescale of a few nanesconds, the liquid contracts toward a sphere. During this contraction the center of mass moves upward, which can lead to detachment of droplets from the surface due to inertia. The velocity of the detaching nanodroplets is measured with a light barrier technique[1]. The experiment shows (see figure 1a) that the velocity of the detached droplet is constant over a large range of laser energy densities. This supports the model of a dewetting driven process: The droplet gains surface energy by contracting toward a sphere which is then converted into kinetic energy. Results are shown for different materials, where different surface tensions result in different velocities.

Further we show impact experiments where the droplets are landed on another substrate. The particles cool down during the flight due to thermal radiation. They solidify either during flight or when impacting on the substrate. By catching the particles at different distances, the landing temperature can be varied. A droplet which is still molten at impact, spreads (and, under certain circumstances, even rebounds) until the heat loss into the substrates leads to solidification of the particle. Snapshots of different stages of droplet impact are shown (see figure 1b).

*University of Konstanz, Dept. of Physics, LS Prof. Dr. Leiderer, D-78457 Konstanz, Germany.
[1]Habenicht et al., *Science* **309**, 2043 (2005).

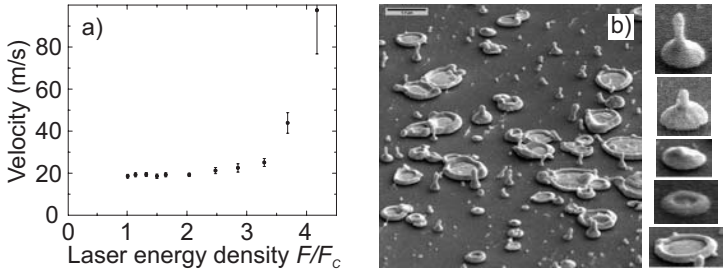

Figure 1: (a) Velocity of the detached gold particles as a function of the energy density of the melting laser. The velocity is constant of a large area of energy densities due to conversion of surface energy into kinetic energy (b) Impact of gold droplets with different sizes on silicon. Depending on the landing temperature (and thus the size of the particle) the droplets solidify at different stages (shown on the right) of droplet impact.

Boundary conditions and the effect of an electrical field gradient in the water dripping dynamics.

J. C. Sartorelli[a], T. N. Nogueira[a], and J. S. Ribeiro[a]

We have studied the effect of different nozzle shapes on the dynamics of water drop formation using two metallic nozzles with different levels. By keeping fixed the level of the water reservoir and having the faucet opening *(S)* as a control parameter we measured the time (T_n) between successive drops as well as their average volume[1]. For each nozzle, we have obtained regular, chaotic, and intermittent behaviors, boundary and interior crises. Comparing the two routes to chaos we have observed: a) for the same water flow (Φ) the reconstructed attractors T_{n+1} vs. T_n are not necessarily the same and neither the dripping rate *(f)*; b) At the crises, in spite of the sudden changes in the attractors shape and in the mean dripping rate, the water flow remained fixed because the average drops volume also changed; and c) for each nozzle we have observed hysteresis in the faucet opening/closing loop[2].

We have established an electrical field gradient in the region where the drop formation took place by assembling one of the nozzles inside a metallic cylindrical shell in which we applied an electrical voltage[3] *(V)* that was used as a second control parameter, while the metallic nozzle was kept grounded. This way, by keeping the faucet opening at a fixed position, the pendant water columns were polarized by the electrical field gradient that in turn was distorted by the column. The drops were ejected with net electrical charge proportional to the applied voltage. For V<1.8kV, the bifurcation diagram is similar to the one obtained with the faucet opening (*S*) as control parameter. Taking some snapshots for some selected control parameters values of *S* and *V* we could observe the same reconstructed chaotic attractors. Above 1.8kV the two bifurcations are quite different since the drops mass decreases while the water flow remains fixed suggesting a decreasing in surface tension due to the electric charges in the water column surface.

---

[a] Universidade de São Paulo, Instituto de Física, Brasil.

[1] Sartorelli et al., *Phys. Rev. E* 49, 3963 (1994).
[2] Sauer T, *Phys. Rev. Lett.* **72**, 3811 (1994).
[3] Fornés et al. *J. Appl. Phys.* **80**, 6021 (1996).

Oscillations of Thin Liquid Shells under Acoustic Forcing

J. Sznitman*, A. Kempe * and T. Rösgen*

Vibrations induced in two-dimensional soap films have been extensively studied both analytically and experimentally in the past[1,2]. In contrast however, oscillations of three-dimensional soap bubbles, a common example of a thin liquid film shaped into a spherical shell, have received comparably little attention and the literature on the subject remains surprisingly scarce. Indeed, for what may seem an intuitive and classic problem, there still lacks both experimental and analytical descriptions of the vibrations of such spherical liquid shells containing a cavity filled with gas.

In the present investigation, we study the oscillations induced by acoustic forcing of soap bubbles placed in ambient air. Using a simple experimental setup, air-filled soap bubbles (size range: 5-20mm diameter) are produced at the tip of a syringe and excited by a loudspeaker at low (1-1000Hz) and high (1-20kHz) frequencies. Both oscillation displacements of the spherical liquid shell and the resulting power spectrum are obtained using a low-coherence interferometric setup[3]. Results for the oscillations of three-dimensional soap bubbles are compared with our measurements for two-dimensional soap films using low-coherence interferometry and in particular, resonance frequencies are sought. In a next step, we implement a PIV algorithm to investigate the possible influence of acoustic forcing on the internal flows present in the cavity. The experimental setup is then slightly modified where particle-laden soap bubbles are now observed under a microscope. Our first results show that not only may acoustic forcing induce flows within the bubble cavity, but moreover, internal convective flow fields are inherently present within the bubble, regardless of the liquid shell oscillations, due to the natural motion of the liquid film which generates a flow inside the cavity, consistent with the no-slip boundary condition at the liquid shell surface.

*Institute of Fluid Dynamics, ETH Zurich, Switzerland

[1] L. Bergmann, *J. Acoust. Soc. Am.* **28**, 6 (1956).
[2] A. Boudaoud et al., *J. Acoust. Soc. Am.* **82**, 19 (1999).
[3] A. Kempe et al., *Optics Letters*, **28**, 15 (2003).

Pinch-off of a giant bubble

D. van der Meer*, R. Bergmann*, M. Stijnman*, M. Sandtke*,
A. Prosperetti*†, and D. Lohse*

Self-similarity has been the paradigmatic picture for the pinch-off of a drop[1]. Here we will show through high-speed imaging and boundary integral simulations that the inverse problem, the pinch-off of an air bubble in water, is *not* self-similar in a strict sense. In our plunger-experiment a disk is quickly pulled through a water surface, leading to a giant, cylindrical void which after collapse creates an upward and a downward jet. The neck radius h scales only in the limiting case of large Froude number as $h(-\log h)^{1/4} \propto \tau^{1/2}$, as expected in the purely inertial regime. For any finite Froude number the collapse is slower, and a second length-scale, the curvature of the void, comes into play. Both length-scales are found to exhibit power-law scaling in time, but with different exponents. The exponents depend on the Froude number, which leads to the conclusion that the pinch-off of a giant bubble is a *non-universal* process.

In all cases we find the profile to be symmetric around the minimum void radius, until the airflow in the neck starts to deform the interface. We find excellent agreement between the experimental profiles and the boundary integral results, up to the point where the effects of air become appreciable.

*Physics of Fluids, University of Twente, P.O. Box 217, 7500 AE Enschede, The Netherlands
†Department of Mechanical Engineering, The Johns-Hopkins University, Baltimore, Maryland 21218, USA

[1]See, e.g., J. Eggers, *Rev. Mod. Phys.* **69**, 865 (1997).

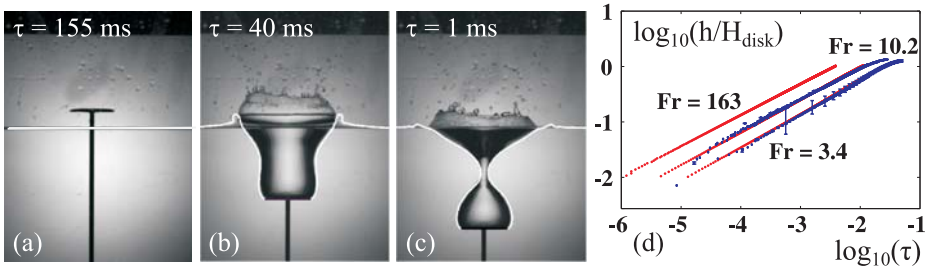

Figure 1: (a-c) Three snapshots of the formation and collapse of a surface void in the plunger experiment. The white lines (overlay) are the void profiles obtained from boundary integral simulations with the same initial condition, and without the use of any free parameter. (d) Doubly logarithmic plot showing the power-law scaling of the neck radius h as a function of the collapse time τ for three different Froude numbers.

3D chaotic mixing inside drops driven by transient electric field

Xiumei Xu[a] and G. M. Homsy[a]

We study the 3D chaotic trajectories inside a neutrally buoyant drop driven by periodically switching a uniform electric field through an angle α. The extent of the chaotic mixing is related to two parameters: the angle α and modulation period T. In a static electric field, the streamlines internal to the drop are axisymmetric Taylor circulations with two rings of center fixed points (CFP) at the top and bottom hemispheres corresponding to the vortex center. Periodically switching the field is equivalent to periodically changing the axis of symmetry, and thus the position of these CFPs. There are always common CFPs during the field rotation, and there are either 4 or 8 depending on the range of α. When α equals π/2, although the trajectories are three dimensional, Poincare maps show that for all modulating periods, the 3D trajectories are confined to certain KAM surfaces, determined only by initial positions, which limit the mixing. For α other than π/2, chaotic mixing is generated inside the drop, but there are ordered regions near the common CFPs, with more regions for the larger number of common CFPs (Figure 1). Inside the ordered regions, trajectories move around the common CFPs in complicated way, and the Poincare maps can exhibit highly ordered fractal structures. The mixing also depends on the modulating period, and our numerical results show that by modifying T it is possible to break the ordered islands and achieve global chaotic mixing. These results suggest there are optimum operating conditions that maximize mixing.

[a] University of California-Santa Barbara, Santa Barbara, 93106, USA

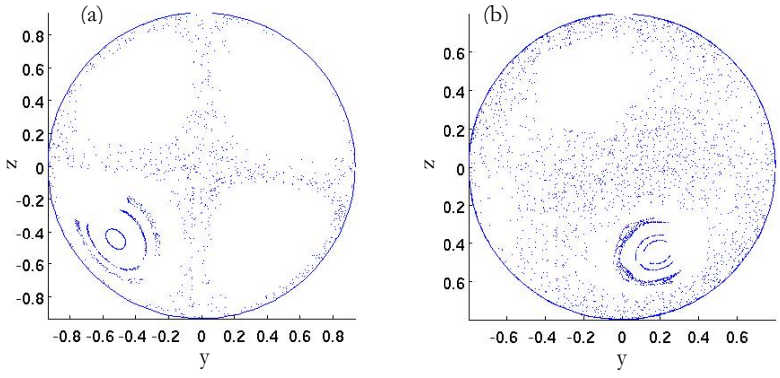

Figure 1: Typical Poincare maps, T=6, (a) α=0.45 π, the case of 8 common center fixed points; (b) α=0.25 π, the case of 4 common center fixed points.

Study of the entrainment mechanism in a negatively buoyant jet developing in an ambient medium of high viscosity

M. S. Manikandan[a], V. Mukund[b] and K. R. Sreenivas[b]

Entrainment process in turbulent free-shear flows is of interest in many applications and is controlled by many factors like whether the flow is driven by initial momentum or buoyancy[1], volumetric heating[2], external magnetic field and pressure gradient[3]. We present results from experiments on the effects of ambient fluid viscosity on the dynamics and entrainment-process of a negatively buoyant jet. In our experiments viscosities of the ambient fluid were altered by the addition of suitable amounts of Sodium carboxymethyl cellulose (Na- CMC). Fluorescence dye was added to the inlet fluid for flow visualization purposes. For a given Reynolds number jet, as the ambient viscosity is increased, jet spread rate decreases (Fig. 1). From Fig. 1, it is also evident that the coherent eddy structures that are prevalent in low viscosity ratio case ($\nu_2 = 15\,\nu_1$) are completely absent in the case of viscosity ratio equal to 47. As the coherent structures are progressively disrupted, by increasing the ambient viscosity, the scalar spread rate decreases. Seeding of the ambient medium indicated the flow structure in the vicinity of the jet. These pictures (Fig 2) show a predominately radial-inward flow when the ambient viscosity is low and it changes to an axial co-flow with the increase in ambient viscosity. These changes are explained by vortex dynamics based model. Results from our study clearly demonstrate the strong correlation between the coherent structures and associated entrainment process. The key mechanism in the suppression of the coherent structures is the stabilization of the shear layer by the high ambient viscosity. The results help in relating shear layer instability to the entrainment process in free-shear flows. This approach will be helpful in modeling their behavior and can address the observed entrainment variations in free-shear flows subjected to different body forces. Results also highlight the importance of looking at the scalar spreads rather than the velocity spreads, in quantifying entrainment in free-shear flows.

[a] Department of Mechanical Engineering, Massachusetts Institute of Technology, MA-USA
[b]EMU, Jawaharlal Nehru Centre for Advanced Scientific Research, Bangalore- 560 064, INDIA.

[1]J.S.Turner, *J. Fluid Mech.* **173**, 431, 1986.
[2]G.S. Bhat and R. Narasimha, *J. Fluid Mech.* **329**, 303, 1996.
[3]D.W. Choi *et. al.* , *J. Fluids Engg.*, **108**, 39,1986.

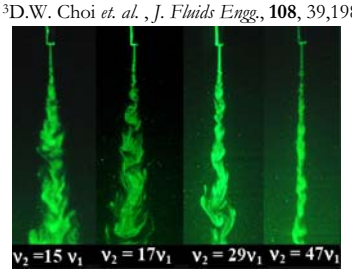

Figure 1: Instantaneous picture of the vertical cross-section of negatively buoyant jets with viscosity ratio changing from 15 to 47.

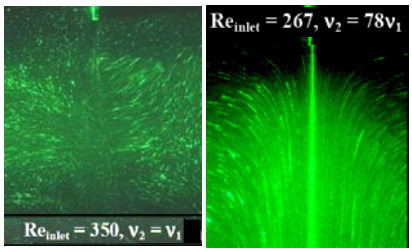

Figure 2: Change of flow field in the vicinity of the jet from inward flow to axial co-flow when viscosity ratio increased from 1 to 78.

The interaction between negatively buoyant jets and wave motion: a laboratory model

G. Querzoli[a] and S.Ferrari[a]

A negatively buoyant jet develops when a fluid is released in a less dense receiving environment, as in the case of brine discharges from desalination plants, dense effluents from wastewater treatment plants, oil and/or gas drilling facilities and mineral salt industries, gypsum wastes from fertilizer factories, etc. As these releases tend to go downwards driven by negative buoyancy, they are typically released upwards, with a certain angle on the horizontal, to increase the path before they impact the sea bottom and so to improve dilution.

As stated by Chin[1], the dilution in a persistent wavy environment is significantly higher than in a stagnant environment; moreover, whether on one hand the interaction between wave motion and vertical buoyant jets has been largely discussed, on the other the present case has not yet been investigated.

For these reasons, with the aim to clarify the influence of surface waves on the behavior of a negatively buoyant jet released upwards at a certain angle, a laboratory model was designed. The experiments were carried out, by means of Light Induced Fluorescence, in a flume furnished with a wavemaker. Buoyant jets with different densimetric Froude numbers were released in both a stagnant and a wavy environment, with ratios between water depth and wave length characteristic of transformation and deep water waves, for various values of wave amplitudes, periods and lengths. These latter values were chosen using data from the Alghero's buoy (North-West Sardinia), to simulate some typical waves of the Mediterranean Sea. The behavior of the jet is analyzed using the overall mean and variance values together with the ones obtained phase by phase.

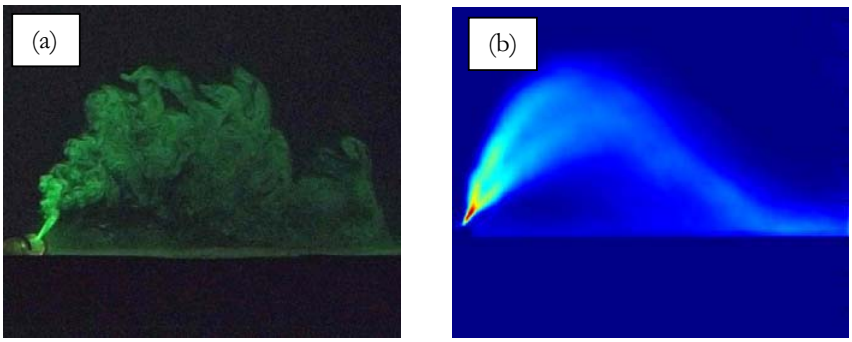

Figure 1: (a) Instantaneous picture and (b) mean value of the concentration field for the run with Froude = 28.1, wave period = 1.05 s and wave amplitude = 1.25 cm.

[a] DIT (Dipartimento di Ingegneria del Territorio), University of Cagliari, piazza d'Armi, 09123 Cagliari, Italy.

1 Chin, *J. Hydraulic Engineering Division,* **113(8)**, 1006 (1987).

Measurements of buoyancy driven turbulence in a vertical pipe

Murali R. Cholemari*, Jaywant H. Arakeri*

We present measurements of a buoyancy driven turbulent flow in long (length-to-diameter ratio = 9) vertical pipes. The flow is created by the density difference across the ends of the vertical tube. We use brine and fresh water for creating the density difference. The flow represents an 'overturning process' of the two fluids through the pipe. Since the pipes are long, an axially homogeneous region of turbulence exists away from the ends. In this region the flow is driven by a linear unstable density gradient. The ratio of the diffusivities of momentum and salt, given by the Schmidt number, $Sc = \nu/\alpha$, is about 670. The Rayleigh number based on the diameter d of the pipe and the density gradient, $Ra_g = g(\Delta\rho/\rho L)d^4/\nu\alpha$, which gives the relative importance of the buoyancy and diffusive effects, is of the order of 10^8. The experimental data consisted of measurements of salt concentration using a conductivity probe and velocity measurements using planar particle image velocimetry (PIV).

Velocity measurements show that there is no mean flow. Flow visualization and spatial velocity correlations show that large scales are of the order of the pipe diameter. One dominant motion seems to be heavier particles going down accompanied by lighter particles rising up on the sides. Another motion inferred from the data is the collision of falling and rising fluid particles. The flow is anisotropic, both at large scales as well as at the smallest scales measured[1].

The turbulence in the fully developed region involves the dominance of a single length scale, comparable to the diameter of the pipe. A mixing length model incorporating this feature is shown to agree very well with the experimental measurements of the scalar (salt concentration) flux and velocity measurements. The Nusselt number scales as $\sim Ra_g^{1/2}Sc^{1/2}$ suggesting that the molecular effects are negligible. This may be compared to the $\sim Ra_g^{1/3}$ scaling obtained in turbulent Rayleigh-Bénard convection[2].

The unique feature about the present flow is that it is a axially homogeneous purely buoyancy driven turbulent flow.

*Department of Mechanical Engineering, Indian Institute of Science, Bangalore 560012 INDIA.

[1]Cholemari, *PhD thesis, Indian Inst. Sci.*, (2004).

[2]Cholemari and Arakeri, *Int. J. Heat Mass Transfer.* **48**, 4467 (2005).

Coherent Large-Scale Structures and Hysteresis in Turbulent Convection

A. Eidelman, T. Elperin, N. Kleeorin, I. Rogachevskii,
I. Sapir-Katiraie

Department of Mechanical Engineering
Ben-Gurion University of the Negev
POB 653, Beer-Sheva 84105
ISRAEL

We studied theoretically and experimentally coherent large-scale circulations (semi-organized structures) in turbulent convection in an air flow in a rectangular chamber. Particle Image Velocimetry was used to determine the turbulent and mean velocity fields, and a specially designed temperature probe with twelve sensitive thermocouples was employed to measure the temperature field. We found the hysteresis phenomenon in turbulent convection by varying the temperature difference between the hot bottom wall and cold top wall of the chamber. The hysteresis loop comprises the one-cell and two-cells flow patterns while the aspect ratio is kept constant. We developed a new mean-field theory of turbulent convection. In a shear-free turbulent convection this theory predicts the convective wind instability which causes formation of large-scale semi-organized fluid motions in the form of cells. The developed theory of formation of semi-organized structures in turbulent convection is in agreement with the experimental observations. The observed coherent structures are superimposed on a small-scale turbulent convection. Thermal structure inside the large-scale circulations is neither homogeneous nor isotropic. The warm thermal plumes accumulate at one side of the large-scale circulation, and cold plumes accumulate at the opposite side of the large-scale circulation. The redistribution of the heat flux plays a crucial role in the formation of coherent large-scale circulations in turbulent convection. Predictions of the developed theory are also in a good agreement with the observed semi-organized structures in the atmospheric turbulent convection.

Effect of inflow conditions on the near field of a turbulent annular jet

F. Picano*, G. Troiani*, F. Salvadore*, P. Gualtieri*

The dynamics of the near field of an annular jet is characterized by a recirculating region at the exit of the nozzle, which is crucial for a stable anchoring of turbulent premixed flames. Several difficulties arise when attempting to model by DNS such features, which strongly depend on the specific geometry of the nozzle and on the details of the inflow boundary conditions. It is well known that the far field of annular jets attains the universal self-similar state of classical jets, as confirmed by the DNS data shown in figure 1-left [1, 2]. Here we present a detailed comparison between DNS results for an annular jet at moderate Reynolds number, and experimental data obtained by PIV for the same nozzle configuration (see figure 1-right) [3, 4].

Different configurations will be exploited both in the numerical simulation and in the experiments in order to characterize the dependence of the near field on the inlet conditions, e.g. turbulence intensity and velocity profiles. Both a closed and an open bottom will be used around the nozzle exit to address the effect of the entrainment on the behavior of the recirculating zone.

*Department of Mechanics and Aeronautics, University of Rome "La Sapienza", Italy

[1] Hussein et al., *J. Fluid Mech.* **258**, (1994)
[2] Warda et al, *Flow Meas. and Instr.* **10**, (1999)
[3] Ko and Chan, *J. Fluid Mech.* **84**, 4 (1978)
[4] Kassab et al., *Flow Meas. and Instr.* **10**, (1999)

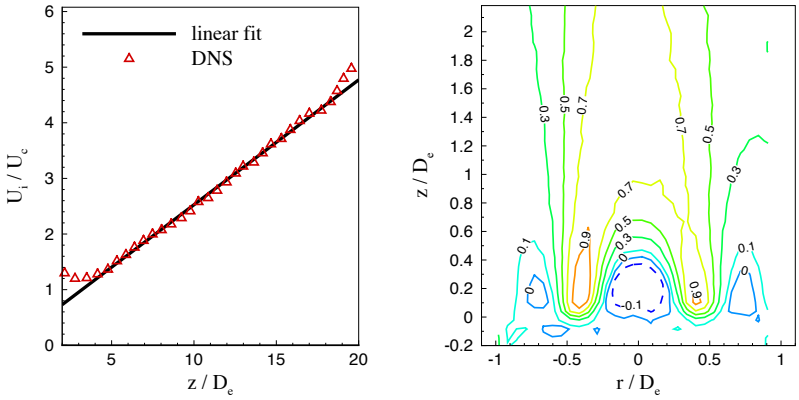

Figure 1: Left: DNS data at $Re = 5100$. Symbols: inverse of normalized mean axial velocity at the centerline *vs* normalized axial position. Line: linear fit, whose slope is $\frac{1}{5.7}$ accordingly with self-similarity of classical jets. Right: PIV measurements, isolines of local axial velocity normalized by exiting velocity.

Turbulent mixing in the entry region of confined coaxial jets

P. M. Areal*and J.M.L.M. Palma*

Coaxial jets is a flow configuration common in many engineering devices (aircraft reactors, combustion chambers, etc.) where mixing is important. In case the velocity ratio is different from 1, these flows usually exhibit large turbulent structures and can be most appropriate to be dealt by the Large-Eddy Simulation (LES) approach to turbulence modelling.

In this work, previous experiments[1], using simultaneously LDV for the velocity field and LIF (laser induced fluorescence) for the passive scalar, were re-analysed and insight on the turbulent mixing was sought using LES. The flow geometry comprised 2 coaxial water flows, with a diameter ratio of 2.5 (42/17 mm). The Reynolds numbers, based on bulk velocity, are 29400 for case 1 and 35000 for case 2, with annular to central bulk velocity ratio equal to 0.8 (0.83/1.08 ms^{-1}) and 3.5 (0.83/0.26 ms^{-1}). A fractional-step, 2nd order, LES code[2] was adapted to the cylindrical geometry with a non-orthogonal grid. To account for the effects of the filtered small scales on the large resolved ones, a Lagrangian dynamic subgrid model[3] was used for the velocity field and extended to the scalar field assuming a uniform turbulent Schmidt number of 1.

The results showed the ability of the LES to capture the main features of the flow. Deficiencies of the current set of results (figure) are expected to be removed by reverting to a fully dynamic model for the scalar subgrid terms[4] (whose implementation is currently underway), with a spatially variable turbulent Schmidt number, and alternative treatments of the inlet conditions.

*Faculdade de Engenharia da Universidade do Porto, Research Centre for Wind Energy and Atmospheric Flows, Rua Dr. Roberto Frias s/n, 4200-465 Porto, Portugal.

[1]Lima, M. and Palma, J.M.L.M., http://in3.dem3.dem.ist.utl.pt/lxlaser2002/papers.asp, (2002).
[2]Silva Lopes A. and Palma J.M.L.M., Journal of Computational Physics, **175**,713 (2002).
[3]Armenio V. and Piomelli U., *Flow, Turbulence and Combustion* **65**, 51 (2000).
[4]Keating A. *et al J. of Turbulence*, **5**, 20 (2004).

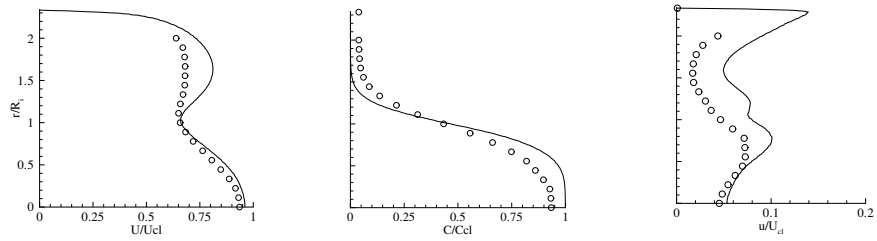

Figure 1: Mean longitudinal velocity (U), mean concentration (C) and fluctuating longitudinal velocity ($\sqrt{\overline{uu}}$), made dimensionless by the mean centerline values.

Interaction of two unequal corotating vortices

R. R. Trieling*, O. U. Velasco Fuentes† and G. J. F. van Heijst*

Previous high-resolution contour dynamics calculations[1] have shown that the inviscid interaction between unequal like-signed vortices with uniform vorticity is not always associated with vortex growth and may lead to vortices smaller than the original vortices. In the present study[2], we investigate whether these results also hold for vortices with continuous vorticity distributions. Similar flow regimes are found as for uniform vorticity patches, but the variation of the flow regimes with the initial vortex radii and peak vorticities is more complicated and strongly dependent on the initial shape of the vorticity profile. It is found that the 'halo' of low-value vorticity, which surrounds the cores of continuous vortices, significantly increases the critical distance at which the weaker vortex is destroyed. The halo also promotes the vortex cores to merge more efficiently, since it accounts for a substantial part of the loss of circulation into filaments. Simple transformation rules and merger criteria are derived for the inviscid interaction between two Gaussian vortices. The strong dependence of the flow regimes on the initial vorticity distribution partly explains why previous laboratory experiments in an electron plasma[3] show complete merger of two unequal vortices in a range of parameter space where contour dynamics simulations with uniform vorticity patches predict partial merger or partial straining-out of the smaller vortex. It is shown that the measured times for complete merger are in reasonable agreement with inviscid dynamics when the vortices are very similar. For more distinct vortices the weaker vortex is often observed to be destroyed on a time scale much smaller than expected from inviscid numerical simulations. An explanation for this discrepancy is given by the combined effects of vortex stripping and viscous diffusion, which leads to an enhanced erosion of the weaker vortex. These results are verified by laboratory experiments in a conventional (rotating) fluid, see figure 1.

*Fluid Dynamics Laboratory, Eindhoven University of Technology, The Netherlands.
†Departamento de Oceanografía Física, CICESE, México.
[1]Dritschel and Waugh, *Phys. Fluids* **4**, 1737 (1992).
[2]Trieling et al., *Phys. Fluids* **17**, 087103 (2005).
[3]Mitchell and Driscoll, *Phys. Fluids* **8**, 1828 (1996).

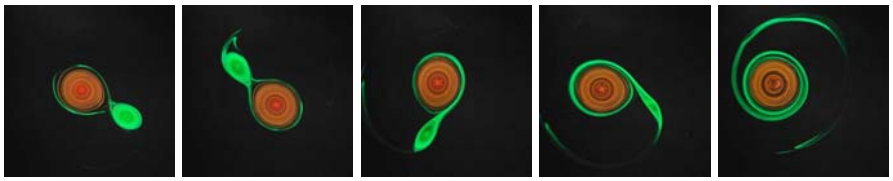

Figure 1: Dye visualization of the evolution of two unequal corotating vortices in a rotating water tank.

Instabilities of co-rotating vortices.

P. Orlandi*

Co-rotating vortices have a particular relevance in the wake of aircraft wings. Laboratory experiments were performed to understand the merging of the two vortices and the influence of 3D instabilities. Meunier & Leweke (JFM, **533**, 2004) designed the experiment to look at vortices of infinite length, which can be considered as time evolving. Chen *et al.* (JFM, **382**, 1999), on the other hand, investigated the more realistic condition of space developing vortices. The common feature is that the merging depends on the Reynolds number and on the separation of the vortices. The pairing should be different because the vortices are generated in a different way.

To understand the differences numerical simulations can be a useful since all the quantities are accessible, in particular pressure and vorticity components. The present study is devoted to look at the details of the merging by simulations in 2D, in 3D with periodic conditions in the direction of the axes (x_3), and in the space developing case where at $x_3 = 0$ a constant axial velocity (u_3) and two Gaussian vorticity distributions of ω_3 are assigned. In all cases the vortices have a radius $a_0 = 0.35$, and are located in a computational box of size 2π, large enough to consider the vortices isolated. Three values for the ratio between the separation b_0 and the radius a_0 are assigned $a_0/b_0 = 0.17, 0.21$ and 0.25.

To investigate the effects of a axial disturbances, undulations of the distance b_0 in phase, and out of phase were given. In the former case the rotation of the two vortices does not vary along the axis, while in the latter case it varies. The centre of the vortex can be detected by the location of the minimum pressure, thus the merging of the two vortices can be appreciated by the time evolution of $|P|_{max}$. In Fig.1a the evolution of this quantity is plotted versus $t^* = t(8\pi^2)Re(a_0/b_0)^2$ for 2D and for 3D with in phase disturbances. Large differences occur for $a_0/b_0 = 0.21$. For the out of phase disturbances the differences are more relevant because one region merges before the other.

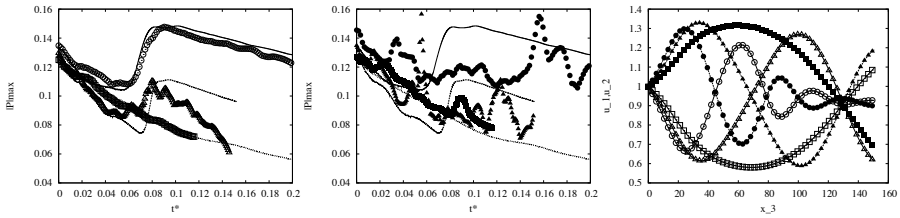

Figure 1: a) 2D+ in phase, b) 2D+ out of phase, c) space developing; $\circ$ $a_0/b_0 = 0.25$, $\triangle$ $a_0/b_0 = 0.21$, $\square$ $a_0/b_0 = 0.17$ in c) solid $i = 2$, open $i = 1$

The same values of b_0 were assigned in the space developing simulations; the streamwise variations of the velocity rms scaled by the values at the inlet give a picture of the merging. Fig.1c shows that the rms grow before the merging and that it is damped after. This is better appreciated for $a_0/b_0 = 0.25$.

*Dip. Mecc. Aer. Università di Roma "La Sapienza" Rome, Italy

Instabilities in co-rotating vortices with axial flow

N. Schaeffer*, L. Lacaze†, S. Le Dizès*

The wake shed by an aircraft is initially composed of several co- and counter-rotating vortices with axial jet whose strength and number depend on the spanwise load distribution on the wings. For instance, a wing equipped with a single flap generates in the near field a wing tip and a co-rotating outboard flap tip vortex. When axial flow is not taken into account, this system of two vortices is known to be unstable with respect to a short-wavelength elliptical instability.[1] This instability has been shown to strongly affect the merging process of the vortices[2] and its subsequent dynamics. In the present work, our goal is to analyze the effect of the axial flow on the instability and the dynamics of the vortex pair.

We consider the three-dimensional temporal evolution of two interacting parallel Batchelor vortices (in the regime where each vortex is inviscidly stable). From a theoretical point-of-view, each vortex is considered separately and the effect of the other vortex is modeled by a rotating strain field. In this framework, the elliptic instability results from the resonant coupling of two Kelvin waves of the vortex with the rotating strain field. Without axial flow, the most unstable mode is known to be a combination of two helical Kelvin waves of azimuthal wavenumber $m = -1$ and $m = 1$ leading to a sinuous deformation of each vortex. When axial flow is considered, the symmetry between left and right propagating waves is broken such that the combination of the two helical waves $m = -1$ and $m = 1$ is no longer a sinuous deformation. In addition, one of the two waves becomes damped by the appearance of a critical layer such that the resonance between these two waves is suppressed above an axial flow threshold. However, the elliptical instability does not disappear: other combinations of Kelvin waves $m = -2$ and $m = 0$, then $m = -3$ and $m = -1$ are shown to become progressively unstable as axial flow is increased.

A theoretical model for the instability growth rate is proposed. It is based on the local estimate of the elliptical instability growth rate in the vortex center.[3] It also uses a large wavenumber asymptotic analysis[4] in order to provide the characteristics of the resonant waves and an estimate of the damping rate associated with the critical layers. The theory is validated by the numerics. Temporal growth rates and unstable mode structures are shown to be well-reproduced by numerical simulations of the linearized perturbation equations for a Batchelor vortex pair. Direct numerical simulations of the complete Navier-Stokes equations are also performed to analyze the nonlinear development of the instability. The influence of the instability on the merging process and its impact on the global dynamics of the vortex system in the aeronautical context are discussed.

This work is supported by the European Community (FAR-Wake project) and the French Agency for Research (ANR).

*IRPHE, 49 rue F. Joliot Curie, BP 146, F-13384 Marseille cedex 13, France.
†IMFT, 1 Allée du Professeur Camille Soula, F-31400 Toulouse, France.

[1] Le Dizès and Laporte, *J. Fluid Mech.* **471**, 169–201 (2002).
[2] Meunier and Leweke, *J. Fluid Mech.* **533**, 125-159 (2005).
[3] Waleffe, *Phys. Fluids* **A 2**, 76–80 (1990).
[4] Le Dizès and Lacaze, *J. Fluid Mech.* **542**, 69–96 (2005).

Experiments on vortex pair dynamics in ground effect

C. Cottin* and T. Leweke*

We investigate experimentally the 3D dynamics of a pair of counter-rotating vortices approaching a solid wall. In addition to its fundamental interest, this configuration has relevance for the problem of aircraft trailing vortices at take-off and landing.

The vortices are generated in water at the edges of two impulsively rotated flat plates, and visualised using fluorescent dye. Measurements were performed using image analysis and Particle Image Velocimetry. The set-up and procedure are similar to the ones described in Ref. 1. Reynolds numbers, based on the circulation of one vortex, were in the range 1500-5500.

In the major part of the experiments, the vortex pairs were generated close to 3 vortex separation distances away from the wall. This is short enough for the flow not to develop long-wavelength displacement instabilities or elliptic core instabilities[1], before the wall effect becomes important. As the vortices approach the surface due to their mutually induced motion, secondary vorticity is generated at the wall (see figure 1), which is lifted off the surface and rolls up into a secondary vortex orbiting the primary one and causing its rebound. During this stage, short-wave perturbations grow at the periphery of the primary vortices (fig. 1a). At a later time, an instability with a larger axial wavelength develops on the secondary vortex (fig. 1b), leading to a rapid decay of the whole system into small-scale structures shortly afterwards. We will present evidence that these phenomena are caused by a centrifugal instability of the primary vortex and an elliptic instability of the secondary vortex, respectively.

Some qualitative results on the interaction of a ground effect with the long-wavelength Crow instability will also be presented.

*IRPHE, CNRS/Universités Aix-Marseille, B.P. 146, F-13384 Marseille Cedex 13, France.

[1]Leweke and Williamson, *J. Fluid Mech.* **360**, 85 (1998)

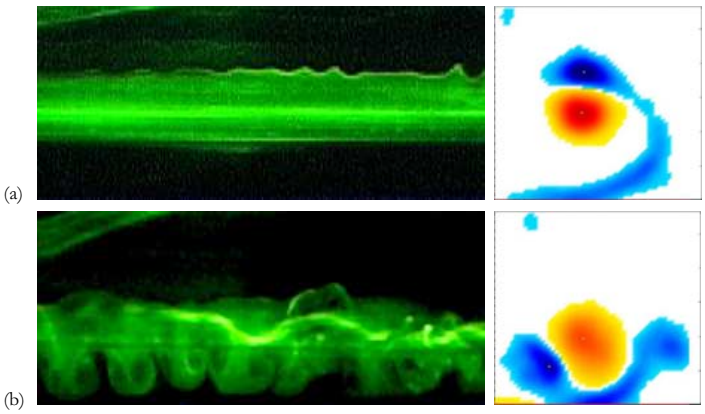

Figure 1: Dye visualisation (side view) and vorticity levels (cross-cut of one vortex only) of a vortex pair in ground effect at Re = 3500. (a) $t^* = 4.5$, (b) $t^* = 6.4$.

On the time evolution of a pulsed jet

G. Querzoli[1], M. Falchi[2] and G. P. Romano[2]

The formation of vortex rings from sudden release of fluid through an orifice or a nozzle has been extensively investigated in the past[a]. Anyway most of authors focussed on flow rate that were constant or increasing until the vortex ring complete formation or stopped suddenly at a given instant, forcing the end of the vortex formation. In the present work, the velocity field generated by a pulsed jet is investigated. The flow-rate is periodic. It is modulated gradually so that there is a well defined phase of acceleration, followed by a gradual deceleration. Different flow-rate laws have been tested varying the overall shape of the curve and the relative duration of the acceleration and deceleration phases, and stroke-volumes, whereas the period was kept constant (T = 1 s). For each phase and curve 50 velocity field have been acquired and the average is considered.

The jet is generated by a sharp-edged orifice (3.0 cm in diameter) on a thin plate placed inside a parallelepipedal vessel, 110 x 40 x 40 cm. On the upstream side of the vessel a small chamber hosts the water inlet and the piston-cylinder device that drives the flow. The flow develops in a 60 cm long chamber. Both water inlet and outlet are connected to a constant-head tank through two one-way valves in order to avoid back-flow during the periodic motion of the piston. The velocity field is measured on a middle plane by means of the Robust Image Velocimetry (RIV)[b]. RIV is a velocimetry based on image analysis that uses robust statistics instead of cross-correlation (as PIV does) to compare interrogation windows. The measuring plane is illuminated by a Nd-Yag laser and couples of particle images are acquired by a cross-correlation camera, 1376 x 1040 x 12 bit in resolution.

An example of the resulting velocity (vectors) and vorticity (colour) field is shown in figure 1. In figure 2 the time laws of the piston motion used during the experiment are shown. The analysis of the results suggests that the vortex ring is affected only by the accelerated ejection.

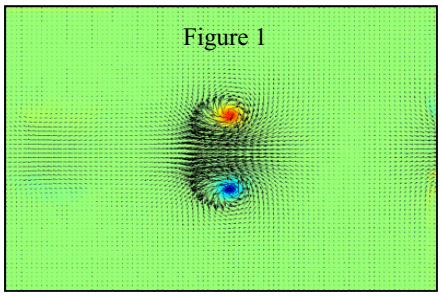

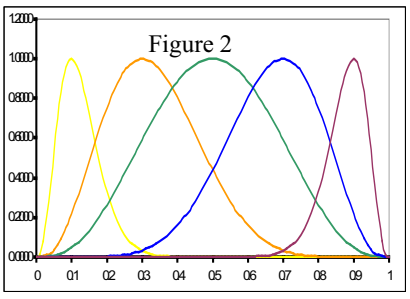

1 Dipartimento di Ingegneria del Territorio, Università di Cagliari, Italia. e-mail: querzoli[@unica.it
2 Dipartimento di Ingegneria Meccanica e Aeronautica, Università di Roma "La Sapienza", Italia

a Shariff and Leonard, *Ann. Rev. Fluid Mech.*, **24**, 235, (1992); Gharib M; Rambod E; Shariff K, *J. Fluid Mech.,* **360**, 121(1998)
b Falchi, Querzoli Romano, *Experiment in Fluids*, submitted (2005).

List of authors

Ordinary lectures and mini-symposia

LIST OF AUTHORS

LIST OF AUTHORS

LIST OF AUTHORS

LIST OF AUTHORS

LIST OF AUTHORS